

ABSTRACT

Title of dissertation: PCB DESORPTION FROM RESUSPENDED HUDSON RIVER SEDIMENT

Abby Ruth Schneider, Doctor of Philosophy, 2005

Dissertation directed by: Professor Joel E. Baker
Marine Estuarine and Environmental Science

From the late 1940's until 1977 two General Electric Plants discharged 200,000 - 1.3 million pounds of polychlorinated biphenyls (PCBs) into the upper Hudson River. Field studies and detailed modeling efforts indicate that PCB release from sediments under realistic mixing conditions determines the efficiency of both 'natural recovery' and proposed dredging operations. In this study, Hudson River sediment was resuspended into clean water in large mesocosms. The desorption rates of individual PCB congeners were determined by measuring dissolved PCB concentrations using solid-phase microextraction.

Immediately following the initiation of resuspension, large particles with an average median diameter of $140 \pm 14 \mu\text{m}$ were lifted into the water column. Dissolved PCBs rose rapidly and after two hours of resuspension 6 to 38% of the PCBs in the water column were in the dissolved phase. Rate constants for this rapid release ranged from 0.04 to 0.34 hour^{-1} and decreased significantly as $\log K_{ow}$ of the PCBs increased. Both

the total suspended solids concentration and dissolved PCBs reached steady state in 24 hours. At steady state the flocs volume median diameter averaged $112 \pm 3 \mu\text{m}$, porosity averaged 0.90 ± 0.02 , and 15-50% of the resuspended PCBs were dissolved. The PCB concentration on resuspended particles was an average of two times greater than the bulk sediment PCB concentration and 8% of the resuspended mass did not settle after twenty hours without mixing. At steady state the particle-water PCB partition coefficients were similar to values measured in the Hudson River and constant across the range of congeners examined. With only one-day quiescence between resuspension events the percent of dissolved PCBs at steady state decreased significantly from the first to the third resuspension event ($p = 0.02$). When quiescent time was increased to four days, there was no change in the percent dissolved PCBs at steady state for the low molecular weight congeners ($\text{Log } K_{ow} \leq 5.85$, $p = 0.45$). This analysis suggests there was a large release of PCBs from particles when they were initially resuspended; however, chronic resuspension resulted in less PCB release per event due to the slow recharge of a labile pool.

PCB DESORPTION FROM RESUSPENDED HUDSON RIVER SEDIMENT

by

Abby Ruth Schneider

Dissertation submitted to the Faculty of the Graduate School of the
University of Maryland, College Park in partial fulfillment
of the requirements for the degree of
Doctor of Philosophy
2005

Advisory Committee:

Professor Joel E. Baker, Chair
Professor William P. Ball
Dr. Brian J. Eadie
Professor Robert P. Mason
Professor Lawrence P. Sanford

©Copyright by
Abby Ruth Schneider
2005

Acknowledgements

Science is a collaborative process and there are many people I'd like to thank for their assistance and fruitful discussions about this work. First and foremost I'd like to thank my advisor Dr. Joel Baker for his patience, guidance, and inspiration. I have enjoyed working in his lab, learned lots of useful skills, and had a great time. I'd like to thank my committee members; I've had many long discussions with each of them about my results, how to present them, and most of all how to interpret them. I really appreciate their assistance. I'd also like to thank Dr. Upal Ghosh at the University of Maryland, Baltimore County. I consider him an honorary member of my committee; I've presented my work to him since the beginning and he has helped guide my analysis of the data. I'd like to thank Harry Zahakos of Quantitative Environmental Analysis, LLC for his help with the labile/resistant modeling. It was fun working with someone as enthusiastic and interested in PCB release during resuspension events as I am. I'd also like to thank Frank Estabrooks of the New York State Department of Environmental Protection for providing a boat, suggesting a good sampling site, and taking us out on the Hudson River to collect sediment. Finally, of course, I am indebted to the Hudson River Foundation for funding this project. I also really enjoyed presenting my work at the meetings they organized.

My thesis project was very labor intensive and I am grateful to all my lab mates for their help and to my advisor for letting them help me. It took the whole village of Baker lab students and FRA's to raise the tent over the STORM tanks so that my experiments could be conducted in the dark. I especially appreciate Andy Stephenson for his assistance during the STORM experiments. He was there every morning to tend to

the LISST and his sense of humor kept me laughing throughout the day. Nearly everyone in my lab group helped filter water samples including Susan Klosterhaus, Alessandra Paolicchi, and Megan Toaspern. Eileen Beard provided moral support throughout the project and greatly assisted with the analysis of the filter samples. Even the high school students working in our lab, Taylor Woodburn-Camp and Marie Hurst, came in on the weekend to help duct tape Mylar to create a reflective tarp tent for the STORM tanks. Bernie Crimmins and Dan Leibert helped me assemble the SPME temperature control room and taught me how to cut 1/8 inch tubing without crunching it. Pat Dickhut in Dr. Sanford's group at the Horn Point Laboratory allowed me to call him in the early hours of the morning when I couldn't get the LISST working. I'd especially like to thank Dr. Elka Porter, who designed the STORM tanks and assisted with the day-to-day operation of the experiment. I never would have been able to complete this project without all the help from my lab mates and friends and am forever grateful to all of you.

I'd like to take this opportunity to say a final thank you to my family and friends for their love and support throughout the years. My parents encouraged me to pursue my interest in science since I was ten years old and for that I will be forever grateful and appreciative. My husband loves and supports me and thinks it is incredibly cool to be married to someone pursuing a PhD. He understood when I had to work at night and on weekends and kept me laughing. I was lucky enough to pursue my PhD in a great environment where everyone from the maintenance workers and administrative assistants to the professors were supportive and encouraging. I will miss my friends, kayak buddies, and girls' night parties very much and will treasure our memories together.

LIST OF TABLES	vii
LIST OF FIGURES	viii
CHAPTER 1: INTRODUCTION.....	1
1.1 BACKGROUND.....	1
1.2 PCB DESORPTION.....	4
1.3 DESORPTION RATE MODELS	9
1.4 IMPACT OF SHEAR STRESS AND TURBULENCE	14
1.5 OBJECTIVES	19
1.6. STRATEGY.....	20
1.7 EXECUTIVE SUMMARY.....	24
1.7.1 Chapter 2	24
1.7.2 Chapter 3	25
1.7.3 Chapter 4	26
1.7.4 Chapter 5	28
1.8 IMPLICATIONS	29
CHAPTER 2: THE USE OF SOLID PHASE MICROEXTRACTION TO RAPIDLY MEASURE DISSOLVED PCBS IN NATURAL WATERS	32
2.1 INTRODUCTION	32
2.2 EXPERIMENTAL SECTION	36
2.2.1 SPME fibers	36
2.2.2 Standards	37
2.2.3 Gas Chromatography	37
2.2.4 Revolving SPME Apparatus.....	39
2.2.5 Spiked Water Calibration	39
2.2.6 Matrix Interference Evaluation.....	41
2.2.7 XAD Comparison.....	42
2.3 RESULTS AND DISCUSSION.....	44
2.3.1. Analytical Verification of GC Technique.....	44
2.3.2 Method Precision.....	45
2.3.3 Kinetics of PCB Uptake	46
2.3.4 Dissolved Phase Calibration	52
2.3.5 Detection Limits.....	53
2.3.6 Matrix Effects.....	53
2.3.7 XAD/SPME comparison.....	55
2.4 SUMMARY	57
CHAPTER 3: A MESOCOSM EXAMINATION OF COHESIVE HUDSON RIVER SEDIMENT RESUSPENSION AND SETTLING.....	61
3.1 INTRODUCTION	61
3.2 MATERIALS AND METHODS	66
3.2.1 STORM Tanks	66
3.2.2 Sampling Strategy.....	69
3.2.3 Ancillary Water Measurements.....	69

3.2.4 LISST Measurements	70
3.2.5 Grain Size Analysis.....	71
3.3. RESULTS AND DISCUSSION.....	71
3.3.1 Grain Size Analysis.....	72
3.3.2 Water Column Properties	72
3.3.3 Particle Size Distribution.....	75
3.3.4 Settling	81
3.3.5 Multiple Resuspension Events in Tank A.....	85
3.3.6 Tank B: Two days quiescence between resuspension events.....	88
3.3.7 Tank C: Four days quiescence between resuspension events.....	92
3.4 CONCLUSIONS.....	92
CHAPTER 4: PCB PARTITIONING TO FLOCCULATED HUDSON RIVER SEDIMENT: RECHARGE OF THE LABILE POOL DURING QUIESCENT PERIODS.....	95
4.1 INTRODUCTION	95
4.2 MATERIALS AND METHODS	101
4.2.1 STORM Tanks	101
4.2.2 Sampling Strategy.....	102
4.2.3 Analytical Procedure	104
4.2.4 Quality Control and Assurance	106
4.3 RESULTS AND DISCUSSION.....	107
4.3.1 Flocculation and Disaggregation.....	107
4.3.2 Sediment and Suspended Particles	109
4.3.3 Steady State PCB Partitioning.....	111
4.3.4 Labile/Resistant Model	115
4.3.5 Black Carbon	125
4.4 IMPLICATIONS.....	130
CHAPTER 5: KINETICS OF PCB RELEASE FROM RESUSPENDED HUDSON RIVER SEDIMENT	132
5.1 INTRODUCTION	132
5.2 MATERIALS AND METHODS	138
5.2.1 STORM Tanks	138
5.2.2 Sampling Strategy.....	139
5.2.3 Analytical Procedure	139
5.3 PCB DESORPTION MODELS	141
5.3.1 One Compartment Model.....	142
5.3.2 Radial Diffusion Model.....	143
5.4 RESULTS AND DISCUSSION.....	146
5.4.1 Initial Release	146
5.4.2 Impact of Quiescent Time	159
5.4.3 Impact of Repeated Resuspension.....	162
5.6 Implications.....	167
APPENDIX.....	170

Appendix A: Ancillary Water data.....	170
Appendix B: LISST data.....	174
Appendix C: Dissolved PCB data.....	181
Appendix D: Particulate PCB data.....	188
Appendix E: Sediment PCB data.....	198
Appendix F: Matlab Code of Radial Diffusion Model.....	200
REFERENCES.....	202

LIST OF TABLES

1.1	Labile rate constants for PCB desorption.	13
1.2	The impact of floc formation on the time to hexachlorobenze sorptive equilibrium (data from Tye et al. 1996).	16
2.1	Kinetic constants for the uptake of PCBs onto the SPME fibers (n = 4).	51
2.2	Regression statistics for the relationship between dissolved PCB concentrations and mass measured on the SPME fiber (n = 4).	54
3.1	The initial (after 45 minutes of mixing) and steady state properties of the resuspended flocs in all STORM experiments.	74
5.1	Literature values of the labile rate constants for PCB desorption and the labile rate constants measured in this study.	136
5.2	Properties of the PCB congeners measured in the STORM tanks. The molecular diffusion coefficient in water (D_m) was calculated using the Wilke-Chang equation. The K_p value was calculated using Karickhoff's equation given that the particles were 12% organic carbon.	155

LIST OF FIGURES

1.1	Map of the Upper Hudson River.	2
1.2	Organic carbon normalized partition coefficients of various PCB congeners measured in the Hudson River compared to the values predicted by Karickhoff.	6
1.3	Schematic of the sequence of resuspension events conducted in each STORM tank. The high TSS corresponds to periods when mixing was turned on. The low TSS corresponds to periods when mixing was turned off and the tank sat with only ~ 1 cm of overlying water.	23
2.1	Schematic of a SPME fiber prior to injection into the GC.	38
2.2	A Schematic of the revolving SPME apparatus	40
2.3	The uptake of PCBs onto SPME fibers deployed in DI water spiked with 5 $\mu\text{g L}^{-1}$ of Aroclor 1248 for sampling times ranging from 5 – 120 minutes at 25°C.	47
2.4	Uptake curves of selected PCBs onto the SPME fibers deployed in DI water spiked with 5 $\mu\text{g L}^{-1}$ of Aroclor 1248. The SPME fibers sampled the water continuously for time periods ranging from five minutes to 12 hours at 25°C.	49
2.5	SPME measurements of the dissolved concentrations of PCB congeners measured in DI water, DI water plus DOC, and DI water plus suspended solids.	56
2.6	A comparison of dissolved PCB concentrations measured by the revolving SPME technique to measurements made by traditional XAD extraction.	58
2.7	The average percent difference between XAD and SPME measurements for each PCB congener.	59
3.1	Schematic of the sequence of resuspension events conducted in the STORM tanks. The high TSS corresponds to periods when mixing was turned on. The low TSS corresponds to periods when mixing was turned off and the tank sat with only ~ 1 cm of overlying water.	68
3.2	Changes in ancillary water measurements during the first three-day resuspension event in Tank A.	73

3.3	Changes in the (A) number (B) volume and (C) surface area median diameter during the course of the first resuspension event in Tank A, B, and C.	77
3.4	The particle size distribution expressed as fraction of total (fot) by (A) number (B) volume and (C) Surface Area during the first resuspension event in Tank A 45 minutes after resuspension was initiated and at steady state.	78
3.5	(A) The total volume concentration of various size classes of particles as they settle through STORM Tank A. (B) The corresponding measured total suspended solids concentration.	83
3.6	The volume median diameter of the settling particles in STORM Tank A.	86
3.7	The settling particles collected on glass fiber filters and magnified to 2.5 power.	87
3.8	The volume median diameter of resuspended flocs in the STORM tanks during multiple resuspension events.	89
3.9	Initial and steady state porosity of the resuspended flocs.	90
4.1	Organic carbon normalized partition coefficients of various PCB congeners measured in the Hudson River compared to the values predicted by Karickhoff.	98
4.2	Schematic of the sequence of resuspension events conducted in the STORM tanks. The high TSS corresponds to periods when mixing was turned on. The low TSS corresponds to periods when mixing was turned off and the tank sat with only ~ 1 cm of overlying water.	103
4.3	Steady state conditions in Tank A for resuspension event 1 (A) total suspended solids concentration and fraction organic carbon (B) a few dissolved PCB congeners (C) a few particulate PCB congeners.	108
4.4	The PCB concentration of (A) the resuspended particles and (B) the sediment. Panel C shows the enrichment of the resuspended particles as the percent difference between the particulate and sediment PCB concentration	110
4.5	Log K_{oc} values measured in the Hudson River (data from Butcher et al. 1999) and in the STORM tanks at steady state for resuspension event 1.	114

4.6	The dissolved PCB concentration in Tank A when resuspension event 3 was extended for seven days.	116
4.7	Particulate, dissolved and log K_{oc} values at steady state for resuspension event 1 and 3 in Tank A.	118
4.8	The percentage of PCBs in the dissolved phase at steady state during resuspension event 1 and 3.	120
4.9	The percent difference in Log K_{oc} between the third and first resuspension event for STORM Tank A, B and C.	121
4.10	Log K_{oc} values measured in Tank A, B, and C at steady state for resuspension event 1 and 3.	123
4.11	The percent of PCBs in the labile phase at steady state during resuspension event 1 and 3 for Tank A, B, and C.	126
4.12	The estimated PCB-charcoal partition coefficient and the adjusted Karickhoff partition coefficient bound the measured $K_{oc-STORM}$ values.	128
5.1	Schematic of the sequence of resuspension events conducted in the STORM tanks. The high TSS corresponds to periods when mixing was turned on. The low TSS corresponds to periods when mixing was turned off and the tank sat with only ~ 1 cm of overlying water.	140
5.2	Dissolved PCBs in STORM Tank A during resuspension event 1.	147
5.3	Percent of PCBs in the dissolved phase after two hours of resuspension.	149
5.4	Dissolved and particulate PCB 52 measured in the STORM tanks and the calculated partition coefficient.	150
5.5	The labile rate constant k_l , full rate constant k_{comp} , and re-absorption rate constant k_d for resuspension event 1 in Tanks A, B and C.	151
5.6	The relationship between the labile and re-absorption rate constants and log K_{ow} during the first resuspension event in all three tanks.	152
5.7	The measured PCB concentration in STORM Tank A event 1 (dots) compared to the concentration predicted by the radial diffusion model (solid line) when Karickhoff's partition coefficient is input into the model along with floc radius, porosity, and density.	156

5.8	The measured PCB concentration in STORM Tank A event 1 (dots) compared to the concentration predicted by the radial diffusion model (solid line) when the partition coefficient is held constant at $5 \cdot 10^4 \text{ L Kg}^{-1}$ and the measured floc radius, porosity, and density are input into the model.	157
5.9	The measured PCB concentration in STORM Tank A event 1 (dots) compared to the concentration predicted by the radial diffusion model (solid line) when Karickhoff's partition coefficient is input into the model and particle porosity and radius are allowed to vary.	158
5.10	Dissolved PCB 18 during the course of each resuspension event in the three STORM tanks.	160
5.11	The measured PCB concentration in STORM Tank A event 3 (dots) compared to the concentration predicted by the radial diffusion model (solid line) when the partition coefficient is held constant at $5 \cdot 10^4 \text{ L Kg}^{-1}$ and the measured floc radius, porosity, and density are input into the model.	163
5.12	Dissolved PCB 52 during the first six hours of resuspension compared to the concentration of fine particles in Tank A.	165
5.13	The total PCB concentration on the particles remaining in the water column after 20 hours of settling at the end of resuspension event 1 and 3.	166

Chapter 1: Introduction

1.1 Background

Polychlorinated Biphenyls (PCBs) were once widely used as insulators in electrical products such as transformers and capacitors. They were produced in the United States from the late 1940s until the Toxic Substance Control Act banned their production in 1979. During this time period, the General Electric Corporation (GE) used PCBs at two plants along the upper Hudson River in the manufacturing of electrical capacitors. Estimates indicate that while these two plants were in operation they released between 200,000 and 1.3 million tons of PCBs into the Hudson River (USEPA 2001). There are 209 possible PCB compounds or congeners, each with a different number or pattern of chlorine atoms bonded to the biphenyl structure. The mixture used at the General Electric plants, known as Aroclor 1242, contained primarily tri and tetra chlorinated PCBs. These PCBs were in an oily liquid form and readily bind to sediments and soils when released into the environment.

The upper Hudson River runs 40 miles from Hudson Falls, NY to the Federal Dam in Troy, NY. This stretch of the river is surrounded by farmland and recreational use of the river is an important part of local residents' lifestyle. In 1984, all fishing in this area was banned because of high PCB concentrations in fish. This ban has since been replaced by a catch and release policy, but fish consumption is still prohibited (NYS DH, 1998). PCBs released from the two GE plants concentrated in an area just south of the plants known as the Thompson Island Pool (TIP, Figure 1.1). The PCB concentration of the sediment in this area is as high as 100 ug g^{-1} . PCB release over the dam transports

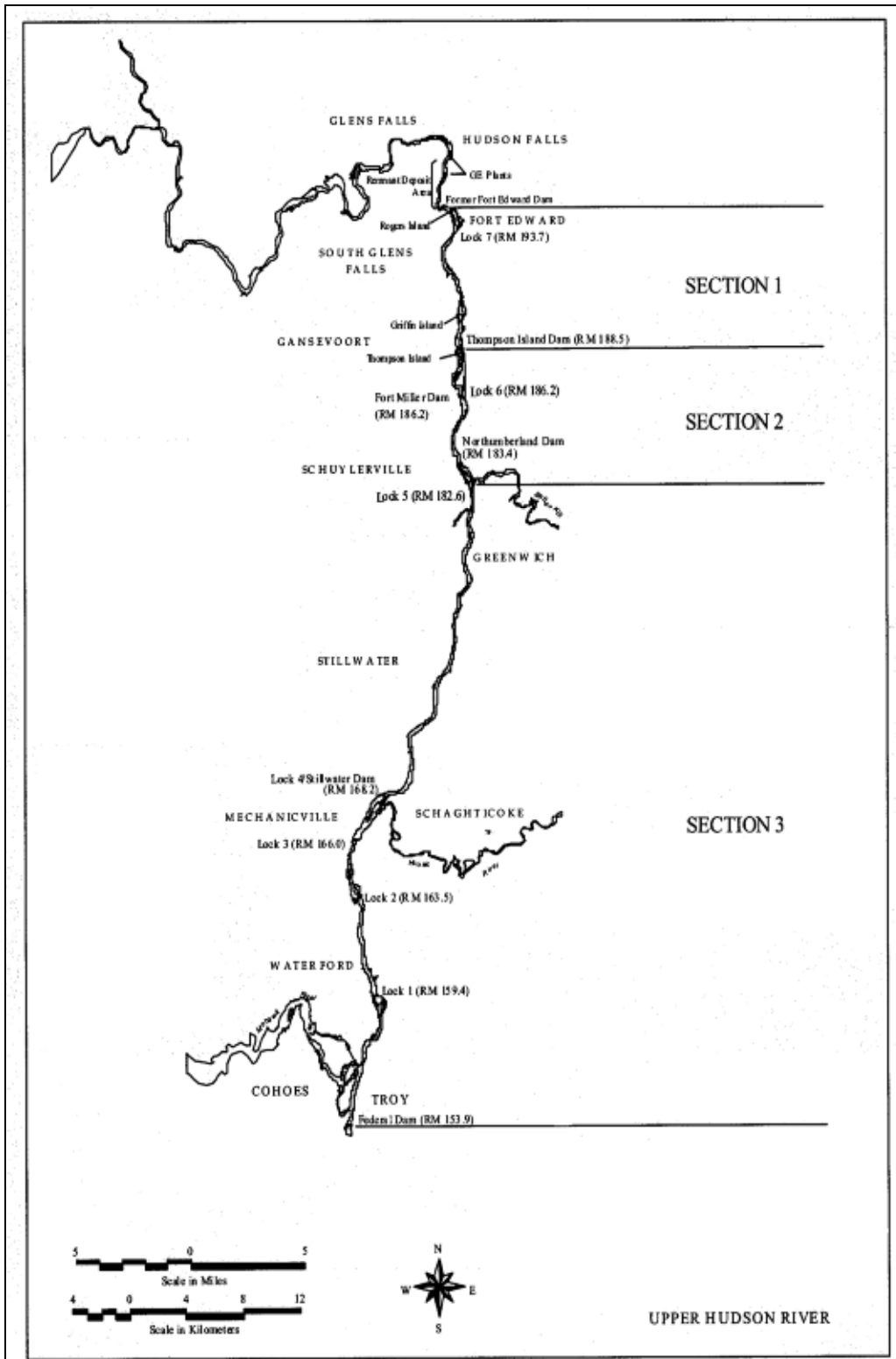


Figure 1.1. Map of the Upper Hudson River (from Baker et al. 2001).

contaminants as far down river as New York City. The entire 200-mile stretch of the river from Hudson Falls to the Battery in New York City was declared a “Superfund” site in 1984 due to severe PCB contamination. It is among the largest Superfund sites in the country (USEPA, 2000).

The river’s sediment is the largest reservoir of the PCBs in the system and the primary source of PCBs to the water column (Thomann et al. 1991). A mass balance analysis based on the total PCB concentration (dissolved + particulate) of water flowing into and out of the TIP highlights the contribution of the sediment to the PCB burden in the water column. Water flowing from Fort Edward transports approximately 30 kg PCBs year⁻¹ into the TIP, water flowing out of the TIP transports 180 kg PCBs year⁻¹ down river suggesting 150 kg PCBs year⁻¹ are released from the sediment in TIP (Baker et al., 2001). PCBs can be remobilized from the sediment back into the water column by diffusion or resuspension. Only PCBs that are dissolved, desorb, or are associated with colloidal particles can exchange from the bedded sediment to the water column by diffusion. Since most of the PCBs in the sediment are bound to non diffusing particles, resuspension and subsequent desorption impacts the dissolved PCB concentration more than diffusion from bed sediment. Resuspension of surficial sediments occurs naturally during high river flows. Mass balance calculations indicate these events are adding large amounts of PCBs to the Hudson River (Baker et al., 2001).

The clean up of PCB contaminated sites such as the Hudson River focuses on minimizing the concentration of PCBs in fish. This emphasis is based on the mission of the Environmental Protection Agency (EPA) to protect human health. The primary risk to humans from PCB contaminated waters is through the consumption of contaminated

fish (USEPA, 2000). When humans consume fish from the Hudson River they ingest PCBs, which are considered a probable human carcinogen. PCBs bioaccumulate or increase in concentration as trophic level increases. Aquatic organisms accumulate contaminants from both their food and the surrounding water. For example, fish obtain their PCB burden from their prey and from diffusion of PCBs into their system from the dissolved phase as water passes over their gills. In order to reduce the concentration of PCBs in fish, the PCB concentration of the lower trophic organisms (their prey) needs to be reduced and dissolved PCBs should be lowered (USEPA, 2000). Ultimately this means the concentration of PCBs in the river needs to be reduced.

To accomplish this goal, the EPA recommends dredging nearly 40 miles of the Upper Hudson River to remove contaminated sediment and decrease the amount of PCBs in the system (USEPA, 2000). One of General Electric's criticisms of the EPA's plan to dredge the Hudson River is that it might "resuspended PCBs, increasing PCB levels in fish in the rest of the Upper Hudson" (GE, 2001). In contrast, the EPA estimates that current dredging technology can minimize the release of PCBs and any increases in fish PCB burdens as a result of dredging will only be temporary. One of the reasons dredging is the EPA's preferred remedy is because it thought to be the fastest way to reduce PCB concentrations in fish (USEPA, 2000).

1.2 PCB Desorption

The release of PCBs to the dissolved phase during resuspension events is typically modeled by incorporating resuspension rates generated in sediment transport models into PCB fate models. Connolly *et al.* (2000) modeled PCB transport in the Upper Hudson

River by linking sub-models for hydrodynamics, sediment transport, PCB fate and PCB bioaccumulation. The sediment transport model predicted resuspension rates for cohesive and non-cohesive sediments that were incorporated into a PCB fate model. The flux of PCBs from the sediment during resuspension events was calculated by coupling the resuspension rates with the surficial sediment PCB concentrations. The PCB fate model assumed the resuspended particles had the same PCB concentrations as the surficial sediment and that the resuspended particles instantly equilibrated with the dissolved phase. These two assumptions are commonly made in PCB fate models and play an integral role in evaluating the impact of remediation plans.

Karickhoff et al. (1979) observed that the partitioning of hydrophobic organic contaminants (HOCs) to a variety of sediment types depended on the octanol water partitioning (K_{ow}) coefficient of the hydrophobic organic contaminant (HOC) and the fraction of organic carbon present in the sediment. They developed an equation to predict the equilibrium-partition coefficient based on these two parameters and formulated a new parameter, the organic carbon normalized partition coefficient (K_{oc}). Field measurements, however, have only found weak correlations between measured partition coefficients, suspended solids organic carbon content, and K_{ow} . Additionally, there is wide scattering in field measurements of K_{oc} and for a single congener the measured K_{oc} value often varies by over an order of magnitude at a given site (e.g. Baker et al. 1991, Gobas et al. 2003, Sobeck et al. 2004). In the Hudson River, the deviation from Karickhoff's prediction is especially pronounced for the low molecular weight congeners (Figure 1.2 data from Butcher et al., 1998). Explanations for these

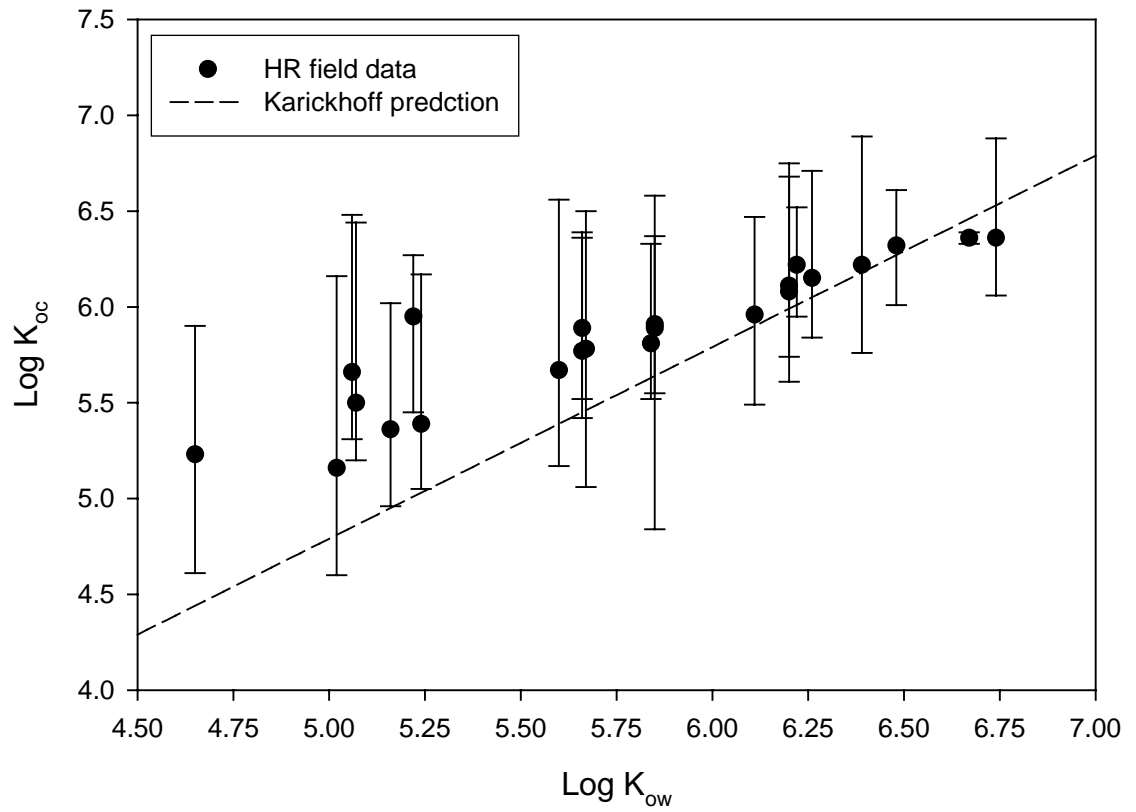


Figure 1.2. Organic carbon normalized partition coefficients of various PCB congeners measured in the Hudson River compared to the values predicted by Karickhoff (data from Butcher et al. 1998).

observations fall into three categories: colloidal interference, non-equilibrium, or the presence of a super sorbent.

In the colloid theory, the inclusion of colloids in the dissolved phase measurement biases the calculation of the partition coefficient. For example, Butcher et al. (1998) theorized that DOC bound PCBs in the Hudson River accounted for a significant fraction of the measured dissolved concentration of high molecular weight PCBs. They suggest that the truly dissolved concentration was lower than measured by XAD extraction. In this case correcting for DOC would actually enhance the observed deviation from Karickhoff's prediction. However, the slope of the relationship would be similar to the slope predicted by Karickhoff. The non-equilibrium theory attributes the natural variability in partition coefficients to the amount of time the particles were resuspended in the water column. Valsaraj and Thibodeaux (1999) re-analyzed field data from a variety of studies and showed the variation in K_{oc} could be caused by differences in the amount of time the particles had been suspended in the water column. As with the colloidal theory, correcting for this effect would enhance the observed deviation more for the high K_{ow} congeners since they equilibrate more slowly. In the super sorbent theory black carbon absorbs PCBs more strongly than organic carbon. Natural suspensions of particles are heterogeneous mixtures containing both organic and black carbon. Partition coefficients measured in the field reflect partitioning to all forms of carbon. The presence of even small concentrations of black carbon greatly increases the binding of PCBs to particles. As a result, this phenomenon could explain why field measurements are higher than predicted by Karickhoff. It is possible that a combination of these theories may apply in the field.

A large body of literature shows that desorption of hydrophobic organic contaminants from suspended sediment is slow relative to the time scales of sediment transport and resuspension events (e.g., Wu and Gschwend, 1986; Jespen and Lick, 1996). During resuspension events, sediment particles are not in the water column long enough for the particulate PCB concentration to reach equilibrium with dissolved phase. For example, Jespen and Lick (1996) conducted batch mixing experiments with sediment and water spiked with carbon-14 labeled 4, 4' dichlorobiphenyl (DCB). Equilibrium between the dissolved and particulate phase of DCB was achieved only after five to 15 days. Higher molecular weight congeners, such as the hexachlorobiphenyls, took up to 30 days to reach equilibrium (Jespen and Lick, 1996). Resuspension events typically last on the order of hours to a few days, significantly shorter than the time needed to reach equilibrium.

Cheng *et al.* (1995) compared the time scale to reach equilibrium (t_e) to the resuspension time scale (t_r) for particles in the Buffalo River. The magnitude of t_e depended on the properties of the sediment, such as radius and porosity, whereas the magnitude for t_r depended on the flow conditions and density of the particle aggregates. The authors estimated the resuspension time scale using four different scenarios. The first two scenarios assumed that the particles settled according to Stokes Law. The second two scenarios assumed turbulence also influenced the particle settling velocity. Under all four conditions $t_r \ll t_e$ and equilibrium assumptions were not valid. The dynamics of the system governed the amount of PCB desorbing from the particles.

1.3 Desorption Rate Models

Numerous studies demonstrate that PCB desorption from sediment and soil can be modeled as a two-stage process; the first ('labile') is rapid and the second ('resistant') is slow. For example, Carroll et al (1994) observed this two-stage desorption of PCBs from Hudson River sediment. A rapid (labile) fraction was defined as that which desorbed in 24 hours and a resistant (slowly) desorbing fraction was identified and shown to require over one year to fully desorb. Girvien et al. (1997) examined PCB desorption from contaminated soils and found that a labile fraction could be defined as that which desorbed in 48 hours whereas the remaining resistant fraction continued to desorb for the entire six month duration of the study. Cornelissen et al. (1997) suggested that PCB desorption might be more effectively modeled as a three stage process, the first rapid labile phase was defined as the portion lasting ~ 10 hours, the second slow resistant phase was defined to lasts weeks, and a third very slow or very resistant phase continued to desorb for months.

The exact mechanisms underlying the multiple stage desorption process are not known. One model to describe the observed biphasic desorption is the radial diffusion model described by Wu and Gschwend (1986, 1988). In this model sediment particles are considered homogeneous spheres with uniform tortuosity and porosity and diffusion is assumed to occur only in the aqueous phase. The rate of aqueous diffusion of the sorbate within the particle, or the effective diffusivity, limits the amount of desorption. The effective diffusivity of the sorbate within the particle is described by the following equation where ϕ is the porosity of the aggregate, D_m is the molecular diffusivity in water (cm^2s^{-1}), ρ_s is the dry density (g cm^{-3}), and K_p is the partition coefficient (cm^3g^{-1}).

$$D_{eff} = \frac{D_m \phi^2}{(1 - \phi) \rho_s K_p + \phi} \quad (1)$$

In the above equation the numerator represents the reduction in molecular diffusion due to the tortuosity of the particle and the denominator reflects the retardation of diffusion due to local microscale partitioning. Larger particles approach equilibrium more slowly than smaller particles because they have longer diffusion path lengths. Resuspensions contain heterogeneous mixtures of particle sizes and the observed multi-staged aggregate diffusion is modeled as the sum of diffusion from different sized particles (e.g. Wu and Gschwend 1988, Ball and Roberts 1991, and Kleineidam et al. 2004). Such diffusion models are inherently non-linear due to the fact that the rate of diffusion scales to the size of the particle.

Organic matter diffusion (OMD) models or permeant/polymer diffusion models are an alternative to the radial diffusion model for describing the sorption of HOCs onto particles (see review by Pignatello and Xing, 1996). These models consider organic matter to be a polymer and diffusion through different phases of the polymer accounts for the observed two stages of desorption. The first rapid phase of desorption represents diffusion through the open rubbery form of the organic matter and the second slower phase represents diffusion through the glassy and condensed form of the organic matter. Carroll *et al.* (1994) modeled HOC desorption from Hudson River sediment using a permeant/polymer diffusion model and literature data describing the diffusion of 4-chlorobiphenyl in glassy polystyrene to represent diffusion in the rubbery open phase of the organic matter. The diffusion coefficient in the glassy condensed phase was then calculated based on the coefficient in the glassy phase. Variations in natural organic matter make choosing a polymer to model organic matter difficult and limit the

widespread applicability of this approach. Additionally, diffusion kinetics in polymers is highly variable and depends on a range of factors including polymer structure and particle size distribution (Pignatello and Xing, 1996).

Both the radial diffusion model and permeant/polymer diffusion model describe the two-phased sorption of HOCs onto particles. Unfortunately both models require detailed knowledge about specific particle properties that are not easily measured. Several other kinetic models of the desorption process have also been proposed including first order (ten Hulscher et al. 1999), multiple first-order (e.g. Cornelisen et al. 1997), and one compartment models (e.g. Karickhoff and Morrison 1985). These models do not have mechanistic underpinnings for desorption and rate constants are estimated by fitting the models to the data.

There are several methods to model the first labile phase of desorption as a first order kinetic process and the diffusion coefficient in the Wu and Gschwend model is correlated to the first order rate constant according to the equation below (Wu and Gschwend, 1988)

$$k = \alpha(D_{\text{eff}}/r^2) \quad (2)$$

where k is the first order kinetic coefficient (s^{-1}), D_{eff} is an apparent diffusion coefficient ($\text{cm}^2 \text{s}^{-1}$), r is the particle radius (cm), and α is a correction factor that depends on K_p and ρ_s . This modified first order model matches the radial diffusion model at $t_{1/2}$ because k is set according to this criterion. The deviation of the kinetic model from the radial diffusion model increases with $K_p\rho_s$. While this model does not fit experimental data as well as the radial diffusion model, kinetic models similar to this one accurately predict

desorption during the first rapid phase of the process (Pignatello *et al.* 1993; Pedit and Miller, 1994).

Estimates of the labile rate constants vary widely and range from 0.0003 to 0.2 hours⁻¹ (Table 1.1) depending on the type of sediment examined, the model used to estimate the rate constant, and the molecular weight of the PCB. The percent of PCBs in the labile pool also varies considerably. For example, Cornelissen *et al.* (1997) spiked sediment with PCBs and found between 70-85% were in the labile pool when the sediment was only allowed to equilibrate for 2 days before desorption experiments were initiated. When the equilibration time increased to 37 days, 33-52% of the PCBs were in the labile pool. Carroll *et al.* (1994) found that between 55-76% of the PCBs in Hudson River sediment were in the labile fraction. Resistant rate constants are estimated to be two to three orders of magnitude less than the labile rate constants (Ghosh *et al.* 1999, Cornelissen *et al.* 1997). Since resuspension events typically last on the order of hours to days and it is unlikely particles in rivers are suspended into the water column long enough for the resistant fraction to desorb.

It is unclear whether the labile pool is replenished from the resistant pool as sediments sit unmixed on the river bottom. If PCBs rapidly migrate from the resistant pool to the labile pool, then every time a particle is lifted from the sediment bed it will undergo the first rapid labile stage of the desorption process. On the other hand, if PCBs diffuse slowly into the labile pool, desorption during resuspension events will largely be a result of the second slower resistant stage of the desorption curve. Spectroscopic investigations of the binding of 1,2 dichloroethane (DCA) to humic and fulvic acids by Aochi and Farmer (1997) showed two different sorbed species. The first species was

Sediment	PCB congener	k labile (hours ⁻¹)	Source
Rhine River	PCB 28	0.20	Ten Hulscher et al. 2002
Hudson River	tPCBs	0.008	Carroll et al. 1994
Hudson River	PCB 18	0.008	Lamoureux and Brownawell 1999
	PCB 49	0.037	
	PCB 52	0.044	
	PCB 101	0.032	
Laboratory contaminated for 2 days	PCB 65	0.058	Cornelissen et al. 1997
	PCB 118	0.045	
Laboratory contaminated for 34 days	PCB 65	0.12	Cornelissen et al. 1997
	PCB 118	0.11	
Laboratory contaminated for 110 days	¹⁴ C TCBP	0.05-0.17	Kukkonen et al. 2003
Laboratory contaminated for 60 days	¹⁴ C HCBP	0.03-0.16	Kukkonen et al. 2003
Laboratory contaminated for 2 days	¹⁴ C TCBP	0.08-0.15	Leppanen et al. 2003
Alcoa sediment at 25°C	di-chlorinated PCBs	0.11	Ghosh et al. 1999
	tri-chlorinated PCBs	0.04	
	tetra-chlorinated PCBs	0.02	
	tetra-chlorinated PCBs	0.01	
Soils from utility industry stations	PCB 18	0.004-0.06	Girvin et al. 1997
	PCB 28	0.001-0.05	
	PCB 33	0.003-0.08	
	PCB 40	0.002-0.06	
	PCB 42	0.002-0.05	
	PCB 44	0.002-0.06	
	PCB 49	0.002-0.06	
	PCB 52	0.002-0.05	
	PCB 66	0.001-0.05	
	PCB 70	0.0005-0.05	
	PCB 87	0.0002-0.02	
	PCB 97	0.0002-0.01	
	PCB 101	0.0003-0.03	

Table 1.1 Labile rate constants for PCB desorption.

labile and sorbed to the organic matter within 30 minutes. The second species was detected only after several hours of sorption and increased in intensity throughout the experiment. Results from this experiment suggest chemicals may rapidly diffuse into and out of the labile portion of the particles during resuspension and settling; however, PCBs are much larger molecules than DCA.

1.4 Impact of Shear Stress and Turbulence

The surfaces of cohesive particles are charged and electrostatic interactions as well as Van der Waals forces cause the particles to attract each other. As a result, in the water column cohesive sediment particles do not behave as individual grains but instead interact and form flocs. Flocculation changes the porosity and density of the resuspended particles and, as predicted by the radial diffusion model, it might also change the rate of PCB desorption. Fluid shear stress, Brownian motion, total suspended solids concentration, salinity, and differential settling are the critical factors affecting floc formation and breakup (Burban et al., 1990; Manning and Dyer, 1999; Tsai et al., 1987). The common approach to study PCB desorption involves vigorously shaking or mixing sediment water slurries. This mixing at high solids concentrations results in the rapid formation of small dense particles and prevents an evaluation of the impact of floc formation on the rate of PCB desorption.

Lick and colleagues conducted a series of experiments to evaluate the impact of flocculation on the sorption process using sediment collected from the Detroit River (Borglin *et al.* 1996; Lick and Rapaka, 1996; Tye *et al.* 1996; Jespen and Lick, 1996; Jespen *et al.* 1995). These studies found that the higher the initial suspended sediment

concentration, the longer the dissolved and particulate phase of hexachlorobenzene (HCB) and several PCBs took to reach equilibrium. Floc formation significantly impacted this result (Table 1.2). At a total suspended solids (TSS) concentration of 10 mg L⁻¹, floc formation and sorptive equilibrium both reached steady state in approximately 60 hours. At this suspended solids concentration the flocs were light and watery with a density of 1.008 g cm⁻³ and a porosity of 0.995. As the suspended sediment concentration increased, flocs formed more quickly and sorptive equilibrium was reached more slowly. At a TSS concentration of 500 mg L⁻¹ steady state floc formation was reached in 4.5 hours but sorptive equilibrium wasn't reached for 480 hours. At this TSS concentration the bulk density of the flocs was 1.41 g cm⁻² and the porosity of the flocs was 0.74 (Tye et al. 1996). Most laboratory studies examining the rate of PCB desorption were conducted at high total suspended solids concentrations and it is likely the rate of desorption would be faster at lower suspended solids concentrations.

In addition to flocculation, the amount of sediment resuspended also impacts the rate of PCB desorption. Sediment resuspension or erosion occurs when the bottom shear stress exceeds the critical shear stress required to lift a particle off of the bed. The critical shear stress required to initiate resuspension determines the amount of sediment resuspended and depends on the properties of the sediment bed and. For example, in Baltimore Harbor, the critical shear stress for resuspension is 0.5 dynes cm⁻² when a bottom floc layer is present and 1 dyne cm⁻² for consolidated beds (Maa et al., 1998). It is difficult to realistically resuspended sediment in the laboratory and simultaneously measure PCBs. As a result, only a few studies have attempted to simulate the bottom shear stress typically encountered in a river.

Concentration (mg L ⁻¹)	Time to Steady State Floc Formation (hours)	Time to Sorptive Equilibrium (hours)	Implications
2	228	24	T _{floc formation} >> T _{sorptive equilibrium}
10	63	60	T _{floc formation} ≈ T _{sorptive equilibrium}
100	8.5	288	T _{floc formation} << T _{sorptive equilibrium}
500	4.5	480	T _{floc formation} << T _{sorptive equilibrium}
2,000	2.5	520	T _{floc formation} << T _{sorptive equilibrium}
10,000	1.2	840	T _{floc formation} << T _{sorptive equilibrium}

Table 1.2. The impact of floc formation on the time to hexachlorobenze sorptive equilibrium (data from Tye et al. 1996).

Latimer et al. (1999) used a particle entrainment simulator (PES) to resuspend sediment at regulated shear stresses. The PES created shear stress by oscillating a grid in the water column over a sediment core. This movement produced realistic bottom shear stresses but the water column turbulence was unrealistically high. The authors measured particulate PCBs but not dissolved PCBs due to water volume limitations. This study found that at a bottom shear stress of 2 dynes cm^{-2} , the resuspended particles were enriched in PCBs and organic carbon relative to the bulk sediment. As shear stress was increased, both the organic carbon content and PCB concentration of the resuspended particles decreased. At a shear stress of 5 dynes cm^{-2} , the PCB concentration of the resuspended material was the same as the bulk sediment. Alkhatib and Weigand (2002) used a PES to examine the release of PCBs from sediment spiked with PCBs in the laboratory. This study also found that the mass of PCBs resuspended at 2 dynes cm^{-2} was greater than the bulk sediment PCB concentration. These studies suggest that models assuming the PCB concentration of particles resuspended at low shear stress is equal to the sediment concentration will underestimate PCB release into the dissolved phase.

In rivers, bottom shear stress and water column turbulence are closely linked. Together these two parameters determine the amount of sediment resuspended and the properties of the resuspended flocs. Previous studies show that both phenomena reach steady state on similar time scales (Lick et al., 1995; Maa et al., 1998). However, the apparatus used to study resuspension and flocculation did not generate realistic levels of water column turbulence and bottom shear stress simultaneously. As a result, laboratory studies often examine these two processes separately. In the flocculation studies conducted by Lick and colleagues, suspended solids were added to an apparatus that

could apply shear to the water column. The sediment could not be lifted off the bed in these studies. The studies examining the impact of shear stress on PCB resuspension did not accurately simulate water column turbulence levels (Latimer et al. 1999, Alkhatib and Weigand 2002). In order to realistically conduct resuspension studies and examine PCB desorption under natural conditions, several key variables need to be reproduced including turbulence intensity, energy dissipation, bottom shear velocity and mean flow speed (Sanford, 1997).

The amount of PCBs released from the sediment during resuspension events depends on the amount of sediment resuspended, the residence time of the particles in the water column, and the rate of desorption. Both the physical mixing of the water column and the chemical properties of the HOCs and sediment influence these variables. For example, water column turbulence and bottom shear stress govern the residence time of particles in the water column. The percent of organic matter on the particle, the size of the resuspended particle, and the molecular weight of the PCB play a key role in determining the rate at which PCBs are released from particles. Previous desorption experiments were conducted under unrealistic environmental conditions and the physical process of resuspension was not accurately reproduced. Multiple factors need to be considered in order to calculate the amount of PCBs lost from the sediment during resuspension events.

Achman *et al.* (1996) used field data to estimate PCB fluxes in the lower Hudson River estuary. The desorption rate of PCBs from resuspended particles was calculated using a first order model that was interpreted in terms of radial diffusion based on the approximation suggested by Wu and Gschwend (1988). The initial particle concentration

was set equal to the sediment concentration and they assumed a closed system in which the sediment was resuspended into water containing an initial dissolved load of PCBs equal to the concentration in the bottom water. They found there could be a significant release of PCBs into the dissolved phase during resuspension events. Chang and Sanford (2005) coupled a physical model to a biogeochemical model to explore the influence of hydrodynamic forcing factors, such as tidal current and shear velocity, on pyrene cycling. In this model, pyrene was input into a clean system with uncontaminated sediment. Model simulations suggest that tidally resuspending sediment increased dissolved pyrene concentrations in the water column by up to 22%. Understanding the release of PCBs during resuspension events is critical for assessing remediation plans and evaluating their impact on dissolved concentrations.

1.5 Objectives

The primary objective of this thesis is to determine the release of PCBs from river sediment when it is resuspended under realistic bottom shear stress and water column turbulence. Specific objectives addressed in each chapter include:

- (1) Develop an in-situ method to rapidly measure dissolved PCBs in natural system without removing water or disturbing dissolved-particle distributions.
- (2) Characterize the properties (porosity, density, median diameter, and settling velocity) of particles resuspended under realistic levels of constant bottom shear stress and water column turbulence.
- (3) Examine how the size distribution of resuspended particles evolves over time during a resuspension event and assess the effects of both sediment consolidation

time and quiescent time between resuspension events on the properties of the resuspended particles.

- (4) Measure PCB partitioning at realistic levels of constant bottom shear stress and water column turbulence.
- (5) Examine the impact of particle reworking on PCB partitioning by allowing the sediment to sit on the bottom for various lengths of time to recharge the labile pool from the resistant pool.
- (6) Measure the rate of PCB release from resuspended sediment under constant shear stress and turbulence.
- (7) Determine the dependence of the desorption rate on the properties of the PCBs and the resuspended particles, and the frequency and duration of resuspension events.

1.6. Strategy

To accomplish these objectives a method was first developed to measure dissolved PCBs in natural waters on 30-minute time frames using non-equilibrium solid phase microextraction (SPME). SPME fibers were made from optical cable, inserted into a glass tube, and attached to the shaft of a motor that revolved at 130 rpm. This sampling device enabled the SPME fiber to revolve in the water as it was being sampled in order to minimize the thickness of the unstirred water layer. The fibers could easily be removed from this device for essentially continuous sampling of dissolved phase PCB concentrations. This technique enabled the measurement of dissolved PCBs without removing water from the mesocosms. In Chapter 2 of this thesis I discuss the details of

this method and compare dissolved PCB measurements made by this technique to the more traditional XAD extraction method. This paper is currently being prepared for publication and will be co-authored by Alessandra Paolicchi, an REU summer student that worked in our laboratory, and Professor Joel Baker.

Resuspension experiments were conducted in three outdoor Shear Turbulence Resuspension Mesocosm (STORM) tanks described previously in Porter et al. (2005 and 2004). In each STORM tank a paddle rotated just above the bottom around a central shaft, resuspending sediment without generating excessive water column turbulence. The tanks sit in series with the motor driving the paddles at one end (Porter et al., 2005). The sediment surface area in the STORM tanks was 1m^2 and the water column was 1 m deep with a total water volume of 1000 L (Porter et al., 2005). Sediment was collected from the upper Hudson River near Griffin Island ($43^\circ 12.246' \text{ N}$, $70^\circ 34.891' \text{ W}$, river mile 189.75), homogenized in a cement mixer, added to the STORM tank to a depth of 5 cm. The tanks were slowly filled with clean well water just prior to the start of resuspension with minimal disturbance to the sediment surface. Unlike in previous experiments using the STORM tanks that simulated tidal cycle resuspension (Kim et al., 2004), every resuspension event lasted three days. Mixing began in the morning of the first day and continued at a constant level for the entire three-day period. The bottom shear maintained the TSS concentration in the water column at a constant level. At the end of each three-day resuspension event, mixing was turned off and the particles were allowed to settle through a still water column for approximately 20 hours. Following settling, the water was pumped out of the tank and the sediment sat undisturbed on the bottom for 1, 2

or 4 days in Tank A, B, and C respectively (Figure 1.3). This process was repeated three times in each tank.

The STORM tanks were sampled most intensively on the first day of each three-day resuspension event. During the first two hours of resuspension, samples were collected every half hour. After the first two hours, samples were collected once an hour for four hours. On the second and third day of each resuspension event the tanks were sampled twice daily, once in the morning and once in the afternoon. At each sampling time point SPME measured the dissolved PCBs for 30 minutes. Mid-way through the SPME sampling period, water was collected from mid depth (0.5 meters above bottom) through a siphon (flow rate $\approx 3000 \text{ mL min}^{-1}$) for particulate PCBs, total suspended solids (TSS), particulate carbon and nitrogen (CHN), chlorophyll *a* and pheopigments, and dissolved organic carbon (DOC) analysis. In addition, at each sampling time point a LISST-100C (Sequoia Scientific, Inc.) was deployed at mid depth (0.5 mab) for 5 minutes to measure the volume concentration of particles.

Chapter 3 of this thesis discusses the properties of the resuspended particles, presents the LISST results, and examines the settling experiments conducted in the STORM tanks. This chapter is being prepared for publication and will be co-authored by Dr. Elka Porter at the University of Maryland, Chesapeake Biological Laboratory, Professor Lawrence Sanford at the University of Maryland, Horn Point Laboratory, and Professor Joel Baker. Chapter 4 discusses the steady state results in the STORM tanks. The apparent PCB partition coefficients are presented and the impact of quiescent time on PCB partitioning at steady state is assessed. This chapter is currently being prepared for publication and will be co-authored by Dr. Joel Baker. Chapter 5 discusses

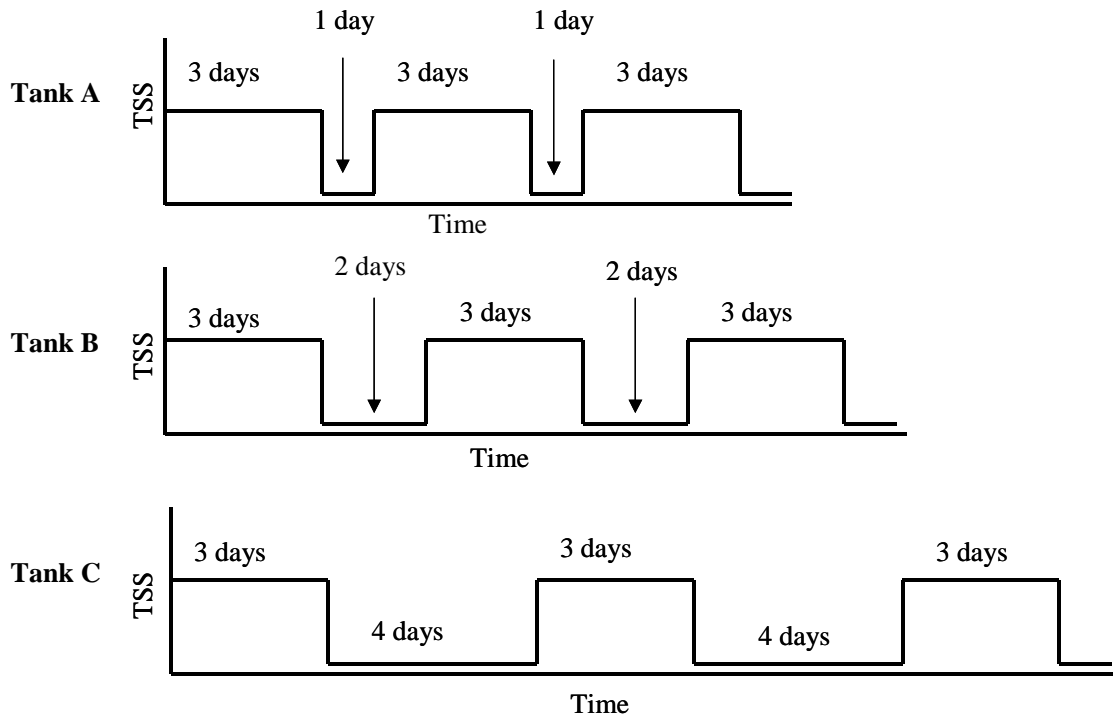


Figure 1.3. Schematic of the sequence of resuspension events conducted in the STORM tanks. The high TSS corresponds to periods when mixing was turned on. The low TSS corresponds to periods when mixing was turned off and the tanks sat with only 1 cm of overlying water.

the initial release of PCBs during the first day of each resuspension event. PCB desorption rates are calculated and the impact of short term resuspension events on dissolved PCB concentrations is evaluated. The chapter is also being prepared for publication and will be co-authored by Dr. Joel Baker.

1.7 Executive Summary

1.7.1 Chapter 2

Pawliszyn and colleagues (1990) first developed the principles of solid phase microextraction (SPME) in 1990 to allow more rapid measurements of dissolved organic chemicals. SPME is an analytic technique in which a fused silica rod coated with a polymer such as polydimethylsiloxane (PDMS) is exposed to the aqueous environment. Dissolved PCBs diffuse from the water into the polymer coating and the fiber is then directly injected into the gas chromatograph (GC) for analysis. The rate of diffusion into the SPME fiber depends on the thickness of the polymer coating, the diffusion coefficient of the analyte in water, and the thickness of the boundary layer or unstirred water layer (UWL) between the SPME fiber and the water. The rate limiting step in this process is diffusion through the UWL surrounding the SPME fiber (Meyer et al. 2003). Agitating or stirring the water sample limits the thickness of this layer. Various agitation methods, such as a magnetic stirring, vortex mixing, and sonication have been used to minimize the thickness of the UWL and each has its own advantages and disadvantages (Pawliszyn 1999, Zygmunt et al. 2001). None of these techniques can be employed in the field to collect in-situ SPME measurements.

This chapter presents a method using non-equilibrium SPME to measure dissolved PCBs in natural waters on 30-minute time frames. Calibration curves relating the dissolved PCB concentration to the mass measured on the SPME fiber were developed, detection limits ranged from 0.6 to 5.2 ng L⁻¹, and the relative standard deviation between replicate samples ranged from 3-20%. To test for matrix interferences, revolving SPME fibers were deployed in three solutions with different matrices. The dissolved PCB concentration in each solution was maintained by equilibration with air contaminated with PCBs. Dissolved PCB measurements made in the presence of 8 mg L⁻¹ of DOC and 200 mg L⁻¹ of suspended solids were not significantly different from measurements made in deionized water, demonstrating that neither suspended particles nor natural organic matter interferes with SPME measurements of dissolved PCBs. PCB concentrations measured by traditional XAD extraction were slightly greater than SPME measurements illustrating the impact of dissolved organic carbon on XAD measurements.

1.7.2 Chapter 3

It is difficult to realistically resuspended sediment in the laboratory and only a handful of studies have attempted to simulate the bottom shear stress or water column turbulence levels typically encountered in a river. Mimicking both water column mixing and benthic boundary-layer flow the STORM tanks simulate resuspension and settling conditions more realistically than previous apparatus used to study these processes (Porter et al., 2004; Porter et al., 2005). Results from the LISST data show that immediately following the initiation of resuspension large particles with an average median diameter of $140 \pm 14 \mu\text{m}$ were lifted into water column. As resuspension time progressed the volume median diameter of the resuspended particles decreased and flocs

disaggregated. At steady state the flocs average volume median diameter was 112 ± 3 μm , the porosity was 0.90 ± 0.02 , and the bulk density was 1.13 ± 0.02 g cm^{-3} . Varying the quiescent time between resuspension events did not change the steady state properties of the flocs. However, increasing the quiescence time between resuspension events initially produced less porous flocs. The particles that were initially resuspended after two or four days of quiescence between resuspension events had an average porosity of 0.86 ± 0.02 compared to an average porosity of 0.92 ± 0.01 in the tank with one day of quiescence.

After mixing was stopped there was a clear change in the composition of the particles remaining in the water column. During the first three minutes of settling large flocs and detritus remained in the water column and the total volume concentration of particles remained constant while the TSS concentration decreased. After 20 minutes of settling, the large organic detritus settled through the water column and both the TSS concentration and the total volume concentration decreased. Several methods of calculating the rapid settling velocity during the first 20 minute after mixing stopped suggests the particles settled at a rate of 0.10 ± 0.02 cm s^{-1} . After 60 minutes of settling, 30% of the particles by mass and 20% of the particles by volume still remained in the water column. Even after 20 hours without mixing, this material did not fully settle out of the water column.

1.7.3 Chapter 4

The STORM tanks ability to easily start and stop resuspension events allowed the exploration of the movement of PCBs between a labile and more resistant pool. In this experiment, increasing quiescent time between resuspension events increased the

resistant to labile pool recharge time. Steady state PCB partitioning occurred on the same time scale as floc disaggregation and was reached by the start of the second day of resuspension. The PCB concentration of the resuspended particles was two times greater than the bulk sediment concentration. The log K_{oc} values measured at steady state in the STORM tanks were similar to values measured in the Hudson River indicating these mesocosm experiments successfully mimicked field conditions. Measured steady state K_{oc} values did not systematically vary with the octanol water partition coefficient and K_{oc} values for the lower molecular weight PCBs were higher than predicted by Karickhoff et al. (1979) and other models that predict K_{oc} based on K_{ow} .

In all three tanks, the steady state log K_{oc} values for the third resuspension were higher than the log K_{oc} values for the first resuspension event. However, there was much less of a difference in the K_{oc} values in Tank C, the tank with four-days quiescence, as compared to the tanks with one and two days quiescence. These changes in K_{oc} were driven by changes in the dissolved PCB concentration. The particulate PCB concentration was relatively constant between events. In Tank A the percent of PCBs in the dissolved phase decreased an average of 8% from event 1 to event 3 but in Tank C the percentage of di, tri, and tetra-chlorinated dissolved PCBs remained constant between events. Only the penta-chlorinated PCBs decreased significantly from event 1 to event 3 in Tank C. This analysis suggests there was a large release of PCBs from particles when they were initially resuspended. However, chronic resuspension resulted in less PCB release per event due to the slow recharge of the labile pool. For the low molecular weight congeners ($\log K_{ow} < 5.85$) the labile pool recharged after approximately three to

four days of quiescence. For the penta-chlorinated congeners the recharge rate was slower and four days of quiescence was insufficient to replenish the labile pool.

1.7.4 Chapter 5

This study examined the initial release of PCBs from the resuspended sediment before the steady state dissolved concentration was reached. After two hours of resuspension event 1 all three tanks had an average of $22 \pm 3\%$ of resuspended PCBs in the dissolved phase. After six hours of resuspension, $30 \pm 8\%$ of the resuspended PCBs were dissolved. There was no relationship between the percent of dissolved PCBs and PCB molecular weight. In all three tanks, the amount of PCBs released into the dissolved phase decreased with each subsequent resuspension event. After two hours of resuspension an average of $18 \pm 10\%$ of the PCBs were dissolved during event 2 and only $16 \pm 8\%$ of the PCB were in the dissolved in event 3 at this time point.

Assuming the resistant pool was non-desorbing, the one compartment model was used to calculate a labile rate constant, re-absorption rate constant, and full rate constant. During the first resuspension event, the labile rate constant ranged from 0.03 to 0.34 hours⁻¹ and decreased significantly as the log K_{ow} of the PCB congeners increased. The labile rate constant of PCB 4+10, unresolved di-chlorinated congeners, was an average of 4 times greater than the labile rate constant of PCB 110, a penta-chlorinated congener. The labile rate constants calculated from our data are at or just above the upper end of the range reported in the literature. The full one compartment rate constant encompassing re-adsorption and desorption calculated using the entire three day data set of dissolved PCB concentrations ranged from 0.18 to 0.58 hour⁻¹ and was not correlated to the octonal water partition coefficient. The re-absorption rate constant, k_d , calculated by subtracting

the labile rate constant from the full rate constant ranged from 0.02 to 0.48 hour⁻¹ and increased significantly as the log K_{ow} of the PCB congeners increased.

Floc volume median diameter as a function of time along with floc porosity and density were input into the radial diffusion model to evaluate its ability to predict the observed rate of desorption in the STORM tanks. If the partition coefficient varied as a function of K_{ow} , then the radial diffusion model predicted desorption of the di-chlorinated congeners would occur too quickly and desorption of the penta-chlorinated congeners would occur too slowly. On the other hand if the partition coefficient did not vary as a function of K_{ow} , the radial diffusion model accurately predicted desorption in the STORM tanks. One partition coefficient was sufficient to reproduce the observed rate of desorption for all PCB congeners. This result is consistent with the measurements made in the STORM tank and in the field (Butcher et al. 1999) showing that K_p does not vary as a function of K_{ow} .

1.8 Implications

The major implications and findings of this thesis are as follows

1. This study found that the PCB concentration of the resuspended material was an average of two times greater than the bulk sediment PCB concentration. Current models that calculate PCB release based on bulk sediment PCB concentrations will underestimate the amount of PCBs that enter the water column during resuspension events by roughly a factor of two.

2. In this study, a large fraction of the total mass of resuspended particles did not settle out of the water column even after 19 hours without mixing. The PCB concentration of these non-settling particles was 4 times greater than the PCB concentration of the resuspended material and 8 times greater than the bulk sediment PCB concentration. If proper precaution is not taken these light PCB enriched particles could potentially be transported large distances downstream during the dredging of the upper Hudson River.

3. There was a large initial release of PCBs immediately after the sediment was resuspended. This “burp” was not accounted for by release from pore water or the expulsion of interstitial floc water. After just two hours of resuspension an average of $22 \pm 3\%$ of resuspended PCBs were in the dissolved phase. This suggests a significant amount of dissolved PCBs could be added to the Hudson River during dredging or storm events.

4. Recharge of the labile pool does not occur fast enough for replenishment on the time scale of tidal cycle resuspension (~ 6 hours). This study indicates it takes at least three days or more for a labile pool of PCBs to recharge from a more resistant pool. If resuspension events occur infrequently (i.e. storms) the time between events might be long enough to replenish the labile pool and result in a large release of PCB. Conversely, resuspension events that occur frequently (i.e. tidal cycles) might result in less release of PCBs per event.

5. This study found no relationship between PCB partitioning and Log K_{ow} . Both the measured partition coefficients and the partition coefficients derived using the radial diffusion model did not vary over the range of K_{ow} examined in this study. As a result, using a partition coefficient that varies as a function of K_{ow} in the radial diffusion model underestimates the time to initial steady state of the dichlorinated PCB congeners by five hours and overestimates the time to initial steady state of the penta-chlorinated PCB congeners by 115 hours.

6. An analysis of the PCB congeners examined in this study found a greater fraction of the penta-chlorinated PCBs were in the labile pool than lower chlorinated PCB congeners. The labile pool might represent PCBs bound to the surfaces of particles and the resistant pool might represent PCBs bound in the pore spaces of the particles. The larger compounds might be too big to fit into the pore spaces of the particle and were unable to enter the resistant pool. Alternatively, since the penta-chlorinated PCB congeners diffuse more slowly than the lower chlorinated PCB congeners, they might not have been exposed to the particles long enough to enter a more resistant pool.

Chapter 2: The use of solid phase microextraction to rapidly measure dissolved PCBs in natural waters

2.1 Introduction

Despite the fact that hydrophobic organic contaminants (HOCs) in natural waters are primarily bound to particles and colloids, the dissolved phase is the most bioavailable to aquatic organisms and even low dissolved concentrations (i.e. pg L^{-1}) are important (DiToro et al., 1991). Historically, measuring dissolved concentrations of HOCs in natural waters has been time consuming and expensive. Traditional methods involve filtering large volumes of water to remove particles, passing the filtrate through a resin, and then extracting the resin (Bamford et al., 2002; Totten et al., 2001). Small particles and colloids may pass through the filters and be included in the dissolved measurement.

Passive sampling devices (PSDs) were developed as an inexpensive and practical alternative to traditional water sampling methods. For example, semi-permeable membrane devices (SPMDs) are designed to mimic organism exposure by measuring only the dissolved or bioavailable HOCs. SPMDs are made by filling polyethylene tubing with model lipids; only dissolved HOCs can pass through the membrane and partition into the lipid (Huckins et al., 1990). Rates of uptake of HOCs into SPMDs depend on the surface area of the SPMD, the thickness of the boundary layer surrounding the SPMD, and the diffusion coefficient of the HOCs (Huckins et al., 1993). Rantalainen et al. (2000) found that uptake rates for polychlorinated biphenyls (PCBs) into SPMDs range from 50-95 $\text{m}^{-2}\text{-day}^{-1}$. Therefore, SPMDs need to be deployed in aqueous environments for several days in order to obtain a sufficient mass for HOC analysis using standard

extraction and analytical techniques. Such PSDs cannot capture short-term variability in dissolved concentrations.

Pawliszyn and colleagues first developed the principles of solid phase microextraction (SPME) to allow more rapid measurements of dissolved organic chemicals (Arthur and Pawliszyn, 1990). SPME is an analytic technique in which a fused silica rod coated with a polymer such as polydimethylsiloxane (PDMS) is exposed to the aqueous environment. Dissolved HOCs diffuse from the water into the polymer coating and the fiber is then directly injected into the gas chromatograph (GC) for analysis. Diffusion into the SPME fiber is much faster than diffusion into other passive sampling devices due to its small size. However, HOCs can take anywhere from hours to days to reach equilibrium with the SPME fiber depending on the extraction conditions (Mayer et al., 2000a; Poerschmann et al., 2000; Yang et al., 1998).

The rate of diffusion into the SPME fiber depends on the thickness of the polymer coating, the diffusion coefficient of the analyte in water, and the thickness of the boundary layer or unstirred water layer (UWL) between the SPME fiber and the water (Arthur and Pawliszyn, 1990). The rate limiting step in this process is diffusion through the UWL surrounding the SPME fiber (Mayer et al., 2000). Agitating or stirring the water sample reduces the thickness of this layer. Various methods, such as a magnetic stirring, vortex mixing, and sonication are used and each has its own advantages and disadvantages (Pawliszyn, 1999; Zygmunt et al., 2001). For example, Yang et al. (1998) was able to reduce the time it takes dissolved PCBs to reach equilibrium with the SPME fiber to less than 5 hours by continuously agitating the samples with a magnetic stir bar. However, the PCBs also absorbed onto the magnetic stir bar and were removed from the

system. The various agitation techniques decrease the time it takes high molecular weight HOCs to reach equilibrium from days to hours (Mayer et al., 2000a; Porschmann et al., 1998; Yang et al., 1998). However, this time scale is still not fast enough to measure short-term variations in dissolved concentrations. Additionally, none of the current techniques provide agitation to SPME fibers deployed directly into natural waters.

Non-equilibrium SPME is used to conduct more rapid measurements of dissolved concentrations. In this technique, the SPME fiber is exposed to a sample just long enough to be able to readily detect the higher molecular weight compounds, typically 20 to 90 minutes (Landin et al., 2001; Langenfeld et al., 1996; Potter and Pawliszyn, 1994). In order to quantify the concentration of HOCs on the fibers, the exposure time and mixing conditions are kept constant for all samples and external calibration solutions (Cardoso et al., 2000; Langenfeld et al., 1996; Llompert et al., 1998). This technique is less sensitive than the equilibrium technique but measures HOC concentrations on shorter time scales. Non-equilibrium SPME assumes the amount of HOCs extracted from the aqueous solution does not appreciably change the dissolved concentration with time, and therefore equilibrium distributions to particles are not disturbed. If other components of the sample do not interfere with the kinetics of uptake onto the SPME fiber, a one compartment kinetic model describes the uptake of dissolved chemical onto the SPME fibers (Vaes et al., 1996).

$$\frac{d[X]_{SPME}}{dt} = k_1[X]_d - k_2[X]_{SPME} \quad (1)$$

where $[X]_{SPME}$ is concentration on the SPME fiber (mass/volume), $[X]_d$ is the dissolved concentration (mass/volume), and k_1 and k_2 are rate constants (1/time) representing the

uptake and release of X from the SPME fiber coating. At equilibrium the concentration of X on the SPME fiber is defined by a constant K_{SPME}

$$K_{spme}(X) = \frac{k_1}{k_2} = \frac{[X]_{SPME,EQ}}{[X]_d} \quad (2)$$

Integrating equation 1 gives an equation for the concentration on the SPME fiber at any given time t assuming the dissolved concentration does not change with time (Oomen et al., 2000)

$$[X]_{SPME,t} = \frac{k_1}{k_2} [X]_d (1 - e^{-k_2 t}) \quad (3)$$

In order to use non-equilibrium SPME to measure dissolved concentrations of HOC, other matrices present in the water cannot interfere with the rate uptake of dissolved HOCs into the SPME fibers. That is, the presence of suspended solids, dissolved organic carbon, and other material in the water column cannot influence the partitioning of HOCs into the SPME fiber. Several studies have examined this issue in detail and found matrix effects to be negligible for suspended solids concentrations ranging from 20 mg L⁻¹ to 1 g L⁻¹ (Kopinke et al., 1999; Langenfeld et al., 1996; Oomen et al., 2000; Porschmann et al., 1998; Ramos et al., 1998). However, these studies focused on a single compound and the impact of matrix effects needs to be tested more thoroughly for a wider range of compounds.

In this study, we present a method using non-equilibrium SPME to measure dissolved PCBs in natural waters on 30-minute time frames. Calibration curves between the dissolved PCB concentration and the mass measured on the SPME fiber were

developed, and the variability of this method was examined. We measured the uptake (k_1) and release (k_2) rate constants for this method and calculated K_{SPME} equilibrium values. Experiments were also conducted to examine any potential matrix effects that might occur due to particles and dissolved organic carbon present in natural waters. Dissolved PCB concentrations measured using this new SPME technique were compared to measurements made by traditional XAD resin extraction of natural waters.

2.2 Experimental Section

2.2.1 SPME fibers

Optical cable (Fiberguide Industry, Stirling, NJ) consisted of a 210 μm diameter glass core and a 10 μm thick PDMS coating. The volume of the PDMS coating was 6.6 μl PDMS per meter of fiber. The cable came with a Nylon cladding 20 μm thick that covered the PDMS coating. The fibers used in this study were obtained from the same source as used and evaluated in previous studies (Mayer et al., 2000b). To make the SPME fibers, the cable was cut into 7.1 cm sections and the Nylon cladding was removed from the bottom 8 mm, according to the manufacture's directions, by dipping one end of the fiber into propylene glycol heated to 180°F for 20 seconds. After heating, any remaining Nylon was wiped away. The fibers were further conditioned by soaking in methanol for 10 minutes and rinsing with deionized (DI) water prior to use. For injection into the GC, a 5 mm silicone rubber septum (Supelco, Bellefonte, PA) was attached to the top of the SPME fiber and then inserted into a 22-gauge Rheodyne needle. Prior to inserting the SPME fiber into the needle, an 11 mm flat disk septum (Agilent

Technologies, Palo Alto, CA) was attached to the end of the needle. A tight seal formed between the two septa when the SPME fiber was injected into the GC. In this design, only 8 mm of the fiber are inserted into the GC (Figure 2.1).

2.2.2 Standards

An Aroclor 1248 standard in hexane purchased from Ultra Scientific (North Kingston, RI) is a mixture of various PCB congeners. The mixture was diluted with hexane to a concentration of 2 μg total PCB ml^{-1} . The dominant PCBs in this mixture are tri and tetra chlorinated congeners (Frame et al., 1996). Results presented in this paper will focus on the major PCB congeners in the Aroclor 1248 mixture (those > 2% by weight) i.e. PCB congener number 18, 17, 31 and 28 (unresolved), 52, 49, 44, 74, 70, 66, 95, 101, 110 and 77 (unresolved), and 118.

2.2.3 Gas Chromatography

The fibers were analyzed using cool on-column injection into an Agilent model 6890 GC equipped with a ^{63}Ni electron capture detector (GC-ECD). Hydrogen was used as the carrier gas and nitrogen was used as the make-up gas. The column was a 30-m DB-5 with a stationary phase thickness of 250 μm attached to a guard column with an internal diameter of 520 μm . The inlet temperature was held at 100°C until the fiber was inserted into the column. After insertion, the temperature in the injection port rose at 350°C min^{-1} until reaching a final temperature of 290°C in 50 seconds. The fiber was held at the head of the column for 1.5 minutes. The oven was held at initial temperature of 70°C for 2 minutes, then heated at a rate of 12° Cmin^{-1} to 140°C, 2.5°C min^{-1} to

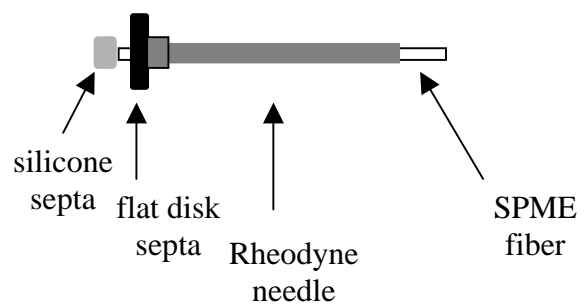


Figure 2.1. A schematic of a SPME fiber prior to injection into the GC.

230°C, and 10°C min⁻¹ to 300°C where it was maintained for 1 minute. The total run time was 51.82 minutes.

2.2.4 Revolving SPME Apparatus

In order to utilize SPME fibers in natural waters, the thickness of the unstirred water layer needs to be minimized and reproducibly controlled. Motors from Tamiya Inc (Shizuoka, Japan) were powered by two AA batteries and configured to spin a shaft at 130 rpm. Glass tubes 300 mm in length and 10 mm in diameter were attached to the motors' shaft. One end of the tube was sealed and four holes < 1 mm in diameter were punched in the end of it. Glass wool was then inserted down the barrel of the tube to hold the SPME fibers in place and one SPME fiber was inserted into each hole allowing for pseudo-replicate samples to be collected. The SPME fibers were inserted into the glass tube such that 8 mm of PDMS coated fiber extended from the end of the tube (Figure 2.2). The glass tube with the four SPME fibers on the end of it could be easily attached or detached from the motor for sampling. In this method of sampling the SPME fibers revolve in the water; all other uses of non-equilibrium SPME involve stirring or agitating the water and holding the SPME fiber still (Arthur and Pawliszyn, 1990; Poerschmann et al., 2001; Mayer et al., 2000, Yang et al., 1998, Zygmunt et al., 2001; Porschmann et al., 1998).

2.2.5 Spiked Water Calibration

Standard water solutions containing Aroclor 1248 were made to calibrate the mass that accumulated on the revolving SPME fiber to measured dissolved concentrations. Five solutions of Aroclor 1248 were prepared in clean 4 L glass

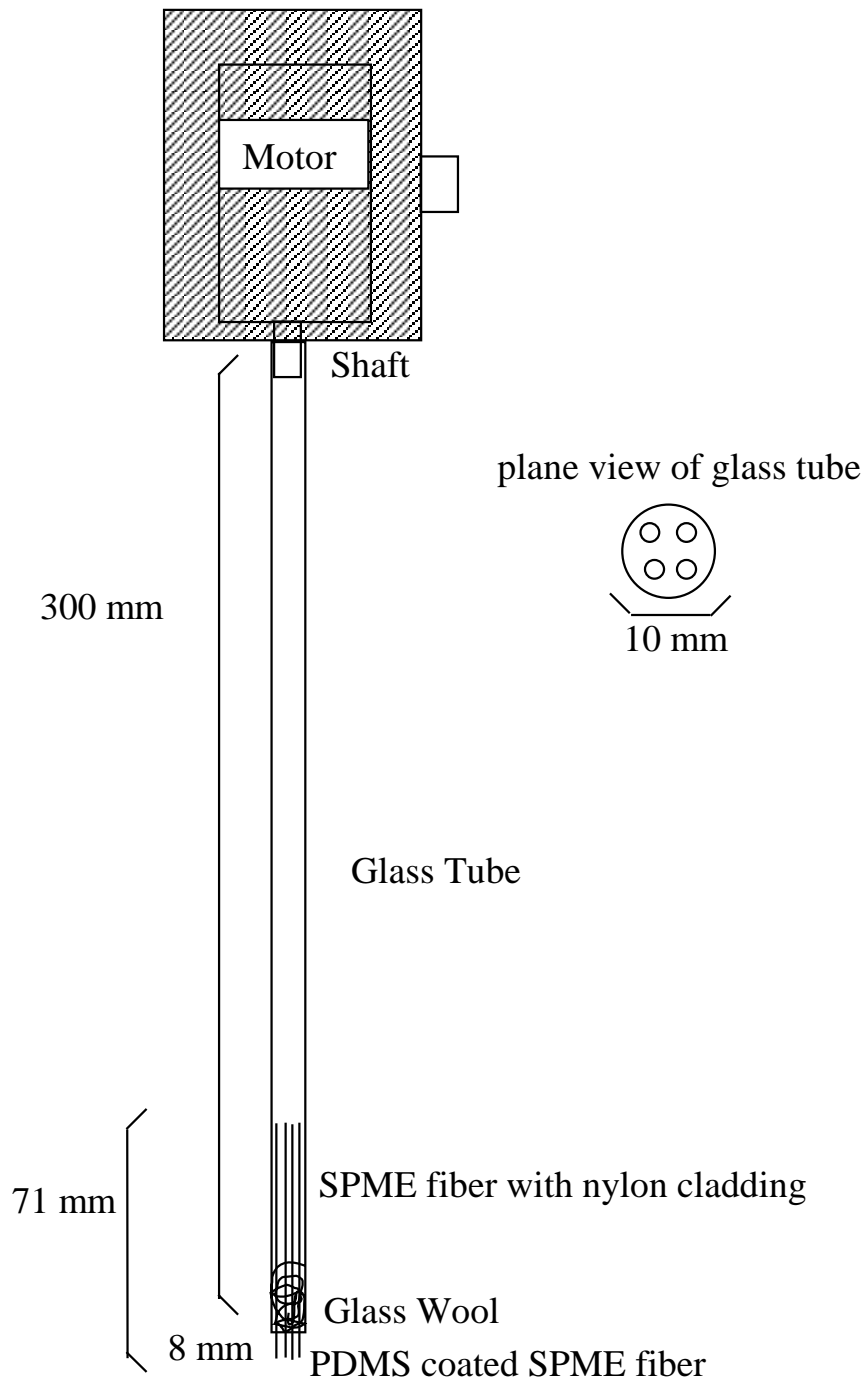


Figure 2.2. A schematic of the revolving SPME apparatus.

bottles. Various amounts of Aroclor 1248 were placed in a syringe and slowly dripped into the empty bottles. The hexane was allowed to evaporate and the vials were then completely filled with DI water. Five concentrations of Aroclor 1248 were prepared containing 0, 0.25, 0.5, 1, 2 $\mu\text{g L}^{-1}$ total PCBs respectively. The bottles equilibrated for seven days at 25 °C before they were analyzed. Water from each bottle was analyzed using SPME and our laboratory's standard liquid/liquid extraction procedure (Bamford et al., 1999). The solubility of the PCB congeners examined ranged from 0.04 to 2.0 mg L^{-1} (Shiu and Ma, 2000) and the concentration of each PCB congener in DI water was well below the solubility limit.

2.2.6 Matrix Interference Evaluation

To test for matrix interferences when using the revolving SPME technique, dissolved PCB concentrations were made by equilibrating known gas phase PCB concentrations with DI water and more complex aqueous solutions/suspensions. The procedure to generate dissolved PCB concentrations is described in detail by Kucklick et al. (1991) and briefly summarized here. Gas-phase generator columns were prepared as follows: neat PCB congeners (Ultra Scientific, North Kingston, RI) were dissolved in methylene chloride (DCM). Chromosorb W beads (Alltech, Inc., Deerfield, IL) were cleaned in an oven at 450 °F for four hours prior to use. The PCB solutions were poured over the Chromosorb beads, slowly evaporated, and the PCB coated Chromosorb was poured into a generator column. Air flowing through the generator columns became saturated with PCBs, and this air was diluted with clean humidified air and bubbled through 150 ml of DI water. The time to equilibrium was established by trapping air exiting the bubbler on polyurethane foam adsorbents (PUF). Analysis of multiple PUFs

showed that equilibrium was established in three days. Once equilibrium was reached, the bubbling was shut off and SPME was used to measure the dissolved PCB concentration.

Dissolved organic carbon (DOC) enriched water was collected from Battle Creek Cypress Swamp located in Calvert County, Maryland. This water was filtered through a 47 mm Whatman glass fiber filter (0.7 μm pore size) to remove suspended solids and placed into a bubbler. The DOC concentration of the filtered water was 8 mg L⁻¹. PCB saturated air was bubbled through 150 ml of this filtered water and allowed to come to equilibrium. Once equilibrium was reached, the gas was shut off and SPME was used to measure the dissolved PCB concentration. Sediment was collected from Fishing Bay, an embayment of the Chesapeake Bay. Dry sediment was added to deionized water for a total suspended solids concentration of 200 mg L⁻¹. PCB saturated air was bubbled through 150 ml of this suspension until it came to equilibrium. Once equilibrium was reached, the bubbling was shut off and SPME was used to measure the dissolved PCB concentration. While the matrices added to the bubblers might have contained PCBs such that the total PCB concentration was higher in those bubblers than in the bubbler with just DI water, the dissolved phase concentration in the bubblers was controlled by equilibrating with PCB contaminated air.

2.2.7 XAD Comparison

To compare this revolving SPME technique to the more traditional dissolved phase PCB measurements made by XAD extraction, twelve contaminated water samples were first analyzed by SPME and then the water was filtered and pumped through an XAD column. The PCB contaminated water was collected in 18 L stainless steel tanks as

part of another on-going study in our laboratory (Chapter 4 and 5). The stainless steel tanks were shaken and then the SPME fibers were deployed in the tanks for 30 minutes. After SPME deployment, the dissolved and particulate phase were separated by pumping the water through a glass fiber filter (Schleicher and Schuell, Keene, NH; no 25; 0.7 μ m pore size) and an Amberlite XAD-2 macroresin (Sigma Aldrich, St. Lois, MO). The XAD analysis followed the standard protocol of our laboratory and is briefly summarized here (Bamford et al., 1999). The samples were spiked with PCB surrogate standards 3,5-dichlorobiphenyl (IUPAC #14), 2,3,5,6-tetrachlorobiphenyl (IUPAC #65), and 2,3,4,4',5,6-hexachlorobiphenyl (IUPAC #166) and Soxhlet extracted for 24 hours in 1:1 acetone/hexane. Following a liquid/liquid extraction of the acetone/hexane mixture using DI water and hexane, the samples were rotoevaporated down to 1mL, and eluted through a Florisil column (60-100 mesh; J. T. Baker Co., Phillipsburg, NJ). The purified extracts were concentrated and analyzed using a Hewlett-Packard 5890 gas chromatography with a 60 meter DB-5 column and a ^{63}Ni electron capture detector (GC-ECD). Each sample was analyzed for 55 individual PCB congeners and 28 chromatographically unresolved congener groups. Internal standards consisting of 2,3,6-trichlorobiphenyl (IUPAC #30) and 2,2'3,4,4', 5,6,6'-octachlorobiphenyl (IUPAC #204) were added to each sample prior to instrumental analysis to calculate relative response factors for each congener. Each PCB congener was identified based on its retention time relative to a standard mixture of PCB Aroclors 1232, 1248, and 1262 (Ultra Scientific, Kingston, RI).

2.3 Results and Discussion

2.3.1. Analytical Verification of GC Technique

Prior to conducting experiments, tests were run to verify the consistency of the SPME fibers and the precision of the GC injections. Ten nanograms of Aroclor 1248 were dripped onto the end of a fiber which was analyzed on the GC. This procedure was repeated ten times using new fibers for each repetition. The detector responses of each congeners were compared to determine the precision of this method. The relative standard deviation (RSD) ranged from 2.3 -7.6 % for all congeners and there was no trend in RSD with PCB solubility or K_{ow} . These results are similar to the precision of head space SPME analysis for various PCB congeners (Landin et al., 2001).

Even though these SPME fibers are designed to be disposable, carryover after one use was examined to analyze the efficiency of desorption in the injection port. To do this analysis, 10 ng of Aroclor 1248 were added to a SPME fiber and analyzed. After this first run completed, the fiber was re-injected into the GC. Carryover was less than 1% for all congeners examined, indicating this method of analysis had a desorption efficiency of over 99%. Landin et al. (2001) also found no significant carryover of PCB congeners when commercially available SPME fibers (Supelco, Bellefonte, PA) were injected into a GC/MS/MS system. However, other studies examining the carryover of PCB congeners have found carryover rates as high as 25% (Potter and Pawliszyn, 1994; Yang et al., 1998). A variety of conditions contribute to the wide range of carryover rates observed in the literature, including the amount of time the fiber is held in the GC and temperature of desorption. In the method described in this paper SPME fibers were not reused and carryover between GC runs was therefore not an issue.

Since SPME injections into the GC are done manually it is desirable to store the fibers in the freezer before analysis. However, some studies suggest PCBs might volatilize or become irreversibly bound to the SPME fibers during storage. Lighter more volatile compounds are especially prone to loss if not stored properly (Chai and Pawliszyn, 1995; Muller, 1999). To examine the loss of PCBs during freezing, 10 ng of Aroclor 1248 was dripped on several SPME fibers and the fibers were frozen inside a glass capillary tube for 30 days. There was no significant difference in the detector response between stored fibers and freshly prepared fibers ($p > 0.05$, $n = 5$). PCBs were not lost during storage and no additional unknown contaminant peaks were detected on the SPME fibers as a result of freezing.

2.3.2 Method Precision

In order to examine the precision of the revolving fiber technique, multiple samples were collected from various concentrations of dissolved PCBs. The variation in detector response among the four SPME fibers on a single rotating glass tube was compared to the variation among different glass tubes. SPME fibers deployed in all of the calibration solutions for 30 minutes showed similar variability, and the between tube RSD for all of the calibration points ranged from 3.0 – 18.9 % and did not vary with concentration. The RSD of the four SPME fibers on the same glass tube was similar to the between tube relative standard deviation and ranged from 3.2 – 16.7% in the $5 \mu\text{g L}^{-1}$ PCB solution. This suggests there is no sampling bias among the different positions on the rod and that PCBs partition into all the fibers on a glass tube at the same rate. There was no trend in RSD with PCB solubility or K_{ow} , and the method is not biased toward better reproducibility for the congeners with lower K_{ow} values. These results are

consistent with RSD values reported in the literature for other non-equilibrium SPME techniques. For example, Potter and Pawliszyn (1994) exposed SPME fibers to aqueous solutions containing among other compounds PCB 18 and PCB 87 for 20 minutes and found RSD values of 19 and 16% respectively. Yang et al. (1998) spiked natural water samples with a variety of PCBs and found RSD values ranging between 5-26% when SPME fibers were exposed to the agitated water samples for 15 minutes.

2.3.3 Kinetics of PCB Uptake

The goal of developing a non-equilibrium technique was to measure individual PCBs in the dissolved phase with suitable detection limits in 30 minutes. In order to examine the uptake of PCBs into the revolving fibers, they were exposed for various lengths of time, ranging from 5 minutes to 12 hours, in 4 L bottle spiked with $5 \mu\text{g L}^{-1}$ of Aroclor 1248 in DI water (Figure 2.3 and 2.4). The bottle equilibrated for seven days at 25°C before analysis to allow the PCBs to have sufficient time to absorb to the glass walls and ensure the dissolved phase concentration would remain constant for the SPME measurements. For all PCB congeners examined, the 30-minute sampling period falls well within the linear range of uptake onto the SPME fibers, indicating it was a suitable exposure time to use with our method (Figure 2.3).

Since the goal of this project was to develop a method to measure dissolved PCBs on 30 minutes time scales, a detailed analysis of the uptake of PCBs onto the fiber during exposure times ranging from 5-120 minutes was conducted. During this time period there was a linear relationship between mass extracted and SPME sampling time, the correlation coefficient ranged from 0.88-0.98 for various PCB congeners (Figure 2.3). This linear relationship suggested diffusion through the UWL was the rate-limiting

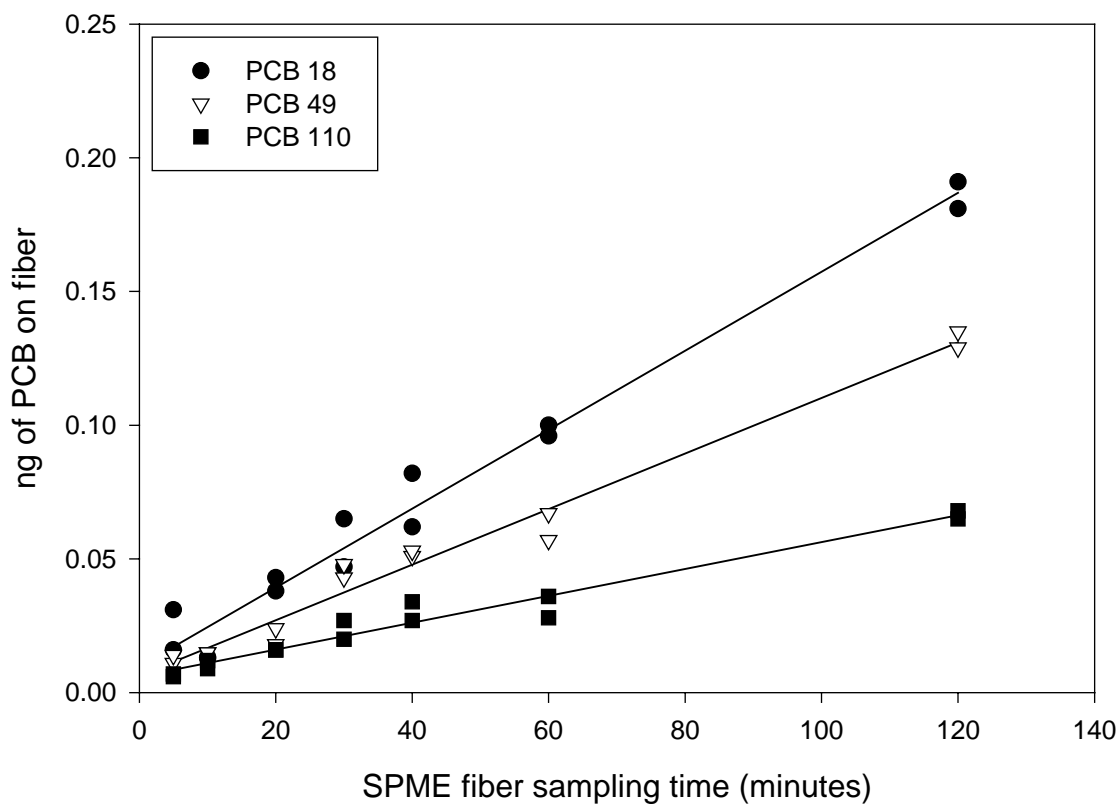


Figure 2.3. The uptake of PCBs onto SPME fibers deployed in DI water spiked with $5 \mu\text{g L}^{-1}$ Aroclor 1248 for sampling times ranging from 5 – 120 minutes at 25°C . For clarity only results from a few selected congeners are depicted. Multiple data points for a given time indicate pseudo-replicate measurements.

uptake step since longer exposure times resulted in more mass accumulating on the SPME fiber. The slope of the line represents a mass uptake rate, which ranges from 0.0002 to 0.0022 ng min⁻¹ for the various congeners. The rate of uptake of PCBs onto the SPME fibers was positively correlated with the molecular diffusion coefficient in water ($r^2 = 0.51$) further indicating that diffusion through the UWL was the limiting step in the uptake process. The rate of diffusion of PCBs into the PDMS coating is controlled by diffusion through the UWL if the thickness of the UWL is greater than the thickness of the PDMS coating divided by K_{SPME} (Pawliszyn, 1997). For PCBs, K_{SPME} ranges from 10^5 to 10^6 and diffusion through the UWL is almost always the rate limiting step.

Sukola et al. (2001) found that the uptake rate of aromatic hydrocarbons into SPME fibers coated with a mixed porous solid adsorptive coating was proportional to the molecular diffusion coefficient in water. The exposure times in that study were much shorter than those examined in our study because the chemicals more readily diffused into the SPME fibers and the stirring rates were much faster. In that study an examination of the uptake kinetics of aromatic hydrocarbons at different stirring speeds demonstrated that the extraction rate of analytes is controlled by diffusion through the UWL. For ethylbenzene, increasing the sample velocity from 1 cm s⁻¹ to 75 cm s⁻¹ decreased the thickness of the UWL from 45 μm to 3 μm.

Over the 12 hour exposure time examined, uptake for the tri-chlorinated congeners appeared to follow the predicted one compartment model to equilibrium (Figure 2.4). At equilibrium there was 0.05 g L⁻¹ of the tri-chlorinated congener PCB 18 in the SPME fiber's PDMS coating. Assuming straight chains of PDMS, the mole fraction of PCB 18 on the fiber was 0.0006. The higher molecular weight congeners did

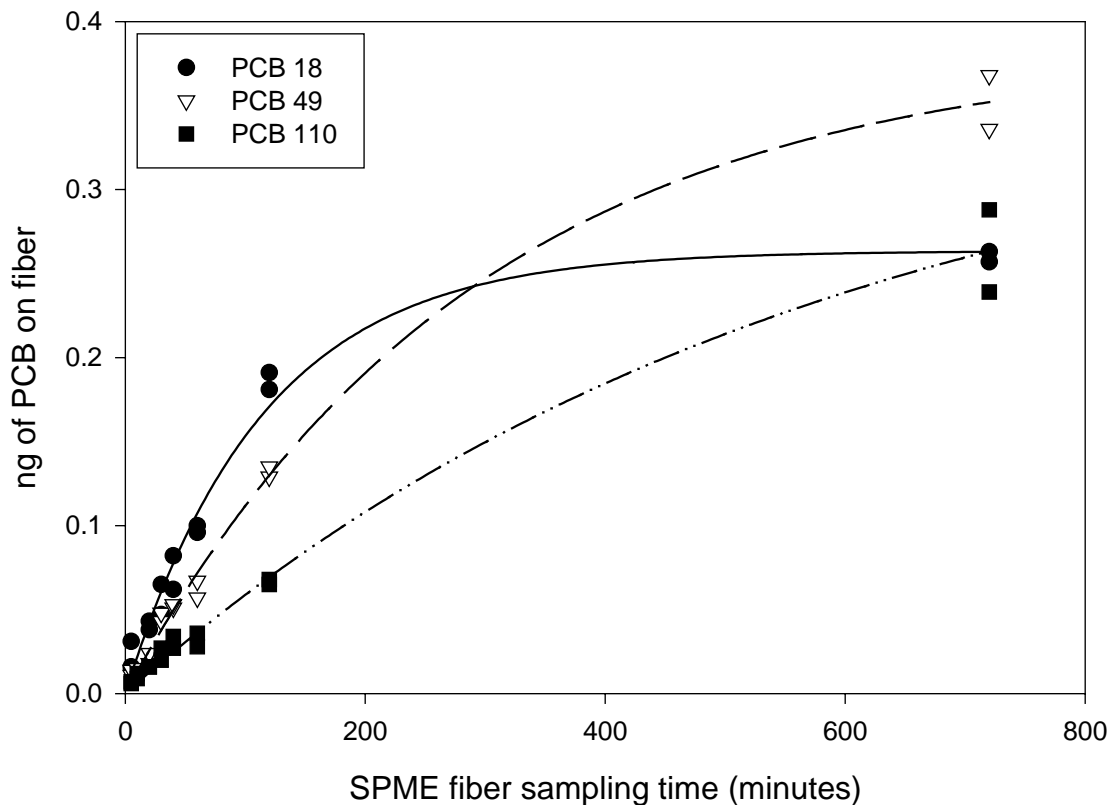


Figure 2.4. Uptake curves of selected PCBs onto the SPME fibers deployed in DI water spiked with $5 \mu\text{g L}^{-1}$ Aroclor 1248. The SPME fibers sampled the water continuously for time periods ranging from five minutes to 12 hours at 25°C . Multiple data points for a given time indicate pseudo-replicate measurements.

not appear to reach equilibrium after twelve hours of exposure (Figure 2.4). Since the utility of this SPME technique depends on short sampling periods, longer fiber exposure times were not examined in great detail. Nevertheless it is useful to calculate rate constants for our sampling technique in order to compare our results to literature values. Uptake and elimination rate constants were determined by curve fitting the model to our data. For this method the uptake rate constant (k_1) ranged from 350 ± 100 to 950 ± 170 min^{-1} , the elimination rate constant (k_2) ranged between 0.0023 ± 0.0002 and 0.0089 ± 0.0006 min^{-1} , and $\text{Log } K_{\text{SPME}}$ ranged from 4.96 to 5.31 (Table 2.1, $n = 4$).

There are only a limited number of studies examining the kinetics of PCB uptake onto SPME fibers in the literature. Oomen et al. (2000) vibrated 1 mm long fibers in PCB spiked water using the Varian 8200 CX autosampler. In that study, PCB 52 had an uptake rate constant of 6700 ± 1200 min^{-1} and an elimination rate constant of 0.014 ± 0.003 min^{-1} ; and PCB 118 had uptake and elimination rate constants of 9600 ± 1200 and 0.017 ± 0.003 min^{-1} respectively. Ramos et al. (1998) measured the uptake of dissolved PCB 77 in a solution that was stirred at a rate of 1000 rpm and calculated a k_1 value of 1530 ± 170 min^{-1} and a k_2 value of 0.025 ± 0.004 min^{-1} . The literature values of k_1 and k_2 are an order of magnitude higher than those found in this study. The uptake (k_1) and elimination (k_2) rate constant depend on the specific technique used to vibrate or shake the fibers in the sample. In these studies the SPME fiber was vibrated more vigorously than in our study resulting in a thinner UWL and greater uptake and elimination rate constants. Since mass accumulation onto a SPME fiber depends on diffusion through the UWL, different techniques will result in different uptake and elimination rate constants.

IUPAC name	congener number	k₁ (min⁻¹) ±SE	k₂ (min⁻¹) * 10⁻³ ±SE	Log K_{SPME} ±SE
2,2',5-trichlorobiphenyl	18	810 ± 100	8.9 ± 0.6	4.96 ± 0.05
2,2',4-trichlorobiphenyl	17	430 ± 60	6.0 ± 0.7	4.85 ± 0.05
2,4',5 and 2,4,4'-trichlorobiphenyl	31, 28	650 ± 90	6.0 ± 0.8	5.04 ± 0.05
2,2',4,6'-tetrachlorobiphenyl	52	700 ± 60	3.0 ± 0.2	5.37 ± 0.05
2,2',4,5'-tetrachlorobiphenyl	49	950 ± 170	5.0 ± 0.8	5.28 ± 0.05
2,2',3,5'-tetrachlorobiphenyl	44	800 ± 150	4.3 ± 0.7	5.27 ± 0.06
2,4,4',5-tetrachlorobiphenyl	74	720 ± 190	3.6 ± 0.8	5.30 ± 0.06
2,3',4',5-tetrachlorobiphenyl	70	480 ± 50	2.3 ± 0.2	5.32 ± 0.05
2,3',4,4'-tetrachlorobiphenyl and 2,2',3,5',6-pentachlorobiphenyl	66, 95	800 ± 160	4.2 ± 0.7	5.28 ± 0.06
2,2',4,5,5'-pentachlorobiphenyl	101	720 ± 190	3.6 ± 0.8	5.30 ± 0.06
2,3,3',4',6-pentachlorobiphenyl	110	740 ± 190	3.6 ± 0.8	5.31 ± 0.06
2,3',4,4',5-pentachlorobiphenyl	118	350 ± 100	3.5 ± 0.9	5.00 ± 0.07

Table 2.1. Kinetic constants for the uptake of PCBs onto the SPME fibers (n = 4).

Studies such as those conducted by Baltussen et al. (1999) and Mayer et al. (2000) found a linear relationship between the K_{SPME} and K_{ow} . This relationship was not observed in our SPME technique; however, our values are within the range of K_{SPME} values reported in the literature. For example, for PCB 52 the log K_{SPME} calculated in this study was 5.37, Meyer et al. (2000) measured a log K_{SPME} of 5.38, Oomen et al. (2000) calculated a log K_{SPME} of 5.7, Poerschmann et al. (2000) measured a log K_{SPME} of 5.21, and Baltussen et al. (1999) measured log K_{SPME} values ranging from 5.11-5.44 depending on the amount of PDMS coated to fused silica beads. For PCB congener 118, Poerschmann et al. (2000) measured a log K_{SPME} of 5.60, this study found a log K_{SPME} of 5.0, and Meyer et al. (2000) measured a log K_{SPME} value of 5.9.

2.3.4 Dissolved Phase Calibration

To correlate the mass on the SPME fiber to actual dissolved concentrations the revolving SPME fibers were deployed for 30 minutes in solutions of DI water spiked with 0, 0.25, 0.5, 1 and 2 $\mu\text{g L}^{-1}$ of Aroclor 1248. After SPME fiber deployment, a liquid/liquid extraction of the water was conducted using our laboratory's standard extraction procedure. For each PCB congener, the mass measured on the SPME fiber was correlated to dissolved phase concentration measured by liquid/liquid extraction. For all PCB congeners, uptake onto the SPME fibers was linear over the range of dissolved concentrations examined with coefficients of determination ranging from 0.91 to 0.99 (Table 2.2). These strong linear relationships demonstrate that the measured mass on the SPME fiber was directly related to the dissolved concentration. At the highest Aroclor concentration examined the concentration of each PCB congener in the PDMS fiber was less than 0.01 g L^{-1} PDMS. No relationship was observed between uptake onto the

SPME fiber and PCB properties such as molecular weight. However, only tri, tetra, and penta-chlorinated congeners were examined in this study.

2.3.5 Detection Limits

The method detection limit (MDL) was defined as three times the average mass in the deionized water blank samples. This mass was then converted to concentration using the calculated calibration curves. The MDL for the congeners examined in this study ranged from 0.6 to 5.2 ng L⁻¹ (Table 2.2). For all congeners the MDL was below the lowest concentration sampled in the calibration curve. The detection limits obtained using this method are similar to the detection limits obtained by other researchers. For example, Martinez et al. (2002) obtained detection limits of 10-20 ng L⁻¹ when they immersed vials of PCB spiked water into a boiling water bath and used SPME to measure the PCB concentration in the headspace on a time scale of 30 minutes. Potter and Pawlyszyn (1994) obtained detection limits of 2-3 ng L⁻¹ for PCB 18 and 86 when they placed SPME fibers in PCB spiked water vigorously mixed with a stir bar for 10 minutes. Yang et al. (1998) obtained detection limits of 5 ng L⁻¹ for a variety of PCB congeners when SPME fibers were deployed for 15 minutes in samples that were agitated at 1000 rpm.

2.3.6 Matrix Effects

In order to use this revolving SPME technique to measure PCBs in natural waters, other matrices present in the water, such as dissolved organic carbon, could not interfere with the uptake of PCBs onto the fibers. The bubbler system maintained constant dissolved PCB concentrations and was designed to test for matrix interferences with this

Congener number	Slope \pm SE (mL)	Coefficient of Determination (r^2)	MDL (ng/L)
18	0.57 \pm 0.01	0.91	1.9
17	0.71 \pm 0.01	0.95	0.6
31, 28	0.50 \pm 0.06	0.96	5.2
52	0.68 \pm 0.06	0.97	3.5
49	0.68 \pm 0.07	0.97	2.2
44	0.55 \pm 0.09	0.92	5.3
74	0.50 \pm 0.03	0.99	0.9
70	0.38 \pm 0.05	0.97	2.0
66, 95	0.58 \pm 0.04	0.99	2.6
101	0.66 \pm 0.06	0.98	0.2
110	0.41 \pm 0.03	0.99	0.7
118	0.29 \pm 0.03	0.98	1.9

Table 2.2. Regression statistics for the relationship between dissolved PCB concentrations and mass measured on the SPME fiber (n = 4).

SPME technique. For various PCB congeners, the dissolved PCB measurements made in DI water were not significantly different from the dissolved measurements made in the presence of DOC or suspended solids (Figure 2.5, $p > 0.05$ for all congeners, $n = 6$). This result indicates that the revolving SPME technique is suitable to measure PCBs in natural waters and the presence of matrices does not influence the uptake of PCBs onto the SPME fibers. This finding confirms results found by other researchers for both the equilibrium (Kopinke et al., 1999; Porschmann et al., 1998) and non-equilibrium techniques (Oomen et al., 2000; Ramos et al., 1998). For example, Ramos et al. (1998) prepared two solutions of dissolved PCB 77; one contained 20 mg L^{-1} humic acid and the other did not. An air bridge connected the round bottom flasks containing the two solutions. The authors found no significant difference in the detector response to SPME fiber measurements made in both flasks, indicating humic acid did not interfere with the uptake of PCBs onto SPME fiber. Oomen et al. (2000) conducted a similar study comparing the impact of artificial soil on SPME measurements of PCB 52. However, this study was conducted at a much higher solids concentration of 1 g L^{-1} . Despite the high solids concentration, this study also found no significant difference between SPME measurements made in pure water and those made in water spiked with artificial soil. These studies and others (Kopinke et al., 1999; Langenfeld et al., 1996) indicate that matrix effects do not interfere with measuring dissolved concentrations in natural waters.

2.3.7 XAD/SPME comparison

The revolving SPME technique was used to sample well water that was mixed with PCB contaminated sediment from the Hudson River (Chapter 4 and 5). After the revolving SPME fibers were deployed in the water for 30 minutes, the water was pumped

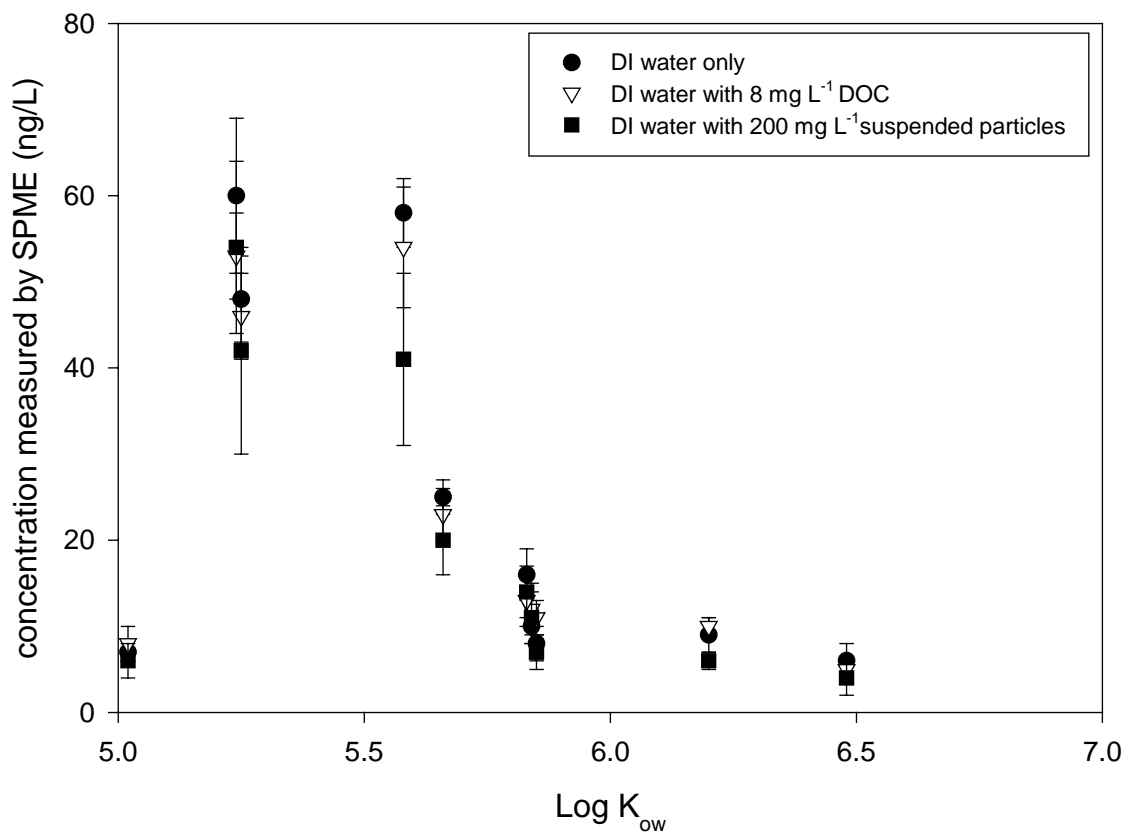


Figure 2.5. SPME measurements of the dissolved concentrations of PCB congeners measured in DI water, DI water plus DOC, and DI water plus suspended solids. The error bars represent the standard deviation between pseudo-replications and multiple tube measurements ($n = 6$).

first through a glass fiber filter to remove particles and then an XAD column to measure the dissolved phase. A total of 12 XAD/SPME pairs were analyzed and compared. Information in the literature suggests PCB concentrations measured by XAD should be higher than those measured by SPME because XAD measurements typically include PCBs bound to DOC (Lee et al., 2003) and SPME measurements do not. Results from this study confirm this hypothesis; dissolved PCB concentrations measured by SPME were slightly lower than dissolved concentrations measured by XAD (Figure 2.6) even though the DOC concentration in the water was only $1.32 \pm 0.23 \text{ mg L}^{-1}$. On average the XAD measurements were 12% higher than the SPME measurements (Figure 2.7). These results are consistent with the study by Zheng et al. (2004) that found SPME fibers deployed as passive samplers measured DDE concentrations that were not statistically different from XAD extractions. The relationship between the XAD and SPME measurements strongly suggests this revolving SPME technique is suitable for measuring PCB concentrations in the field.

2.4 Summary

This technique rapidly measures dissolved PCB congeners in natural waters in 30 minutes with detection limits ranging from 0.6 to 5.2 ng L^{-1} . Revolving the SPME fibers at 130 rpm rather than agitating the water reproducibly minimizes the thickness of the UWL and allows sufficient mass to diffuse onto the SPME fibers for reasonable detection limits. The mass that accumulates on the fiber is linearly related to the dissolved concentration, and the presence of both DOC and suspended solids does not interfere with the dissolved measurements made using this technique. The relative standard

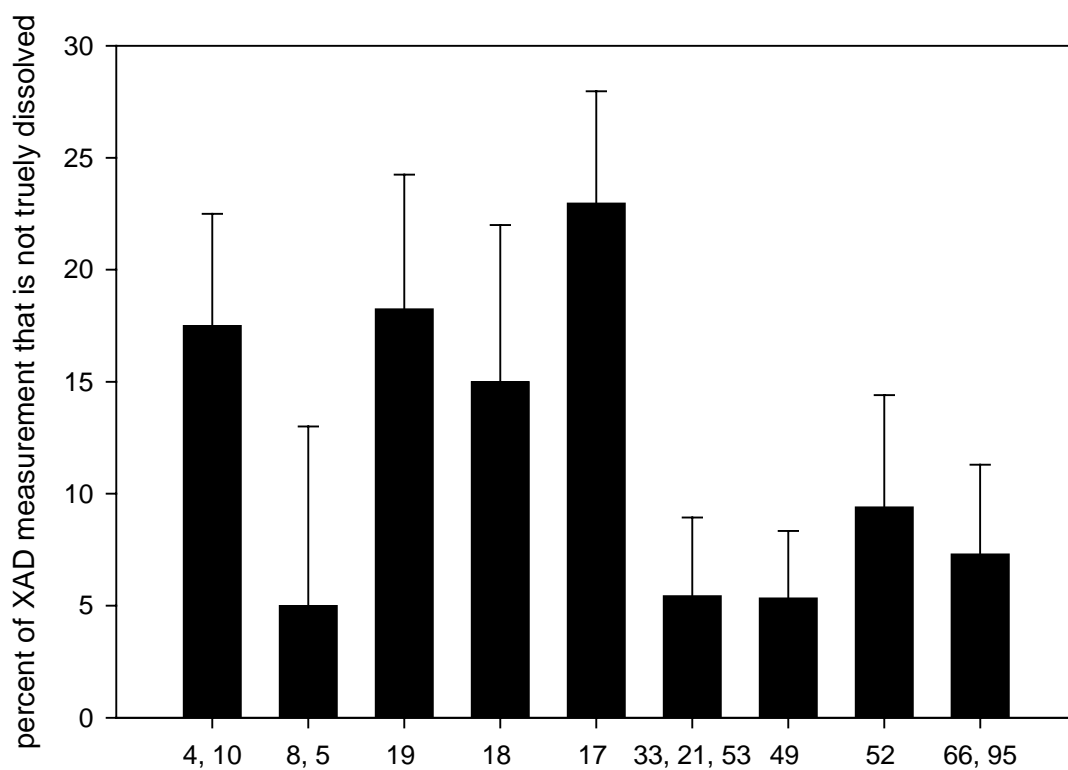


Figure 2.7. The average percent difference between XAD and SPME measurements for each PCB congener. Congener 110 was not detected by this SPME technique and XAD measurements indicate the concentration was $\sim 0.5 \text{ ng L}^{-1}$, below the SPME detection limit.

deviation between replicate SPME samples ranges from 3 to 20%. A comparison with XAD extraction of natural water shows that this SPME technique reliably and consistently measures dissolved PCB concentrations in natural waters.

Current field applications of SPME are best suited for time weighted average measurements because the commercially available devices are essentially passive samplers (Muller, 1999). This revolving SPME technique can be used on shorter timescales to less expensively and more rapidly monitor short-term variability in dissolved concentrations of contaminants. Pseudo-replicate samples are easily collected to assess analytical variability. Although this technique requires manual injection, the fibers can be safely stored in the freezer until they are analyzed. This type of SPME device can be made relatively cheaply by buying the SPME fibers from an optical fiber company and motors from a local hobby shop; it eliminates the need for expensive lab equipment to conduct SPME analysis and provides a more economical way to conduct field studies. This technique is currently being used to quantify PCB desorption from contaminated sediments (Chapters 4-5).

Chapter 3: A mesocosm examination of cohesive Hudson River sediment resuspension and settling

3.1 Introduction

The upper Hudson River in New York State (USA) is severely contaminated with polychlorinated biphenyls (PCBs). The river's sediments are the largest reservoir of PCBs in the system and release from the sediment is the primary source of PCBs to the water column (Thomann et al., 1991). One of the keys to assessing PCB release from the sediment is an understanding of the processes of resuspension and settling. The amount of PCBs released from resuspended sediment is governed by three primary factors: the amount of sediment resuspended, the residence time of the particles in the water column, and the rate of PCB desorption. In previous studies examining PCB release from sediment, sediment-water slurries were vigorously mixed or shaken (Brusseau et al., 1991; Carroll et al., 1994; Lamoureux and Brownawell, 1999). These experiments did not mimic natural conditions and neither the amount of sediment resuspended nor the residence time of the particles in the water column was similar to resuspension events caused by storms or other high flow conditions. One of the major uncertainties in remediation plans for the upper Hudson River is the calculation of the amount of PCBs that will be released during proposed dredging activities (Connolly et al., 2000).

Sediment resuspension or erosion occurs when the bottom shear stress exceeds the critical shear stress required to lift a particle off of the bed. The critical shear stress required to initiate resuspension depends on the properties of the sediment bed. In Baltimore Harbor, Maryland the critical shear stress for resuspension is $0.5 \text{ dynes cm}^{-2}$

when a bottom floc layer is present and 1 dyne cm^{-2} for consolidated beds (Maa et al., 1998). Tolhurst et al. (2000) deployed a variety of instruments used to measure critical shear stress in the muddy sediment of the Humbar estuary and determined critical shear stresses ranged from 1.9 to 2.6 dynes cm^{-2} , depending on the apparatus used. The surficial sediment of cores collected from the Sheboygan River in Wisconsin had critical shear stresses averaging $1.6 \text{ dynes cm}^{-2}$. As erosion depth increased, the critical shear stress for resuspension increased and at depths of 4 to 5 cm below the surface the critical shear stress averaged $2.0 \text{ dynes cm}^{-2}$. This change in critical shear stress with depth occurred because the core became more compacted and bulk density increased with depth (Lee et al., 2004). In the Great Lakes, the critical shear stress is about 1 dyne cm^{-2} for sediment beds that have consolidated 1 to 7 days but is considerably less for beds that have consolidated for less than 1 day (Lick et al., 1994). Additionally, bed consolidation time affects the amount of sediment resuspended at a given shear stress. For example, in an annular flume study conducted at a shear stress of 2 dynes cm^{-2} , 120 mg L^{-1} of sediment was resuspended if the bed consolidated for only two days. If bed consolidation time increased to seven days, only 30 mg L^{-1} of solids were resuspended (Tsai and Lick, 1988).

The surfaces of cohesive particles are charged and electrostatic interactions as well as Van der Waals forces cause the particles to attract each other. As a result, in the water column cohesive sediment particles do not behave as individual particles but instead aggregate and form flocs. The components of flocs are both organic and inorganic in origin and include humic substances, clay minerals, manganese oxyhydroxides, biogenic silicates, extracellular polymeric substances, bacteria, viruses,

and other microorganisms. Fluid shear stress, Brownian motion, total suspended solids concentration, ionic strength, and differential settling are the critical factors affecting floc formation and breakup (Burban et al., 1990; Manning and Dyer, 1999; Tsai et al., 1987). Fluid shear stress enhances the frequency of collisions between particles and increases the chances of floc formation. However, it also breaks apart larger flocs and promotes disaggregation of the particles. For example, the median diameter of a suspension of Detroit River sediment, with a pre-suspension median diameter of 4 μm , decreased from 110 μm to 50 μm as shear increased from 1 dyne cm^{-2} to 4 dynes cm^{-2} at 100 mg L^{-1} (Tsai et al., 1987). At this suspended solids concentration, floc formation reached steady state in two hours or less for all levels of applied shear stress. At a given shear, time to steady state floc formation decreases as TSS increases. For example, at a shear stress of 2 dynes cm^{-2} and 800 mg L^{-1} of TSS, steady state floc formation was reached in 30 minutes compared to 1 hour at 100 mg L^{-1} of TSS (Tsai et al., 1987). Additionally, the floc size at steady state changes with TSS. At a stress of 2 dyne cm^{-2} , suspended mud decreased in diameter from 160 μm to 95 μm as the TSS concentration decreased from 200 mg L^{-1} to 80 mg L^{-1} (Manning and Dyer, 1999). At higher suspended solids concentrations, the direction of this relationship changes as the flocs collide more frequently. For example, Tsai et al. (1987) found the steady state median diameter of flocs was 80 μm at 100 mg L^{-1} and decreased to 26 μm at an 800 mg L^{-1} TSS.

Water column turbulence and total suspended solids also influence floc properties such as porosity and density, which in turn affect floc settling speeds (Burban et al., 1990; Droppo et al., 1997; Manning and Dyer, 1999). Burbán et al. (1990) found that flocs generated at lower turbulence and suspended solids concentrations had lower

settling speeds than flocs produced at higher turbulence and suspended solids concentrations. Droppo *et al.* (1997) showed that as floc size increased the porosity and settling rate of the flocs increased and floc density decreased. Recently investigators have begun using laser in-situ scattering transmissometry (LISST) to examine the relationship between particle size, density, porosity, and settling velocity in the field (Fugate and Friedrichs, 2002; Van der Lee, 2000; Voulgaris and Meyers, 2004; Xia *et al.*, 2004). The LISST measures the total volume concentration of particles and flocs ranging in diameter from 2.5 to 500 μm . Coupled to TSS measurements or settling velocity observations, the LISST data can be used to calculate floc porosity and effective density (Mikkelsen and Pejrup, 2001; Xia *et al.*, 2004, Sanford *et al.*, 2005). For example, Xia *et al.* (2004) used the LISST to examine changes in floc diameter and settling velocity along the Pearl River Estuary in China. By attaching a LISST to a settling tube, the researchers examined changes in settling velocity over a range of particle size classes and in turn studied how the effective density of the particles changed with size class. This study found an inverse relationship between apparent density and particle size- as particle size increased apparent density decreased. There was only a slightly positive correlation between particle size and the settling velocity, and there was no clear relationship between total suspended solids, settling velocity and particle size.

In rivers, bottom shear stress and water column turbulence are closely linked. Together these two parameters determine the amount of sediment resuspended and the properties of the resuspended flocs. Previous studies show that both phenomena reach steady state on similar time scales (Lick *et al.*, 1995; Maa *et al.*, 1998). However, the apparatus used to study resuspension and flocculation did not generate realistic levels of

water column turbulence and bottom shear stress simultaneously. As a result, laboratory studies often examine these two processes separately. In the flocculation and settling studies discussed earlier, suspended solids were added to an apparatus that could apply shear to the water column. The sediment could not be lifted off the bed in these studies (Burban et al., 1990; Manning and Dyer, 1999; Tsai et al., 1987). The studies examining the critical shear stress needed for resuspension did not accurately simulate water column turbulence levels. Laboratory annular flume studies and shaker table studies generated realistic bottom shear stresses for resuspension but the water column turbulence was too high to study the properties of resuspended particles (Lick et al., 1994; Lick et al., 1995; Tsai and Lick, 1988). Field apparatus designed to determine the in-situ critical shear stress needed for resuspension did not have the capability to also examine the size distribution of the resuspended particles (Hawley, 1991; Maa et al., 1998). In order to realistically conduct resuspension studies, several key variables need to be reproduced including turbulence intensity, energy dissipation, bottom shear velocity and mean flow speed (Sanford, 1997).

In this study we use the Shear Turbulence Resuspension Mesocosms (STORM) tanks to examine the changes in particle size distribution of sediment as it is resuspended and settled under realistic bottom shear stress and water column turbulence. These tanks resuspend sediment while generating only minimal water column turbulence. Mimicking both water column mixing and benthic boundary-layer flow, the STORM tanks simulate resuspension and settling conditions more realistically than previous apparatus used to study these processes (Porter et al., 2004; 2005). We deployed a LISST 100C (Sequoia Scientific, Redmond, WA) in the STORM tanks to observe how the particle size

distribution changes as both cohesive sediment resuspension and flocculation reach steady state. The objective of this paper is to characterize the properties (porosity, density, median diameter, and settling velocity) of particles resuspended at a constant shear stress. Specifically, this paper examines how the size distribution of resuspended particles evolves over time during a resuspension event, assesses the effects of both sediment consolidation time and quiescent time between resuspension events on the properties of the resuspended particles, and determines the settling velocity of the particles in the STORM tank. This study is part of a larger project examining the release of PCBs from resuspended Hudson River sediment.

3.2 Materials and Methods

3.2.1 *STORM Tanks*

Resuspension experiments were conducted in three outdoor Shear Turbulence Resuspension Mesocosm (STORM) tanks described previously in Porter et al. (2005). In each STORM tank a paddle rotated just above the bottom around a central shaft, alternating directions periodically. This form of stirring resuspended sediment without generating excessive water column turbulence. Sets of three tanks were driven by a single motor, with mechanical linkages designed to ensure uniformity in stirring characteristics (Porter et al., 2005). The instantaneous maxima bottom shear stress of about 1 dyne cm^{-2} resulted in significant resuspension, but the time and spaced averaged bottom shear stress was $0.07 \text{ dyne cm}^{-2}$. The sediment surface area in the STORM tanks was 1 m^2 and the water column was 1 m deep with a total water volume of 1000 L (Porter et al., 2005). A large reflective tarp tent was constructed over the STORM tanks so that

all experiments were conducted in the dark in order to minimize biological growth. The water temperature throughout the experiments was 25°C

Sediment was collected from the upper Hudson River near Griffin Island (43° 12.246' N, 70° 34.891' W or river mile 189.75), homogenized in a cement mixer, added to the STORM tank to a depth of 5 cm, and smoothed to create an even surface.

Sediment samples of the homogenized mixture were collected for grain size analysis prior to lowering the sediment into the tank. The moist sediment sat on the bottom of each tank with a small amount of over lying water and consolidated for 10, 11, or 14 days in the dark before the first resuspension event was initiated. The tanks were slowly filled with clean well water just prior to the start of resuspension minimizing disturbance to the sediment surface. The freshwater used in this study was low in dissolved organic carbon (1.00 mg C L⁻¹).

Unlike in previous experiments using the STORM tanks that simulated tidal cycle resuspension (Kim et al., 2004), every resuspension event lasted three days. Mixing began in the morning of the first day and continued at a constant level for the entire three-day period. The bottom shear maintained the TSS concentration in the water column at a constant level. At the end of each three-day resuspension event, mixing was turned off and the particles were allowed to settle through a still water column for approximately 20 hours. Following settling, the water was pumped out of the tank and the sediment sat undisturbed in the dark on the bottom with ~ 1 cm of overlying water for 1, 2 or 4 days in Tank A, B, and C respectively (Figure 3.1). This resuspension cycle was repeated three times in each tank.

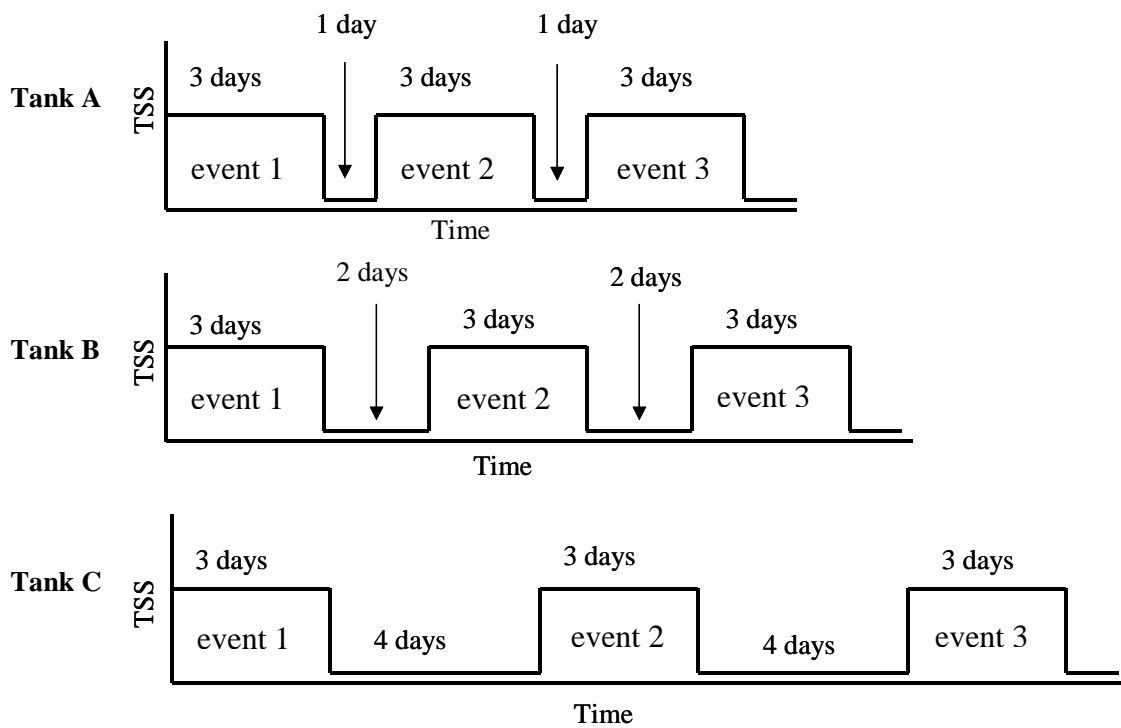


Figure 3.1. Schematic of the sequence of resuspension events conducted in the STORM tanks. The high TSS corresponds to periods when mixing was turned on. The low TSS corresponds to periods when mixing was turned off and the tanks sat with only 1 cm of overlying water.

3.2.2 Sampling Strategy

The STORM tanks were sampled most intensively on the first day of each three-day resuspension event. During the first two hours of resuspension, samples were collected every half hour. After the first two hours, samples were collected once an hour for four hours. On the second and third day of each resuspension event the tanks were sampled twice daily, once in the morning and once in the afternoon. At each sampling time point water was collected from mid depth (0.5 meter above bottom) through a siphon (flow rate $\approx 3000 \text{ mL min}^{-1}$) for total suspended solids (TSS), particulate carbon and nitrogen (CHN), chlorophyll *a* and pheopigments, and dissolved organic carbon (DOC) analysis. In addition, at each sampling time point a LISST-100C (Sequoia Scientific, Inc.) was deployed at mid depth to measure the volume concentration and size distribution of particles. Details of the LISST deployment are discussed in section 3.2.4.

3.2.3 Ancillary Water Measurements

The Nutrient Analytical Services Laboratory in Solomons, MD analyzed all water samples according to their standard procedures. After filtration, all filters were folded in half, stored in aluminum foil pouch, and frozen at -20°C until analysis. TSS was measured by filtering 100 ml of water through pre-weighed Whatman glass fiber filters (47 mm, $0.7 \mu\text{m}$ pore size), which were then dried at 105°C overnight and re-weighed. Samples for particulate carbon, hydrogen, and nitrogen analysis (CHN) were collected by filtering 50 ml of water through pre-combusted glass fiber filters (25 mm, $0.7 \mu\text{m}$ pore size). Prior to analysis the filters were removed from the freezer and dried in an oven at 45°C overnight. The samples were then combusted in an Exeter Analytical CE-440

Elemental Analyzer to measure carbon (as CO₂), hydrogen (as H₂O) and nitrogen (N₂). Chlorophyll *a* (chl *a*) and phaeopigments were collected by filtering 200 ml of water through Whatman glass fiber filters (47 mm, 0.7 μm). The filters were extracted in acetone and analyzed using a Sequoia Turner Fluorometer Model 112. Dissolved organic carbon (DOC) samples were collected in Teflon screw top bottles after water was filtered through a 0.7 μm pore size Whatman glass fiber filter and frozen at –20°C until analysis. The samples were thawed at room temperature before analysis using an OI Analytical Model 700 TOC Analyzer.

3.2.4 LISST Measurements

The LISST-100C (Sequoia Scientific, Inc.) uses laser diffraction to measure the volume concentration (μL L⁻¹) of particles 2.5-500 μm in diameter in 32 logarithmically spaced bins as long as beam transmission is greater than 30% (Traykovski et al., 1999). The conversion from light scattering to volume concentration assumes the particles in the water column are spherical and therefore the diameters reported here are spherical equivalent diameters. The LISST was deployed in the STORM tanks for five minute sample periods and collected data once every five seconds. Prior to deployment the lens of the LISST was cleaned and the cleanliness was verified by measuring light transmission through distilled water in a test chamber. Light transmission for these background scattering tests averaged 99%. For each sampling period, the average volume concentration of particles in each size bin was computed and this average profile is used for discussion and calculations in this paper. Beam transmission remained above 45% for all sampling periods. The study by Traykovski et al. (1999) showed the LISST was not able to resolve the size of sand grains greater than 250 μm. A careful

examination of our data also suggested this to be true as there was a large variance in total volume concentration for the 250-500 μm size bins during any five-minute sampling period. As a result, these size classes are not considered in the analysis of the LISST data presented in this paper. We also excluded the smallest size class in our analysis (median size 2.5 μm) because the volume concentration of this bin is incorrect when there are particles smaller than 2.5 μm in the water column (Traykovski et al., 1999).

3.2.5 Grain Size Analysis

Grain size analysis was conducted using the Beckman Coulter LS100 Laser Diffractometer. This instrument works on the same principles as the LISST and measures the size distribution of suspensions of nonsieved sediments 0.4 to 900 μm in diameter using the laser diffraction technique. Recoveries were close to 100% and measured values for the reference material were within one standard deviation of the expected values.

3.3. Results and Discussion

For comparison purposes sections 3.3.2- 3.3.4 focus on results from the first resuspension event in all three tanks. Since the initial condition in all three tanks was the same, the first resuspension event represents replicate treatments. After the first resuspension event the three tanks did not receive the same treatment because they had different quiescent times between resuspension events. In sections 3.3.5 through 3.3.7 the results of multiple resuspension events are presented for each tank individually.

3.3.1 Grain Size Analysis

The size distribution of the homogenized Hudson River sediment was tri-model with a large peak in the volume size distribution at 145 μm and two lesser peaks at 61 and 473 μm respectively. The volume median diameter of the sediment grains was 63 μm .

3.3.2 Water Column Properties

All tanks had the same applied bottom shear stress and reached steady state by the start of the second day of resuspension. The steady state total suspended solids concentration for resuspension event 1 was $60 \pm 4 \text{ mg L}^{-1}$ (Figure 3.2), $79 \pm 4 \text{ mg L}^{-1}$, and $79 \pm 5 \text{ mg L}^{-1}$ in tanks A, B and C respectively (Table 3.1) and the inter tank relative standard deviation was 15%. The differences in TSS concentration between the tanks at steady state could either be due to experimental variability or sediment consolidation time. Each three-day resuspension event began after slightly different sediment consolidation times ranging in duration from 10 to 13 days. The long consolidation time coupled with the lack of correlation between TSS concentration and consolidation time suggests it is unlikely that TSS differences are caused by consolidation time. The differences in TSS levels at steady state are more likely caused by slight variations in the experimental setup (Porter et al., 2005). In previous experiments using the STORM tanks all three tanks had the same consolidation time, yet it was also observed that Tank A had a lower TSS concentration than Tanks B and C although other variables did not vary between tanks (Porter et al., 2005).

There were no differences in the other ancillary water properties between tanks and for clarity only the results from Tank A are going to be discussed here. The organic carbon content of the resuspended particles did not change significantly during the course

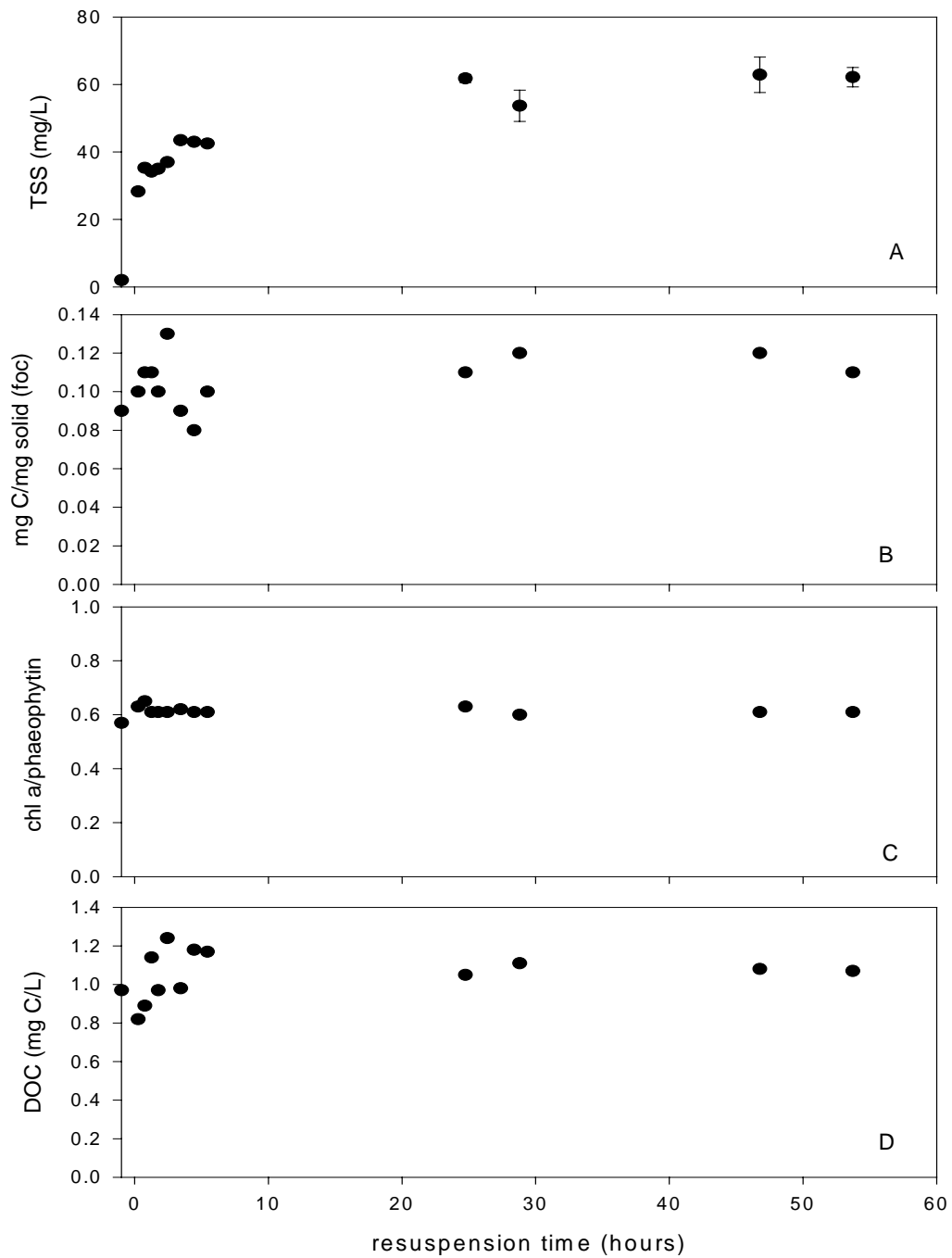


Figure 3.2. Changes in ancillary water measurements during the first three-day resuspension event in Tank A. Mixing was turned on at time zero (A) TSS (B) fraction organic carbon (C) Ratio of chl a/phaeophytin (D) DOC. Mixing was turned on at time zero and TSS reaches steady state by the start of the second day of resuspension.

	Tank	time in bed prior to mixing (days)	Initial					Steady State						
			TSS (mg/L)	TVC ($\mu\text{L/L}$)	floc porosity	bulk density (g/cm^3)	volume median diameter (μm)	TSS (mg/L)	TVC ($\mu\text{L/L}$)	floc porosity	bulk density (g/cm^3)	volume median diameter (μm)	Stokes' settling velocity (cm/s)	
Event 1	A	11	35	154	0.90	1.13	164	60	258	0.89	1.14	112	0.08	
	B	13	65	360	0.92	1.10	161	79	331	0.90	1.13	112	0.08	
	C	10	46	233	0.91	1.11	127	79	332	0.90	1.13	104	0.08	
Event 2	A	1	35	179	0.91	1.10	134	52	279	0.92	1.11	112	0.07	
	B	2						88	387	0.90	1.13	112	0.09	
	C	4	52	145	0.84	1.21	128	75	419	0.92	1.11	112	0.07	
Event 3	A	1	38	173	0.90	1.12	136	50	248	0.91	1.11	112	0.06	
	B	2	52	177	0.87	1.17	133	70	235	0.87	1.16	113	0.11	
	C	4	27	72	0.84	1.22	135	60	236	0.89	1.15	116	0.09	

Table 3.1. The initial (after 45 minutes of mixing) and steady state properties of the resuspended flocs in all STORM experiments.

of the resuspension event and at steady state the particulate organic carbon content was $11.5 \pm 0.6\%$ with $6.9 \pm 0.5 \text{ mg C L}^{-1}$ resuspended into the water column (Figure 3.2). The resuspended particles were enriched in organic carbon relative to the bulk sediment, which had an average organic carbon content of 5.5%. For comparison, the survey of water in the upper Hudson River found suspended organic carbon ranged from 0.4 to 3.4 mg C L^{-1} with an average of 1.4 mg C L^{-1} (Butcher et al. 1998). The ratio of chl *a* to phaeopigments remained constant at 0.6 for the entire duration of the experiment (Figure 3.2). This low ratio indicates the particles in the water column consisted of recycled material. The experiments were conducted in the dark and there was no phytoplankton growth during the resuspension event. DOC remained constant throughout the experiment (Figure 3.2) and was similar to the source water. At steady state the DOC was $1.08 \pm 0.03 \text{ mg C L}^{-1}$ (Figure 3.2). There was no evidence of DOC release from resuspended particles.

3.3.3 Particle Size Distribution

This section discusses the LISST data from the first resuspension event in all three tanks and uses these results to calculate floc density and porosity. For clarity the results from Tank A are presented first and then compared to results from Tanks B and C. The LISST data provides the particle size distribution in terms of the volume concentration of particles. Assuming spherical particles, the volume concentration of each size class of particles (n_{vj}) can be converted to a number concentration of each size

class of particles $n_j = \frac{n_{vj}}{\frac{4}{3}\pi r^3}$ and a surface area concentration of each size class of

particles $n_A = \frac{n_j}{4\pi r^2}$ where r is the median radius of each particle size class. The volume based size distribution highlights the presence of flocs, as most of the volume of resuspended particles is in flocs. The number and surface area distributions were dominated by small particles. In Tank A, the initial number median diameter of resuspended particles after the first 45 minutes of resuspension was 11 μm and at steady state it was 8 μm (Figure 3.3). This shift in the number median diameter with time was due to the increase in the number of particles in the 3-5 μm diameter range (Figure 3.4). Both the volume median diameter and the surface area median diameter decreased with time. Initially these particle size distributions were dominated by large particles; the volume median diameter was 162 μm and the surface area median diameter was 81 μm (Figure 3.3). At steady state, 24 hours later, the volume median diameter was 112 μm and the surface area median diameter was 54 μm (Figure 3.3).

Most of the changes in these size distributions with time occurred in the larger size classes of particles whose number distribution is near zero (Figure 3.4). For example, the particles with a median diameter of 219 μm decreased 46% by volume and 64% by surface area from the initial to steady state size distribution. The median diameter of the number, surface and volume distributions decreased between 30-40% first resuspended and then broken up with time until a steady state particle size during the course of the resuspension event (Figure 3.3). It appears that large flocs were first resuspended and then broken up with time until a steady state particle size distribution was reached. The changes in surface area and volume distribution support the idea of floc break-up in the water column. Floc disaggregation could also add smaller particles

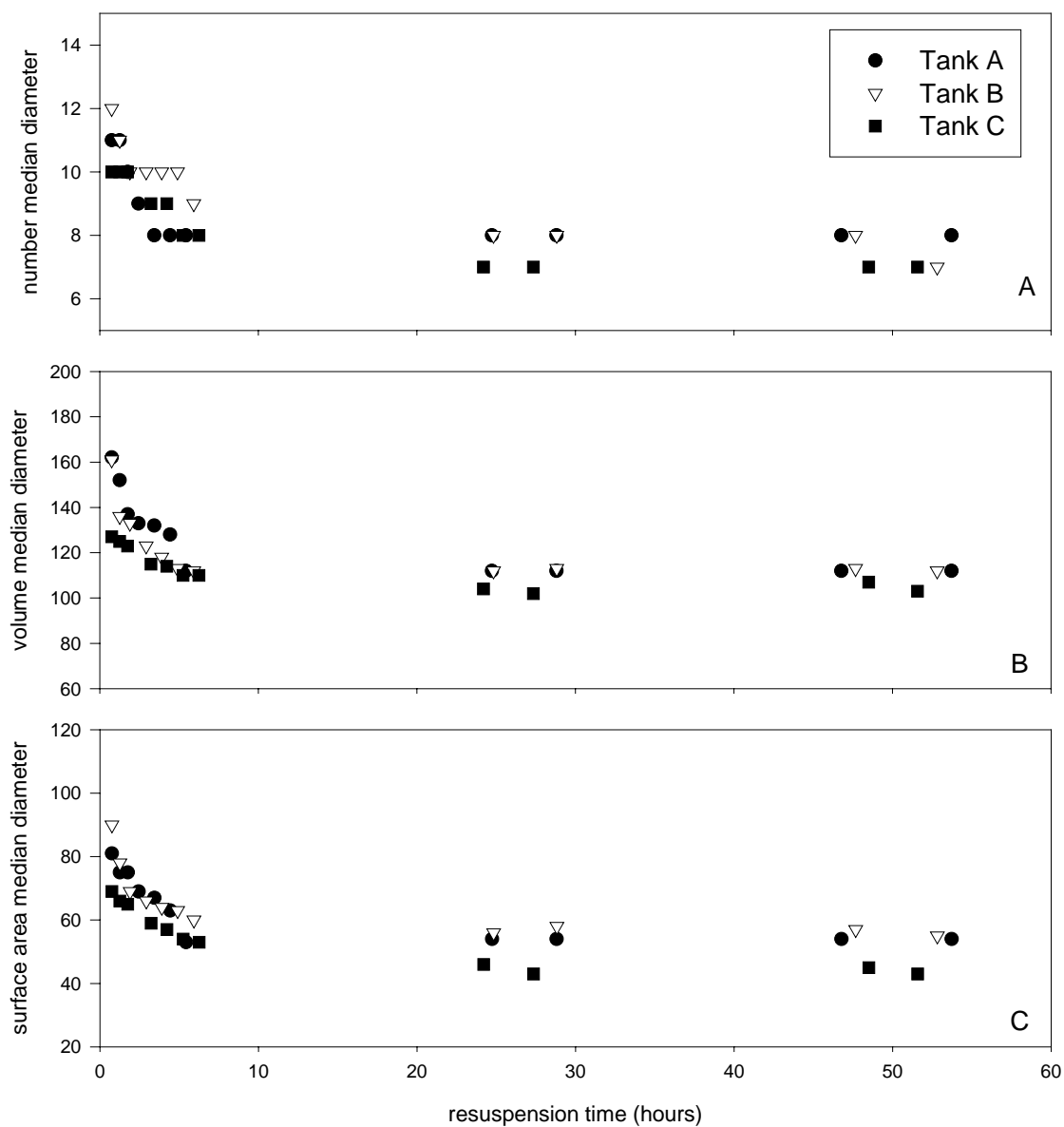


Figure 3.3. Changes in the (A) number (B) volume and (C) surface area median diameter during the course of the first resuspension event in Tank A, B, and C. Steady state is reached by the start of the second day of resuspension.

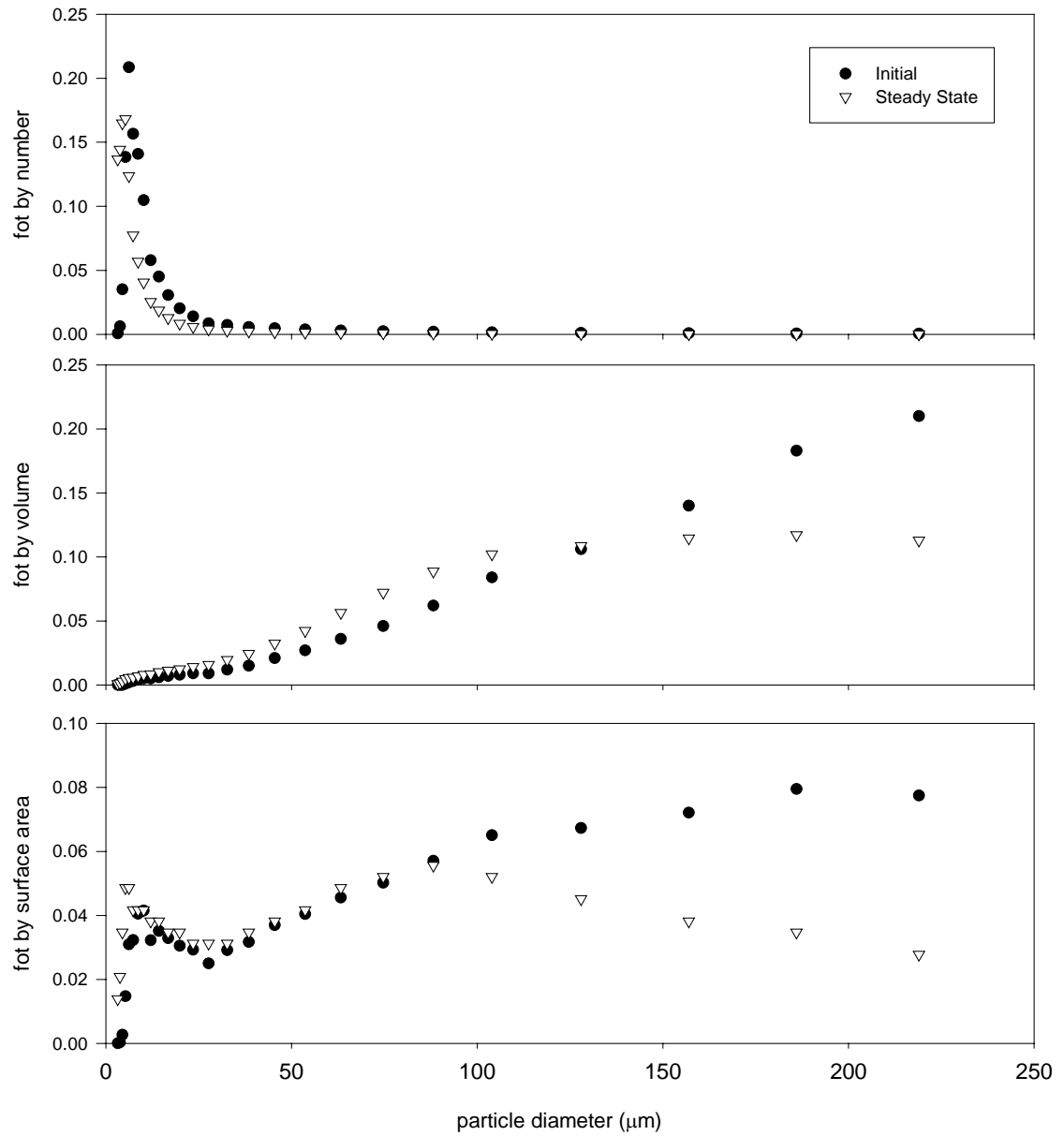


Figure 3.4. The particle size distribution expressed as fraction of total (fot) by (A) Number (B) Volume and (C) Surface Area during the first resuspension event in Tank A 45 minutes after resuspension was initiated and at steady state.

to the water column, accounting for the change in number distribution with resuspension time.

Since the changes in the surface area and number median diameter mirror the changes in the volume median diameter during the course of a resuspension event (Figure 3.3), only results of the volume median diameter are going to be discussed further in this paper. This choice was made because there is more data about the volume median diameter of resuspended particles in the literature (Mikkelsen, 2002; Van der Lee, 2000; Xia et al., 2004). There was only minimal inter-tank variability in particle size distribution during the replicate resuspension events (Table 3.1). Initially after 45 minutes of resuspension, the relative standard deviation between tanks was 13% and the volume median diameter of the flocs was 162 μm , 162 μm , and 127 μm in tank A, B and C respectively (Figure 3.3). At steady state, the relative standard deviation between tanks decreased to only 4% and the volume median diameter was 112 μm in tank A and B and 104 μm in tank C (Table 3.1). These slight differences in particle size distribution are attributed to experimental variability.

In the Dollard estuary, the mass weighted average floc diameter measured using a video camera was 150 μm and did not vary seasonally (Van der Lee, 2000). Near the Danish coast in the North Sea, the volume median diameter of aggregates as measured by a LISST was 322 μm in June and 117 μm in April (Mikkelsen, 2002). This same study found the volume median diameter of flocs in the Horsens Fjord ranged between 23 and 164 μm in June and September (Mikkelsen, 2002). The volume median diameter of particles along the Pearl River in China measured by the LISST-ST during the wet and dry season ranged from 8.7 to 105.6 μm (Xia et al., 2004). During the wet season the

volume median diameters were larger because the particles flocculated more than during the dry season. In that study floc size was only weakly correlated to salinity. None of these studies converted volume distributions to surface area or number distributions.

The LISST data and TSS measurements were used to calculate the gross bulk density and porosity of the resuspended flocs following procedures in Sanford et al. (2005). Again, for clarity only results from Tank A are discussed in this section and results from Tanks B and C are discussed in sections 3.4 and 3.5, respectively. These calculations cannot be conducted for each size class of particles because the TSS measurement is for the bulk particles in the water column. Nevertheless, it is useful to examine the bulk properties of the particle populations. Here TVC is the total volume concentration measured by the LISST, Vol_w is the water volume, ρ_s is the density of the solid, ϕ_s is the solids fraction of the floc, Vol_f is the floc volume, and $\phi = 1 - \phi_s$ is the porosity. The following equations assume that the $Vol_w \gg Vol_f$.

$$TSS = \frac{\text{mass of particle}}{Vol_w} = \frac{Vol_f * (\rho_s \phi_s)}{Vol_w} \quad (1)$$

$$TVC = \frac{Vol_f}{Vol_w + Vol_f} \approx \frac{Vol_f}{Vol_w} \quad (2)$$

$$\frac{TSS}{TVC} = \rho_s \phi_s \quad (3)$$

If ρ_s is assumed to be a linear combination of the mineral solids density (2.65 g cm^{-3}) and the density of the organic matter on the particle (1.05 g cm^{-3}) then the above equations can be solved for the porosity of the particle (Sanford et al. 2005). In the STORM tanks the resuspended particles consisted of 24% organic matter (foc*2.1) and 76% mineral solid so $\rho_s = 2.27$ g cm^{-3} , and the porosity of the resuspended flocs averaged 0.91 ± 0.01 (n = 12) during event 1, and did not change systematically with resuspension

time. The bulk density of the floc, ρ_f , was then calculated using the following equation (Sanford et al., 2005):

$$\rho_f = \rho_s \phi_s + \rho_w \phi \quad (4)$$

Floc bulk density averaged $1.12 \pm 0.02 \text{ g cm}^{-3}$ ($n = 12$) during event 1 and there was no trend in bulk density with resuspension time (Table 3.1). The high porosity and low bulk density is further evidence that the resuspended particles were light, watery flocs. For comparison, in the upper Chesapeake Bay bulk densities calculated using the same method ranged from 1.02 to 1.30 g cm^{-3} (Sanford et al. 2005). Calculated bulk densities in the San Pablo Straight based on a video camera observations and TSS measurements averaged 1.08 g cm^{-3} (Kranck and Milligan, 1992). Estimates for aggregated sediment bulk densities made using a viscometer averaged 1.14 g cm^{-3} in the San Francisco Bay and 1.07 g cm^{-3} in the Brunswick Harbor (Krone, 1976). Xia et al. (2004) calculated bulk densities of particles in the Pearl River from their observed settling velocities, finding that $100 \mu\text{m}$ particles had an average bulk density of 1.02 g cm^{-3} .

3.3.4 *Settling*

There are many different methods for calculating the settling velocity of the resuspended flocs, each with its own limitations. One method is to utilize the results of equations 1 through 4 and Stokes' law. This method calculates a settling velocity based on the steady state conditions in the STORM tanks. Again for clarity only results from Tank A are presented in this section. The excess density, $\Delta\rho$, is calculated based on the density of the floc determined in equation 5:

$$\Delta\rho = \rho_f - \rho_w \quad (5)$$

Once the effective density is determined, Stokes' law can be applied as long as the Reynold's number is less than 1 and spherical particles are assumed.

$$W_s = \frac{gd_{mv}^2 \Delta\rho}{18\mu} \quad (6)$$

In the above equation d_{mv} is the volume median diameter, μ is the dynamic viscosity of water, and g is acceleration due to gravity. Applying the above equations to the STORM tank data at steady state yields an apparent settling velocity of 0.08 cm s^{-1} .

The LISST data can also be used to calculate a settling velocity. The LISST was placed into the STORM tank just prior to turning off the mixing and measured the change in volume concentration over the first 60 minutes of settling. With the mixing turned off the STORM tanks became large settling chambers. There was no change in the total volume concentration during the first seven minutes of settling for any of the size classes of particles (Figure 3.5) after which the volume concentration of the larger particles began to decrease rapidly. If it is assumed that this time period represents the delay before the settling particle front passed the LISST, than a rough estimate of settling velocity is to divide the depth at which the LISST was deployed (50 cm) by seven minutes. This calculation results in a settling velocity of 0.12 cm s^{-1} .

The TSS data can be used to calculate the settling velocity by yet another method. The TSS data did not exhibit frontal settling; instead TSS declined from the moment mixing was turned off (Figure 3.5). The decrease in total suspended solids was also confirmed by optical backscatter (OBS-3, D&A Instrument Company). Estimating settling velocity from this decline in total suspended solids data in TSS and is a bit imprecise because it is assumed the TSS decrease linearly with time. One method is to determine the time it took for half the mass to settle through the tank. Since all the TSS

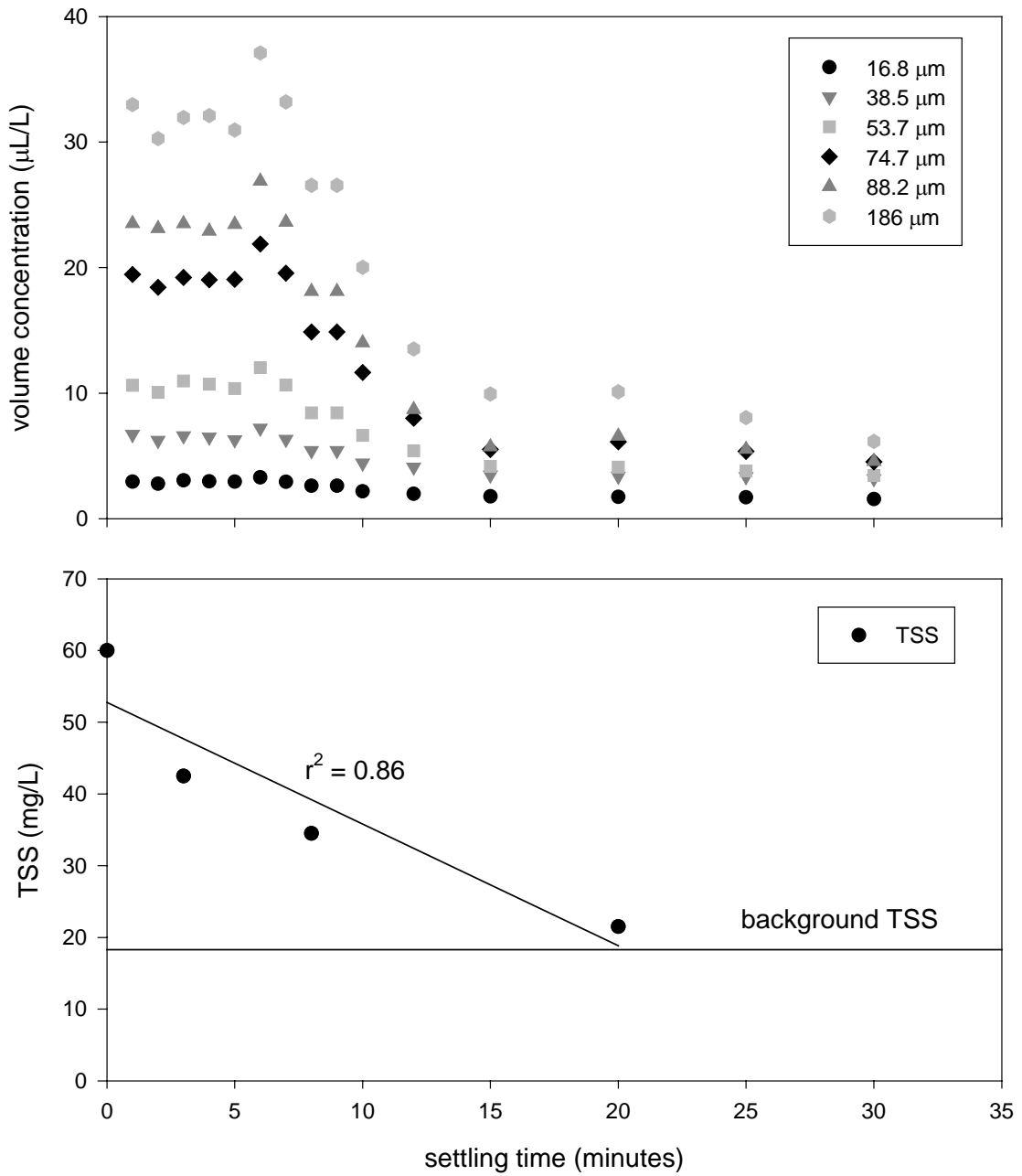


Figure 3.5. (A) The total volume concentration of various size classes of particles as they settle through STORM Tank A. (B) The corresponding measured total suspended solids concentration.

did not settle out of the water column during the twenty hours of settling, this calculation depends on a chosen final TSS concentration. To better compare this data with the LISST data, the final concentration was selected to be the TSS concentration at 60 minutes (see Figure 3.5). This calculation results in a settling velocity of 0.10 cm s^{-1} . In spite of the uncertainties in the three individual estimates, the fact that all three methods yield very consistent settling velocities averaging $0.10 \pm 0.02 \text{ cm s}^{-1}$ is reassuring.

A LISST attached to a settling column was used to measure the settling velocity of particles at various locations throughout the Pearl River (Xia et al., 2004). At TSS concentration ranging from 20.4 and 39 mg L^{-1} , the particles had median settling velocities ranging between 0.0064 to 0.024 cm s^{-1} . A video camera deployed in the Dollard estuary where the suspended solids concentration was 350 mg L^{-1} measured the average settling velocity of $110 \text{ }\mu\text{m}$ flocs to be 0.2 cm s^{-1} (Van der Lee, 2000). Van Leussen (1999) compiled literature data on in-situ measurements of median settling velocities of mud flocs as a function of suspended solids concentration. For TSS concentrations ranging between 60-100 mg L^{-1} , settling velocities ranged from 0.004 cm s^{-1} to 0.04 cm s^{-1} in saline waters. Fugate and Friedrichs (2002) deployed an Acoustic Doppler Velocimeter at the Cherrystone site in the Chesapeake Bay where the TSS concentration ranged from 15 to 55 mg L^{-1} and calculate settling velocities ranging from 0.07 to 0.13 cm s^{-1} . Floc settling velocities derived from video settling tube estimates in the upper Chesapeake Bay ranged between 0.02 - 0.50 cm s^{-1} , with a mean of 0.15 cm s^{-1} (Sanford et al. 2005).

The TVC data suggests there was a change in the particle composition during settling. Prior to the start of settling the volume median diameter of the resuspended

particles was 112 μm and strands of detritus too large to be measured by LISST were suspended in the water column. After 60 minutes of settling the volume median diameter of the particles in the water column was 72 μm (Figure 3.6). Examining particles collected on GFF filters throughout the settling event under a microscope illustrated this change in particle composition (Figure 3.7). During resuspension and even after three minutes of settling, large flocs and detritus remained in the water column. During this three-minute time period the TVC did not change but the TSS decreased. This could happen if flocculation and settling were occurring simultaneously such that new large flocs were being formed at roughly the same rate as they were settling out or small dense flocs were rapidly settling out of the water column. After 20 minutes of settling, when the TVC had changed dramatically, no large pieces of detritus remained in the water column and only smaller particles were collected on the filter. Nineteen hours after the paddle was turned off small fine particles still remained in the water column (Figure 3.7). The fraction of organic carbon on the settling particles decreased from 12% to 9% after 60 minutes of settling, consistent with the settling out of organic rich detritus.

3.3.5 Multiple Resuspension Events in Tank A

A total of three resuspension events each three days in duration were conducted in STORM Tank A. There was one day of quiescence between each event to allow the sediment to consolidate during which only a thin layer of water remained over the sediments (Figure 3.1). The steady state TSS concentration was $60 \pm 4 \text{ mg L}^{-1}$, $52 \pm 2 \text{ mg L}^{-1}$ and $50 \pm 4 \text{ mg L}^{-1}$ for resuspension events 1, 2 and 3 respectively (Table 3.1). The steady state volume median diameter was the same for all three resuspension events averaging $112 \pm 2 \text{ }\mu\text{m}$ ($n = 12$; Table 3.1). The particle size distributions differed

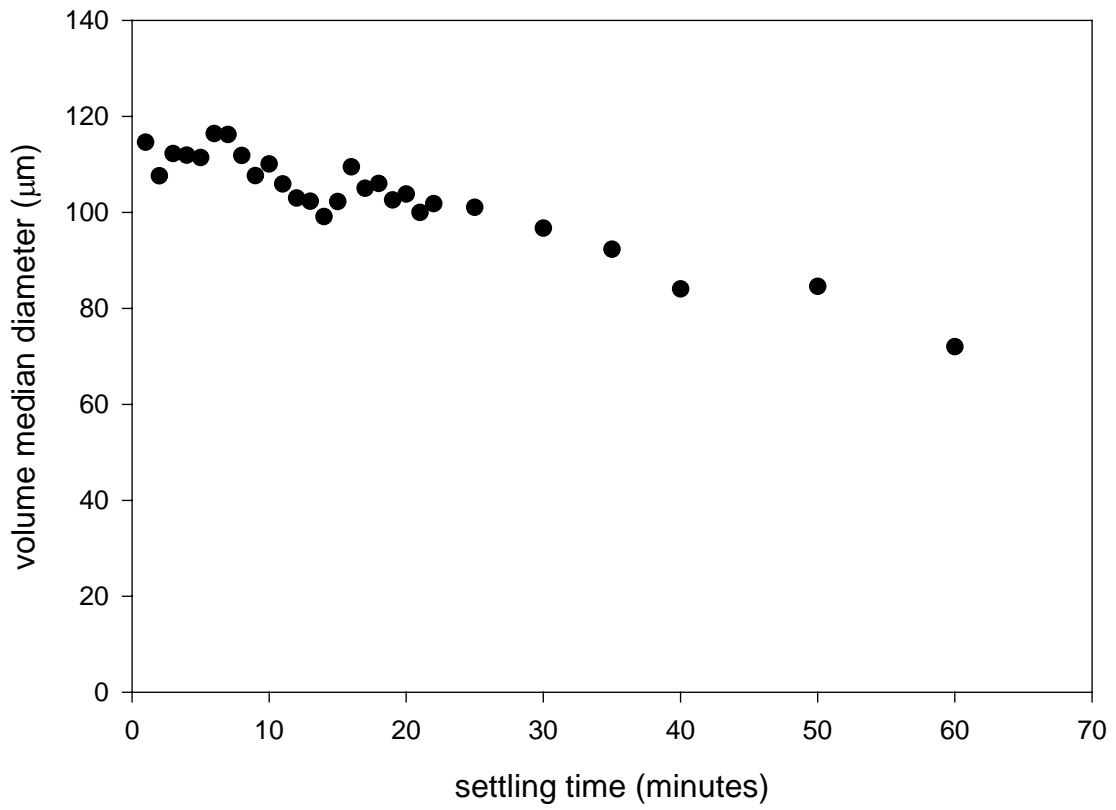
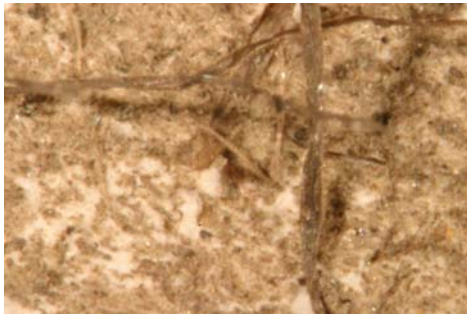
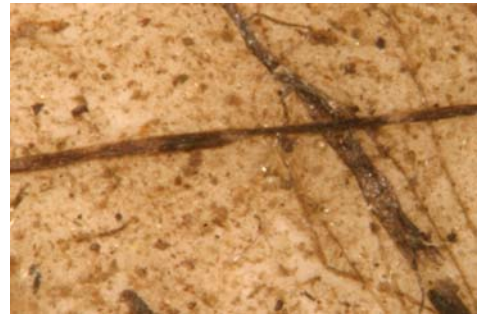


Figure 3.6. The volume median diameter of the settling particles in STORM Tank A.



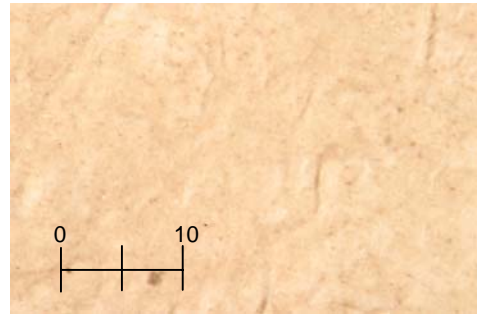
resuspension on



3 minutes of settling



20 minutes of settling



19 hours of settling

Figure 3.7. The settling particles collected on glass fiber filters and magnified to 2.5 power. The scale shows ten microns.

between the resuspension events when mixing first began. After the first 45 minutes of resuspension the volume median diameter was 162 μm , 134 μm , and 136 μm for resuspension events 1, 2 and 3 respectively (Figure 3.8). The initial similarity of event 2 and 3's particle size distributions suggests the approach to steady state of resuspension event 1 represents an initial adjustment period. Previous studies in the STORM tanks support this hypothesis. For example, in experiments with Baltimore Harbor sediment it took several six-hour periods of tidal cycle resuspension (4 hours of mixing, 2 hours off) before the TSS concentration resuspended to a constant value when mixing was turned on (Kim et al. 2004). While that study did not examine the size distribution of the resuspended particles, it suggests there might be an initial experimental adjustment period.

For all resuspension events in our experiments there was no systematic change in porosity (Figure 3.9) or aggregate bulk density during the course of each resuspension event and there were no significant differences between resuspension events. For all three resuspension events the calculated porosity of the resuspended particles averaged 0.92 ± 0.02 ($n = 35$) and the calculated bulk density averaged $1.11 \pm 0.02 \text{ g cm}^{-3}$ ($n = 35$; Table 3.1).

3.3.6 Tank B: Two days quiescence between resuspension events

In the series of three resuspension events conducted in Tank B there was two days quiescence between the end of one event and the start of the next event (Figure 3.1). Unlike in the other tanks, the first time the sediment in this tank was resuspended the TSS concentration rose to 65 mg L^{-1} in the first 45 minutes of resuspension. This concentration represents 82% of the steady state value of $79 \pm 5 \text{ mg L}^{-1}$. For comparison,

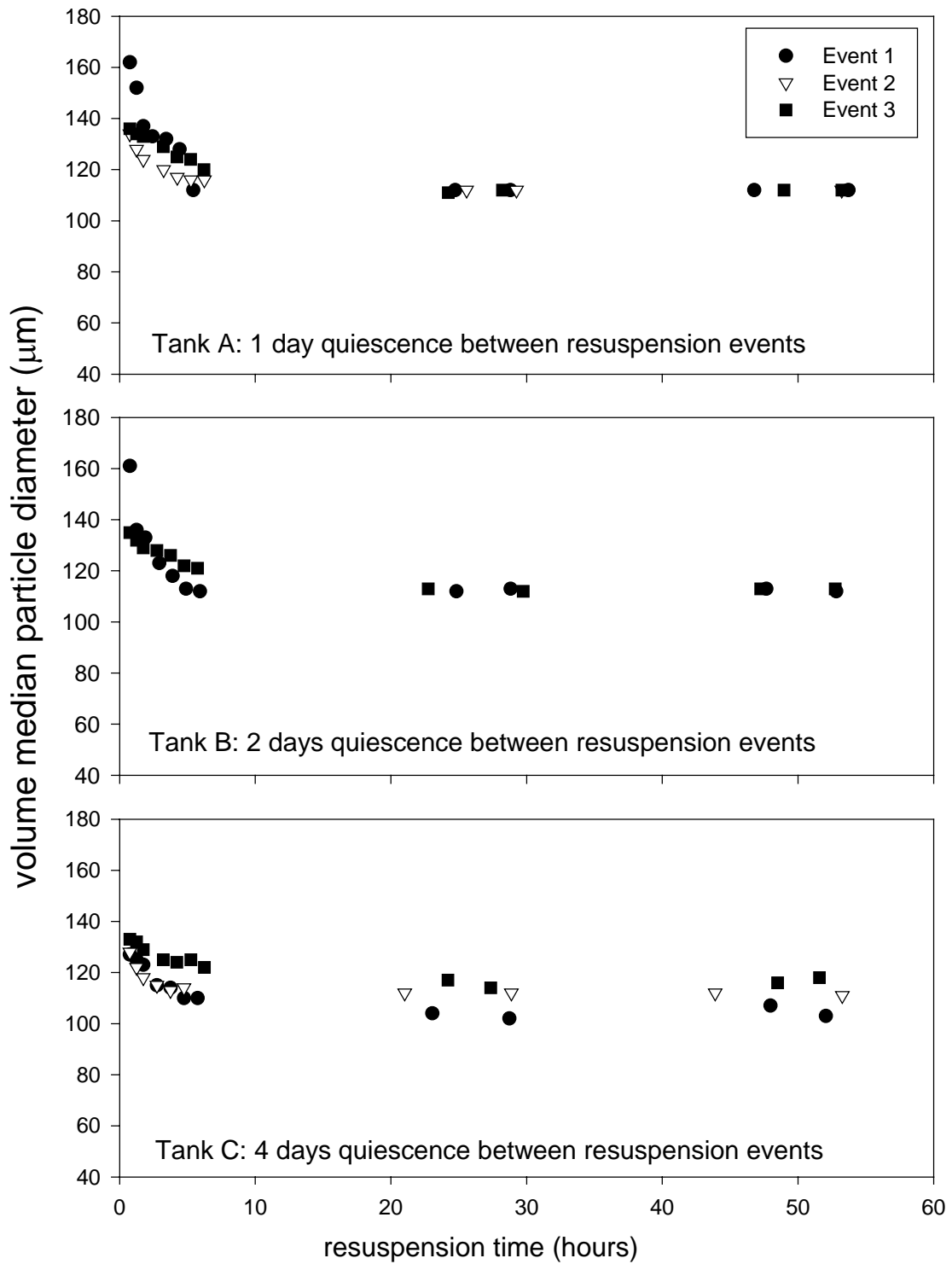


Figure 3.8. The volume median diameter of resuspended flocs in the STORM tanks during multiple resuspension events.

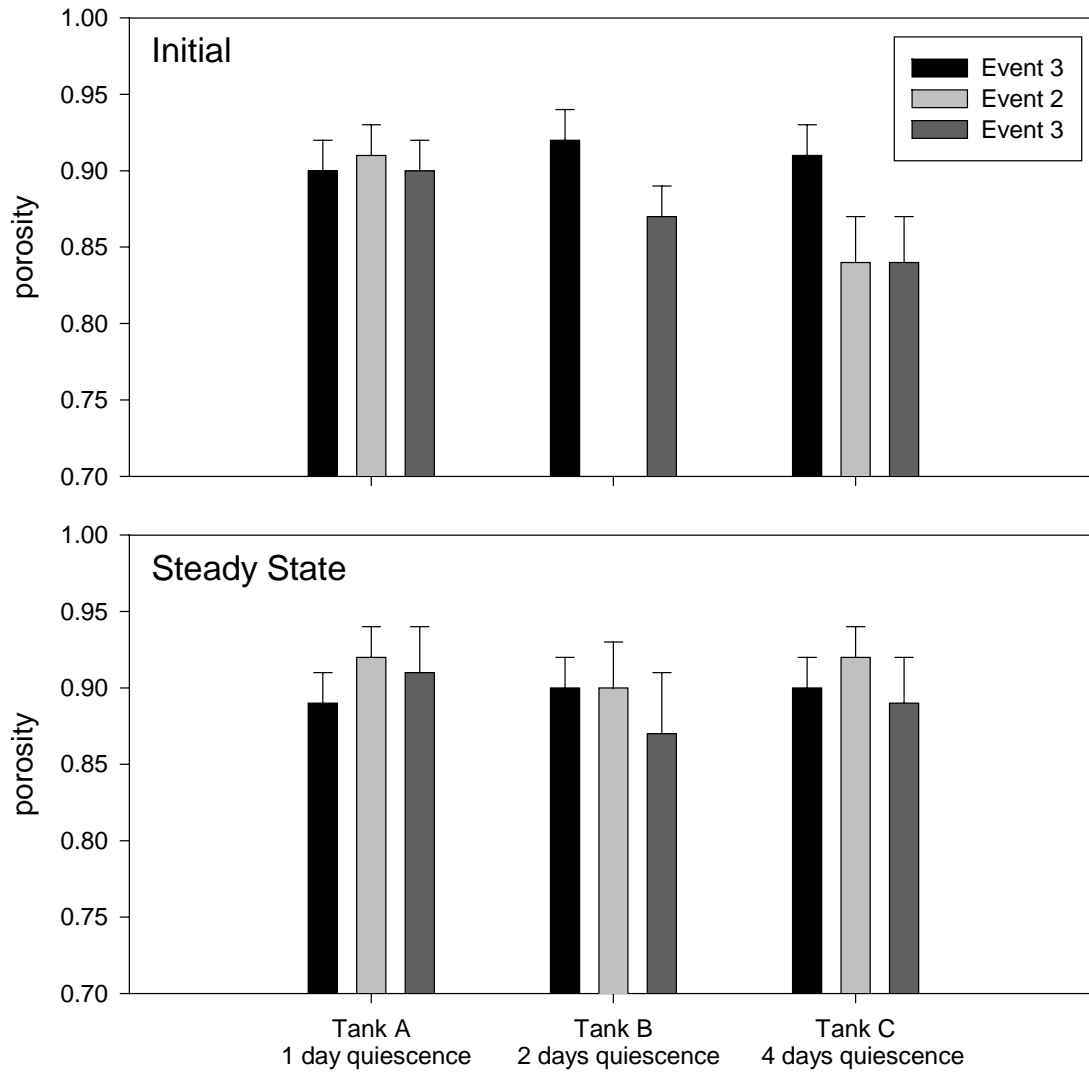


Figure 3.9. Initial and steady state porosity of the resuspended flocs. The initial floc porosity in Tank B and C was lower for event 2 and 3 than for event 1. There were no significant differences in steady state porosity between tanks or events.

in both Tank A and Tank C after 45 minutes of resuspension the TSS concentration was 58% of the steady state (Table 3.1). The LISST data for resuspension event 2 shows that a slug of sediment entered the water column during the initial resuspension period when an object was dropped into the tank. As a result, the data from the first day of this resuspension event was excluded from analysis. Steady state conditions from this resuspension event were examined because the impact of dropping an object into the tank did not last beyond the first day and subsequent examination of the sediment surface did not reveal much sediment disturbance.

Despite differences in total suspended solids, the change in volume median diameter over the course of the resuspension event was similar to the other STORM tanks (Figure 3.8). Initially after 45 minutes of resuspension the volume median diameter was 161 μm and 135 μm for resuspension event 1 and 3 respectively. Again it appears as if the first event's approach to steady state represents an initial adjustment period. At steady state the volume median diameter averaged $113 \pm 1 \mu\text{m}$ ($n = 12$) for all three resuspension events (Table 3.1).

Initially at the start of the first resuspension event calculated floc porosity and density were 0.92 ± 0.02 and $1.10 \pm 0.03 \text{ g cm}^{-3}$ (Table 3.1). When the third resuspension event began after two days of quiescence the particles re-eroded as denser less porous flocs ($\rho = 1.17 \pm 0.02 \text{ g cm}^{-3}$, $\phi = 0.87 \pm 0.01$, Figure 3.9). However, the steady state properties of the flocs for all three resuspension events were not significantly different, the porosity averaged 0.89 ± 0.03 ($n = 12$) and bulk density averaged $1.15 \pm 0.03 \text{ g cm}^{-3}$ ($n = 12$; Table 3.1).

3.3.7 Tank C: Four days quiescence between resuspension events

In Tank C a similar series of resuspension events was conducted but there were four days of quiescence between each resuspension event (Figure 3.1). At steady state the TSS concentration was $79 \pm 4 \text{ mg L}^{-1}$ for event 1, $75 \pm 9 \text{ mg L}^{-1}$ for event 2, and $60 \pm 6 \text{ mg L}^{-1}$ for event 3 (Table 3.1). There was no difference in the median diameter of the particles among resuspension events. For all three events, the initial volume median diameter averaged $129 \pm 3 \text{ }\mu\text{m}$ ($n=3$). The particles disaggregated with time and at steady state the average volume median diameter was $111 \pm 6 \text{ }\mu\text{m}$ ($n=12$; Figure 3.8 and Table 3.1).

After the first resuspension event and four days of quiescence, the resuspended flocs were less porous and re-eroded as denser particles (Table 3.1). During the approach to steady state the flocs became more porous and less dense (Figure 3.9). This change in the initial properties of the resuspended particles between events was similar to the change observed in Tank B. At steady state the density and porosity of the particles in Tank C was similar to the other tanks (Figure 3.9). The calculated steady state porosity averaged 0.90 ± 0.02 ($n=12$), and the corresponding bulk density averaged $1.13 \pm 0.02 \text{ g cm}^{-3}$ ($n=12$) for all three resuspension events (Table 3.1).

3.4 Conclusions

Large particles were lifted into the water column immediately following the initiation of resuspension. As resuspension time progressed the volume median diameter of the resuspended particles decreased and flocs disaggregated. The quiescent time between resuspension events did not affect the steady state properties of the resuspended particles. For all resuspension events, a steady state size distribution was reached by the

start of the second day of resuspension and the volume median diameter of the flocs was $112 \pm 3 \mu\text{m}$ ($n = 36$). When both realistic bottom shear stress and water column turbulence were simulated in the same experiment the resuspended particles took longer to reach steady state than either bottom shear or water column turbulence experiments conducted alone predict (Manning and Dyer, 1999; Tsai et al., 1987; Tsai and Lick, 1988). At steady state the resuspended flocs had an average porosity of 0.90 ± 0.02 ($n = 36$). These open watery flocs were had an average steady state bulk density of $1.13 \pm 0.02 \text{ g cm}^{-3}$ ($n = 36$). The median diameter, porosity, and bulk density of the resuspended particles were similar to those observed in the field, further validating the use of the STORM tanks to simulate resuspension and settling events.

During the initial time period when mixing first began, a quiescent times of one day between resuspension events resulted in particles with similar porosities and densities. When the quiescent time was increased to two or four days it appears as if the flocs that formed initially were less porous than in Tank A (Figure 3.9). The flocs that formed at the start of the second and third resuspension event in Tanks B and C were less porous and denser than at the start of the first resuspension event. During the approach to steady state the flocs became more porous and less dense. Despite initial differences in the properties of the resuspended flocs between the tanks, quiescent time did not affect the steady state properties.

The particles in the STORM tank did not settle according to a first order loss process and it was difficult to precisely calculate a settling velocity. Both the TSS and the LISST data clearly showed the settling velocity of the particles changed with time. Several methods of calculating the settling velocity for the first sixty minutes after

mixing was turned off suggest that the particles first settled at a rate of $0.10 \pm 0.02 \text{ cm s}^{-1}$. There was a clear change in the particle composition with time after mixing stopped. During the first three minutes of settling, the total suspended solids declined but the total volume concentration remained constant. An examination of the settling particles under the microscope showed that the organic detritus rapidly settled through the water column during the first 20 minutes of settling leaving behind the light fine-grained material. After 60 minutes of settling, 30% of the particles by mass and 20% of the particles by volume still remained in the water column. Even after 19 hours without mixing, this material did not fully settle out of the water column. In the Hudson River, this non-settling material could potentially be carried downstream transporting PCBs far from the original site of contamination.

Chapter 4: PCB Partitioning to Flocculated Hudson River Sediment: Recharge of the Labile Pool During Quiescent Periods

4.1 Introduction

The upper Hudson River in New York State (USA) is severely contaminated with polychlorinated biphenyls (PCBs). The river's sediments are the largest reservoir of PCBs in the system, and mass balance calculations show that long-term, chronic releases of PCBs from the sediments can account for the PCB inventory in the water column (Thomann et al., 1991). Resuspension of surficial sediments occurs naturally during high river flows and tidal cycles. Understanding the release of PCBs during these events is critical for assessing remediation plans and evaluating the impact on dissolved PCB concentrations. However, most studies examining PCB partitioning to sediment do not mimic resuspension under realistic physical conditions. Typically PCB desorption is studied by vigorously mixing, shaking or rolling contaminated sediment in clean water (Borglin et al., 1996; Brusseau et al., 1991; Carroll et al., 1994; Lamoureux and Brownawell, 1999).

It is difficult to realistically resuspend sediment in the laboratory and only a handful of studies have attempted to simulate the bottom shear stress or water column turbulence levels typically encountered in a river. Latimer et al. (1999) used a particle entrainment simulator (PES) to resuspend sediment at regulated shear stresses. The PES created shear stress by oscillating a grid in the water column over a sediment core. This movement produced realistic bottom shear stresses but the water column turbulence was unrealistically high. The authors measured particulate PCBs but not dissolved PCBs due to water volume limitations. This study found that at a bottom shear stress of 2 dynes

cm^{-2} , the resuspended particles were enriched in PCBs and organic carbon relative to the bulk sediment. As shear stress was increased, both the organic carbon content and PCB concentration of the resuspended particles decreased. At a shear stress of 5 dynes cm^{-2} , the PCB concentration of the resuspended material was the same as the bulk sediment. This suggests that models assuming the PCB concentration of particles resuspended at low shear stress is equal to the sediment concentration will underestimate PCB release into the dissolved phase.

Lick and colleagues took a different approach to simulating resuspension events (Borglin et al., 1996; Jepsen et al., 1995; Jepsen and Lick, 1996; Lick and Rapaka, 1996; Tye et al., 1996). In this series of experiments they added specific suspended solids concentrations to the water column rather than resuspending sediment off the bed. They used this design to examine the influence of particle flocculation on hexachlorobenzene partitioning. At a total suspended solids (TSS) concentration of 10 mg L^{-1} , floc formation and sorption reached steady state in approximately 60 hours. At this suspended solids concentration the flocs were light and watery with a density of 1.008 g cm^{-3} and a porosity of 0.995. As the suspended sediment concentration increased, flocs formed more quickly and apparent equilibrium was reached more slowly. At a TSS concentration of 500 mg L^{-1} steady state floc formation was reached in 4.5 hours but apparent sorptive equilibrium was not reached for 480 hours (Tye et al., 1996). At this TSS concentration the bulk density of the flocs was 1.41 g cm^{-3} and the porosity of the flocs was 0.74. Lick et al. concluded that the time to reach equilibrium varied greatly with TSS because of the changes in the properties of the resuspended flocs (Lick and Rapaka, 1996).

One unresolved question is whether resuspended particles remain in the water column long enough to reach sorptive equilibrium. Karickhoff et al. (1979) observed that the partitioning of HOCs to a variety of sediment types depends on the octanol water partition (K_{ow}) coefficient of the HOC and the fraction of organic carbon present in the sediment. They developed an equation to predict the equilibrium partition coefficient based on these two parameters and formulated a new parameter, the organic carbon normalized partition coefficient (K_{oc}). Field measurements, however, have only found weak correlations between measured partition coefficients, suspended solids organic carbon content, and K_{ow} . Additionally, there is wide scattering in field measurements of K_{oc} and for a single congener the measured K_{oc} value often varies by over an order of magnitude at a given site (Baker et al., 1991; Gobas and MacLean, 2003; Sobek et al., 2004). In the Hudson River, the deviation from Karickhoff's prediction is especially pronounced for the low molecular weight congeners (Figure 4.1, data from Butcher et al. 1998).

Explanations for these observations traditionally fall into three categories: colloidal interference, non-equilibrium, or particle heterogeneity. In the colloid theory, the inclusion of colloids in the dissolved phase measurement biases the calculation of the partition coefficient. For example, Butcher et al. (1998) theorized that DOC bound PCBs in the Hudson River accounted for a significant fraction of the measured dissolved concentration of high molecular weight PCBs. They theorized that the truly dissolved concentration was lower than measured by XAD extraction. In this case, correcting for DOC would enhance the observed deviation from Karickhoff's prediction. The non-equilibrium theory attributes the natural variability to the amount of time the particles

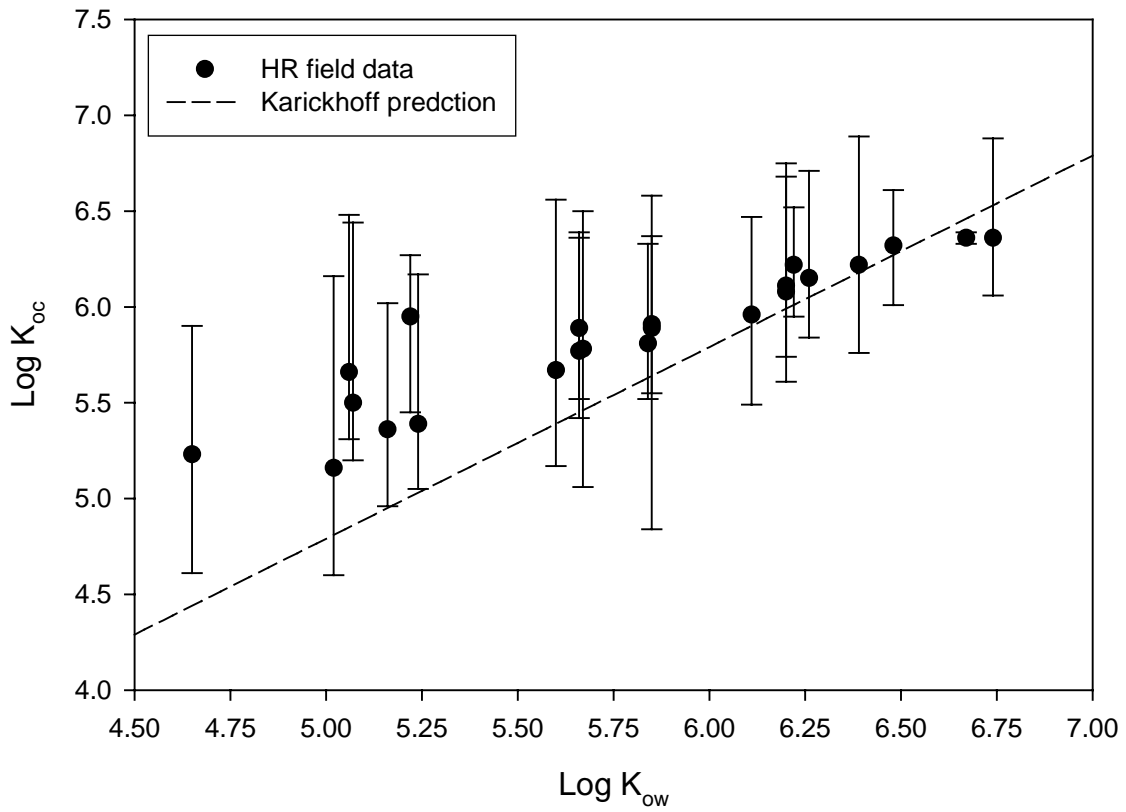


Figure 4.1. Organic carbon normalized partition coefficients for various PCB congeners measured in the Hudson River (average, maximum, and minimum) compared to the values predicted by Karickhoff (data from Butcher et al. 1998).

were resuspended in the water column. Valsaraj and Thibodeaux (1999) re-analyzed field data from a variety of studies and showed the variation in K_{oc} could be caused by differences in the amount of time the particles had been suspended in the water column.

A third theory to explain why partition coefficients are higher than predicted based on the percent of organic carbon present in the particles is the super sorbent theory. In this paradigm, particles suspensions are heterogeneous mixtures of both organic carbon and black carbon (Accardi-Dey and Gschwend, 2003). The black carbon absorbs PCBs more strongly than organic carbon and acts as a “super” sorbent. Partition coefficients measured in the field reflect partitioning to both forms of carbon. The presence of even small concentrations of black carbon greatly increases the binding of PCBs to particles because PCB-black carbon partition coefficients (K_{BC}) are 2 to 3 orders of magnitude higher than PCB-organic carbon partition coefficients (Jonkers and Koelmans, 2000). For some types of black carbon, K_{BC} values are not strongly correlated to K_{ow} (Jonkers and Koelmans, 2000).

Laboratory experiments show that desorption of PCBs from particles can be modeled as a two-stage process; the first (‘labile’) is rapid and the second (‘resistant’) is slow. Much of the research into PCB desorption has focused on understanding and modeling the resistant pool (Cornelissen et al., 2000; Pignatello and Xing, 1996; Ten Hulscher et al., 1999; van Noort et al., 2003). However, resuspension events typically last on the order of hours to days and it is unlikely particles in rivers are suspended into the water column long enough for desorption of the resistant fraction to contribute significant amounts of dissolved PCBs. Studies either assume the labile pool is at equilibrium with the water (e.g. Brusseau et al., 1991) or calculate a specific rate constant

for the labile fraction (e.g. Lamoureux and Brownawell, 1999). Estimates of the percent of PCBs in the labile pool vary considerable from study to study. For example, Cornelissen et al. (1997) spiked sediment with PCBs and found between 70-85% were in the labile pool when the sediment was allowed to equilibrate for only 2 days before desorption experiments were initiated. When the equilibration time increased to 37 days, 33-52% of the PCBs were in the labile pool. Carroll et al. (1994) found that between 55-76% of the PCBs in Hudson River sediment were in the labile fraction.

It is unclear whether a labile pool is replenished from a more resistant pool as sediments sit unmixed on the river bottom. If PCBs rapidly migrate from a resistant pool to a labile pool, then every time a particle is lifted from the sediment bed it will undergo the first rapid labile stage of the desorption process. On the other hand, if PCBs diffuse slowly into a labile pool, desorption during resuspension events will largely be a result of the second slower resistant stage of desorption. Spectroscopic investigations of the binding of 1,2 dichloroethane (DCA) to humic and fulvic acids by Aochi and Farmer (1997) showed two different sorbed species. The first species was labile and sorbed to the organic matter within 30 minutes. The second species was detected only after several hours of sorption and increased in intensity throughout the experiment. Results from this experiment suggest chemicals will rapidly diffuse into and out of the labile portion of the particles during resuspension and settling; however, PCBs are much larger molecules than DCA.

This study utilized the Shear Turbulence Resuspension Mesocosms (STORM) to examine the partitioning of PCBs to Hudson River sediment. Unlike other apparatus used to produce resuspension in laboratory settings, the STORM tanks mimic both

bottom shear stress and water column turbulence (Porter et al. 2005). These large tanks resuspend sediment to concentrations of $\sim 80 \text{ mg L}^{-1}$ while generating minimal turbulence. Under these conditions, the resuspended particles adhered to each other and form flocs in the water column (Chapter 3). Solid phase microextraction (SPME) was used to measure dissolved PCBs so that colloids would not be included in our measurement of dissolved PCBs (Chapter 2), enabling a more accurate calculation of K_{oc} values. The STORM tank's ability to easily start and stop resuspension events allowed us to explore the movement of PCBs between a labile and more resistant pool. In this experiment, we varied the quiescent time between resuspension events allowing the sediment to sit on the bottom for various lengths of time in order to examine the recharge of the labile pool.

4.2 Materials and Methods

4.2.1 STORM Tanks

Resuspension events were conducted in three Shear Turbulence Resuspension Mesocosms (STORM) tanks described previously in Porter et al. (2005). In each STORM tank a paddle rotated just above the bottom around a central shaft, resuspending sediment without generating excessive water column turbulence. The instantaneous maxima bottom shear stress of about 1 dyne cm^{-2} resulted in significant resuspension, but the time and spaced averaged bottom shear stress was $0.07 \text{ dyne cm}^{-2}$. Sediment was collected from the upper Hudson River near Griffin Island ($43^{\circ} 12.246' \text{ N}$, $70^{\circ} 34.891' \text{ W}$, river mile 189.75) and added to the STORM tanks to a depth of 5 cm. In each tank

the sediment surface area was 1m² and the water column was 1 m deep with a total volume of 1000 L. To minimize biological growth, a large reflective tarp tent was constructed over the STORM tanks so that all experiments were conducted in the dark.

A series of three resuspension events was conducted in each tank. A detailed description of the resuspension experiments is presented in Chapter 3 and briefly summarized here. Each resuspension event lasted three days; mixing began on the morning of day one and continued uninterrupted for the entire three-day period. The slowly rotating paddle maintained the total suspended solids (TSS) concentration in the water column at a constant level. At the end of each three-day resuspension event, mixing was stopped and the particles were allowed to settle through the water column for approximately 20 hours. Following settling, the water was pumped out of the tank. The sediment sat at the bottom of the tank with only ~1 cm of overlying water until the start of the next resuspension event when clean well water was slowly added back to the tank. In STORM Tank A there was 1 day of quiescence between resuspension events, in Tank B there was two days quiescence between events, and in Tank C there was four days quiescence between events (Figure 4.2). Additionally, a diffusion control tank was setup in the same manner as the resuspension tanks but no paddle was placed in the tank to generate resuspension.

4.2.2 Sampling Strategy

The STORM tanks were sampled most intensively on the first day of each resuspension event. On day two and three of the resuspension event, the tanks were sampled twice daily, once in the morning and once in the afternoon. In this paper only the results from sampling on day two and three are presented. A detailed analysis of the

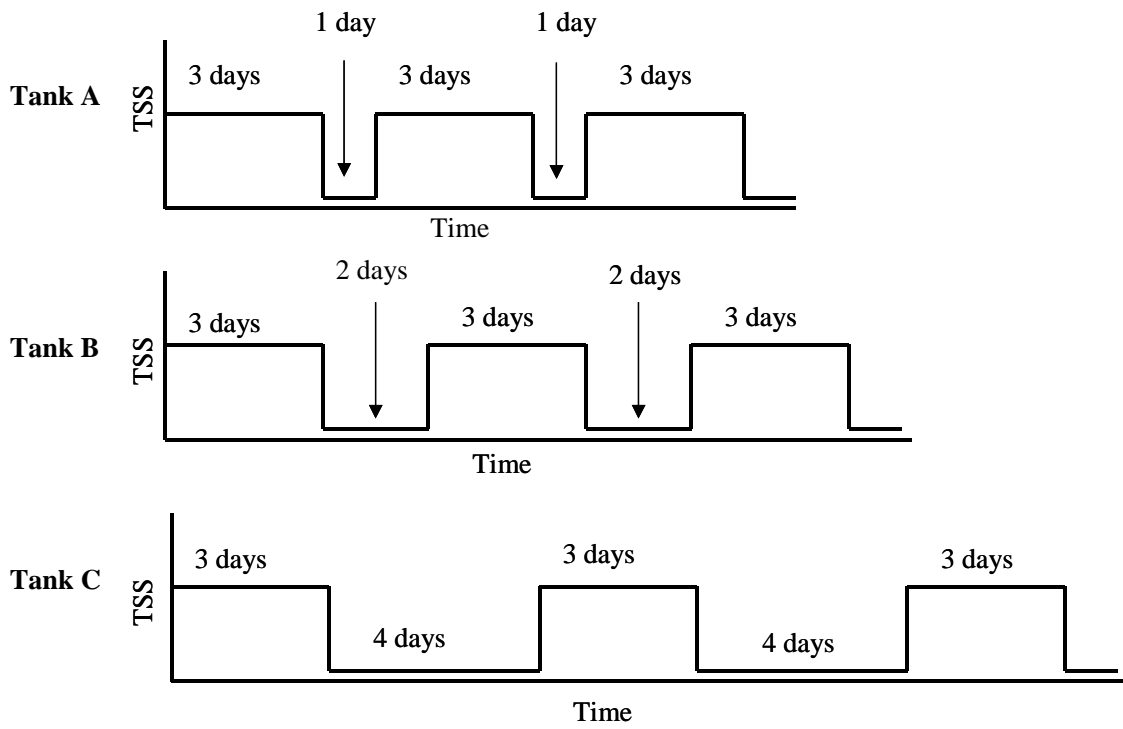


Figure 4.2. Schematic of the sequence of resuspension events conducted in the STORM tanks. The high TSS corresponds to periods when mixing was turned on. The low TSS corresponds to periods when mixing was turned off and the tanks sat with only 1 cm of overlying water.

first day of resuspension will be discussed in Chapter 5. At each sampling time point the dissolved PCB concentration was measured using solid phase microextraction (SPME) and suspended solids were collected for particulate PCB analysis. In addition, water samples were collected for TSS and particulate carbon and nitrogen (CHN) analysis. Laser In-Situ Scattering and Transmissometry (LISST 100C, Sequoia Scientific) measured the volume concentration ($\mu\text{L L}^{-1}$) of particles 3.2-250 μm in diameter in 32 logarithmically spaced bins. Detailed results of the LISST data are presented in Chapter 3. In the diffusion control tank, PCBs were measured using SPME every third day for a total of 30 days.

4.2.3 Analytical Procedure

Dissolved PCB concentrations were measured using non-equilibrium solid phase microextraction (SPME). This technique is described in detail elsewhere (Chapter 2) and briefly summarized here. SPME fibers were inserted into a glass tube that revolved at 130 rpm and deployed in the STORM tanks for 30 minutes to collect half hour time integrated measurement of the dissolved PCB concentration. Immediately after sampling the fibers were placed in glass capillary columns and frozen at -20°C until further analysis. The SPME fibers were analyzed by spiking them with PCB standards, 3,5-dichlorobiphenyl (IUPAC #14), 2,3,6-trichlorobiphenyl (IUPAC #30), 2,3,5,6-tetrachlorobiphenyl (IUPAC #65), 2,3,4,4',5,6-hexachlorobiphenyl (IUPAC #166), and 2,2'3,4,4', 5,6,6'-octachlorobiphenyl (IUPAC #204) obtained from Ultra Scientific, and immediately injecting them into the cool on-column injection port of an Agilent model 6890 gas chromatogram equipped with a 30 meter DB-5 column (J&W Scientific) and a ^{63}Ni electron capture detector (GC-ECD). Each sample was analyzed for 10 PCB

congeners based on retention time relative to a standard mixture of PCB Aroclor 1248. The mass quantified on the SPME fiber was calibrated to dissolved PCB concentrations by conducting both SPME and liquid/liquid extractions of deionized water spiked with various amounts of PCB Aroclor 1248 (Chapter 2).

The collection and analysis of suspended particle samples and sediment from the STORM tanks followed our laboratory's standard procedure, which is described in detail elsewhere (Bamford et al., 2002; Kucklick et al., 1996) and summarized here. Particulate PCB samples were collected by filtering 150 ml of water through glass fiber filters (47 mm, 0.7 μm pore size). Sediment samples were collected in pre-cleaned glass jars from the homogenized sediment mixture before it was added to each tank. All samples were frozen at -20°C until analysis. The sediment was ground with cleaned anhydrous Na_2SO_4 and the filters were extracted without drying. The samples were transferred to Soxhlet flasks, spiked with PCB surrogate standards 3,5-dichlorobiphenyl (IUPAC #14), 2,3,5,6-tetrachlorobiphenyl (IUPAC #65), and 2,3,4,4',5,6-hexachlorobiphenyl (IUPAC #166), and extracted for 24 hours in dichloromethane. The extract was concentrated to 1 mL, transferred into hexane using rotary evaporation, and eluted through a Florisil column (60-100 mesh, J. T. Baker Co.) to remove polar interferences. The purified extracts were concentrated and analyzed using a Hewlett-Packard 5890 gas chromatography with a 60 meter DB-5 column (J&W Scientific) and a ^{63}Ni electron capture detector. Each sample was analyzed for 55 individual PCB congeners and 28 chromatographically unresolved congener groups. Internal standards (Ultra Scientific) consisting of 2,3,6-trichlorobiphenyl (IUPAC #30) and 2,2'3,4,4', 5,6,6'-octachlorobiphenyl (IUPAC #204) were added to each sample prior to instrumental

analysis to calculate relative response factors. Each PCB congener was identified based on its retention time relative to a standard mixture of PCB Aroclors 1232, 1248, and 1262 (Ultra Scientific).

Ancillary water samples measurements were made by the Nutrient Analytical Services Laboratory (Solomons, MD) and followed their standard procedures. To measure TSS 150 ml of water was filtered through pre-weighed glass fiber filters (47 mm, 0.7 μm pore size) and dried overnight at 105 °C. Particulate carbon and nitrogen was measured by filtering 50 ml of water through glass fiber filters (25 mm, 0.7 μm pore size) and combusting the dried filters in a CE-440 Elemental Analyzer (Exeter Analytical, Inc.).

4.2.4 Quality Control and Assurance

This SPME technique does not quantify surrogate recoveries explicitly since the surrogates were added to the SPME fibers just prior to injection into the GC-ECD. Instead the surrogate mass ratio was examined to determine if there were problems with the sample during injection into the GC. If the ratio of IUPAC 14/65, 14/166 or 65/166 deviated from what would be expected based on the mass of PCB added, the sample was discarded. For the suspended particle samples surrogate recoveries were 81% \pm 9% for IUPAC 14, 83% \pm 10% for IUPAC 65, and 85% \pm 8% for IUPAC 166 (n = 100). For the sediment samples surrogate recoveries were 80% \pm 10% for IUPAC 14, 87% \pm 5% for IUPAC 65, and 85% \pm 6% for IUPAC 166 (n = 13). For dissolved, particulate, and sediment samples laboratory and field blanks were incorporated into the analysis to quantify possible contamination due to collection, transport, and analysis. Detection limits were derived from the blanks and defined as three times the mean blank mass of each

PCB congener. Detection limits for the various PCB congeners ranged from 1 to 5 ng L⁻¹ in the dissolved phase, 1 to 120 ng g⁻¹ in particulate phase, and 0.1 to 12 ng g⁻¹ in the sediment. In addition if an individual PCB congener represented over 35% of the total it was considered non quantifiable and removed from the results.

4.3 Results and Discussion

4.3.1 Flocculation and Disaggregation

In all three tanks, the TSS concentration rose rapidly and reached steady state by the start of the second day of resuspension (Figure 4.3 and Chapter 3). During the first resuspension event the steady state TSS concentration was 60 ± 4 mg L⁻¹ in Tank A and 79 ± 5 mg L⁻¹ in Tanks B and C. Results from the LISST data showed that large flocs were lifted into the water column immediately following the initiation of resuspension. As resuspension time progressed the volume median diameter of the resuspended particles decreased and flocs disaggregated. At steady state, there was no significant difference in the particle size distribution among tanks or events and the volume median particle diameter was 112 ± 3 μm (Chapter 3). If the solids density is assumed to be a linear combination of the density of minerals and organic matter, then the LISST data and TSS concentration can be used to calculate porosity and gross bulk density of the resuspended particles. At steady state, the particles had a porosity of 0.90 ± 0.02 and a gross bulk density of 1.13 ± 0.02 g cm⁻³ (Chapter 3).

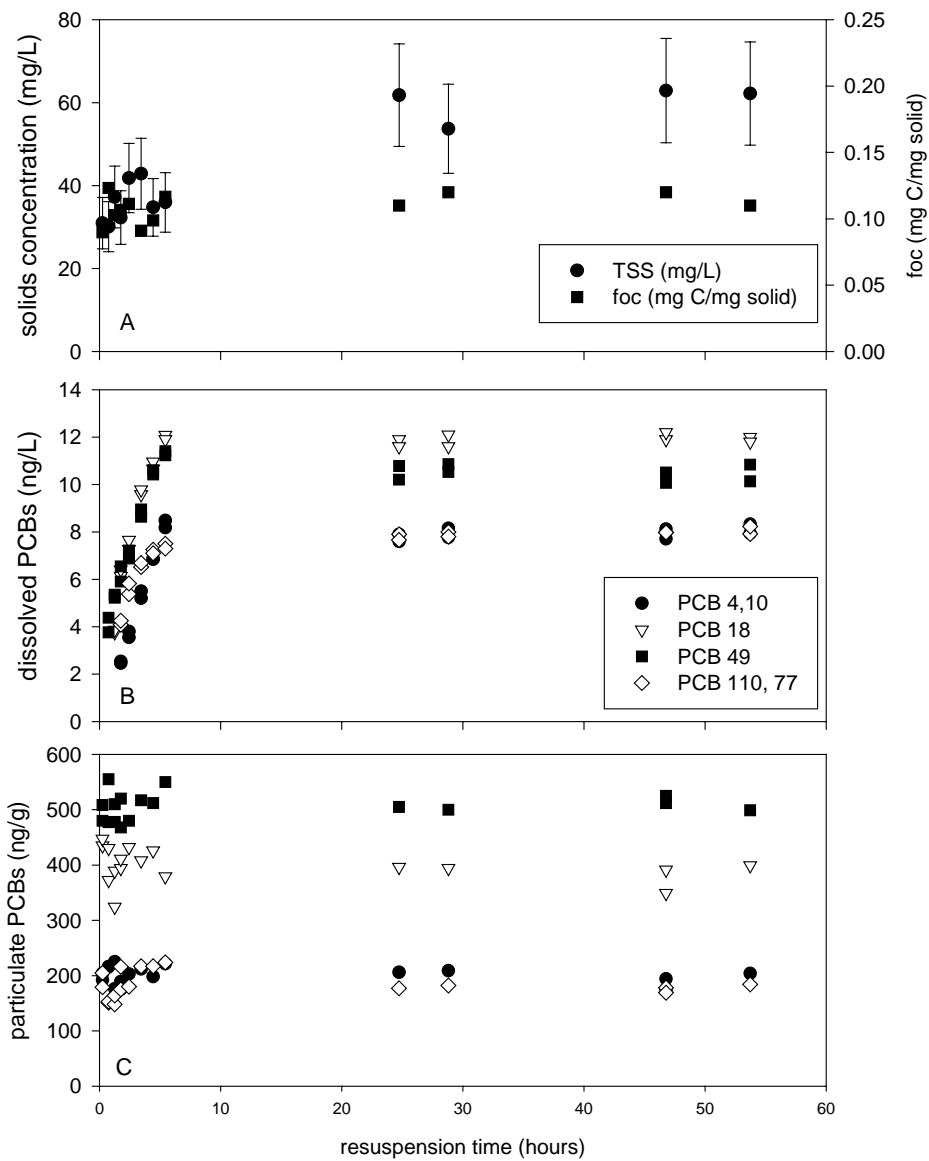


Figure 4.3. Measured parameters in Tank A during event 1 (A) Total suspended solids (TSS) concentration and fraction organic carbon (B) Selected dissolved PCB congeners (C) Selected particulate PCB congeners. In panel B and C multiple data points represent replicate measurements. The error bars in panel A show a 20% error on each TSS measurement.

4.3.2 Sediment and Suspended Particles

At steady state, the organic carbon content of the particles resuspended at an instantaneous maximum bottom shear stress of 1 dyne cm^{-2} shear stress was $0.12 \text{ mg-C mg-solid}^{-1}$ in all three tanks and did not change during the course of each resuspension event (Figure 4.3). The resuspended particles were enriched in organic carbon relative to the bulk sediment, which had an organic carbon content ranging between 0.05 and $0.06 \text{ mg-C mg-solid}^{-1}$ (Chapter 3).

The total PCB concentration in the bulk sediment was $12.6 \pm 0.72 \text{ } \mu\text{g g}^{-1}$ and $11.9 \pm 0.47 \text{ } \mu\text{g g}^{-1}$ in Tank A and B respectively. Due to a handling error the sediment in Tank C was not analyzed for PCBs, and the concentration in that sediment was assumed to equal $12 \text{ } \mu\text{g g}^{-1}$. The resuspended particles were enriched in PCBs by $50 \pm 18\%$ relative to the bulk sediment and this enrichment was not correlated to PCB molecular weight (Figure 4.4). Under these realistic physical conditions, more PCBs were resuspended in the water column than predicted based on bulk sediment PCBs measurements. This suggests that mass balance calculations utilizing sediment PCB concentration and TSS underestimate the mass of PCBs resuspended in the water column.

Latimer et al. (1999) used a particle entrainment simulator to observe changes in resuspended particle PCB concentrations as a function of bottom shear stress for sediment collected from Narragansett Bay, RI. At a bottom shear stress of 2 dynes cm^{-2} , the resuspended sediment was enriched in organic carbon and *t*-PCBs relative to the bulk sediment. Alkhatib and Weigand (2002) also used a PES to examine the release of PCBs from sediment spiked with PCBs in the laboratory. This study also found that the mass of PCBs resuspended at 2 dynes cm^{-2} was greater than the bulk sediment PCB

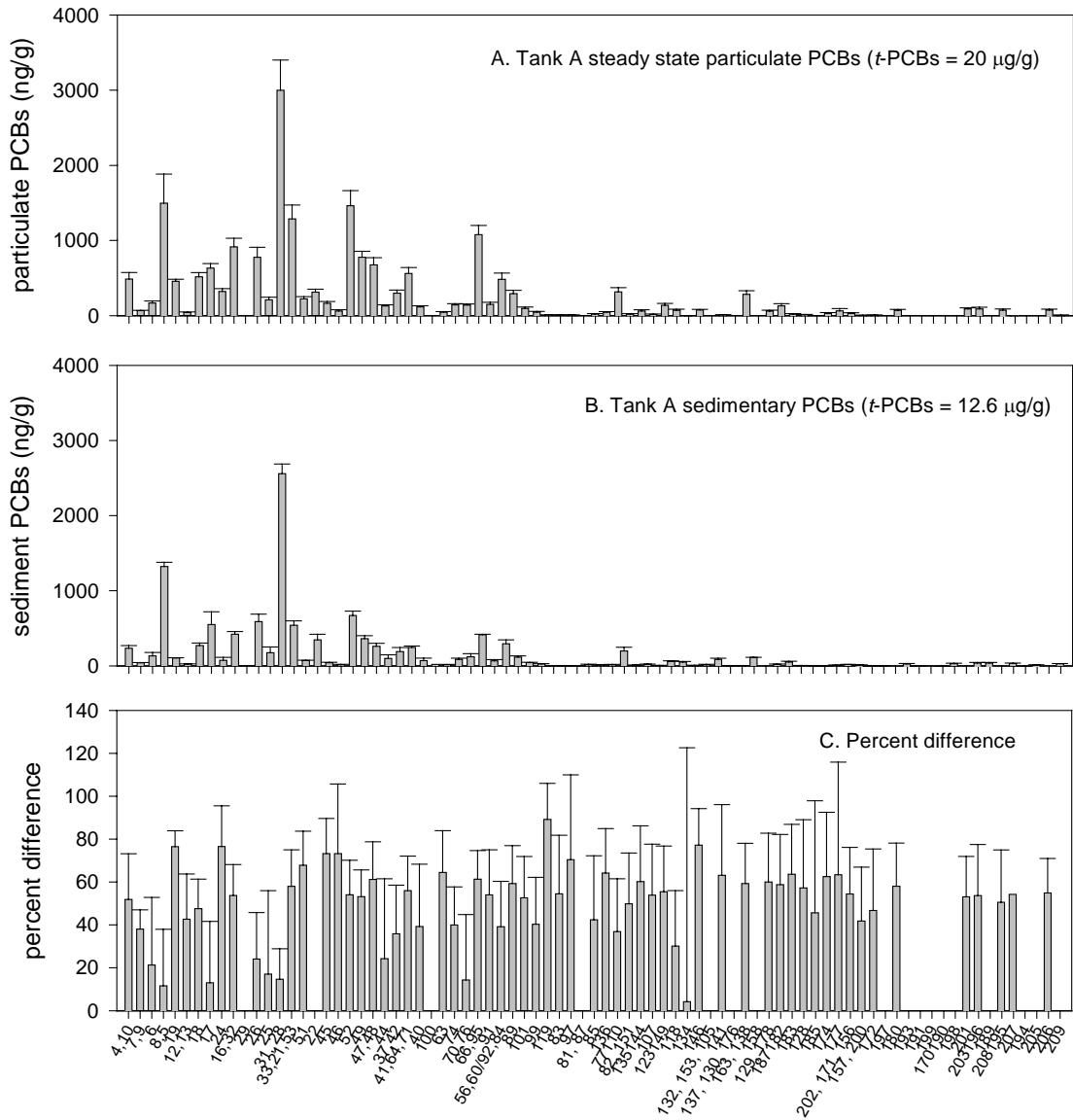


Figure 4.4. The PCB concentration of (A) the resuspended particles and (B) the sediment. Panel C shows the enrichment of the resuspended particles as the percent difference between the particulate and sediment PCB concentration. In panel A and B the error bars represent the standard deviation of replicate measurements ($n = 5$ for the particles $n = 3$ for the sediment). The percent difference error bars were calculated by propagation of the sediment and resuspended particle error.

concentration. Field observations of the PCB concentration on suspended solids in the Hudson River vary temporally due to the heterogeneity of resuspended particles. Suspended solids samples collected in the field consist of autochthonous material, particles eroded from other areas, as well as resuspended sediment. The EPA (1997) compared the PCB concentrations on suspended solids to nearby surficial sediment PCB concentrations. In the Thompson Island Pool at river mile 188.5 the surficial sediment *t*-PCB concentration was $25.1 \mu\text{g g}^{-1}$ and the *t*-PCBs concentration on the suspended particles ranged between 1.9 and $21.3 \mu\text{g g}^{-1}$ with a median concentration of $17.3 \mu\text{g g}^{-1}$. At the four locations examined, *t*-PCBs on the suspended particles were equal to or less than surficial sediment *t*-PCBs. Total PCB concentrations on suspended solids were less than bulk sediment because the solids were diluted by upstream material that was depleted in PCBs.

4.3.3 Steady State PCB Partitioning

The dissolved PCB concentration in each storm tank rose rapidly and reached steady by the start of the second day of resuspension (Figure 4.3). Given the sensitivity limits of SPME, changes in dissolved PCB concentrations less than $0.03 \text{ ng L}^{-1} \text{ hour}^{-1}$ over the three-day time period of each resuspension event would not be detected. Diffusion from the bed sediments did not significantly contribute to dissolved PCB measurements in the three-day resuspension experiments. The flux of PCBs from the bedded sediment in the diffusion control tank ranged from 0.13 to $0.45 \mu\text{g m}^{-2}\text{-day}^{-1}$ and was two orders of magnitude less than the 12 to $53 \mu\text{g m}^{-2}\text{-day}^{-1}$ flux due to resuspension and subsequent desorption measured during the first day of each resuspension event. The flux of PCBs out of the system due to air water exchange was estimated to average of 2.2

$\mu\text{g m}^{-2}\text{-day}^{-1}$, an order of magnitude less than the flux caused by resuspension and subsequent desorption. At first glance it appears that PCB steady state in the STORM tanks was reached faster than predicted from previous studies. For example, in the studies by Lick and colleagues at a TSS concentration of 100 mg L^{-1} sorptive equilibrium for 4, 4' dichlorobiphenyl to sediment was reached in 288 hours (Tye et al., 1996). However, the time to reach steady state or apparently equilibrium observed in our study is consistent with the findings of Carroll et al. (1994). In that study, sediment from the Hudson River was vigorously mixed with XAD resin and over half the PCBs desorbed from the sediment in the first day. The remaining fraction desorbed so slowly with time that the concentration appeared constant over a two day time period. Lamoureux and Brownawell (1999) conducted batch desorption experiments with sediment collected from the New York Harbor and found that desorption of the lower molecular PCB congeners desorption ($\log K_{ow} < 6.2$) occurred rapidly and equilibrium was reached after less than 100 hours. Gong et al. (1998) measured desorption of PCB 52 from laboratory contaminated sediment and found that equilibrium was reached within 50 hours.

At steady state, the PCB data collected in the STORM tanks was used to calculate PCB partition coefficients. For the di, tri, and tetra-chlorinated PCB congeners the steady state partition coefficients in the STORM tanks fell within the range observed in the Hudson River (Figure 4.5 data from Butcher et al. 1999). For the penta-chlorinated PCB congeners the steady state partition coefficients in the STORM tank were lower than in the Hudson River. Butcher et al. (1999) calculated partition coefficients for the lower molecular weight PCBs using ~25 samples. However, they calculated partition coefficients for the penta-chlorinated PCB congeners in only three samples. The Hudson

River data set was generated by collecting suspended particles on glass fiber filters for the particulate measurement and then conducting a liquid/liquid extraction of the water that passed through the filter for the dissolved measurement (Butcher et al., 1999). The inclusion of PCBs bound to DOC in Butcher et al.'s estimate of dissolved PCBs suggests the actual partition coefficient were higher than reported.

As with all field data (Baker et al., 1991; Gobas and MacLean, 2003; Sobek et al., 2004), a wide range of K_{oc} values were measured in the Hudson River. There was less variability in the range of K_{oc} values observed in the STORM tanks than in the field data (Figure 4.5). STORM tank measurements of K_{oc} as well as field data from the Hudson River and elsewhere (Baker et al., 1991; Gobas and MacLean, 2003; Sobek et al., 2004) indicate the partition coefficients for low molecular weight PCB congeners are higher than predictions made by Karickhoff et al. (1979) using the octanol water partition coefficient. This same discrepancy is often seen in laboratory estimates of K_{oc} . For example, Jespen and Lick (1996) measured a log K_{oc} value of 5.73 for 4,4'-dichlorobiphenyl partitioning to sediment from the Detroit River. Karickhoff et al. (1979) predicted the log K_{oc} value for this compound should be 4.4. Updated estimates of K_{oc} as a function of K_{ow} have similar slopes to Karickhoff's equation but increase the intercept (Xia, 1998). This change does not result in a better fit to the observed STORM or Hudson River data (Figure 4.5). Previously, unexpected trends in K_{oc} were explained by invoking dissolved organic carbon (DOC). For example, Butcher et al. (1998) theorized that up to 50% of measured dissolved mono and di-chlorinated PCBs were bound to DOC. The use of SPME in these experiments limits DOC interferences (Chapter 2) and suggests the observed lack of trend with the octanol water partition

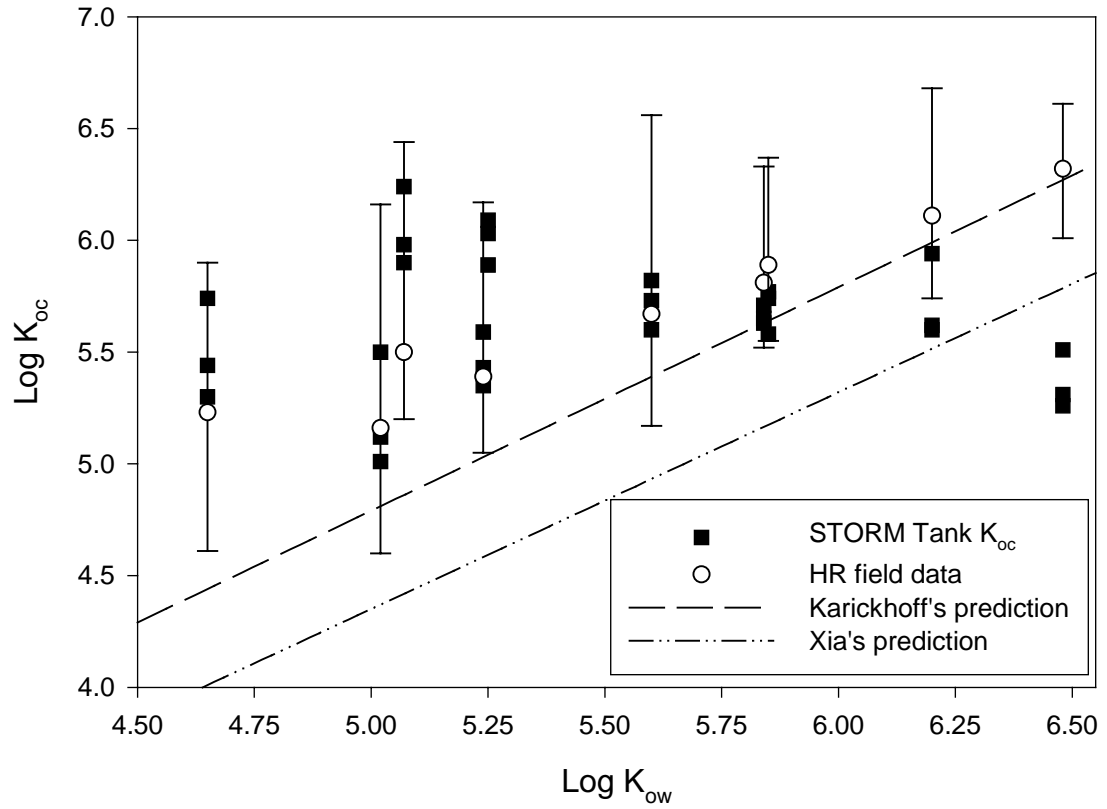


Figure 4.5. $\text{Log } K_{oc}$ values measured in the Hudson River (average, maximum, minimum data from Butcher et al. 1999) and in the STORM tanks at steady state for resuspension event 1.

coefficient is not the result of this analytical bias.

Since PCB desorption is often modeled as a two stage process, it is possible that the steady state dissolved concentration obtained in the tanks was not the true equilibrium concentration with a resistant pool but rather represents equilibrium with a labile pool. In one tank a resuspension event was extended for seven days and after three days the concentration of most congeners increased very slowly with time (Figure 4.6). Even given the sensitivity limits of SPME, after 168 hours of resuspension the dissolved concentration of every congener except PCB 110 was significantly greater than the dissolved concentration at 53 hours ($p = 0.002$). This suggests that if the resuspension event had been extended for a much longer period of time this tank might have reached Karickhoff's predicted K_{oc} . However, the time scale on which this might happen is much greater than the time scale of a sediment resuspension event. In the STORM tanks the steady state obtained after three days might represent equilibrium with a labile phase rather than "true" equilibrium with a resistant phase.

4.3.4 Labile/Resistant Model

The K_{oc} values reported in the previous section were calculated from steady state conditions at the end of the first resuspension event in the three STORM tanks. A total of three resuspension events were conducted in each STORM tank and steady state K_{oc} values were also calculated for each event. For discussion purposes, only the K_{oc} values from the first and third resuspension event are compared. For Tank A with one day quiescence between resuspension events, the K_{oc} values for the third resuspension event were significantly greater than for the first resuspension event (Figure 4.7 $p = 0.45$). This

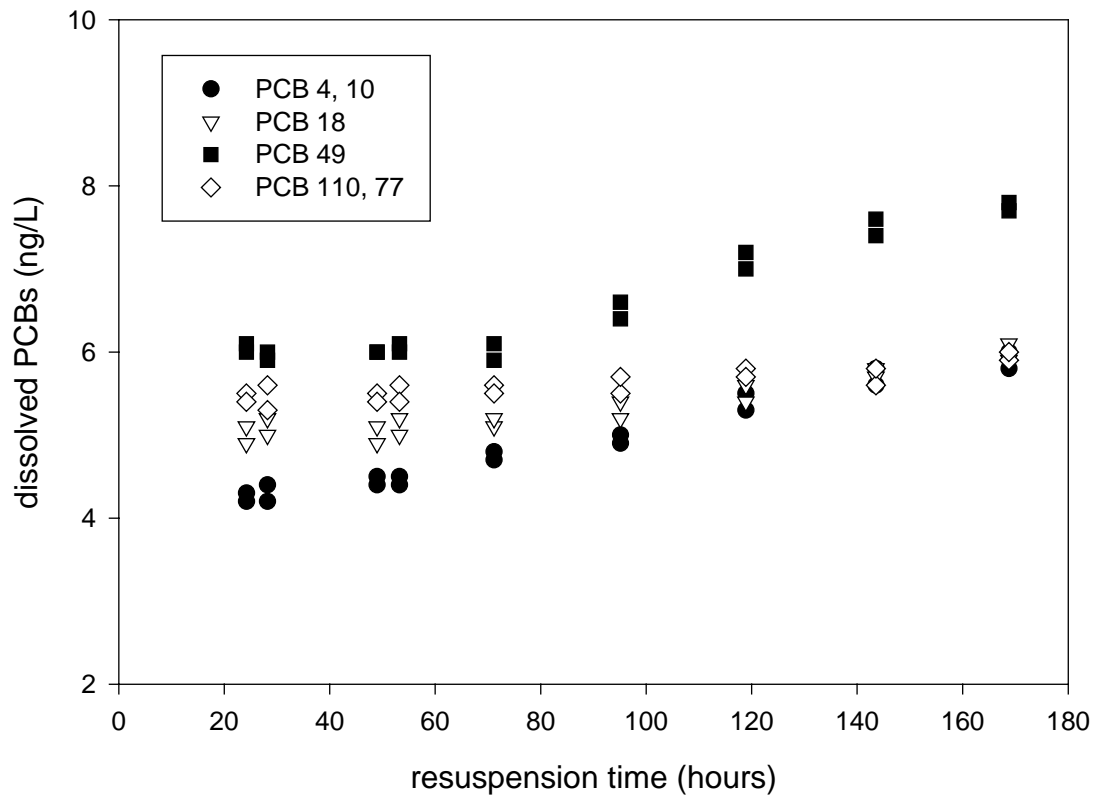


Figure 4.6. The dissolved PCB concentration in Tank A when resuspension event 3 was extended for seven days. Here multiple dots represent replicate samples.

change in K_{oc} is driven by a decrease in dissolved PCB concentrations at steady state for the third resuspension event (Figure 4.7).

As discussed earlier, PCB desorption from particles occurs in two-stages; the labile stage is rapid and the resistant stage is slow. A labile/resistant model was applied to the STORM tank data assuming the steady state obtained after three days represents equilibrium with a labile pool. In the STORM tanks, depletion of a labile pool during the first resuspension event could account for the decrease in dissolved concentrations measured on subsequent resuspension events. If the labile pool did not recharge during the quiescent period between resuspension events, subsequent resuspension events would result in lower dissolved PCB concentrations. One way to test this hypothesis is to vary the quiescent period between resuspension events. If longer quiescent times result in higher dissolved concentrations, it would suggest that PCBs repartition into a labile pool. The replenishment of the labile pool after periods of quiescence could be caused by repartitioning from a resistant or slightly less labile pool within the particle, or even by re-equilibration with bedded sediments labile pool through diffusion of concentrated pore water.

The results presented in Figure 4.7 are from Tank A in which there was one-day quiescence between resuspension events. The same sequence of experiments was conducted in STORM tanks with two and four days of quiescence between resuspension events (Tank B and C respectively). In Tanks A and B, with one or two days quiescence respectively, the percentage of PCBs in the dissolved phase at steady state decreased significantly from resuspension event 1 to resuspension event 3 ($p=0.02$ for both Tank A and Tank B, Figure 4.8). In Tank C, with four days quiescence between events, the

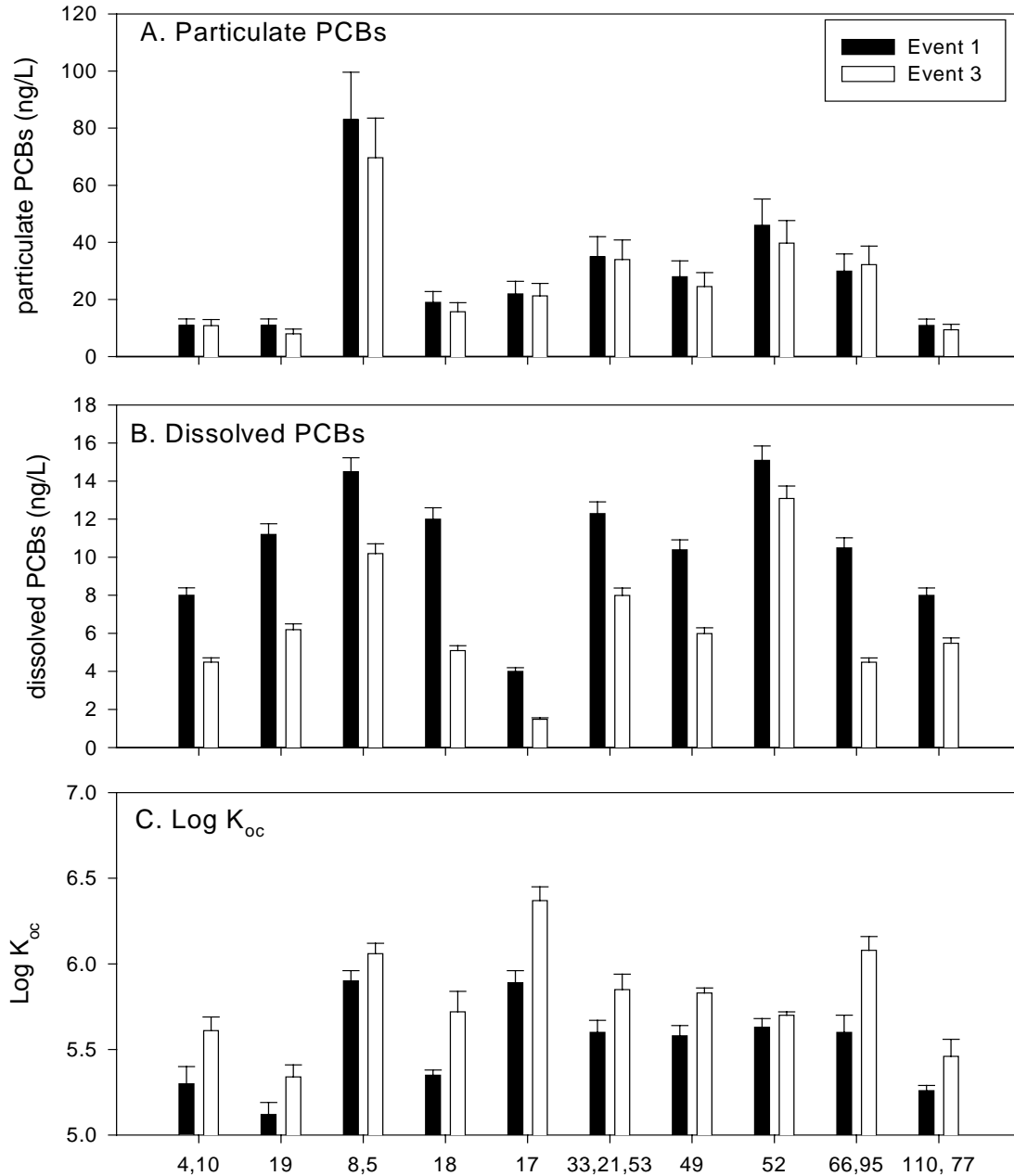


Figure 4.7. Particulate, dissolved and log K_{oc} values at steady state for resuspension event 1 and 3 in Tank A. The difference in K_{oc} between resuspension events is driven by the decrease in the dissolved concentration. An error of 5% for the dissolved measurement and 20% for the particulate measurement was assumed and propagated through to determine the error on log K_{oc} .

percentage of dissolved low molecular weight PCBs ($\log K_{ow} \leq 5.85$) at steady state did not change significantly between events ($p = 0.44$). Only the percentage of higher molecular weight PCBs ($\log K_{ow} > 5.85$) decreased significantly ($p = 0.002$, Figure 4.8). In all three tanks, the steady state $\log K_{oc}$ values for the third resuspension were higher than the $\log K_{oc}$ values for the first resuspension event. However, there was much less of a difference in the K_{oc} values in Tank C, the tank with four-days quiescence, as compared to the tanks with one and two days quiescence (Figure 4.9). For low molecular weight PCBs ($\log K_{ow} < 5.85$) the percent difference in K_{oc} values between the first and third resuspension event is significantly less for Tank C as compared to Tanks A and B (Figure 4.9). In this case it appears that the labile pool recharged during the four days of quiescence. For higher molecular weight PCBs ($\log K_{ow} \geq 5.85$) it appears that the labile pool did not recharge during the quiescent time periods examined in this study (Figure 4.9).

In terms of the labile/resistant model, the total PCB concentration on the resuspended particles is given by the following equation where all variables have units of ng kg^{-1} :

$$C_{\text{total-suspended}} = C_{\text{particle-labile}} + C_{\text{particle-resistant}} \quad (1)$$

where $C_{\text{particle-labile}}$ is the concentration in the labile pool, and $C_{\text{particle-resistant}}$ is the concentration in the resistant pool, and, $C_{\text{total-suspended}}$ is the total PCB concentration measured on resuspended particles prior to desorption. Another method for exploring PCB transfer between a labile and resistant compartment is to compare the measured K_{oc} values in the STORM tanks to the values predicted by Karickhoff. The $\log K_{oc}$ of the lower molecular weight congeners measured in the STORM tank are higher than

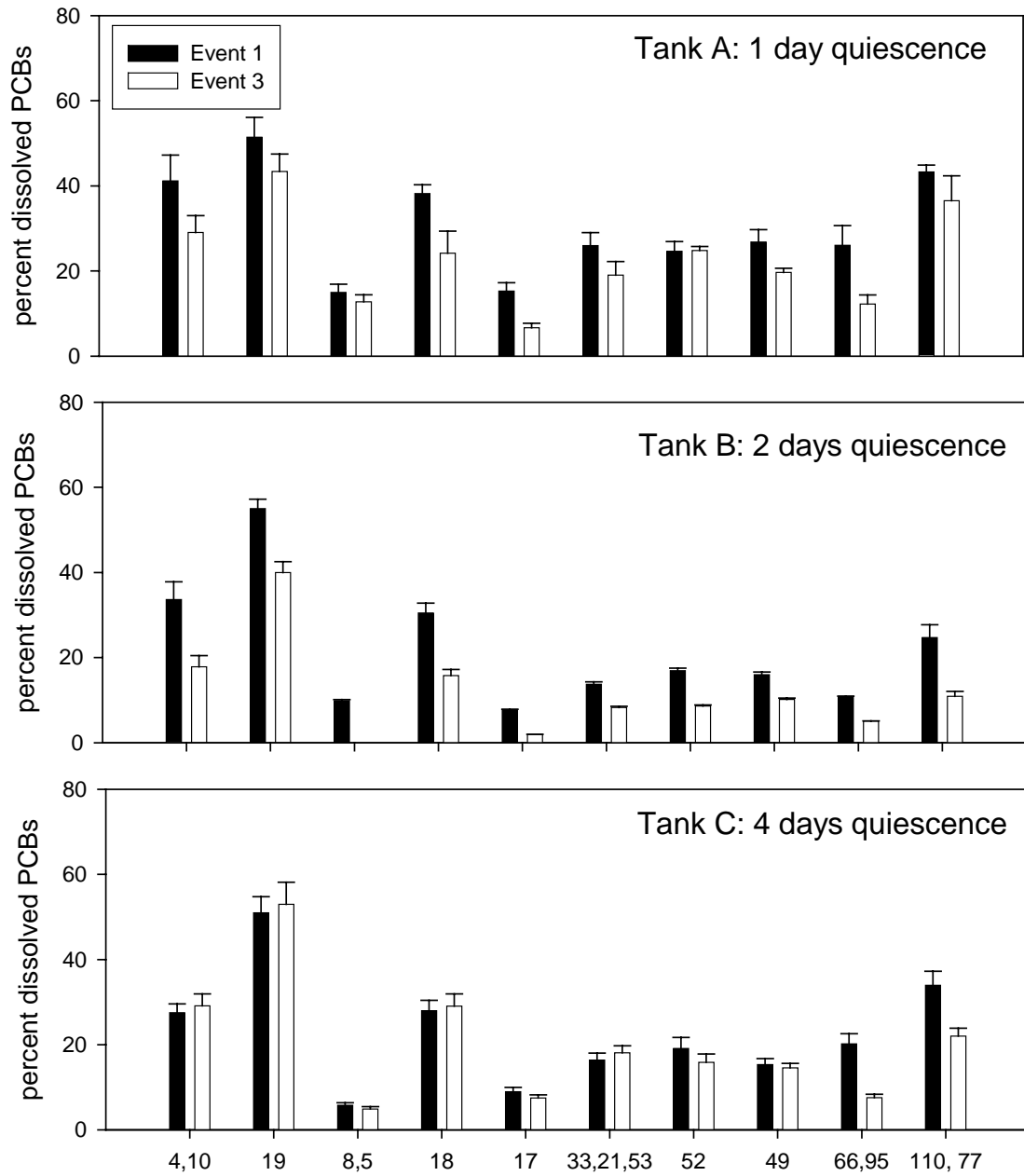


Figure 4.8. The percentage of PCBs in the dissolved phase at steady state during resuspension event 1 and 3.

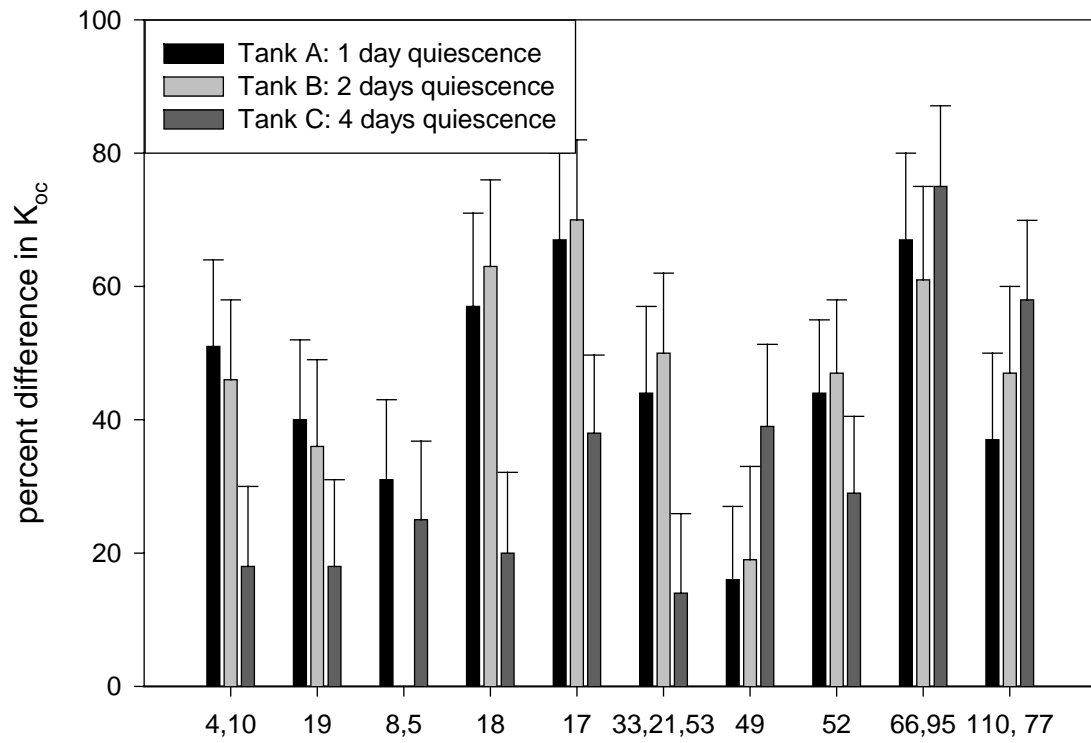


Figure 4.9. The percent difference in K_{oc} between the third and first resuspension event for STORM Tank A, B and C.

predicted by Karickhoff and the log K_{oc} values for the higher molecular weight congeners are lower than predicted by Karickhoff (Figure 4.10). Since DOC bound PCBs are not included in the dissolved measurement, there is no physical reason why the log K_{oc} values for the higher molecular weight congeners should be lower than Karickhoff's prediction. Therefore, the intercept of the Karickhoff line was adjusted so that the average measured K_{oc} value for 2,3,3',4',6-pentachlorobiphenyl (congener 110) was equal to Karickhoff predicted K_{oc} value (Figure 4.10). This adjustment changed the intercept from -0.21 to -1.02 .

Assuming the labile pool reaches equilibrium, the difference between the measured K_{oc} values in the STORM tanks and the adjusted Karickhoff values represents the concentration in a resistant pool. Since the Karickhoff K_{oc} of congener 110 was set equal to the measured value, by definition, 100% of congener 110 is in a labile pool. The lower the molecular weight of the congener, the lower the fraction of PCBs in the labile pool (Figure 4.10). This result may seem counterintuitive since compounds with lower molecular weights diffuse faster than higher molecular weight compounds. One possible explanation for the decrease in percent labile with molecular weight is the larger size of the higher molecular weight congeners. The mono to tetra-chlorination congeners have total surface areas ranging from $200\text{-}260 \text{ \AA}^2$ whereas total surface area of the penta to deca-chlorinated congeners ranges from $270\text{-}345 \text{ \AA}^2$ (Wang et al., 2003). It is possible that these higher molecular weight congeners are too big to diffuse into the micro pore spaces of the particles and enter a resistant pool. Another explanation could be that since the higher molecular weight congeners diffuse more slowly, they might not have been exposed to the particle long enough to enter a more resistant pool.

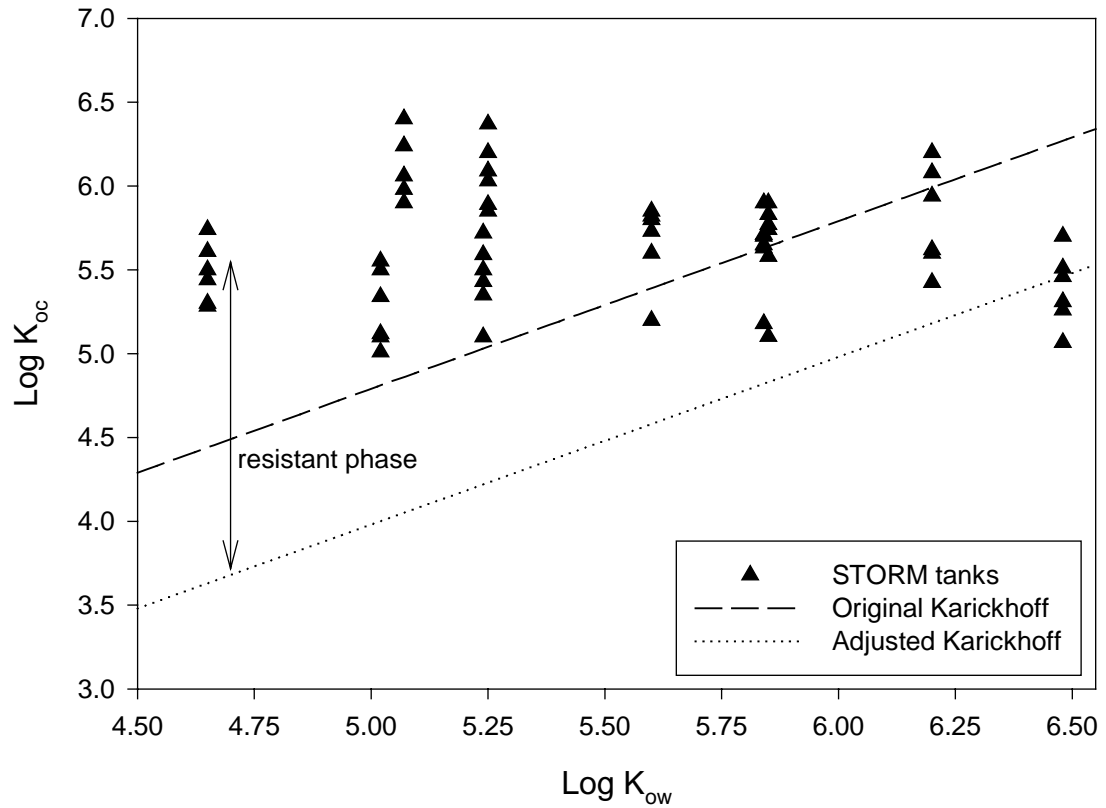


Figure 4.10. Log K_{oc} values measured in Tank A, B, and C at steady state for resuspension event 1 and 3. The dashed lines represent the log K_{oc} values calculated using Karickhoff's original equation and the dotted line represents the adjusted values used to calculate the percent of PCBs in the labile pool.

Using the adjusted Karickhoff equation, the labile concentration on the suspended particles was then calculated according to equation 2 where $K_{kar.adj.}$ is the adjusted K_p value obtained by changing the intercept of Karickhoff's line ($L\ kg^{-1}$), $C_{measured-dissolved}$ is the dissolved concentration in the STORM tank measured using SPME ($ng\ L^{-1}$).

$$C_{particle-labile} = K_{kar.adj.} * C_{measured-dissolved} \quad (2)$$

The resistant concentration on the suspended particles can then be calculated according to the following equation where all concentrations are in units of $ng\ kg^{-1}$.

$$C_{particle-resistant} = C_{total-suspended} - C_{particle-labile} \quad (3)$$

Finally, the total labile pool that was present on the sediment before it was resuspended can be calculated according to the equation below assuming only the labile pool desorbes during resuspension. In equation 4, TSS is the total suspended solids concentration at steady state in units of ($kg\ L^{-1}$).

$$C_{labile-total} = C_{particle-labile} + \left(C_{measured-dissolved} * \frac{1}{TSS} \right) \quad (4)$$

The movement of PCBs between a labile and resistant pool was explored by examining the percent of PCBs in the labile pool. For each resuspension event the percentage of PCBs in the labile pool was calculated using the following equation:

$$\% \text{ labile} = \frac{C_{labile-total}}{C_{total-suspended}} * 100 \quad (5)$$

The speciation of PCBs varied considerable by congener and ranged from 7 to 58% labile (Figure 4.11). In Tank A, where there was one day of quiescence between resuspension events, the fraction of PCBs in the labile pool decreased from resuspension event 1 to event 3 for all congeners (Figure 4.11). This suggests that there was little recharge of the labile pool during the quiescent time period. The total labile pool decreased because after

was removed from the tank at the end of resuspension event 1. Results from Tank B were similar to Tank A and it appears two days of quiescence was insufficient to recharge the labile pool (Figure 4.11). For Tank C, where there was four days quiescence between resuspension events, the percent of low molecular weight congeners ($\log K_{ow} < 5.85$) in the labile pool did not change between resuspension events (Figure 4.11). For the higher molecular weight PCBs ($\log K_{ow} \geq 5.85$) there was a decrease in the percent of PCBs in the labile pool between resuspension events. This result is consistent with the previous calculations and indicates that low molecular weight congeners recharge into the labile pool relatively rapidly (< four days) but the higher molecular weight congeners take longer.

This analysis suggests that there is a large release of PCBs from particles when they are initially resuspended. However, chronic resuspension results in less PCB release per event due to the slow recharge of the labile pool. For the low molecular weight congeners the labile pool recharges after approximately three to four days of quiescence. For the higher molecular weight congeners the recharge rate is slower and four days of quiescence is insufficient to replenish the labile pool. This series of experiments could not elucidate the mechanism by which PCBs in the labile pool were recharged.

4.3.5 Black Carbon

Another explanation for the higher K_p values measured in the STORM tanks than predicted based on the percentage of organic matter could be the presence of a super sorbent such as black carbon. In this case, the measured partition coefficients reflect not only partitioning to the organic matter but also partitioning to the black carbon present on the particles. A microscopic examination of settling particles collected on glass fiber

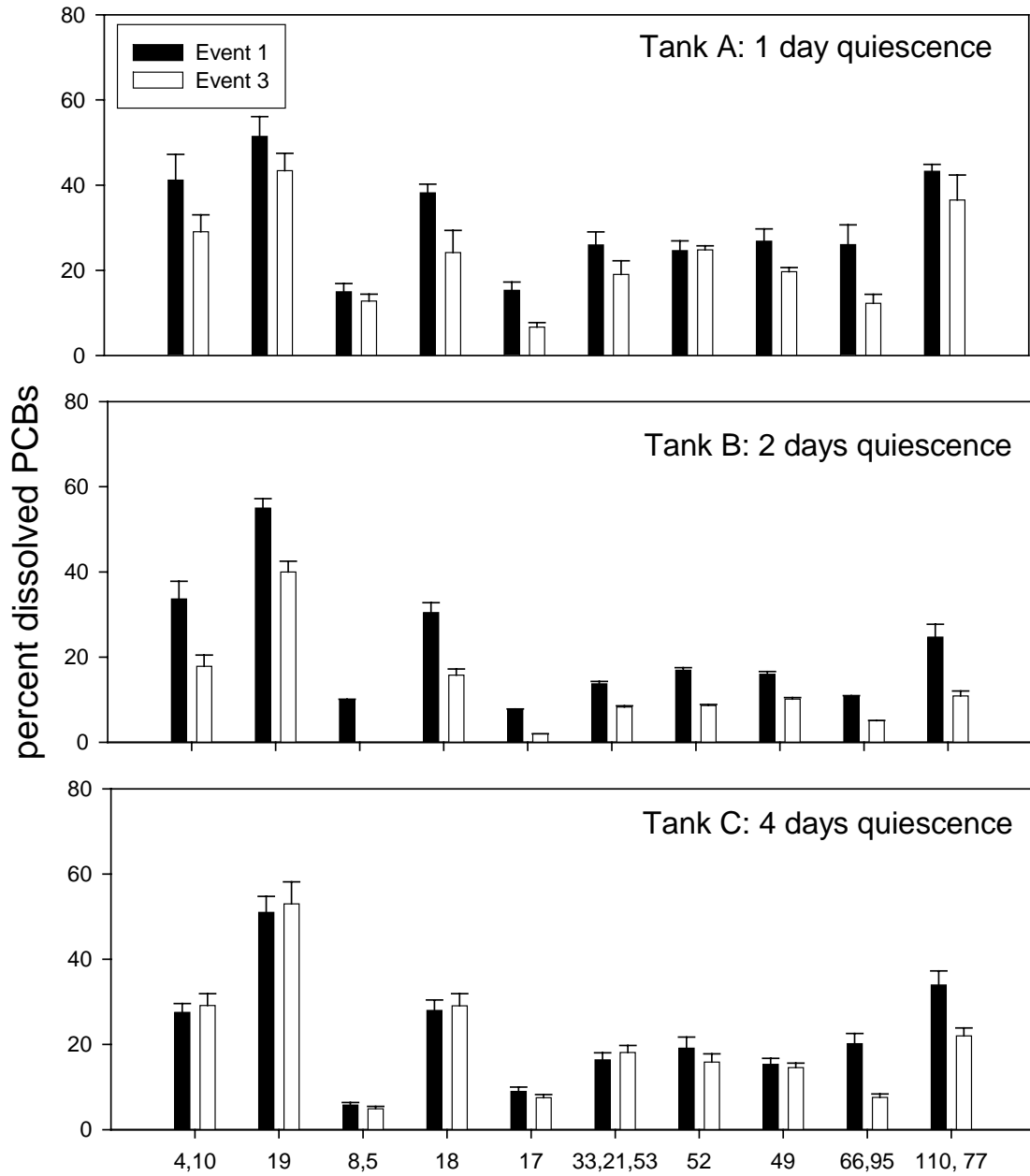


Figure 4.11. The percent of PCBs in the labile phase at steady state during resuspension event 1 and 3 for Tank A, B, and C.

filters found that after the large organic detritus settled out of the water column, black carbon like particles were visible on the filters (Chapter 3). Black carbon, more strongly absorbs PCBs than organic matter (Jonker and Koelmans, 2002). If it assumed that the steady state measurements in the STORM tanks represent equilibrium then an estimate for the percent of black carbon present on the particles can be made using a linear mixing model with the organic matter (Figure 4.12). In equation 5, K_{STORM} is the measured partition coefficient ($L\ kg^{-1}$) f_{BC} is the fraction black carbon, and K_{BC} is the PCB black carbon partition coefficient. It is assumed that fraction of organic matter is equal to $1 - f_{BC}$.

$$K_{STORM} = f_{BC} K_{BC} + (1 - f_{BC}) K_{kar.adj.} \quad (5)$$

In order for the linear mixing model to work, the adjusted Karickhoff equation needs to be used so that fraction of soot and organic matter on the particles remains positive.

The difficulty with this approach is determining the appropriate K_{BC} value to use. It is difficult to measure PCB-black carbon partition coefficients and only a handful of studies have examined PCB partitioning to black carbon (Cornelissen et al., 2004; Ghosh et al., 2003; Jonker and Koelmans, 2002; Lohmann et al., 2005). Jonkers and Koelmans (2002) calculated K_{BC} partition coefficients for 11 PCBs to a variety of types of black carbon. For the purposes of the linear mixing model, the $\log K_{charcoal}$ values measured by Jonkers and Koelmans were plotted according to their $\log K_{ow}$ values ($r^2 = 0.81$) and $K_{charcoal}$ values were estimated for the PCB congeners measured in the STORM tanks. Dissolved concentrations in the Jonker and Koelmans study were on the order of $pg\ L^{-1}$ to $ng\ L^{-1}$, slightly lower than in the STORM tanks ($ng\ L^{-1}$). It has been shown that PAH

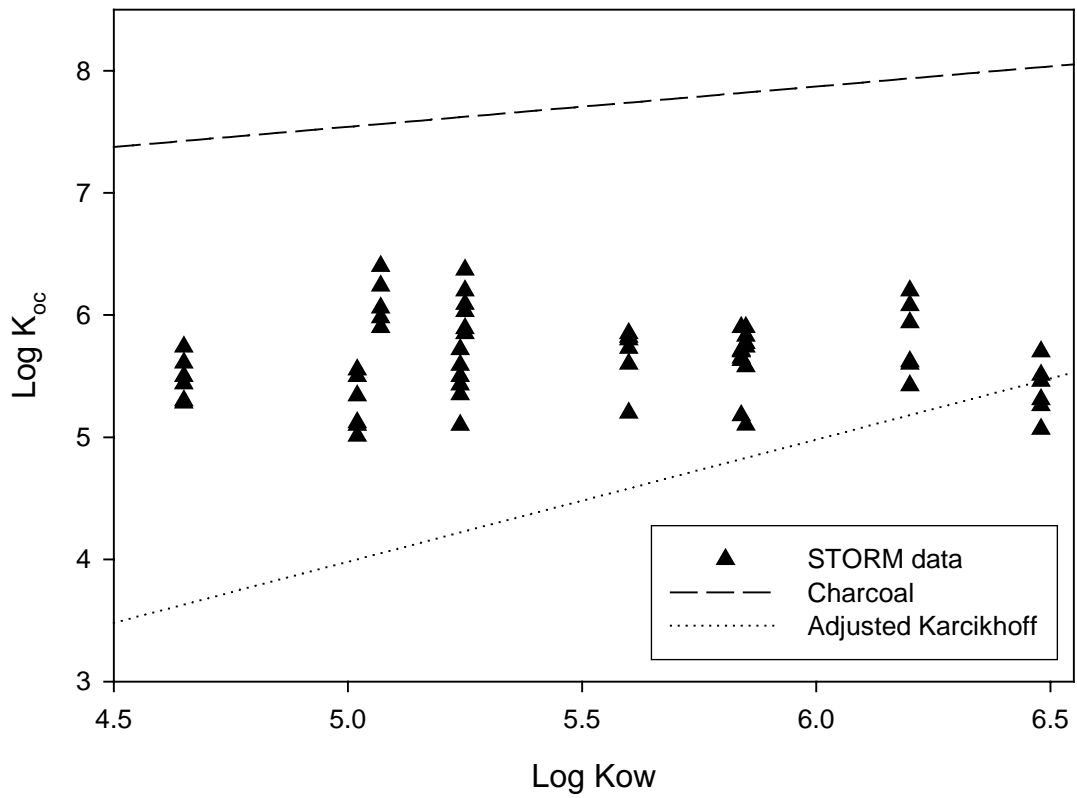


Figure 4.12. The estimated PCB-charcoal partition coefficient and the adjust Karickhoff partition coefficient bound the measured $K_{OC-STORM}$ values.

sorption to black carbon depends non-linearly on the dissolved concentration (Accardi-Dey and Gschwend, 2003). If this is true for PCBs, the K_{charcoal} values in Jonkers and Koelmans might be slightly lower than the partition coefficients in the STORM tanks. As a result, the linear mixing model represents the maximum fraction of charcoal that might be present in the sediment samples in order to account for the observed partition coefficients. Since the slope of the K_{charcoal} line is much less than the slope of the $K_{\text{kar.adj.}}$ (Figure 4.12), the resulting fraction of charcoal was constant across congeners. According to this model, 1% charcoal is enough to account for the observed partition coefficients. This small amount is a realistic estimate of the amount of charcoal present in the resuspended particles.

The problem with invoking soot equilibrium partitioning as the explanation for the elevated observed partition coefficients is that it does not account for the increase in K_{STORM} with subsequent resuspension events. A linear mixing model using the partitioning data from event 3, shows that the fraction of charcoal would have to increase to 2% to explain the data from this event. There is no conceivable mechanism by which the fraction of charcoal in the sediment could have increased while it sat on the bottom of the STORM tanks. If the resuspended particles are not in equilibrium with the organic matter and charcoal phases, the linear mixing model does not apply. In that case, little can be concluded about the observed partition coefficients since neither the amount of black carbon nor the equilibrium and kinetic parameters describing PCB congener-black carbon interactions are known.

4.4 Implications

Steady state PCB partitioning occurred on the same time scale as floc disaggregation. The log K_{oc} values measured in the STORM tanks were similar to values measured in the field indicating these mesocosm experiments successfully mimic field conditions. Measured K_{oc} values did not systematically vary with octanol water partition coefficient and K_{oc} values for the lower molecular weight PCBs were higher than predicted by Karickhoff et al. (1979) and other models that predict K_{oc} based on K_{ow} . The use of solid phase microextraction to measure the dissolved PCB concentrations indicates that DOC partitioning does not account for the discrepancy between measured and predicted K_{oc} values. At steady state the PCB concentration of the resuspended particles was an average of 2 times greater than the bulk sediment PCB concentration. Current models that calculate PCB release based on bulk sediment PCB concentrations will underestimate the amount of PCBs that enter the water column during resuspension events.

When there was only one or two days between resuspension events, the percentage of dissolved PCBs at steady state decreased with subsequent resuspension events. This suggests that recharge of the labile pool does not occur fast enough for replenishment on the time scale of tidal cycle resuspension (~ 6 hours). Extremely frequent resuspension events such as these might result in only minimal release of dissolved PCBs per event. When the quiescent time was increased to four days, the percentage of dissolved di, tri, and tetra-chlorinated PCBs at steady state remained constant with each resuspension event. Only the percentage of penta-chlorinated PCBs declined with four days of quiescence. This indicates it takes at least three days or more

for the labile pool of PCBs to recharge. If resuspension events occur infrequently (i.e. storms) the time between events might be long enough to replenish the labile pool and result in a large release of PCB during each event. In the upper Hudson River, where storm events are the primary cause of sediment resuspension, the time between events might be long enough for the labile pool to be replenished.

Chapter 5: Kinetics of PCB Release from Resuspended Hudson River Sediment

5.1 Introduction

Numerous studies demonstrate that PCB desorption from sediment and soil can be modeled as a two-stage process; the first ('labile') is rapid and the second ('resistant') is slow. For example, Carroll et al (1994) observed this two-stage desorption of PCBs from Hudson River sediment. A rapid (labile) fraction was defined as that which desorbed in 24 hours and a resistant (slowly) desorbing fraction was identified and shown to require over one year to fully desorb. Girvien et al. (1997) examined PCB desorption from contaminated soils and found that a labile fraction could be defined as that which desorbed in 48 hours whereas the remaining resistant fraction continued to desorb for the entire six month duration of the study. Cornelissen et al. (1997) suggested that PCB desorption might be more effectively modeled as a three stage process, the first rapid labile phase was defined as the portion lasting ~ 10 hours, the second slow resistant phase was defined to last weeks, and a third very slow or very resistant phase continued to desorb for months.

The exact mechanisms underlying the multiple stage desorption process are not known. The labile fraction might represent HOCs loosely bound to surface sites on particles while the resistant fraction is adsorbed within the interior of porous aggregates. Alternatively, rapid initial release may result from particle disaggregation, creating colloidal-sized particles from which HOCs rapidly desorb. One model to describe the

first scenario is the radial diffusion model developed by Wu and Gschwend (1986; 1988). In this model, sediment particles are considered homogeneous spheres with uniform tortuosity and porosity. When particles are resuspended, the rate of diffusion of the sorbate within the particle, or the effective diffusivity, limits the amount of desorption.

Ball et al. (1991) interpreted the uptake of tetrachloroethene and 1,2,4,5-tetrachlorobenzene (TeCB) in terms of a retarded intraparticle diffusion model similar to the radial diffusion model. The organic carbon content of the sandy aquifer soil used in that study was less than 1%, the porosity of the particles was less than 0.02, and the internal retardation factor ranged from 47-15400. As a result, the apparent diffusion coefficients were orders of magnitude lower than the aqueous diffusion coefficients and measured uptake rates into the soil were limited by the diffusion of the chemicals into the sandy particles. The chemicals examined by Ball et al. were much smaller in size than PCBs. The total surface area of TeCB, the largest molecule examined by Ball et al., was 175.2 \AA^2 . For comparison, PCBs have total surface areas ranging from 225 \AA^2 for the dichlorinated congeners to 345 \AA^2 for the deca-chlorinated congener (Wang et al., 2003). Larger molecules such as PCBs might not fit in the small pore spaces of the sand sized particles.

Organic matter diffusion (OMD) models or permeant/polymer diffusion models are an alternative to the pore diffusion models for describing the association of HOCs with particles (Pignatello and Xing, 1996). These models consider organic matter to be a polymer and diffusion through the organic matter accounts for the two stage desorption process. The first rapid phase represents diffusion through the open rubbery form of the organic matter and the second slower phase represents diffusion through the glassy and

condensed form of the organic matter. Carroll *et al.* (1994) modeled HOC desorption from Hudson River sediment using a permeant/polymer diffusion model and literature data describing the diffusion of 4-chlorobiphenyl in glassy polystyrene to represent diffusion in the rubbery open phase of the organic matter. The diffusion coefficient in the glassy condensed phase was then calculated based on the coefficient in the rubbery phase. Variations in natural organic matter make choosing a polymer to model organic matter difficult and limit the widespread applicability of this approach. Diffusion rates in polymers are highly variable and depend on a range of factors, including polymer structure and particle size distribution (Pignatello and Xing, 1996).

In the linear driving force model, the rate of desorption is limited by diffusion through the stagnant boundary layer around the particle rather than diffusion within the particle. This model makes similar assumptions of uniform particle porosity and radius as the radial diffusion model and also assumes there is no shear stress between the particle and the fluid (Valsaraj and Thibodeaux, 1999). All of these mass transfer limited models require detailed knowledge about specific particle properties that are not easily measured. Several other kinetic models based on a two stage desorption process have also been proposed including first order (Ten Hulscher *et al.*, 1999), multiple first-order (e.g. Cornelisen *et al.*, 1997), and one compartment models (Karickhoff and Morris, 1985).

Much of the research into PCB desorption has focused on understanding and modeling the resistant pool (Cornelissen *et al.*, 2000; Pignatello and Xing, 1996; ten Hulscher *et al.*, 2002; van Noort *et al.*, 2003). However, resuspension events typically last on the order of hours to days and it is unlikely particles in rivers are suspended into

the water column long enough for desorption of the resistant fraction to contribute significant amounts of PCBs. Studies either assume the labile pool is at equilibrium with water or calculate a specific rate constant for the labile fraction (Carroll et al., 1994; Girvin et al., 1997; Ghosh et al., 1999; Kukkonen et al., 2003). Estimates of the labile rate constants vary widely and range from 0.0003 to 0.2 hour⁻¹ depending on the type of sediment examined, the model used to estimate the rate constant, and the molecular weight of the PCB (Table 5.1).

The large range in estimated rate constants for labile PCB desorption indicates the amount of PCBs released on short time scales is highly variable. The common approach to study PCB desorption involves vigorously shaking or mixing sediment water slurries, which does not simulate the bottom shear stress or water column turbulence levels typically encounter in rivers. When particles are resuspended into the water column they aggregate and form flocs, which could change the rate of PCB desorption. Lick and colleagues (Borglin et al., 1996; Jepsen et al., 1995; Jepsen and Lick, 1996; Lick and Rapaka, 1996; Tye et al., 1996) evaluated the influence of particle flocculation on hexachlorobenzene partitioning to Detroit River sediment. Flocculation changed the porosity and density of the resuspended particles and, as predicted by the radial diffusion model, changed the rate of desorption. Lick and colleagues found that the higher the total suspended solids (TSS) concentration, the slower the rate of desorption because the flocs that formed were more dense and less porous than the flocs that formed at lower TSS. Most laboratory studies examining the rate of PCB desorption were conducted at high total suspended solids concentrations and it is likely the rate of desorption would be faster under more natural conditions.

Sediment	PCB congener	k labile (hour ⁻¹)	Source
Rhine River	PCB 28	0.20	Ten Hulscher et al. 2002
Hudson River	<i>t</i> -PCBs	0.008	Carroll et al. 1994
Hudson River	PCB 18	0.008	Lamoureux and Brownawell 1999
	PCB 49	0.037	
	PCB 52	0.044	
	PCB 101	0.032	
Laboratory contaminated for 2 days	PCB 65	0.058	Cornelissen et al. 1997
	PCB 118	0.045	
Laboratory contaminated for 34 days	PCB 65	0.12	Cornelissen et al. 1997
	PCB 118	0.11	
Laboratory contaminated for 110 days	¹⁴ C TCBP (PCB 77)	0.05-0.17	Kukkonen et al. 2003
Laboratory contaminated for 60 days	¹⁴ C HCBP (PCB 153)	0.03-0.16	Kukkonen et al. 2003
Laboratory contaminated for 2 days	¹⁴ C TCBP (PCB 77)	0.08-0.15	Leppanen et al. 2003
Alcoa sediment at 25 °C	di-chlorinated PCBs	0.11	Ghosh et al. 1999
	tri-chlorinated PCBs	0.04	
	tetra-chlorinated PCBs	0.02	
	tetra-chlorinated PCBs	0.01	
Soils from utility industry stations	PCB 18	0.004-0.06	Girvin et al. 1997
	PCB 28	0.001-0.05	
	PCB 33	0.003-0.08	
	PCB 40	0.002-0.06	
	PCB 42	0.002-0.05	
	PCB 44	0.002-0.06	
	PCB 49	0.002-0.06	
	PCB 52	0.002-0.05	
	PCB 66	0.001-0.05	
	PCB 70	0.0005-0.05	
	PCB 87	0.0002-0.02	
PCB 97	0.0002-0.01		
Upper Hudson River	PCB 4, 10	0.06-0.21	This Study
	PCB 19	0.05-0.22	
	PCB 8, 5	0.06-0.14	
	PCB 17	0.05-0.15	
	PCB 18	0.04-0.15	
	PCB 33, 21, 53	0.06-0.11	
	PCB 52	0.05-0.10	
	PCB 49	0.06-0.13	
	PCB 66, 95	0.03-0.08	
PCB 110, 77	0.03-0.04		

Table 5.1 Labile rate constants for PCB desorption.

Achman *et al.* (1996) used field data to estimate PCB fluxes in the lower Hudson River estuary. The desorption rate of PCBs from resuspended particles was calculated using a first order model that was interpreted in terms of radial diffusion based on the approximation suggested by Wu and Gschwend (1988). The initial particle concentration was set equal to the sediment concentration and they assumed a closed system in which the sediment was resuspended into water containing an initial dissolved load of PCBs equal to the concentration in the bottom water. They found there could be a significant release of PCBs into the dissolved phase during resuspension events. Chang and Sanford (2005) coupled a physical model to a biogeochemical model to explore the influence of hydrodynamic forcing factors, such as tidal current and shear velocity, on pyrene cycling. In this model, pyrene was input into a clean system with uncontaminated sediment. Model simulations suggest that tidally resuspending sediment increased dissolved pyrene concentrations in the water column by up to 22%. Understanding the release of PCBs during resuspension events is critical for assessing remediation plans and evaluating their impact on dissolved concentrations.

Understanding the release of PCBs during resuspension events is critical for assessing remediation plans and evaluating their impact on dissolved concentrations. This study utilized the Shear Turbulence Resuspension Mesocosms (STORM) to examine the release of PCBs from resuspended Hudson River sediment. In this series of experiments contaminated sediment was resuspended into clean well water to maximize the release of PCBs. Unlike other apparatus used to produce resuspension in laboratory settings, the STORM tanks mimic both bottom shear stress and water column turbulence (Porter *et al.* 2005). These tanks resuspended sediment to concentrations of ~80 mg/L

while generating minimal turbulence. Under these conditions, the resuspended particles adhered to each other and formed flocs in the water column (Chapter 3). In order to eliminate colloidal interferences, solid phase microextraction (SPME) was used to measure dissolved PCBs (Chapter 2). The organic carbon normalized partition coefficients measured at steady state in the STORM tank were similar to observed field measurements (Chapter 4). This study examines the initial release of PCBs from the resuspended sediment before a steady state dissolved concentration is reached. The rate constants for PCB desorption are calculated using two models and the release of PCBs on short time scales is assessed.

5.2 Materials and Methods

5.2.1 STORM Tanks

Resuspension events were conducted in three Shear Turbulence Resuspension Mesocosms (STORM) tanks described previously in Porter et al. (2005). The details of the tank set-up were presented in Chapters 3 and 4. This chapter focuses on the PCB results from first day of resuspension in the same series of events discussed in the previous chapters. During each resuspension event mixing began on the morning of day one and continued uninterrupted for the entire three-day period. After three days, at the end of each resuspension event, mixing was stopped and the particles were allowed to settle through the water column for approximately 20 hours. In STORM Tank A there was 1 day of quiescence between resuspension events, in Tank B there was two days quiescence between events, and in Tank C there was four days quiescence between

events (Figure 5.1). A diffusion control tank was also set-up in the same manner as the other three tanks but no resuspension events occurred in this tank.

5.2.2 Sampling Strategy

The STORM tanks were sampled most intensively on the first day of each resuspension event. Samples were collected every half hour for the first two hours of resuspension and then once an hour for the next four hours. On day two and three of the resuspension event, the tanks were sampled twice daily, once in the morning and once in the afternoon. At each sampling time point the dissolved PCB concentration was measured using solid phase microextraction (Chapter 2) and suspended solids were collected for particulate PCB analysis (Chapter 4). In addition, water samples were collected for TSS and particulate carbon and nitrogen (CHN) analysis. Laser In-Situ Scattering and Transmissometry (LISST 100C, Sequoia Scientific) measured the volume concentration ($\mu\text{l/l}$) of particles 3.2-250 μm in diameter in 32 logarithmically spaced bins (Chapter 3). Dissolved PCBs were measured every third day in the diffusion control tank.

5.2.3 Analytical Procedure

Dissolved PCB concentrations were measured using non-equilibrium solid phase microextraction (SPME). Chapter 2 describes this technique in detail and Chapter 4 discusses how SPME was used in the STORM tanks. The collection and analysis of suspended particle samples followed our laboratory's standard procedure, which is described in detail elsewhere (Bamford et al., 2002; Kucklick et al., 1996). Chapter 4 presents the details of the analytical procedure as it relates to the STORM tanks. For the

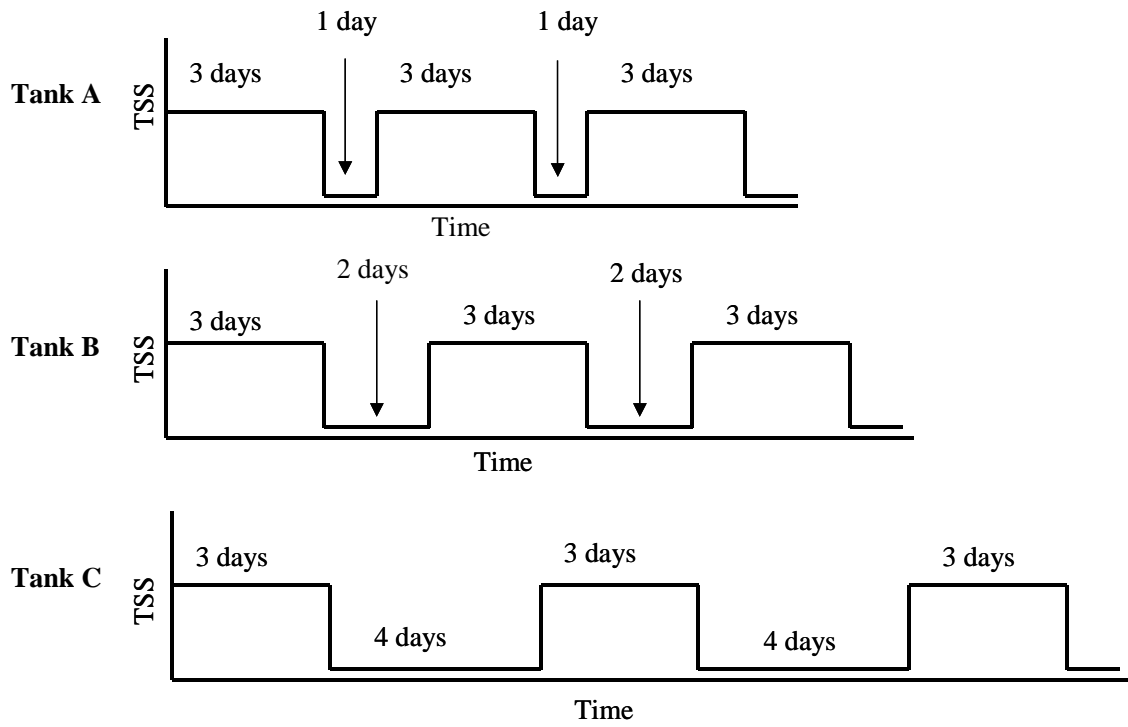


Figure 5.1. Schematic of the sequence of resuspension events conducted in the STORM tanks. The high TSS corresponds to periods when mixing was turned on. The low TSS corresponds to periods when mixing was turned off and the tanks sat with only 1 cm of overlying water.

suspended particle samples surrogate recoveries were $81\% \pm 9\%$ for IUPAC 14, $83\% \pm 10\%$ for IUPAC 65, and $85\% \pm 8\%$ for IUPAC 166 ($n = 100$). For dissolved, and particulate samples laboratory and field blanks were incorporated into the analysis to quantify possible contamination due to collection, transport, and analysis. Detection limits were derived from the blanks and defined as three times the mean blank concentration of each PCB congener. Detection limits for the various PCB congeners ranged from 1 to 5 ng L^{-1} in the dissolved phase, 1 to 120 ng g^{-1} in particulate phase, and 0.1 ng g^{-1} to 12 ng g^{-1} in the sediment. In addition if an individual PCB congener represented over 35% of the total it was considered non quantifiable and removed from the results.

5.3 PCB Desorption Models

As discussed in the introduction there are several different models of PCB desorption. This paper focuses on two models: the one compartment model and the radial diffusion model. The one compartment model was chosen in order to compare the desorption rate constants observed in this study to other literature studies. However, the parameters of the one compartment model were calculated by curve fitting and it is an empirical model with no mechanistic basis. The radial diffusion model was used to assess the impact of floc formation on the rate of desorption. The radial diffusion model takes into account the mechanisms of desorption by considering such factors as particle size and porosity and is semi-empirical in nature (Wells et al., 2004).

5.3.1 One Compartment Model

The total concentration of PCBs on resuspended particles is the sum of the PCB concentration in the labile and resistant pool. Literature estimates of the desorption rate constants show that the labile rate of desorption is two to three orders of magnitude greater than the resistant rate of desorption (Ghosh et al., 1999, Cornelissen et al., 1997). When particles are in the water column for short periods of time, the resistant fraction is effectively non-desorbing. In this case, PCB desorption can be modeled as a one compartment system rather than a two compartment system because PCBs only desorb from a labile pool. The governing equations for this system are as follows, where C_l is the particulate PCB concentration in a labile pool, k_l is the rate constant from the labile pool to the water (desorption), k_d is the rate constant from the water to the particle (re-absorption) and the resistant fraction is neglected (Chapra, 1996).

$$\frac{dC_d}{dt} = k_l C_l - k_d C_d \quad (1)$$

$$\frac{dC_l}{dt} = k_d C_d - k_l C_l \quad (2)$$

$$K_{labile} = \frac{k_d}{k_l} = \frac{C_{l,ss}}{C_{d,ss}} \quad (3)$$

$$C_{total} = C_l + C_d \quad (4)$$

This system of equations can be solved for the dissolved concentration in the STORM tanks given the boundary condition that $C_d(t = 0) = 0$ and $k_l + k_d = \text{constant} = k_{comp}$. In equation 6 below $C_{d,ss}$ is the steady state dissolved PCB concentration (ng L^{-1}).

$$\frac{dC_d}{dt} + (k_l + k_d)C_d = k_l C_{total} \quad (5)$$

$$C_d = C_{d,ss} (1 - \exp^{-k_{comp} t}) \quad (6)$$

The rate constant measured in the above equation is the full one compartment rate constant that accounts for both desorption and re-absorption. At short time periods re-absorption is negligible because C_d is near zero and equation 1 simplifies to equation 7.

$$\frac{dC_d}{dt} = k_l C_l \quad (7)$$

Integrating equation 7 gives an equation for the initial dissolved concentration as a function of time where b is a constant.

$$C_d(t) = k_l C_l t + b \quad (8)$$

In equation 8 both k_l and C_l are unknown. However, the total labile pool that was present on the sediment before it was resuspended ($C_{l,0}$) was calculated in equation 4 of Chapter 4. In this analysis at short time periods $C_{l,0} \cong C_l$. During the first 6 hours of resuspension the rate of desorption was linear and equation 8 was fit to the data to calculate k_l . The full one compartment model was fit to the total three day period of desorption to obtain k_{comp} or $k_l + k_d$. The re-absorption rate constant, k_d , was calculated by subtracting k_l from k_{comp} .

5.3.2 Radial Diffusion Model

In the radial diffusion model the movement of PCBs into or out of aggregates is retarded by local equilibrium between intra-particle pore water and solid matrices such as the organic matter fraction of the aggregate (Wu and Gschwend 1986, 1988). The rate of diffusion of the sorbate within the particle, or the effective diffusivity (D_{eff}), limits the rate of desorption. In the equation below, ϕ is the porosity of the aggregate, D_m is the molecular diffusivity in water ($\text{cm}^2 \text{s}^{-1}$), ρ_s is the dry density (g cm^{-3}), and K_p is the partition coefficient ($\text{cm}^3 \text{g}^{-1}$).

$$D_{eff} = \frac{D_m \phi^2}{(1 - \phi) \rho_s K_p + \phi} \quad (9)$$

In the above equation the numerator represents the reduction in molecular diffusion due to the tortuosity of the particle and the denominator reflects the retardation of diffusion due to local microscale partitioning. Resuspensions contain heterogeneous mixtures of particle sizes and the observed multi-staged aggregate diffusion is modeled as the sum of diffusion from different sized particles (e.g. Wu and Gschwend 1988, Ball and Roberts 1991, and Kleinedam et al. 2004). Such diffusion models are inherently non-linear due to the fact that the rate of diffusion scales to the size of the particle.

The partition coefficient K_p in equation 9 represents equilibrium between the dissolved concentration in the interstitial pore water and the sorbed concentration in the walls of the pores. Wu and Gschwend estimated K_p by calculating bulk partition coefficients from measured dissolved and particulate concentrations. In terms of the one compartment model, these bulk estimates include both the labile and resistant fraction. Since the resistant fraction does not desorb on the time scales of resuspension events, this might not be the most relevant value of K_p . Additionally, this model assumes the partition coefficient within the pore spaces of the particle is the same as that at the surface of the particle.

Assuming a constant sorbate concentration on the surface of the particle, an analytical solution for the fraction of equilibrium obtained at time t is given by the equation below where R = particle radius (cm) (Crank, 1975).

$$\frac{M_t}{M_\infty} = 1 - \frac{6}{\pi} \sum_{l=1}^{\infty} \frac{1}{l^2} \exp\left(-\frac{D_{eff} l^2 \pi^2 t}{R^2}\right) \quad (10)$$

In equation 10 I is the index of series that approximate the solution at $M(t)/M_{\text{infinity}}$ (Appendix F). This solution was used by Cheng et al. (1995) to demonstrate that on time scales relevant to natural resuspension events, hydrophobic organic contaminants do not reach equilibrium between the particulate and dissolved phase.

Enough parameters were measured in the STORM tanks to evaluate the ability of the radial diffusion model to predict desorption. The LISST was deployed in each tank to measure the particle size distribution. Since size specific mass concentration of particles could not be measured porosity was a bulk parameter, and the data generated by the LISST were condensed into one measurement of volume median diameter (see Chapter 3). Alternatively we could have assumed that initially the PCBs were uniformly distributed across all size classes of particles and allowed desorption to occur from the various size classes of particles measured by the LISST. This approach will be explored in the future, for now this analysis focuses on utilizing measurable parameters in the radial diffusion model. For evaluation purposes, the change in median diameter as a function of resuspension time was input into the radial diffusion model. Floc porosity was assumed to be constant since it did not vary systematically with time and dry density was assumed to be a linear combination of the mineral density and organic matter density (Chapter 3). Several values of the partition coefficient were input into the model to explore its effect on the predicted the rate of desorption.

5.4 Results and Discussion

5.4.1 Initial Release

Since the initial conditions in all three tanks were the same, the first resuspension event in each tank represents replicate treatments. This first event occurred after 10-14 days of the sediment sitting on the bottom of the STORM tank (Chapter 3) and represents the initial release of PCBs from quiescent sediment when it is resuspended after a long rest period. Some very labile PCBs were probably lost during the original collection when the sediment was lifted from the bottom of the Hudson River and transported to Maryland, so the data presented in this study could underestimate the release caused by an infrequent storm.

During the first resuspension event, PCB desorption occurred rapidly and the dissolved phase concentration appeared to reach steady state in six hours (Figure 5.2). Several di, tri and tetra-chlorinated PCB were detectable after just 15 minutes of resuspension. This rapid initial release represented an average of 30% of the steady state dissolved PCB concentration. Resuspension of pore water does not account for this “burp” in PCB concentration. Since the resuspension depth was less than 1mm, less than 1L of porewater was mixed into the 1000L water column during resuspension. Assuming the pore water was in equilibrium with the sediment, resuspension could account for dissolved PCB concentrations up to 8 pg L^{-1} of each congener, well below the detection limits of SPME and much less than the “burp” concentrations measured after 15 minutes of resuspension. A similar evaluation was conducted to determine if this initial PCB release could be caused by the exchange of interstitial water during floc disaggregation. The LISST measured an initial volume of resuspended particles of 154 uL L^{-1} and the

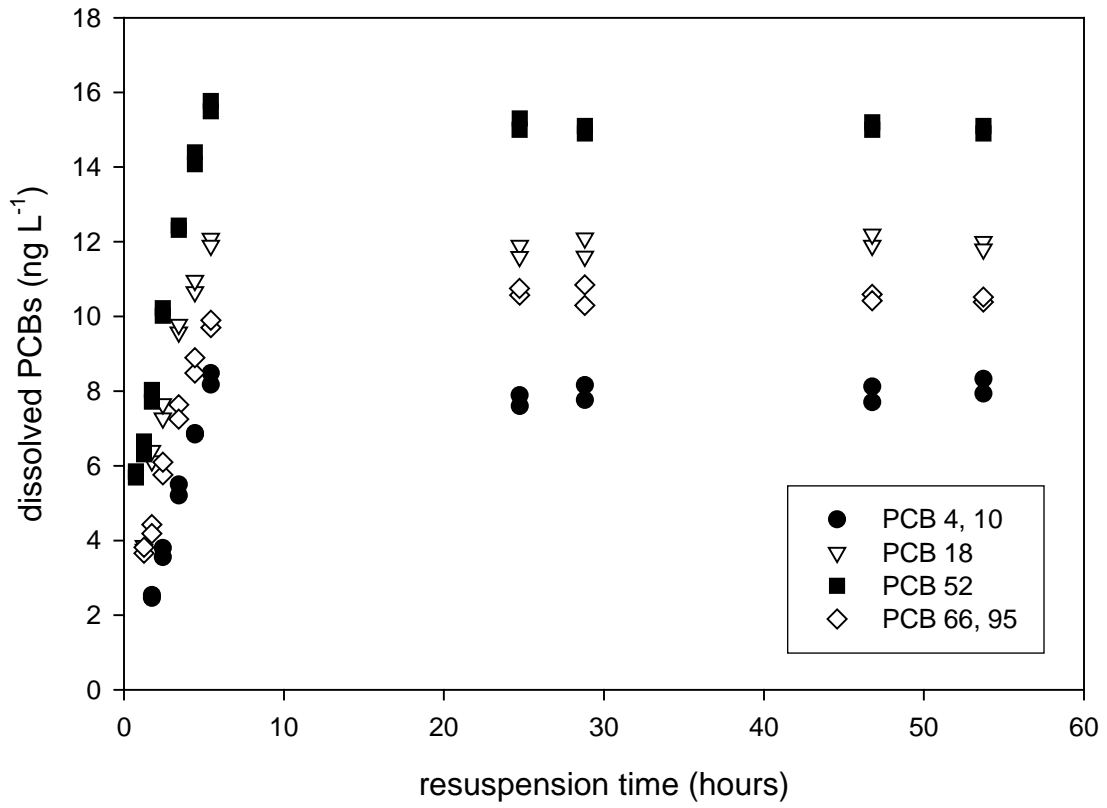


Figure 5.2. Dissolved PCBs in STORM Tank A during resuspension event 1.

calculated porosity of the flocs was 0.90. If all of the intra-floc water was released into the water column instantaneously, $138 \text{ ul}_{\text{floc water}} \text{ L}^{-1}_{\text{water}}$ would exchange with the water column. The release of this volume of water would add up to 5 pg L^{-1} of each congener into the water column, assuming equilibrium between the solid phase and porewater of the floc before resuspension.

After two hours of resuspension, all PCB congeners were detectable and dissolved concentrations were an average of $50 \pm 11\%$ of their steady state values. At this time, the percentage of water column PCBs in the dissolved phase did not vary with molecular weight and averaged $20 \pm 8\%$ in all three tanks (Figure 5.3). During the first six hours of resuspension, the dissolved PCB concentration continued to increase with time, while the particulate concentration was relatively constant. As a result, the organic normalized partition coefficient decreased with time (Figure 5.4).

Labile rate constants, k_1 , calculated using the data collected during the first six hours of resuspension ranged from 0.03 to 0.34 hour^{-1} and were not significantly different between tanks ($p = 0.72$ Figure 5.5). During this time period the dissolved concentration rose linearly with time and this model fit the data well with coefficient of determination ranging from 0.80 to 0.99 . The labile rate constant decreased significantly as the $\log K_{ow}$ of the PCB congeners increased ($p = 0.002$ Figure 5.6). The labile rate constant of PCB 4, 10, unresolved di-chlorinated congeners, were an average of 4 times greater than the k_1 of PCB 110, a penta-chlorinated congener. Literature values of the rate constants for PCB desorption ranged from 0.0002 to 0.20 hour^{-1} (Table 5.1). The rate constants calculated from our data are at or just above the upper end of this range.

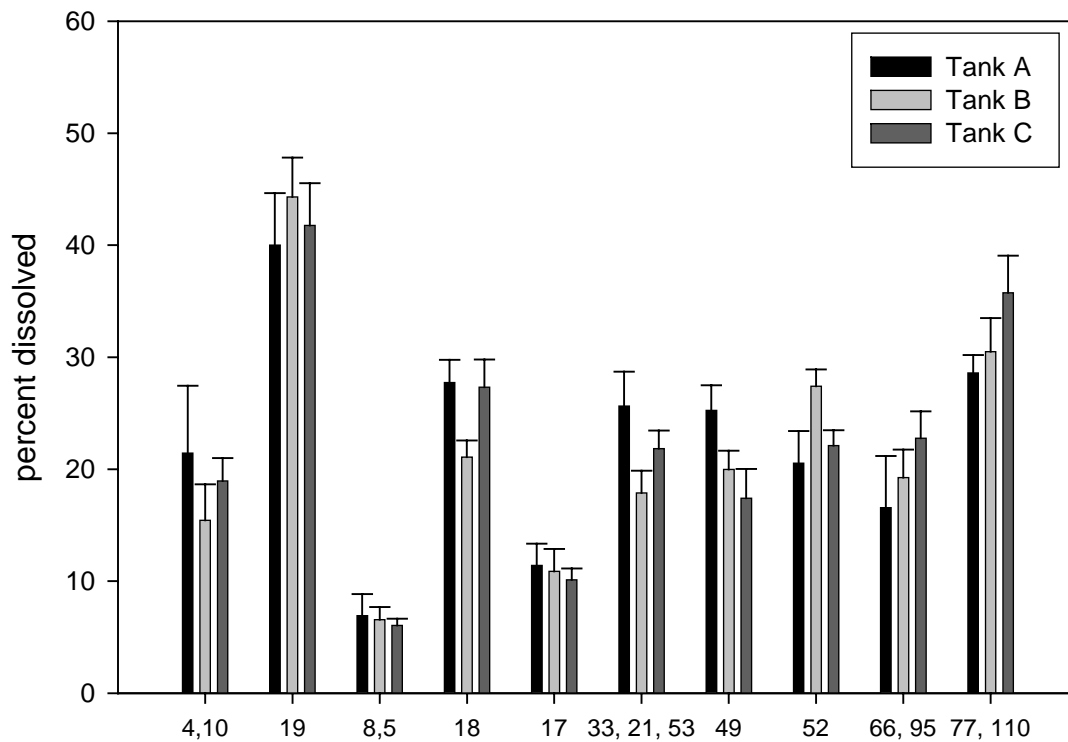


Figure 5.3. Percent of water column PCBs in the dissolved phase after two hours of resuspension.

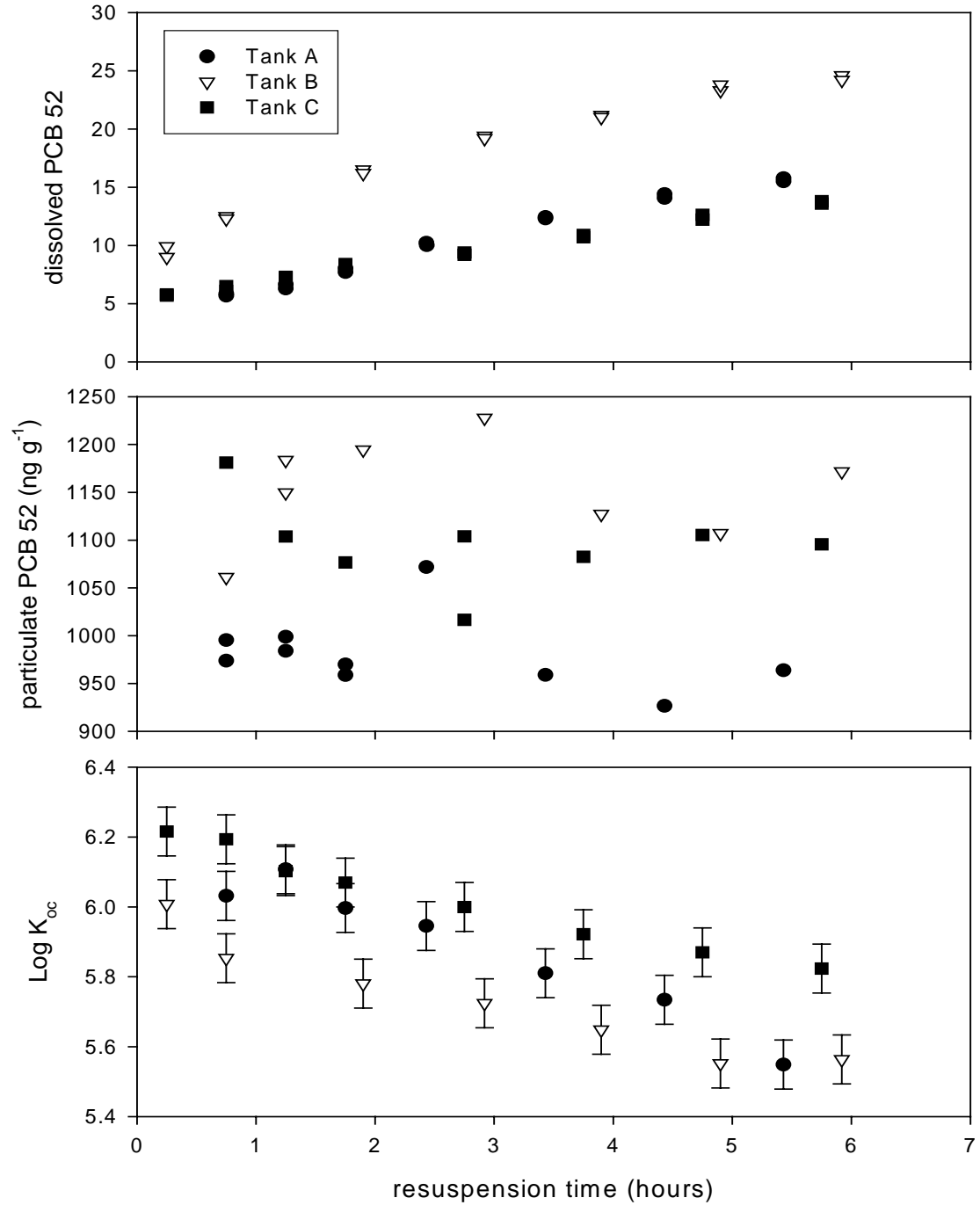


Figure 5.4. Dissolved and particulate PCB 52 measured in the STORM tanks and the calculated partition coefficient. In the top two panels multiple dots represent replicate samples. Error was propagated for the partition coefficient calculation assuming a 5% error in the dissolved measurement and 20% error in the particulate measurement.

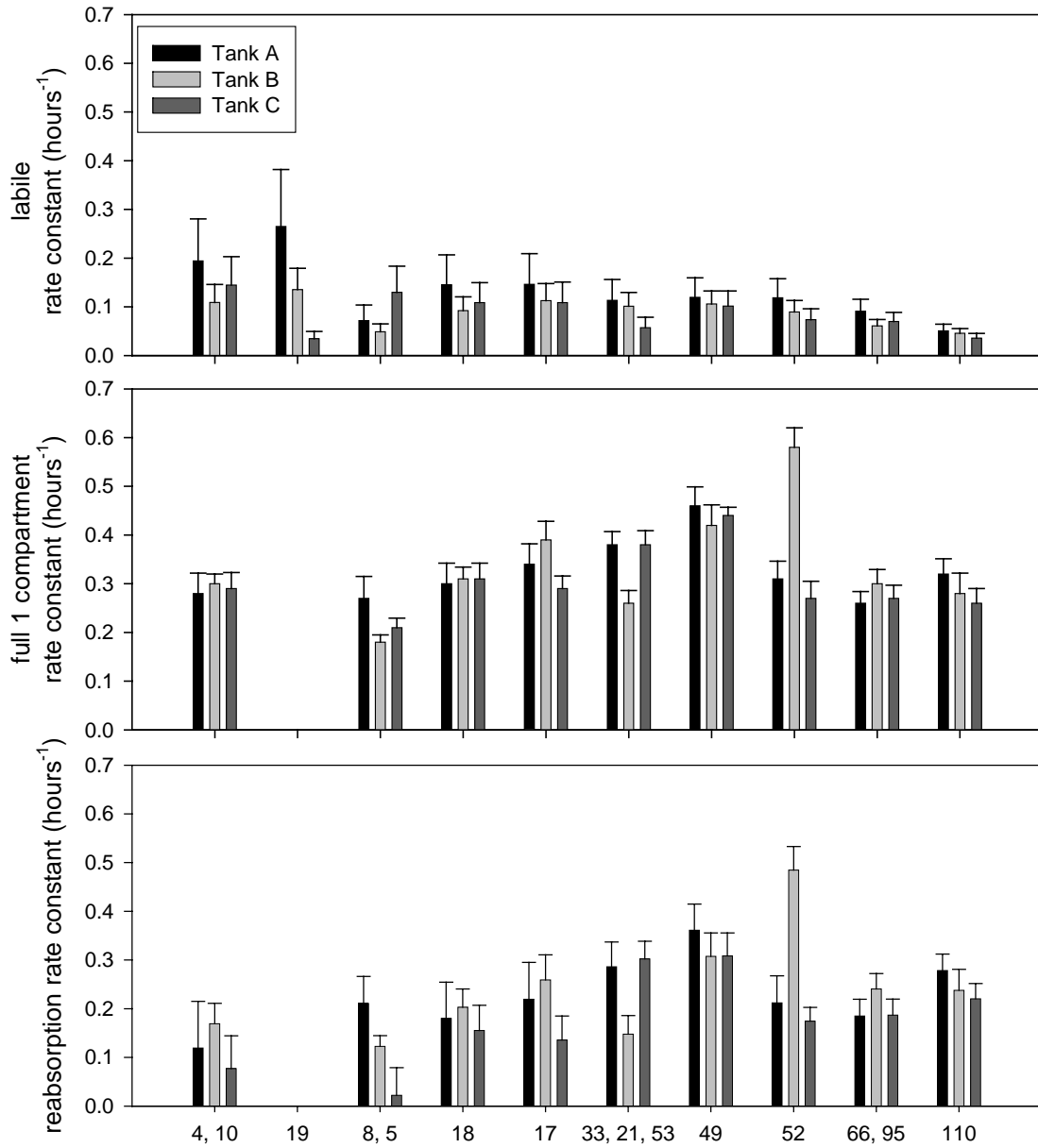


Figure 5.5. The labile rate constant k_l , full rate constant k_{comp} , and re-absorption rate constant k_d for resuspension event 1 in Tank A, B and C.

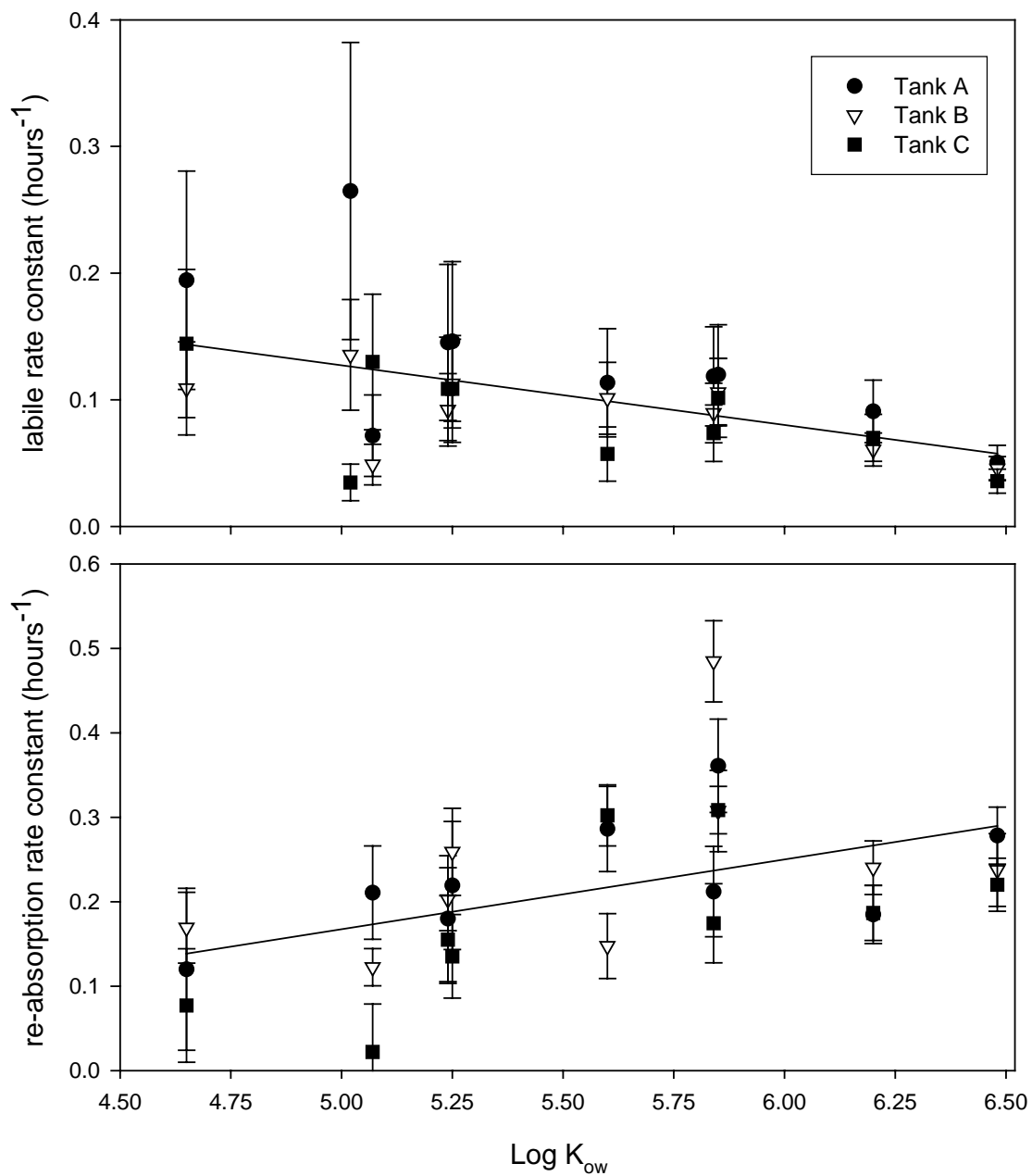


Figure 5.6. The relationship between the labile and re-absorption rate constant and log K_{ow} during the first resuspension event in all three tanks.

The one compartment full rate constant k_{comp} encompassing re-adsorption and desorption calculated using the entire three day data set of dissolved PCB concentrations ranged from 0.18 to 0.58 hour^{-1} with an average of $0.32 \pm 0.08 \text{ hour}^{-1}$ (Figure 5.5). Again there were no significant differences in the full rate constant among tanks ($p = 0.71$). A rate constant for PCB 19 could not be calculated because the dissolved concentration reached steady state more rapidly than predicted by the model and the relative percent error was over 100%. The relative percent error of the other full rate constants averaged $11 \pm 3\%$ and there was no correlation between k_{comp} and PCB molecular weight, in contrast to the labile rate constant. The re-absorption rate constant, k_d , calculated by subtracting the labile rate constant from the full rate constant ranged from 0.02 to 0.48 hour^{-1} . As with the other rate constants, k_d did not vary significantly between tanks ($p = 0.30$, Figure 5.5). The re-absorption rate constant was significantly positively correlated with $\log K_{\text{ow}}$ ($p = 0.01$, Figure 5.6) and the k_d of PCB 110, the penta-chlorinated congener, was an average of two times greater than the k_d of PCB 4, 10, the unresolved di-chlorinated congeners.

The radial diffusion model assumes high molecular weight congeners desorb more slowly than low molecular weight congeners because of their lower aqueous diffusion coefficients. However, the aqueous diffusion coefficient, D_m , only varies from 5.97×10^{-6} to $5.24 \times 10^{-6} \text{ cm}^2 \text{ s}^{-1}$ over the range of congeners examined in this study and the model was not very sensitive to this parameter (Table 5.2). In the first scenario examined, the LISST data were used to input the change in floc volume median diameter as a function of time. Floc dry density was assumed to be a linear combination of the mineral and organic matter density and this information along with the total suspended

solids concentration was used to calculate floc porosity (Chapter 3). Since floc porosity did not vary systematically during the first resuspension event (Chapter 3), it was input as a constant into the model. Various relationships between the partition coefficient and the octanol water partition coefficient (K_{ow}) are presented in the literature (see Allen-King et al. 2002). For evaluation purposes Karickhoff's relationship that $\log K_{oc} = 1.0 * \log K_{ow} - 0.21$ was input into the model (Karickhoff et al., 1979; Table 5.2).

Using a K_{ow} -dependent K_{oc} , the radial diffusion model over-predicted the time to equilibrium for the di-chlorinated congeners, accurately predicted the time to equilibrium for the tri-chlorinated PCB congeners and overestimated the time to equilibrium for the tetra and penta-chlorinated congeners (Figure 5.7, Table 5.2). When the partition coefficient was held constant at $5 * 10^4 \text{ L Kg}^{-1}$ for all congeners, the model more accurately predicted the time to equilibrium (Figure 5.8). This analysis suggests the partition coefficient does not vary as a function of the octanol water partition coefficient. The observation that K_p is constant over the range of octanol water partition coefficients examined in this study is consistent with the observed steady state partition coefficient measured in the STORM tanks (Chapter 4) and in the Upper Hudson River (Butcher et al. 1999).

In the second scenario examined, Karickhoff's relationship between K_{oc} and K_{ow} was input into the radial diffusion model and particle radius and porosity were allowed to vary until the best fit for the data was obtained. Results from this scenario showed that desorption from the different chlorinated congeners was best described by particles with different properties. It was not possible to predict the results observed in the STORM tank using a uniform particle radius and porosity. The best fit to the data was obtain

	# Cl-	D_m (cm ² s ⁻¹)	Log K_{ow}	Log K_p
PCB 4, 10	2	5.97e-6	4.65	3.52
PCB 8, 5	2	5.97e-6	5.07	4.36
PCB 19	3	5.70e-6	5.02	4.31
PCB 17	3	5.70e-6	5.24	4.53
PCB 18	3	5.70e-6	5.25	4.54
PCB 33, 21, 53	3	5.70e-6	5.60	4.89
PCB 52	4	5.46e-6	5.84	5.13
PCB 49	4	5.46e-6	5.85	5.14
PCB 66, 95	4	5.46e-6	6.20	5.49
PCB 110	5	5.24e-6	6.48	5.77

Table 5.2. Properties of the PCB congeners measured in the STORM tanks. The molecular diffusion coefficient in water (D_m) was calculated using the Wilke-Chang equation. The K_p value was calculated using Karickhoff's equation given that the particles were 12% organic carbon.

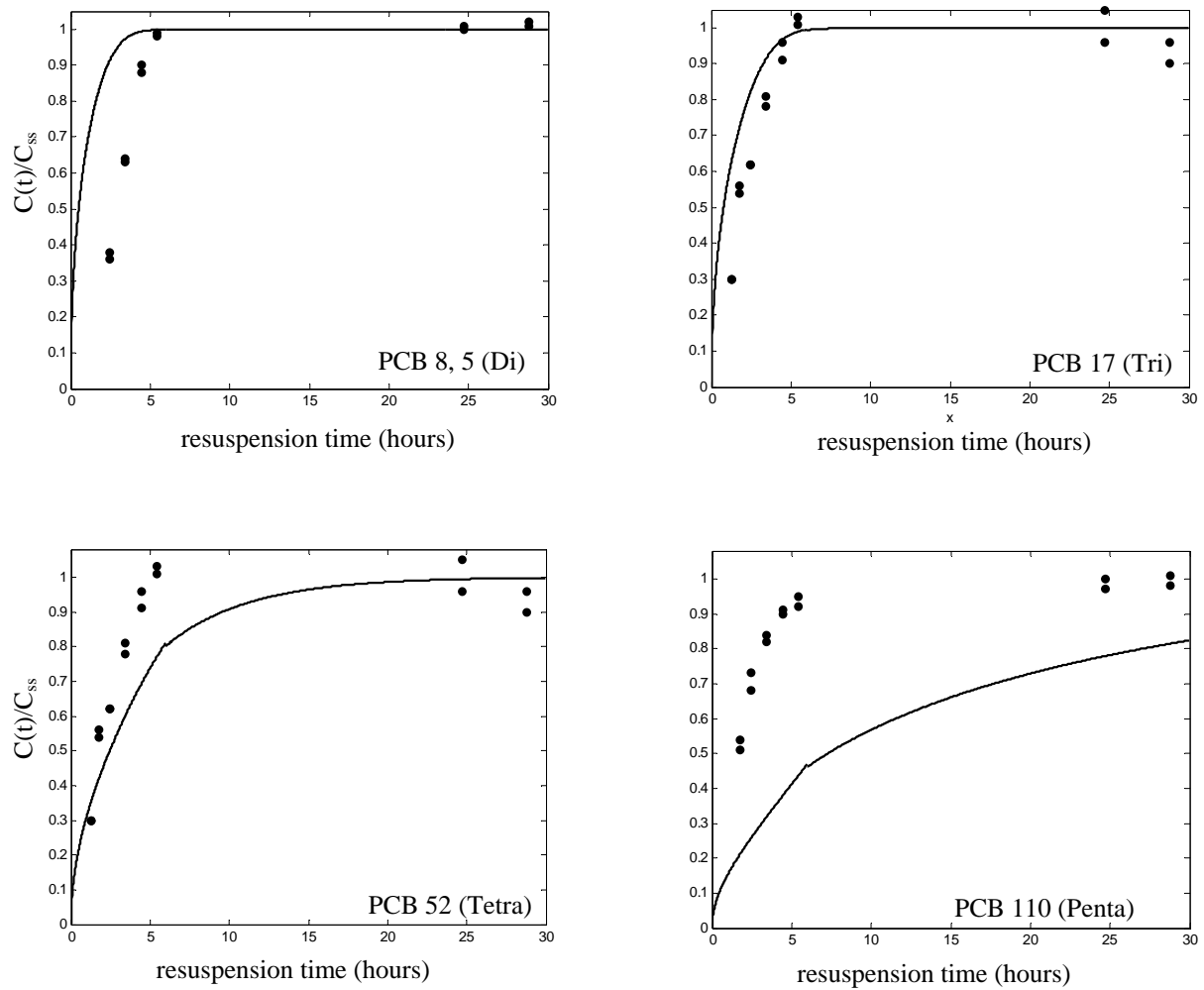


Figure 5.7. The measured PCB concentration in STORM Tank A event 1 (dots) compared to the concentration predicted by the radial diffusion model (solid line) when Karickhoff's partition coefficient is input into the model along with floc radius, porosity, and density.

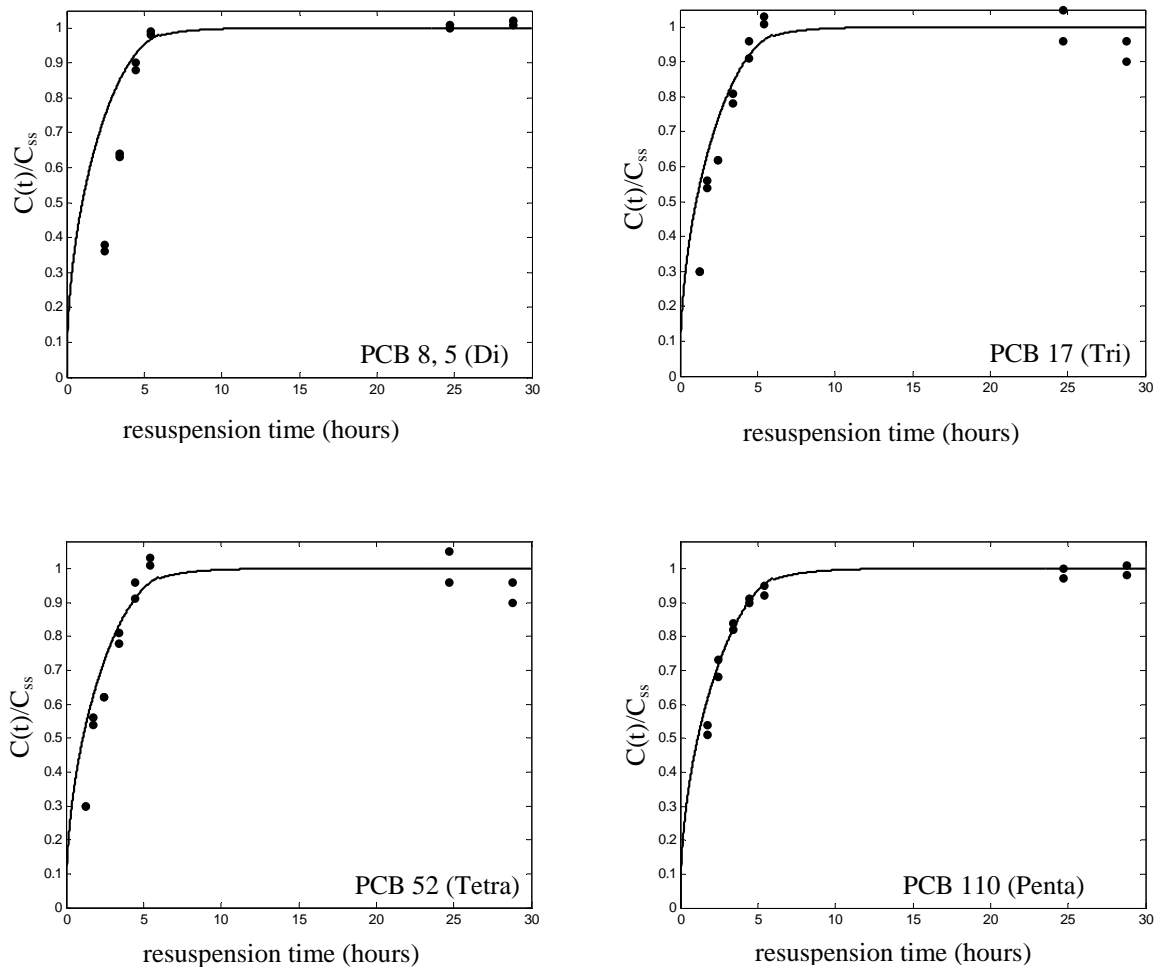


Figure 5.8. The measured PCB concentration in STORM Tank A event 1 (dots) compared to the concentration predicted by the radial diffusion model (solid line) when the partition coefficient is held constant at $5 \cdot 10^4 \text{ L kg}^{-1}$ and the measured floc radius, porosity, and density are input into the model.

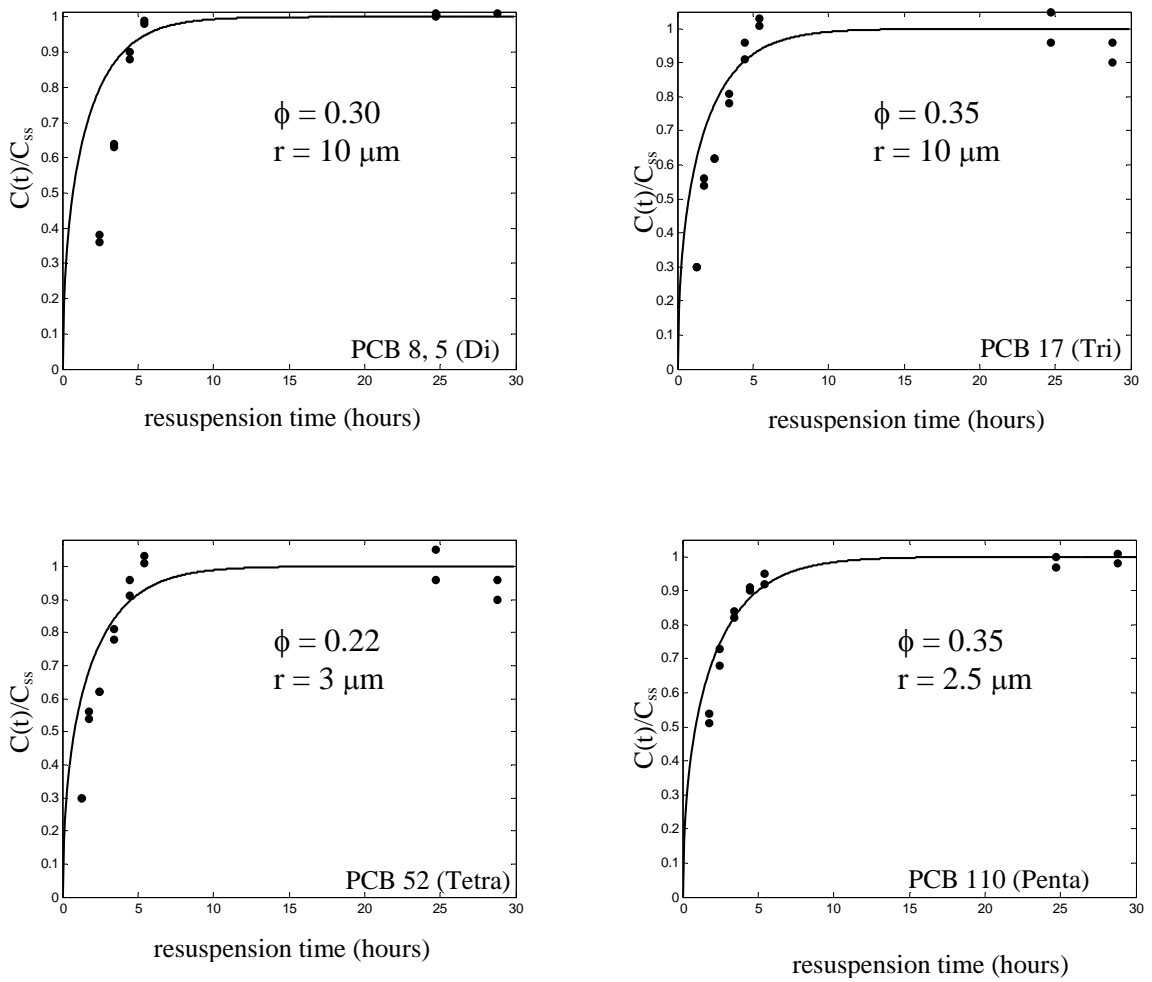


Figure 5.9. The measured PCB concentration in STORM Tank A event 1 (dots) compared to the concentration predicted by the radial diffusion model (solid line) when Karickhoff's partition coefficient is input into the model and particle porosity and radius are allowed to vary.

when the particles ranged in radius from 2.5 to 10 μm and had porosities between 0.22 and 0.35 (Figure 5.9). Using Karickhoff's K_p values suggests that small particles control the rate of desorption in the STORM tank. However, modeling the observed desorption rates with K_p varying as a function of K_{ow} suggests that the various PCB congeners are bound to different sized sediment particles. It is difficult to envision a mechanism by which this could occur and it seems more likely that K_p is constant over the range of K_{ow} examined in this study.

5.4.2 Impact of Quiescent Time

After the first resuspension event, the three tanks did not receive the same treatment because they had different quiescent times between resuspension events. By resuspension event 3 several of the PCBs congeners did not exceed detection limits until the second day of resuspension. For discussion purposes only the congeners that were detected in all three events are compared. For the congeners that were detected in all three events, an average of $22 \pm 3\%$ of the resuspended PCBs were dissolved after two hours of resuspension in event 1. There was no relationship between the percent of PCBs in the dissolved phase and the congener molecular weight for this event or any of the subsequent events. Event 2 and 3 had significantly less dissolved PCBs after two hours of resuspension than event 1 ($p = 0.04$ for event 2 and $p = 0.005$ for event 3, Figure 5.10). At this time point, there were no significant differences between tanks despite the different treatments ($p = 0.35$ for event 2 and $p = 0.54$ for event 3) and by event 3 an average of $16 \pm 8\%$ of the resuspended PCBs were dissolved. After two hours of resuspension, the dissolved concentration reached an average of $60 \pm 10\%$ of the steady state concentration for both event 2 and 3. Repeated resuspension events resulted in less

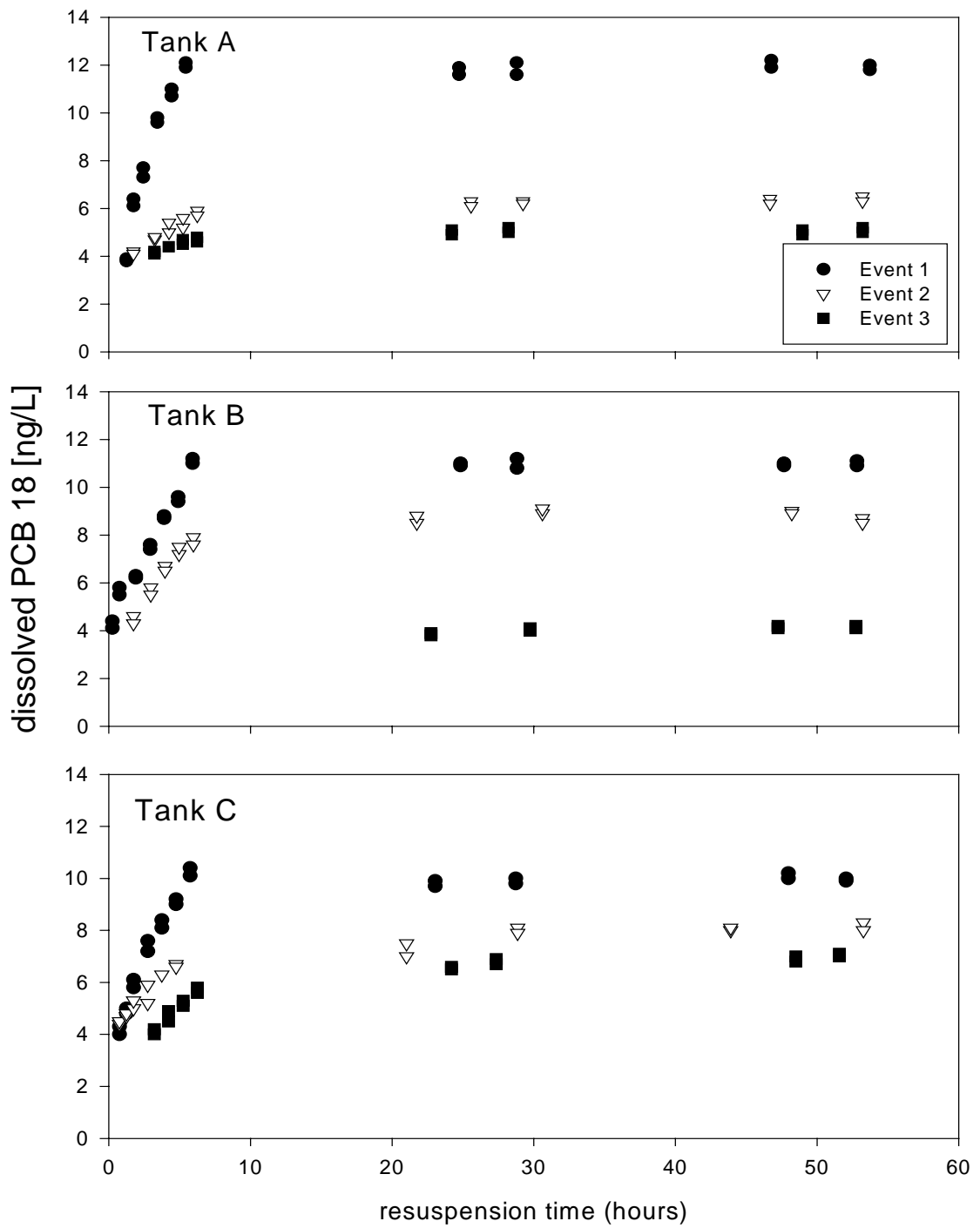


Figure 5.10. Dissolved PCB 18 during the course of each resuspension event in the three STORM tanks.

PCB release per event. Four days of quiescence was insufficient to impact the amount of PCBs released during the first two hours of resuspension.

After six hours of resuspension, the percent dissolved PCBs decreased between events (Figure 5.10). In Tank A, with 1 day of quiescence between events, an average of $33 \pm 10\%$ of the resuspended PCBs were dissolved after six hours of resuspension event 1 but only $19 \pm 8\%$ of PCBs were dissolved at the same time point in resuspension event 2 and 3. In this tank the decrease in dissolved PCBs was significant ($p = 0.005$). In Tank B, with two days of quiescence between events, an average of $30 \pm 10\%$ of the resuspended PCBs were dissolved after six hours of resuspension 1 but only an average of $18 \pm 9\%$ after event 2 and 3. In this tank the decrease was significant at the 90% confidence level ($p = 0.07$). The percent dissolved PCBs in Tank C event 1 averaged of $30 \pm 10\%$ and in event 2 and 3 it averaged $21 \pm 9\%$. Unlike in the other tanks this decrease was not significant ($p = 0.39$). This suggests quiescent time impacts PCBs desorption. During resuspension events longer than a few hours, more PCBs are released from sediment the longer it sits undisturbed on the bottom. However, in all cases repeated resuspension events resulted in less release of PCBs per event.

By the third resuspension event only five of the PCB congeners (PCB 4+10, 17, 18, 33, 21, 53, 49 and 52) were consistently present in the dissolved phase at detectable levels. In all three tanks the labile rate constant (k_1), full rate constant (k_{comp}) and re-absorption rate constant (k_d) decreased significantly from event 1 to event 3, were not significant differences between tanks, and were not significantly correlated to $\log K_{ow}$. However, the limited number of congeners detected in the third event limits the statistical strength of this analysis. By the third resuspension event k_1 ranged from 0.03 to 0.28

hours⁻¹ and averaged 0.07 hours⁻¹, k_{comp} ranged from 0.10 to 0.53 hour⁻¹ and averaged 0.24 hour⁻¹, and k_d ranged from 0.04 to 0.27 hour⁻¹ and averaged 0.13 hour⁻¹. It appears that the quiescent time between resuspension events did not influence the rate constants of PCB desorption and suggests that desorption during subsequent resuspension events occurred from a less labile pool than desorption during the first resuspension event.

The radial diffusion model run using the measured change in floc diameter as a function of time, calculated porosity, and constant partition coefficient of $5 \times 10^4 \text{ L Kg}^{-1}$ accurately predicted desorption during the third resuspension event (Figure 5.11). The change in volume median diameter with resuspension time was described by a different function in each resuspension event. The difference in the function was sufficient to account for the change in desorption behavior between resuspension events. The radial diffusion model run with the LISST input could accurately predict the impact of quiescent time on the rate of desorption.

5.4.3 Impact of Repeated Resuspension

One explanation for the decrease in dissolved PCBs between resuspension events could be changes in the properties of the resuspended particles. If flocculation caused the median diameter of the particles to increase with each resuspension event this would slow the rate of desorption. Desorption occurs more slowly from particles with larger radii. An analysis of the LISST data showed that the particle size distribution did not change with each resuspension event and there were only minimal differences in floc porosity and density between events (Chapter 3). These differences are insufficient to account for the change in the dissolved PCB concentrations observed in the STORM tanks. Chapter 4 explored using a labile/resistant model to explain the differences between resuspension

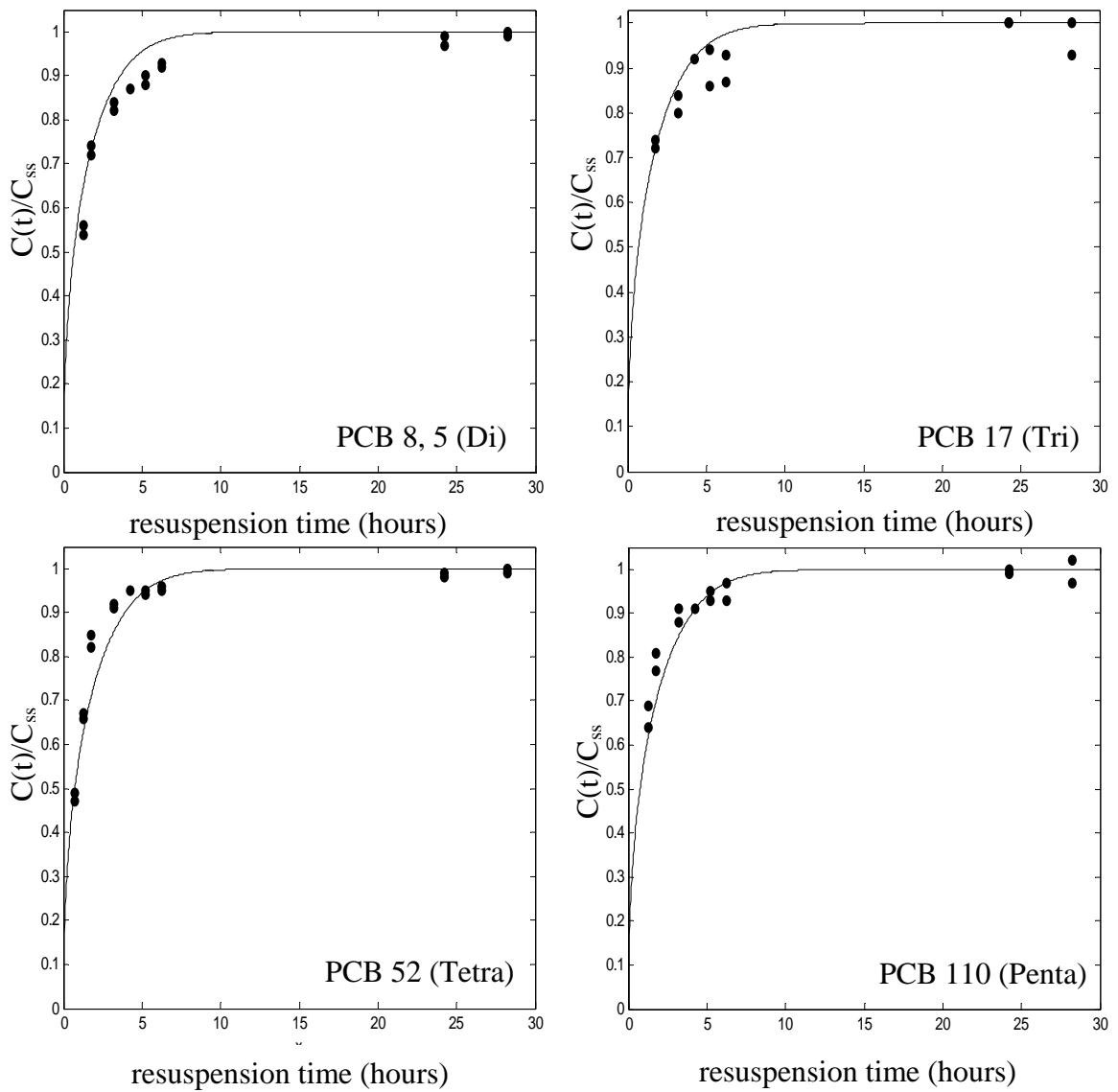


Figure 5.11. The measured PCB concentration in STORM Tank A event 3 (dots) compared to the concentration predicted by the radial diffusion model (solid line) when the partition coefficient is held constant at $5 \cdot 10^4 \text{ L kg}^{-1}$ and the measured floc radius, porosity, and density are input into the model.

events in terms of a change in the percent of PCBs in a labile pool on the particles.

Another possible explanation for the decreased concentration of dissolved PCBs during subsequent resuspension events could be the loss of PCB enriched fine particles when the water was removed at the end of each resuspension event. During each resuspension event, flocs disaggregated with time and the same concentration of small particles was present in each resuspension event. However, the dissolved PCB concentration was lower during event 2 and 3 than event 1 (Figure 5.12). At the end of each resuspension event after ~20 hours of settling an average of 8% of the pre-settling particle mass still remained in the water column (Chapter 3). These particles were then removed from the tanks along with the water. If the particles remaining in the water column after the first event were enriched in PCBs relative to the particles remaining after the second and third event, their loss could account for the lower PCB concentration in subsequent resuspension events. In all three tanks, the PCB concentration of the particles remaining in the water column after resuspension event 1 and 20 hours of settling was an average of 4 times greater than the PCB concentration of the particles remaining after resuspension event 3 and 20 hours of settling (Figure 5.13). These PCB enriched fine particles consisted of such a small percentage of the total particle population that the bulk resuspended particulate PCB concentration did not change between resuspension events.

It is possible that these fine particles controlled desorption in the STORM tanks. However, this explanation does not account for the differences between tanks and the impact of quiescent time on PCB desorption. If it is assumed that the fine particles have a radius of 1 μm , a porosity of 0.5, and the partition coefficient is constant with $\log K_{ow}$

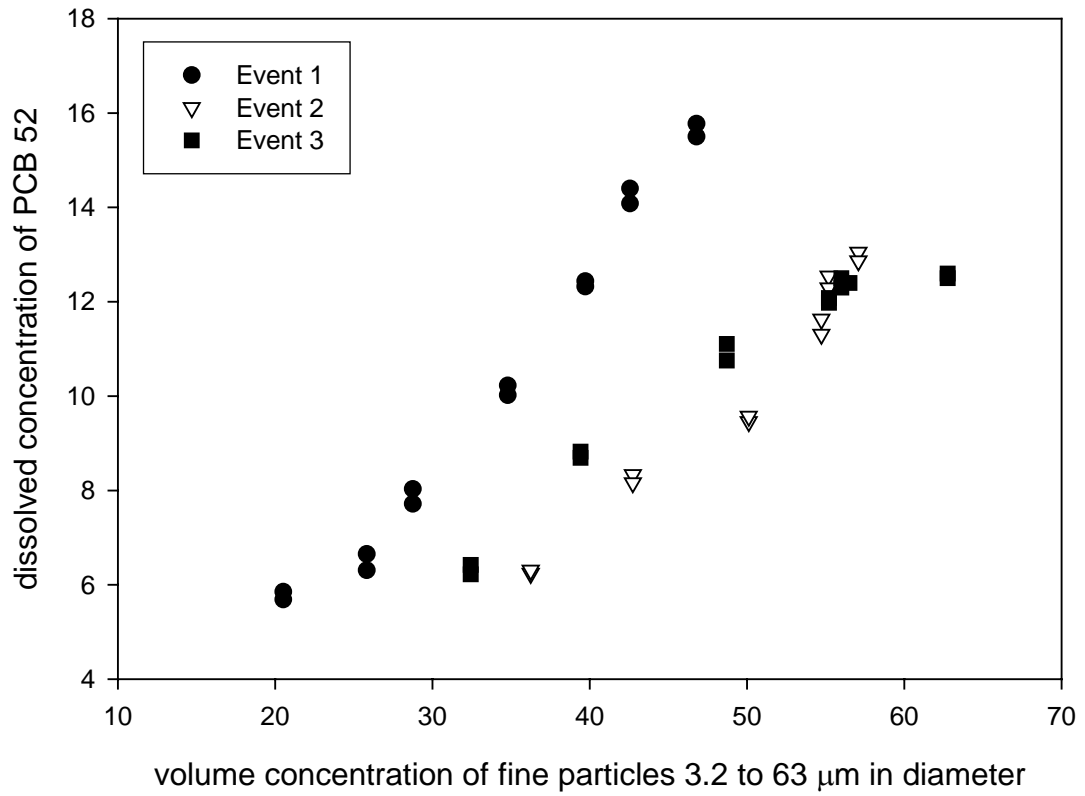


Figure 5.12. Dissolved PCB 52 during the first six hours of resuspension compared to the concentration of fine particles in Tank A.

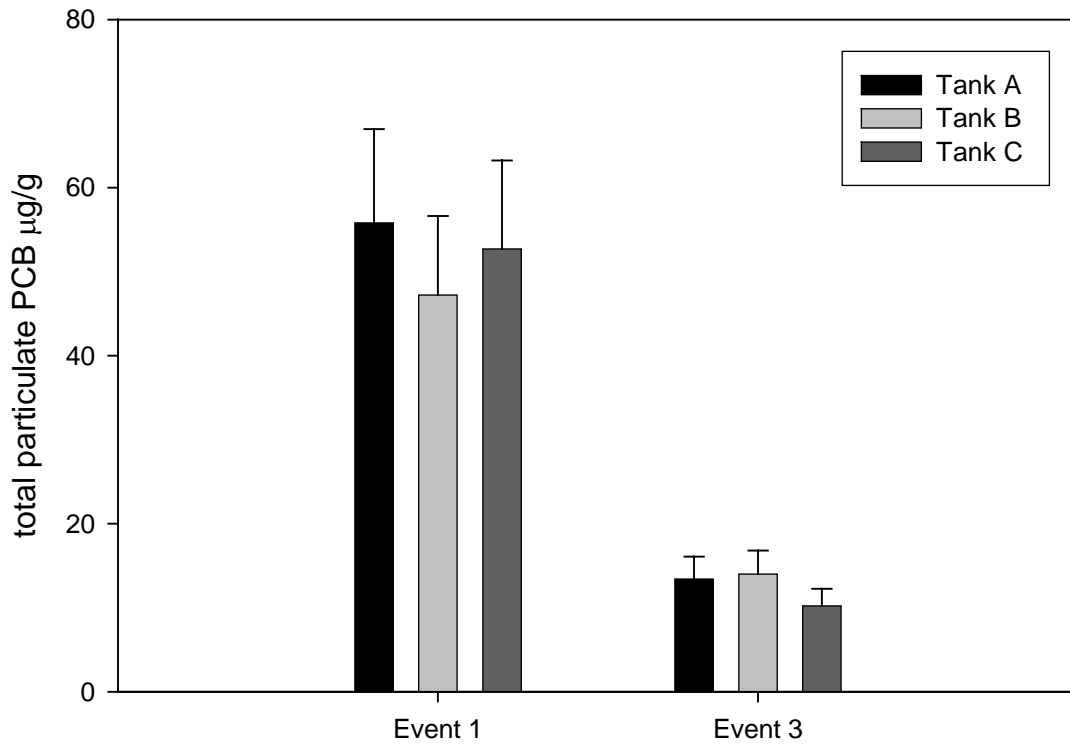


Figure 5.13. Dissolved PCB 52 during the first six hours of resuspension compared to the concentration of fine particles in Tank A.

than the radial diffusion model accurately predicts desorption in STORM Tanks during resuspension event 1. However, in order to model the observed rate of desorption during event 2 and 3 the radius and porosity of the small particles would have to change between resuspension events. If the radius and porosity of the small particles is held constant, then the radial diffusion model does not fit the observed data well (Figure 5.14). Since the LISST cannot measure particles whose radius is less than 1.6 μm it is impossible to know if this occurred.

5.6 Implications

After just two hours of resuspension, an average of 20% of the PCBs were released into the dissolved phase. Resuspension events could therefore add significant amounts of dissolved PCBs to the water column. In the Hudson River where sediment PCB concentrations are as high as 50 ug g^{-1} , a resuspension event of just 25 mg L^{-1} would add 250 ng L^{-1} of dissolved PCBs to the water column. In the three tanks, the amount of PCBs released into the dissolved phase decreased with subsequent resuspension events suggesting the impact of resuspension events diminishes with their frequency. However, even after the third resuspension event an average 16% of the resuspended PCBs were released into the dissolved phase after just two hours. At this rate of decline it would take over 6 resuspension events before only 5% of the resuspended PCB were in the dissolved phase. The labile rate constants calculated in this study fall in the upper end of those reported in the literature and PCBs may desorb faster than predicted in the EPA's assessment of dredging of the Upper Hudson River.

The quiescent time between resuspension events influenced PCB desorption on

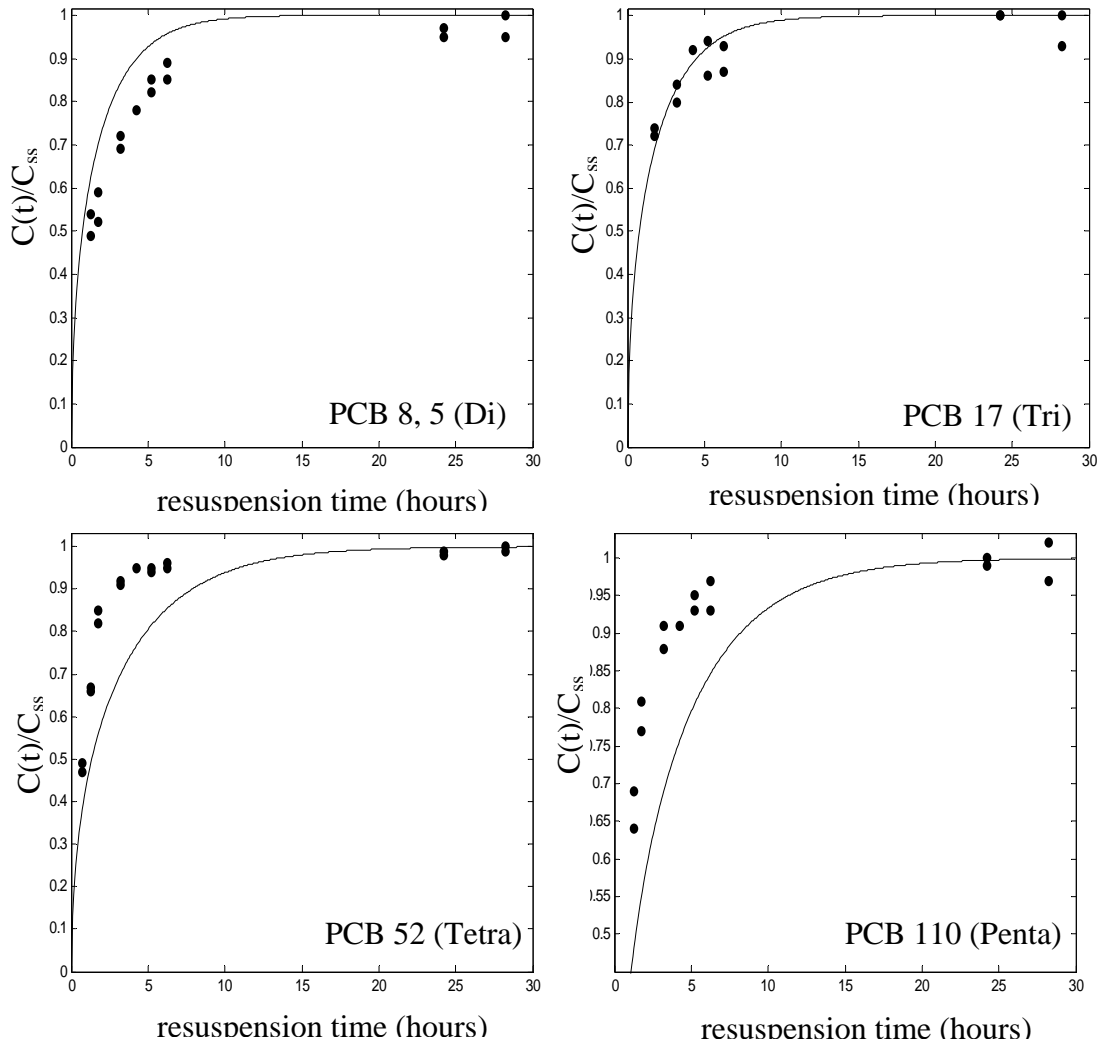


Figure 5.14. The measured PCB concentration in STORM Tank A event 3 (dots) compared to the concentration predicted by the radial diffusion model (solid line) when the partition coefficient is held constant, particle radius is $1 \mu\text{m}$, and particle porosity is 0.5. The model does not fit the data as well as when floc volume as a function of time is input into the radial diffusion model (Figure 5.11).

longer time scales. After six hours of resuspension there were no significant differences in the percentage of dissolved PCBs among the three resuspension events in Tank C, with four days quiescence between events. In Tank A, with one day quiescence between resuspension events, subsequent resuspension events resulted in significantly lower percentages of dissolved PCBs. This suggests that if there was a long enough time period between resuspension events, the desorbable fraction might recharge and release higher than predicted amounts of PCBs into the dissolved phase.

Allowing the partition coefficient to vary as a function of K_{ow} in the radial diffusion model and inputting the measured floc volume median diameter and porosity resulted in the di-chlorinated congeners desorbing faster than observed in the STORM tanks and the penta-chlorinated congeners desorbing more slowly than observed in the STORM tanks. As a result, the radial diffusion model over estimated the time to equilibrium of the di-chlorinated congeners by five hours and under estimated the time to equilibrium of the penta-chlorinated congeners by 115 hours. If the partition coefficient was allowed to vary as a function of K_{ow} and particle radius and porosity were fit to the observed data, then the radial diffusion model suggests the different homologue groups of PCBs are bound to particles with different properties. When measured floc volume median diameter and porosity were input into the model and the partition coefficient was held constant, the model fit the data vary well. This analysis suggests the K_p does not vary as a function of K_{ow} and is consistent with field measured values of K_p . Inputting these measured floc properties into the radial diffusion model and holding the partition coefficient constant was the only way to capture the change in desorption between resuspension events.

Appendix A: Analytical Services Data

A-1: Tank A

A-2: Tank B

A-3: Tank C

Table A-1: Tank A ancillary water sample data

Resuspension event 1

elapsed time (hours)	PN (mg N/l)	PC (mg C/l)	TSS (mg/L)	total chla (ug/l)	phaeo (ug/l)	active (ug/l)	DOC (mg C/l)
0.00	0.01	0.10	2.4	0.19	0.33	0.02	0.97
0.25	0.22	2.78	31.0	3.69	5.87	0.77	0.82
0.75	0.27	3.71	30.1	3.56	5.49	0.83	0.89
1.25	0.32	3.83	37.3	4.36	7.16	0.79	1.14
1.75	0.26	3.45	32.3	3.98	6.48	0.75	0.97
2.43	0.36	4.65	41.8	4.70	7.65	0.89	1.24
3.43	0.31	3.90	42.9	5.31	8.51	1.07	0.98
4.43	0.27	3.43	34.8	3.84	6.26	0.72	1.18
5.43	0.32	4.19	36.0	4.44	7.33	0.79	1.17
24.73	0.65	8.07	61.8	8.66	13.82	1.79	1.05
28.8	0.61	7.69	53.7	4.42	7.37	0.76	1.11
46.77	0.31	4.02	62.9	7.44	12.14	1.40	1.08
53.72	0.51	6.56	62.2	7.66	12.50	1.44	1.07
Off	0.13	1.88	5.4	2.39	4.06	0.37	1.16

Resuspension event 2

elapsed time (hours)	PN (mg N/l)	PC (mg C/l)	TSS (mg/L)	total chla (ug/l)	phaeo (ug/l)	active (ug/l)	DOC (mg C/l)
0.00	0.01	0.12	2.4	0.19	0.30	0.05	0.91
0.25	0.19	2.82	28.3	3.35	5.31	0.71	0.89
0.75	0.23	3.48	35.3	4.30	6.85	0.89	0.90
1.25	0.31	4.47	34.2	4.69	7.60	0.91	0.99
1.75	0.32	4.34	35.0	5.23	7.97	1.26	0.93
3.25	0.29	4.24	37.0	4.88	7.87	0.97	0.90
4.25	0.35	4.46	43.5	6.38	9.78	1.51	1.2
5.25	0.38	5.13	43.0	5.41	8.72	1.07	1.37
6.25	0.33	4.33	42.5	5.38	8.53	1.13	1.13
25.58			53.0				
29.25	0.42	5.54	50.5	6.82	10.89	1.40	1.27
46.68	0.41	5.14	51.0	6.60	10.73	1.26	1.11
53.22	0.45	5.43	47.5	6.72	10.81	1.34	1.4
Off	0.10	0.76	6.5	1.54	2.60	0.25	1.3

Resuspension event 3

elapsed time (hours)	PN (mg N/l)	PC (mg C/l)	TSS (mg/L)	total chla (ug/l)	phaeo (ug/l)	active (ug/l)	DOC (mg C/l)
0.00	0.01	0.12	2.4	0.16	0.27	0.03	0.97
0.25	0.26	3.44	32.0	4.77	7.45	1.06	0.99
0.75	0.37	4.97	37.5	4.40	7.14	0.85	0.95
1.25	0.37	4.84	35.0	4.58	7.38	0.91	0.91
1.75	0.26	3.26	34.5	3.48	5.85	0.57	1.25
3.23	0.26	3.47	37.0	4.02	6.58	0.74	1.01
4.23	0.27	3.40	39.8	4.82	7.67	1.01	1.1
5.23	0.34	4.10	38.5	5.38	8.75	1.03	1.33
6.23	0.41	4.85	42.5	5.24	8.62	0.95	1.10
24.22	0.32	3.87	33.0	4.81	7.96	0.85	1.23
28.22	0.36	4.20	39.5	5.66	9.47	0.96	1.45
48.98	0.52	6.08	45.5	7.24	11.70	1.42	1.68
53.23	0.55	6.93	54.5	7.77	12.77	1.42	1.13
71.17	0.69	8.63	44.5	6.32	10.36	1.16	1.33
95.12	0.45	5.87	42.0	5.78	9.90	0.85	1.49
118.90	0.51	6.03	48.0	7.47	12.00	1.50	1.51
143.55	0.54	6.29	57.0	8.17	13.11	1.65	1.79
168.80	0.64	7.31	58.0	8.16	12.96	1.71	1.73
Off	0.06	0.71	8.2	1.46	2.48	0.22	1.28

Settling

elapsed time (hours)	PN (mg N/l)	PC (mg C/l)	TSS (mg/L)	total chla (ug/l)	phaeo (ug/l)	active (ug/l)	DOC (mg C/l)
before	0.64	7.31	58.0	8.16	12.96	1.71	1.73
3	0.36	4.44	42.5	6.06	10.08	1.05	1.84
8	0.29	3.58	34.5	4.98	8.50	0.76	1.98
20	0.19	2.18	21.5	3.27	5.59	0.48	1.49
60	0.15	1.71	18.3	2.93	4.91	0.48	1.74
120	0.12	1.22	13.8	2.32	3.93	0.37	1.36
1140	0.06	0.71	8.2	1.46	2.48	0.22	1.28

Table A-2: Tank B ancillary water sample data

Resuspension event 1

elapsed time (hours)	PN (mg N/l)	PC (mg C/l)	TSS (mg/L)	total chla (ug/l)	phaeo (ug/l)	active (ug/l)	DOC (mg C/l)
0	0.01	0.29	3.3	0.52	0.89	0.08	0.76
0.25	0.33	4.61	53.5	6.19	10.27	1.08	0.86
0.75	0.30	4.10	64.5	6.39	10.62	1.11	0.79
1.25	0.58	7.85	64.3	8.67	14.55	1.43	1.07
1.90	0.40	4.77	64.3	6.60	11.13	1.06	0.80
2.92	0.33	4.49	64.3	6.49	10.98	1.02	0.98
3.90	0.36	4.85	64.6	7.76	13.02	1.28	0.94
4.9	0.32	4.35	73.4	6.63	11.29	1.01	0.97
5.92	0.56	7.44	72.9	7.41	12.52	1.18	0.88
24.83	0.46	6.14	82.8	7.30	12.67	1.00	0.95
28.82	0.71	9.32	75.9	9.70	16.09	1.69	0.96
47.67	0.71	8.85	81.1	9.17	15.14	1.64	1.43
52.82	0.58	8.24	75.3	8.61	14.53	1.38	1.05
OFF	0.04	0.53	6.00	1.25	2.11	0.20	1.36

Resuspension event 2

elapsed time (hours)	PN (mg N/l)	PC (mg C/l)	TSS (mg/L)	total chla (ug/l)	phaeo (ug/l)	active (ug/l)	DOC (mg C/l)
0	0.03	0.17	2.4	0.45	0.39	0.26	1.04
0.25	0.47	5.68	54.5	7.47	11.74	1.63	1.05
0.75	0.70	8.68	80.0	9.88	16.25	1.80	1.06
1.25	0.91	11.20	103.5	13.02	21.23	2.46	1.21
1.75	0.75	9.56	83.0	10.69	17.30	2.09	1.16
2.97	0.78	10.20	78.8	10.56	16.98	2.11	1.36
3.97	0.84	11.10	90.0	13.27	20.85	2.90	1.06
4.97	0.68	8.76	80.0	11.15	17.24	2.57	1.18
5.97	0.84	11.30	86.5	10.86	17.60	2.10	1.34
21.75	0.92	12.30	81.0	10.21	17.18	1.66	1.09
30.62	0.99	12.20	79.5	11.22	18.78	1.88	1.52
48.22	0.88	10.80	94.5	11.25	19.28	1.65	
53.22	0.86	10.60	88.5	12.26	20.53	2.04	1.95
Off	0.06	0.61	4.8	1.17	2.07	0.14	1.35

Resuspension event 3

elapsed time (hours)	PN (mg N/l)	PC (mg C/l)	TSS (mg/L)	total chla (ug/l)	phaeo (ug/l)	active (ug/l)	DOC (mg C/l)
0	0.01	0.16	2.4	0.33	0.41	0.13	1.09
0.25	0.50	6.87	43.5	6.32	10.52	1.08	1.13
0.75	0.37	4.88	49.5	6.40	11.10	0.88	0.85
1.25	0.55	7.40	52.0	7.75	12.62	1.47	1.04
1.75	0.68	8.53	57.5	8.18	12.99	1.72	1.18
2.75	0.66	8.18	60.5	7.62	12.78	1.26	1.41
3.75	0.59	7.23	63.5	9.07	14.69	1.76	1.17
4.75	0.66	7.99	64.0	9.16	15.17	1.61	1.21
5.75	0.44	5.34	63.0	8.39	14.18	1.34	1.59
22.75	0.66	8.52	65.5	8.37	14.11	1.35	1.44
29.75	0.70	8.77	78.5	9.76	15.90	1.85	1.13
47.25	0.73	9.31	72.5	9.55	16.24	1.47	1.41
52.75	0.57	7.25	63.0	10.07	16.95	1.63	1.26
Off	0.04	0.58	2.5	0.92	1.55	0.15	1.31

Settling

elapsed time (min.)	PN (mg N/l)	PC (mg C/l)	TSS (mg/L)	total chla (ug/l)	phaeo (ug/l)	active (ug/l)	DOC (mg C/l)
before	0.57	7.25	63.0	10.07	16.95	1.63	1.26
3	0.43	5.37	47.5	6.24	10.63	0.95	2.03
8	0.30	3.79	32.0	4.94	8.59	0.67	1.42
20	0.15	2.03	17.0	3.23	5.74	0.38	1.52
60	0.09	1.27	9.5	2.15	3.68	0.32	1.68
120	0.07	0.98	6.8	1.61	2.67	0.28	1.18
1160	0.04	0.58	2.5	0.92	1.55	0.15	1.31

Table A-3: Tank C ancillary water sample data

Resuspension event 1

elapsed time (hours)	PN (mg N/l)	PC (mg C/l)	TSS (mg/L)	total chla (ug/l)	phaeo (ug/l)	active (ug/l)	DOC (mg C/l)
0.00	0.05	0.53	6.5	0.89	1.47	0.16	1.04
0.25	0.51	6.37	48.5	5.81	9.33	1.16	0.96
0.75	0.50	6.16	46.0	6.44	10.26	1.33	0.95
1.25	0.40	5.06	46.0	5.59	9.00	1.11	0.93
1.75	0.39	4.81	43.5	5.79	9.35	1.14	1.07
2.75	0.44	5.57	54.5	6.27	10.20	1.20	1.06
3.75	0.53	6.95	56.5	6.98	10.91	1.55	1.04
4.75	0.58	7.20	56.5	7.40	11.42	1.72	1.12
5.75	0.62	7.76	50.0	8.06	12.91	1.63	1.11
23.05	0.62	7.95	71.0	8.23	13.25	1.64	1.19
28.73	0.73	9.08	80.0	10.31	16.27	2.22	1.22
47.97	0.52	6.44	81.0	9.13	14.66	1.84	0.98
52.05	0.39	4.95	82.0	9.55	15.53	1.82	1.20
Off	0.08	1.02	11.1	2.23	3.81	0.33	1.19

Resuspension event 2

elapsed time (hours)	PN (mg N/l)	PC (mg C/l)	TSS (mg/L)	total chla (ug/l)	phaeo (ug/l)	active (ug/l)	DOC (mg C/l)
0.00	0.02	0.31	6.5	0.80	1.31	0.14	1.13
0.25	0.30	4.13	45.0	4.99	7.82	1.10	1.37
0.75	0.29	3.77	51.5	5.93	9.32	1.29	1.21
1.25	0.35	4.41	54.5	6.76	10.75	1.41	1.36
1.75	0.61	7.80	61.0	7.13	11.33	1.50	1.29
2.75	0.62	8.00	60.5	6.82	10.75	1.47	1.23
3.75	0.50	6.73	64.5	6.88	10.97	1.43	1.36
4.75	0.42	6.27	57.0	7.13	11.32	1.50	1.41
21.02	0.58	6.71	66.5	8.66	14.13	1.63	1.54
28.87	0.79	9.79	87.5	10.10	16.46	1.91	1.46
43.90	0.66	8.16	70.0	9.11	15.11	1.59	1.36
53.27	0.82	9.58	73.5	9.79	15.74	1.96	2.47
Off	0.08	0.65	8.0	1.42	2.45	0.20	1.99

Resuspension event 3

elapsed time (hours)	PN (mg N/l)	PC (mg C/l)	TSS (mg/L)	total chla (ug/l)	phaeo (ug/l)	active (ug/l)	DOC (mg C/l)
0.00	0.01	0.22	2.4	0.14	0.22	0.04	1.39
0.25	0.24	3.04	21.5	3.05	4.82	0.66	1.96
0.75	0.21	2.60	27.0	3.73	5.97	0.76	1.18
1.25	0.33	4.23	34.5	4.28	6.76	0.92	1.04
1.75	0.36	4.43	41.5	4.63	7.30	0.99	1.87
3.22	0.45	5.62	40.0	5.37	8.77	1.00	1.50
4.22	0.40	5.02	42.0	5.85	9.52	1.11	1.20
5.25	0.44	5.64	43.5	6.01	9.84	1.12	1.54
6.25	0.54	7.01	48.5	6.46	10.30	1.34	1.75
24.20	0.74	8.82	57.0	7.10	11.22	1.52	1.24
27.35	0.41	5.02	60.0	8.62	13.72	1.79	1.56
48.50	0.59	7.84	63.0	7.44	12.32	1.31	1.29
51.58	0.53	6.57	59.5	8.13	13.13	1.60	1.06
Off	0.05	0.58	5.0	0.86	1.45	0.14	1.13

Settling

elapsed time (min.)	PN (mg N/l)	PC (mg C/l)	TSS (mg/L)	total chla (ug/l)	phaeo (ug/l)	active (ug/l)	DOC (mg C/l)
before	0.53	6.57	59.5	8.13	13.13	1.60	1.06
3	0.42	5.09	48.0	6.19	10.29	1.07	0.93
8	0.31	3.76	34.0	4.64	7.94	0.69	0.95
20	0.21	2.48	26.5	3.13	5.33	0.48	0.96
60	0.13	1.49	15.0	2.15	3.69	0.32	0.94
120	0.08	0.90	10.5	1.55	2.66	0.23	0.98
1136	0.05	0.58	5.0	0.86	1.45	0.14	1.13

Appendix B: LISST data

B-1: Tank A

B-2: Tank B

B-3: Tank C

Table B-1: Tank A LISST data: volume concentration of particles (uL/L) by size class (um)

Resuspension event 1

particle diameter (um)	elapsed time (hours)													
	0.00	0.25	0.75	1.25	1.75	2.43	3.43	4.43	5.43	24.73	28.8	46.77	53.72	Off
2.73	0.0000	0.0000	0.0000	0.0001	0.0004	0.0034	0.0038	0.0054	0.0247	0.0602	0.0627	0.2123	0.2896	0.6258
3.22	0.0000	0.0000	0.0002	0.0008	0.0018	0.0091	0.0101	0.0142	0.0496	0.1042	0.1093	0.2901	0.3795	0.6373
3.8	0.0000	0.0000	0.0025	0.0064	0.0106	0.0358	0.0403	0.0547	0.1321	0.2319	0.2451	0.4693	0.5797	0.6375
4.48	0.0000	0.0049	0.0229	0.0467	0.0691	0.1614	0.1849	0.2387	0.3821	0.5567	0.5904	0.7975	0.9265	0.6229
5.29	0.0001	0.0486	0.1489	0.2494	0.3316	0.5318	0.6213	0.7526	0.8585	1.0944	1.1578	1.2032	1.3390	0.5507
6.24	0.0022	0.1658	0.3681	0.5280	0.6486	0.8165	0.9654	1.1006	1.1095	1.3769	1.4542	1.4071	1.5529	0.4134
7.36	0.0073	0.2494	0.4535	0.5956	0.6998	0.8117	0.9585	1.0587	1.0946	1.3872	1.4695	1.4646	1.6274	0.2886
8.69	0.0257	0.4217	0.6712	0.8274	0.9470	1.0633	1.2333	1.3506	1.3828	1.7112	1.8292	1.7397	1.9099	0.2540
10.2	0.0546	0.5389	0.8071	0.9607	1.0860	1.2534	1.4353	1.5641	1.6313	1.9909	2.1706	1.9957	2.1646	0.3485
12.1	0.0580	0.4992	0.7439	0.9018	1.0065	1.2074	1.4086	1.5157	1.6914	2.0457	2.2737	2.0893	2.2783	0.4165
14.3	0.0717	0.6465	0.9587	1.1865	1.2991	1.5435	1.8196	1.9546	2.1718	2.5191	2.8038	2.4747	2.7109	0.3773
16.8	0.0771	0.6943	1.0549	1.3044	1.4530	1.7548	2.0424	2.2105	2.4856	2.8198	3.1305	2.7275	3.0407	0.3807
19.9	0.0825	0.7541	1.1580	1.4445	1.6269	1.9897	2.3190	2.5150	2.8152	3.0947	3.4011	2.9075	3.3556	0.3974
23.5	0.0759	0.8731	1.3137	1.6698	1.8818	2.3573	2.7135	2.9703	3.3082	3.5454	3.8753	3.2727	3.9133	0.4382
27.7	0.0541	0.8690	1.3210	1.6958	1.9656	2.5287	2.8586	3.1336	3.6112	3.8952	4.2751	3.6277	4.4500	0.4720
32.7	0.0582	1.2194	1.8169	2.3048	2.6259	3.2504	3.6665	3.9607	4.5460	4.9095	5.4164	4.4522	5.4578	0.4327
38.5	0.0617	1.5458	2.3287	2.9395	3.2721	3.9304	4.4326	4.7241	5.2945	6.2002	6.8163	5.5703	6.5820	0.2837
45.5	0.0963	2.1368	3.2060	3.9837	4.3342	5.1096	5.7402	5.9839	6.4640	8.3162	9.1878	7.5428	8.4339	0.1512
53.7	0.1297	2.8543	4.1370	5.1713	5.4930	6.4362	7.2710	7.4629	7.7552	10.8322	11.9096	10.1656	10.7238	0.0907
63.3	0.1256	4.0211	5.5023	6.9107	7.2652	8.6032	9.7636	9.9213	9.7279	14.3657	15.5123	13.8785	14.3633	0.1061
74.7	0.1305	5.3918	7.1543	8.8605	9.2478	11.2342	12.6144	12.5985	12.1113	18.3727	19.7567	17.3547	18.8588	0.2430
88.2	0.2380	7.2251	9.5966	11.1978	11.7710	14.3665	15.9092	15.9325	15.1093	22.7870	24.9373	20.6092	23.0660	0.5140
104	0.4332	9.7599	12.9074	14.2960	15.3507	18.1520	20.4917	21.2062	19.0355	26.3249	29.4336	24.0870	25.5014	0.5715
128	0.8059	12.9265	16.4310	18.2550	20.2036	21.5359	26.2049	29.0932	21.6212	28.3230	30.5140	25.9300	27.1818	1.0165
157	2.8956	16.7509	21.6002	23.2860	26.8172	24.2314	33.2517	40.6174	22.9581	29.9925	31.4426	27.2793	29.3147	1.9510
186	7.4626	21.1476	28.2236	28.6609	33.9146	24.1759	37.3078	48.2418	21.0899	30.2498	31.5223	28.4664	30.5251	2.3088
219	3.8342	25.0434	32.3678	32.9025	39.2616	21.6201	33.3021	40.2578	19.7387	28.4028	32.4905	26.6743	28.8113	3.5182
259	0.6651	27.5525	30.1364	33.6772	39.2518	20.0806	27.9373	27.0142	16.9068	25.5615	29.4869	23.7220	26.6488	5.2026
293	0.2419	24.7148	23.2245	28.9043	29.1523	19.8153	22.2267	19.3709	14.9317	23.0630	26.0017	21.4814	24.9377	12.2671
332	0.0689	19.0315	18.4454	24.2220	17.8812	18.8151	16.6735	17.4476	12.2228	21.6502	20.7314	20.1942	22.4702	35.9463
391	0.0163	11.5964	13.4771	21.2499	8.6451	15.7680	12.3418	20.6627	10.6624	26.1854	21.1723	22.7965	24.2103	68.2794
462	0.0060	4.4685	4.7947	12.2950	3.0077	10.6327	6.8311	20.0944	8.4550	25.0310	22.8279	27.8275	29.2300	88.6877
TVC	18	203	244	291	291	264	315	365	251	377	398	355	387	228

Resuspension event 2

particle diameter (um)	elapsed time (hours)													
	0.00	0.25	0.75	1.25	1.75	3.25	4.25	5.25	6.25	25.58	29.25	46.68	53.22	Off
2.73	0.0000	0.0000	0.0000	0.0003	0.0014	0.0026	0.0119	0.0043	0.0682	0.0758		0.2038	0.6560	
3.22	0.0000	0.0001	0.0004	0.0016	0.0045	0.0076	0.0185	0.0116	0.1220	0.1303		0.2866	0.5093	
3.8	0.0003	0.0026	0.0049	0.0094	0.0206	0.0329	0.0496	0.0467	0.2796	0.2875		0.4790	0.3900	
4.48	0.0076	0.0247	0.0407	0.0630	0.1144	0.1671	0.1978	0.2145	0.6863	0.6851		0.8384	0.3177	
5.29	0.0597	0.1632	0.2433	0.3274	0.4842	0.6328	0.6706	0.7337	1.3705	1.3392		1.2900	0.3297	
6.24	0.1747	0.4115	0.5654	0.7092	0.9119	1.0924	1.1068	1.1865	1.7140	1.6745		1.5094	0.4652	
7.36	0.2457	0.5225	0.6821	0.8333	1.0043	1.1539	1.1576	1.2271	1.7069	1.6791		1.5631	0.6607	
8.69	0.3957	0.7819	0.9911	1.1837	1.3704	1.5310	1.5176	1.6092	2.0917	2.0735		1.8631	0.7364	
10.2	0.4842	0.9343	1.1780	1.4048	1.6306	1.7900	1.7821	1.8736	2.3854	2.4274		2.1244	0.8237	
12.1	0.4377	0.8664	1.0966	1.3264	1.5740	1.7359	1.7657	1.8392	2.4257	2.4947		2.2280	0.9145	
14.3	0.5562	1.1162	1.4302	1.7185	2.0402	2.2541	2.3092	2.3894	3.0026	3.0721		2.6673	0.8805	
16.8	0.5994	1.2351	1.6175	1.9352	2.3261	2.5958	2.6769	2.7588	3.3935	3.4100		2.9615	0.8702	
19.9	0.6527	1.3813	1.8265	2.1833	2.6540	2.9959	3.0907	3.1792	3.7799	3.6598		3.2141	0.7984	
23.5	0.7678	1.6477	2.1916	2.6124	3.1889	3.6229	3.7049	3.7927	4.3561	4.0994		3.6450	0.7738	
27.7	0.8050	1.7470	2.3280	2.8071	3.4126	3.9213	3.9724	4.0904	4.7673	4.4044		4.0361	0.7940	
32.7	1.1921	2.4631	3.2827	3.8931	4.5682	5.1114	5.1462	5.2759	5.8672	5.4875		4.9863	0.8445	
38.5	1.7108	3.3593	4.4419	5.1781	5.9634	6.4993	6.5039	6.7229	7.5127	7.1060		6.3242	0.9077	
45.5	2.5702	4.6980	6.1388	7.1409	8.1906	8.5893	8.5952	8.8928	10.1353	10.1975		8.6010	1.0349	
53.7	3.5447	6.2895	8.1906	9.4164	10.6556	10.9921	10.9191	11.2317	13.3328	14.3109		11.5821	1.2991	
63.3	4.6114	8.6858	11.1665	12.8070	13.9289	14.7025	14.1415	14.4732	17.2519	19.2381		15.3391	1.5640	
74.7	5.4307	11.2521	14.5163	16.6099	17.7547	19.5699	18.4624	18.7231	20.3967	22.1980		18.4226	1.7325	
88.2	6.4530	14.1932	18.5021	21.0086	22.9037	26.2564	24.6937	24.9424	24.1712	24.9453		21.4050	1.8396	
104	8.5960	17.8974	22.7949	25.8832	27.3975	31.3539	29.5234	30.0021	28.9767	29.8448		25.0912	2.1631	
128	12.6964	21.9259	26.2534	29.9146	29.3791	31.7840	29.6600	30.3124	31.5126	32.3542		26.0684	1.9649	
157	15.6415	23.9734	27.6982	31.5550	30.0866	30.4741	28.5643	29.2039	31.2075	33.9769		25.1906	1.7317	
186	15.3483	25.8993	29.5965	33.9006	33.6865	34.4979	31.8421	32.4506	32.7762	37.8235		25.1382	1.5881	
219	16.9818	27.9554	30.7175	35.4762	35.4836	35.0260	33.7044	33.2141	33.2549	37.6231		23.2668	1.1627	
259	20.4860	30.2071	32.3259	36.8374	37.7547	33.3046	33.9027	33.2412	37.4483	37.7711		22.1198	0.9232	
293	20.7466	31.2502	33.0000	37.3754	39.9662	32.7473	33.6797	34.6301	40.7259	37.8135		22.6301	0.9278	
332	22.4595	31.8057	32.2783	37.6929	36.7426	31.5454	31.0914	34.6946	39.7242	36.5368		23.1324	0.5835	
391	17.2628	19.9464	19.5401	27.4472	25.9188	23.2421	22.1851	27.1188	28.4425	41.4001		25.9544	0.3135	
462	12.5960	12.3849	10.7953	20.0661	18.0823	15.9534	15.0207	24.7143	19.8977	41.9930		28.0807	0.3732	
TVC	194	305	345	409	419	415	402	425	455	502		362	31	

Table B-1: Tank A LISST data: volume concentration of particles (uL/L) by size class (um)

Resuspension event 3

particle diameter (um)	elapsed time (hours)																	Off	
	0.00	0.25	0.75	1.25	1.75	3.23	4.23	5.23	6.23	24.22	28.22	48.98	53.23	71.17	95.12	118.90	143.55		168.80
2.73	0.0582	0.0005	0.0033	0.0035	0.0054	0.0078	0.0214	0.0332	0.0265	0.0232	0.0272	0.0952	0.1622	0.1697	0.3270	0.4141	0.5421	0.7331	1.3603
3.22	0.0587	0.0016	0.0068	0.0086	0.0122	0.0187	0.0429	0.0612	0.0520	0.0463	0.0544	0.1531	0.2333	0.2314	0.3977	0.4733	0.5910	0.7807	0.7661
3.8	0.0613	0.0078	0.0215	0.0305	0.0402	0.0646	0.1165	0.1481	0.1377	0.1250	0.1472	0.3065	0.4035	0.3727	0.5480	0.6015	0.7056	0.9065	0.3814
4.48	0.0636	0.0403	0.0891	0.1242	0.1491	0.2498	0.3420	0.3851	0.3965	0.3722	0.4370	0.6514	0.7346	0.6295	0.7815	0.7898	0.8683	1.0798	0.2045
5.29	0.0634	0.1579	0.2973	0.3825	0.4191	0.7138	0.7694	0.7863	0.8861	0.8791	1.0234	1.1576	1.1656	0.9441	1.0376	0.9959	1.0537	1.2712	0.1713
6.24	0.0610	0.2843	0.4759	0.5801	0.6055	1.0022	0.9688	0.9536	1.1199	1.1944	1.3845	1.4095	1.3670	1.1017	1.1904	1.1469	1.2322	1.4662	0.2652
7.36	0.0582	0.3066	0.4801	0.5735	0.5962	0.9368	0.9065	0.8976	1.0515	1.2114	1.4021	1.4486	1.3952	1.1583	1.2911	1.2668	1.4097	1.6682	0.4140
8.69	0.0565	0.4073	0.6109	0.7154	0.7384	1.1162	1.0785	1.0671	1.2435	1.5408	1.7812	1.7991	1.6508	1.3958	1.5289	1.4793	1.6470	1.9298	0.3835
10.2	0.0566	0.4451	0.6890	0.8068	0.8328	1.2272	1.2116	1.1988	1.3928	1.7886	2.0873	2.1031	1.8604	1.6030	1.7470	1.6888	1.8546	2.1890	0.3725
12.1	0.0590	0.4288	0.6452	0.7774	0.8108	1.1799	1.2145	1.2112	1.3879	1.7847	2.0907	2.2016	1.9137	1.6778	1.8725	1.8151	1.9704	2.3939	0.3766
14.3	0.0730	0.5523	0.8325	1.0233	1.0665	1.5619	1.5844	1.5893	1.8061	2.1889	2.5673	2.6888	2.2911	1.9653	2.1797	2.0713	2.1864	2.7317	0.2834
16.8	0.1014	0.6532	0.9902	1.2333	1.2933	1.9311	1.9325	1.9453	2.2008	2.4621	2.8552	2.9854	2.5735	2.1553	2.4242	2.2986	2.4215	3.0238	0.2361
19.9	0.1279	0.7720	1.1682	1.4738	1.5517	2.3832	2.3647	2.3598	2.6383	2.8155	3.1942	3.2445	2.8518	2.2965	2.6042	2.4437	2.6592	3.2415	0.1713
23.5	0.1463	0.9047	1.3872	1.7607	1.8641	2.8823	2.8701	2.8733	3.1987	3.4859	3.9089	3.7298	3.3016	2.6216	2.9423	2.7222	3.1979	3.6791	0.1233
27.7	0.1468	0.8918	1.4388	1.8229	1.9421	2.9258	3.0507	3.0630	3.3969	4.0241	4.5133	4.1601	3.6988	2.9951	3.3051	3.0307	3.8754	4.2962	0.1006
32.7	0.1555	1.1584	1.8796	2.3753	2.5052	3.6295	3.8549	3.8342	4.2556	5.2244	5.9143	5.3407	4.5533	3.9084	4.0635	3.6973	4.8500	5.4397	0.0704
38.5	0.1976	1.6130	2.6282	3.2880	3.4509	4.9616	5.1610	5.1409	5.7135	6.1265	7.0375	6.7442	5.6941	5.1605	5.0812	4.6775	5.6344	6.8812	0.0513
45.5	0.2521	2.3076	3.7630	4.6651	4.8254	6.9724	7.0603	7.0700	7.8278	7.6237	8.9418	8.8964	7.5722	6.7364	6.7304	6.3990	6.9718	9.2208	0.0402
53.7	0.2700	3.0820	5.0325	6.2142	6.3542	8.9662	9.1111	9.0239	10.0905	10.1952	11.8751	11.2823	10.0278	8.1015	8.8955	8.5750	9.4058	12.0711	0.0364
63.3	0.3102	4.7419	7.6464	9.2545	9.3585	12.4883	12.8803	12.3888	13.9566	13.0375	15.4966	14.3557	13.9020	9.9455	11.5541	11.3775	12.1069	15.7400	0.0390
74.7	0.3824	6.7151	10.5608	12.5081	12.4960	16.0125	16.7086	15.9254	17.7106	15.9924	19.1329	18.2793	18.1994	13.3585	14.2909	13.5512	14.9629	20.1705	0.0452
88.2	0.5233	9.0757	13.6090	15.7574	15.6186	20.6258	20.2851	19.9220	21.4903	20.1918	23.8974	22.6274	22.0063	16.8892	17.3866	16.0825	18.7209	24.6210	0.0565
104	0.6878	11.5533	16.6714	18.6274	18.3967	25.0916	23.1943	23.5615	24.8888	23.7566	28.4534	27.4512	24.8709	20.0644	21.3378	20.4308	22.4467	28.6996	0.0636
128	0.8976	14.3107	20.0115	21.5774	21.2228	29.3585	26.1513	27.0007	28.3378	24.6497	30.8282	29.8293	26.5796	21.9786	22.6195	21.5384	23.8606	30.3990	0.0657
157	1.1409	18.1140	23.8759	25.3656	24.1041	33.9162	30.1381	31.6472	33.4172	24.2121	31.7900	30.7550	27.1364	22.4314	22.3782	20.8687	23.8739	31.6591	0.0758
186	1.1709	22.3309	28.2099	29.1126	26.0743	37.3822	35.2052	35.8321	40.5427	22.7435	30.0172	29.7477	27.3133	21.9912	21.6442	20.9574	21.5105	30.8818	0.1122
219	0.8890	24.4658	29.9009	30.1902	25.3109	36.3979	36.3126	33.4726	42.6181	23.2761	29.4610	30.4709	25.3902	21.8652	21.2219	20.9277	20.1050	29.4870	0.1158
259	0.6804	24.9640	28.8632	29.3912	23.7334	35.2026	35.1711	27.9654	40.3638	22.3570	27.4609	28.0360	24.6160	20.1152	19.5500	19.5267	17.5356	24.2916	0.1169
293	0.9515	23.3507	26.0604	27.2087	22.1293	34.4499	33.7396	22.8558	36.5661	22.6167	29.5295	27.5675	24.6154	20.9967	19.5151	19.6760	17.1289	20.8945	0.1742
332	1.6393	21.1608	24.6513	24.0235	20.0094	39.2069	30.3367	17.9059	33.1689	20.2670	32.0388	26.8951	24.6608	20.7875	20.1227	19.3079	16.1463	19.7127	0.2214
391	2.6367	21.7932	23.0455	22.3285	20.5814	46.4483	28.4957	15.5324	33.0814	15.8607	34.8185	29.7684	23.1202	20.8495	22.0369	21.1290	17.9681	26.7562	0.2731
462	3.5337	18.3442	15.4122	15.7993	17.5017	50.4186	24.9120	10.9705	31.5150	15.3542	36.2795	23.7789	21.8425	19.5332	23.9065	20.2154	17.3612	34.8121	0.2055
TVC	18	235	291	309	286	460	397	339	446	317	430	400	358	296	307	292	297	403	7

Table B-2: Tank B LISST data: volume concentration of particles (uL/L) by size class (um)

Resuspension event 1

particle diameter (um)	elapsed time (hours)													
	0	0.25	0.75	1.25	1.90	2.92	3.90	4.9	5.92	24.83	28.82	47.67	52.82	OFF
2.73	0.0000	0.0000	0.0000	0.0000	0.0003	0.0010	0.0018	0.0027	0.0040	0.0457	0.0328	0.0855	0.1343	0.3779
3.22	0.0000	0.0001	0.0003	0.0021	0.0040	0.0055	0.0076	0.0106	0.0853	0.0641	0.1536	0.2240	0.4157	0.4157
3.8	0.0019	0.0029	0.0050	0.0122	0.0200	0.0258	0.0323	0.0422	0.2082	0.1678	0.3537	0.4689	0.4946	0.4946
4.48	0.0175	0.0292	0.0441	0.0813	0.1190	0.1446	0.1662	0.1976	0.5520	0.4830	0.8729	1.0474	0.5985	0.5985
5.29	0.1150	0.2085	0.2763	0.4003	0.5206	0.5980	0.6431	0.6989	1.1793	1.1024	1.7412	1.9461	0.7277	0.7277
6.24	0.3094	0.5550	0.6709	0.8380	0.9960	1.1083	1.1494	1.1848	1.5129	1.4785	2.1724	2.3906	0.8504	0.8504
7.36	0.4314	0.7517	0.8484	0.9898	1.1197	1.2326	1.2600	1.2787	1.4936	1.4993	2.1613	2.4062	0.9696	0.9696
8.69	0.6903	1.2166	1.2891	1.4365	1.5801	1.7212	1.7368	1.7399	1.8239	1.9006	2.6494	2.9147	1.1081	1.1081
10.2	0.8687	1.5312	1.5910	1.7782	1.9319	2.1038	2.1437	2.1155	2.0629	2.2409	3.0288	3.3009	1.1837	1.1837
12.1	0.8419	1.4548	1.5344	1.7532	1.9181	2.1041	2.1867	2.1498	2.0365	2.2660	3.0531	3.3406	1.2120	1.2120
14.3	1.1216	1.9440	2.0494	2.3341	2.5381	2.7901	2.9072	2.8383	2.4723	2.7942	3.7031	4.0236	1.2961	1.2961
16.8	1.2374	2.1058	2.2882	2.6462	2.8608	3.1463	3.2923	3.2353	2.7640	3.0913	4.0910	4.4810	1.4379	1.4379
19.9	1.3374	2.2737	2.5345	2.9303	3.2222	3.4958	3.6593	3.6456	3.1537	3.4131	4.4423	4.9349	1.5892	1.5892
23.5	1.5261	2.6225	2.9600	3.4132	3.8218	4.0946	4.2826	4.3267	3.8454	4.1209	5.0975	5.7451	1.7781	1.7781
27.7	1.5262	2.6106	3.0281	3.5582	4.0421	4.2959	4.5321	4.6145	4.4134	4.7201	5.5350	6.3127	1.8672	1.8672
32.7	2.0756	3.6498	4.1982	4.8544	5.4255	5.7719	6.0891	6.1046	5.4762	6.0965	6.8453	7.7444	1.9626	1.9626
38.5	2.6386	4.7064	5.3627	6.1829	6.8273	7.3400	7.6926	7.5516	6.4515	7.0707	8.5785	9.4350	2.0838	2.0838
45.5	3.7097	6.5525	7.3951	8.4802	9.2799	9.9690	10.4340	9.8938	8.1848	8.8540	11.2299	11.8525	2.2511	2.2511
53.7	4.9275	8.7917	9.6697	10.9465	11.9506	12.8041	13.2843	12.3010	10.9072	11.5310	14.9372	14.9072	2.8284	2.8284
63.3	6.6141	12.3539	12.9588	14.4755	15.7171	16.5899	16.8469	15.4835	14.3714	15.1548	18.6468	19.6155	3.9258	3.9258
74.7	8.1561	16.7068	16.4526	18.2543	19.2786	20.2830	20.2135	18.6303	17.7328	19.1235	23.8566	26.1166	5.3497	5.3497
88.2	10.2485	23.8669	21.1328	23.2305	23.4717	24.6215	24.6375	22.1395	22.3821	24.1472	31.1512	34.8097	6.7710	6.7710
104	13.5705	37.8207	28.6333	30.2336	29.4916	30.5753	30.8761	26.9604	25.6150	28.9629	39.0016	43.1427	7.7083	7.7083
128	16.5852	55.8401	35.9447	35.3801	34.2443	34.6470	34.8749	30.1597	28.1426	32.3293	43.2428	45.5581	6.7212	6.7212
157	20.4443	73.4541	44.1431	39.2743	38.1191	37.5531	38.5670	32.8897	29.5408	34.6992	45.1224	45.3148	6.5816	6.5816
186	25.9682	76.1051	51.7302	39.9920	40.7324	38.7011	39.8971	34.0090	31.7929	34.6444	46.7874	47.0845	12.4695	12.4695
219	32.7583	60.2423	58.1489	39.1704	40.7934	39.4493	39.2604	35.0234	32.2994	35.7628	49.2533	47.7129	21.0293	21.0293
259	35.9465	38.6201	53.5798	34.8033	37.2824	35.7093	32.8736	31.4083	33.3147	32.5774	47.6993	44.7051	22.3761	22.3761
293	37.1419	31.4359	45.4712	35.1680	36.6574	33.1853	29.5286	30.9667	32.8887	31.2976	45.9410	48.4002	27.7947	27.7947
332	33.0052	33.4416	36.9361	36.2314	33.3983	29.5348	27.8603	28.2636	33.3711	28.6079	41.2782	51.0684	20.6661	20.6661
391	33.6630	41.9386	35.3420	36.0410	30.0763	30.7574	32.5022	26.3966	29.0970	32.1168	38.3711	49.7528	9.6302	9.6302
462	29.2688	36.1050	27.2764	23.5354	24.8441	33.2119	31.3383	21.1485	30.4870	34.5987	37.3058	45.7857	9.3126	9.3126
TVC	327	579	513	458	462	468	465	417	420	447	588	637	185	

Resuspension event 2

particle diameter (um)	elapsed time (hours)													
	0	0.25	0.75	1.25	1.75	2.97	3.97	4.97	5.97	21.75	30.62	48.22	53.22	Off
2.73	0.000	0.000	0.000	0.000	0.000	0.000	0.001	0.001	0.002	0.017	0.113	0.059	0.088	0.641
3.22	0.000	0.000	0.000	0.000	0.000	0.002	0.003	0.005	0.006	0.038	0.193	0.111	0.154	0.410
3.8	0.000	0.000	0.001	0.003	0.005	0.011	0.018	0.027	0.032	0.121	0.415	0.275	0.345	0.244
4.48	0.000	0.006	0.013	0.032	0.048	0.087	0.122	0.169	0.192	0.433	0.955	0.742	0.834	0.158
5.29	0.001	0.062	0.123	0.248	0.327	0.488	0.607	0.772	0.831	1.190	1.800	1.596	1.647	0.150
6.24	0.006	0.233	0.394	0.695	0.832	1.084	1.254	1.499	1.567	1.710	2.195	2.072	2.087	0.233
7.36	0.012	0.377	0.573	0.929	1.049	1.279	1.440	1.661	1.728	1.695	2.166	2.078	2.127	0.365
8.69	0.032	0.668	0.938	1.439	1.565	1.842	2.039	2.297	2.370	2.113	2.587	2.582	2.637	0.379
10.2	0.055	0.857	1.157	1.768	1.907	2.224	2.467	2.761	2.834	2.417	2.913	2.982	3.027	0.395
12.1	0.049	0.772	1.047	1.649	1.812	2.141	2.416	2.711	2.798	2.355	2.939	2.991	3.043	0.407
14.3	0.072	1.008	1.376	2.191	2.434	2.881	3.245	3.634	3.753	2.964	3.622	3.590	3.624	0.329
16.8	0.085	1.139	1.561	2.489	2.798	3.340	3.773	4.229	4.370	3.366	4.199	3.913	3.985	0.300
19.9	0.070	1.291	1.800	2.832	3.214	3.872	4.353	4.909	5.057	3.814	4.857	4.306	4.421	0.252
23.5	0.081	1.487	2.130	3.342	3.860	4.662	5.213	5.897	6.131	4.437	5.695	5.192	5.318	0.227
27.7	0.091	1.412	2.053	3.335	3.885	4.737	5.377	6.083	6.417	4.621	6.094	5.990	6.093	0.220
32.7	0.104	1.889	2.775	4.569	5.246	6.270	7.124	7.882	8.277	5.836	7.424	7.683	7.769	0.184
38.5	0.116	2.389	3.607	5.860	6.646	7.786	8.861	9.544	9.986	7.644	9.614	9.070	9.204	0.134
45.5	0.128	3.317	5.037	8.041	8.947	10.237	11.611	12.374	12.847	10.444	12.915	11.544	11.623	0.109
53.7	0.151	4.374	6.660	10.372	11.303	12.770	14.416	15.374	15.926	13.645	16.755	15.474	15.455	0.118
63.3	0.287	6.465	9.885	14.782	15.762	17.586	19.458	20.962	21.305	19.279	23.320	20.356	19.859	0.120
74.7	0.327	8.990	13.334	20.156	21.139	23.671	25.294	27.914	27.136	25.672	30.382	26.103	24.877	0.124
88.2	0.237	12.063	17.229	27.187	27.484	31.867	32.020	36.793	34.338	32.160	37.849	33.981	32.547	0.151
104	0.253	15.865	22.256	35.778	35.390	42.999	39.646	47.276	42.799	36.776	43.885	41.095	40.379	0.176
128	0.348	21.069	29.212	45.367	44.074	53.831	45.055	54.338	48.960	40.235	49.078	45.084	43.899	0.183
157	0.427	28.057	38.335	57.156	53.557	62.147	49.404	57.844	55.196	41.836	52.635	47.628	44.903	0.198
186	0.498	39.772	47.614	65.975	60.608	63.520	51.184	57.733	58.937	41.713	53.937	47.044	43.166	0.238
219	0.803	47.853	48.394	65.810	61.918	59.501	54.121	57.836	61.478	39.416	50.382	48.810	45.991	0.296
259	1.697	51.197	43.722	55.797	54.221	49.534	51.956	54.139	54.723	39.149	49.087	46.605	46.765	0.327
293	3.636	42.556	36.241	48.912	48.704	44.003	50.188	52.329	49.210	40.164	49.842	47.413	48.536	0.415
332	14.736	34.214	31.759	44.379	41.394	36.400	48.566	48.960	44.058	43.553	53.686	49.384	46.447	0.520
391	20.628	29.021	31.226	44.145	38.627	29.717	53.061	49.971	43.345	45.284	56.165	54.450	45.911	0.713
462	0.774	18.062	21.502	36.646	34.207	20.023	43.887	45.835	33.510	31.745	49.084	58.862	45.206	1.097
TVC	46	376	422	612	593	601	638	694	660	546	687	649	612	10

Table B-2: Tank B LISST data: volume concentration of particles (uL/L) by size class (um)

Resuspension event 3

particle diameter (um)	elapsed time (hours)													Off
	0	0.25	0.75	1.25	1.75	2.75	3.75	4.75	5.75	22.75	29.75	47.25	52.75	
2.73	0.0025	0.0000	0.0000	0.0000	0.0000	0.0000	0.0001	0.0001	0.0002	0.0064	0.0105	0.0308	0.0292	0.1439
3.22	0.0037	0.0000	0.0000	0.0000	0.0001	0.0002	0.0005	0.0013	0.0019	0.0154	0.0241	0.0588	0.0562	0.2001
3.8	0.0068	0.0001	0.0008	0.0012	0.0025	0.0041	0.0058	0.0087	0.0114	0.0537	0.0774	0.1496	0.1455	0.3230
4.48	0.0143	0.0033	0.0121	0.0154	0.0233	0.0360	0.0469	0.0618	0.0767	0.2124	0.2774	0.4193	0.4153	0.5431
5.29	0.0267	0.0341	0.0944	0.1181	0.1585	0.2250	0.2741	0.3210	0.3749	0.6384	0.7619	0.9409	0.9402	0.8030
6.24	0.0340	0.1215	0.2704	0.3345	0.4138	0.5397	0.6286	0.6744	0.7555	0.9623	1.0956	1.2287	1.2458	0.9361
7.36	0.0387	0.1958	0.3704	0.4577	0.5392	0.6648	0.7548	0.7726	0.8473	0.9746	1.1019	1.2020	1.2493	0.9950
8.69	0.0611	0.3608	0.5918	0.7284	0.8327	0.9874	1.1002	1.0896	1.1766	1.2590	1.4043	1.4543	1.5610	1.2117
10.2	0.0878	0.4888	0.7386	0.9010	1.0250	1.2007	1.3304	1.2944	1.3939	1.4577	1.6156	1.6178	1.8063	1.3928
12.1	0.0769	0.4618	0.6842	0.8311	0.9530	1.1236	1.2559	1.2344	1.3309	1.4104	1.5948	1.5566	1.8034	1.4645
14.3	0.0552	0.6026	0.8788	1.0739	1.2383	1.4606	1.6243	1.6162	1.7466	1.7542	2.0100	1.8567	2.1964	1.6840
16.8	0.0265	0.6323	0.9379	1.1521	1.3478	1.6035	1.7748	1.8203	2.0072	1.9309	2.2654	2.0514	2.4182	1.7957
19.9	0.0093	0.6415	0.9989	1.2326	1.4548	1.7515	1.9407	2.0367	2.3069	2.0871	2.4662	2.3015	2.6546	1.8729
23.5	0.0029	0.6499	1.0919	1.3700	1.6316	1.9789	2.1866	2.3296	2.6616	2.3516	2.7808	2.7932	3.2023	2.2267
27.7	0.0009	0.5392	1.0296	1.3156	1.5900	1.9374	2.1755	2.3068	2.6071	2.4310	2.7844	3.2091	3.6692	2.7469
32.7	0.0005	0.6847	1.3500	1.7644	2.1198	2.5537	2.8784	2.9961	3.1352	3.0322	3.2383	4.0575	4.7357	3.5066
38.5	0.0015	0.8922	1.7516	2.3044	2.7490	3.3151	3.7423	3.6388	3.7545	4.0098	4.0335	4.9571	5.6518	4.0579
45.5	0.0183	1.5675	2.7703	3.5736	4.1984	5.0553	5.6698	5.3808	5.5608	5.8678	5.9297	6.5498	7.2726	4.9745
53.7	0.5166	2.9683	4.6935	5.7840	6.6592	7.7622	8.7025	8.3395	9.0117	8.6263	9.8238	9.1890	9.7681	6.3840
63.3	2.0981	4.7044	7.6578	9.1965	10.4673	11.5027	13.1188	12.3216	13.8044	12.1217	14.5790	12.4534	12.7299	7.3717
74.7	0.0865	4.5857	8.7741	10.9265	12.5400	13.8308	15.8884	14.1366	15.1498	14.4617	15.5024	15.6747	16.0891	8.2956
88.2	0.0082	5.1535	10.1636	12.9987	14.7490	17.1725	19.1916	17.1533	18.0878	17.1192	17.5963	20.3475	21.1032	10.3108
104	0.2465	9.3888	15.0310	18.5575	20.4997	23.7537	25.3768	23.7328	24.5005	22.1747	25.1274	24.0897	26.6345	13.0526
128	0.5340	11.3834	17.9398	22.0608	24.2305	27.6184	28.9471	26.6548	26.0703	24.0845	26.4842	26.7093	30.1204	13.3867
157	0.0979	12.1055	18.7453	23.9289	25.9072	29.4430	30.6849	27.1063	26.5395	23.2247	25.1554	27.7578	32.3290	12.0880
186	0.5933	16.1031	22.5644	28.7979	29.7001	33.5446	34.5435	28.3741	28.9484	24.8592	25.9548	28.5635	32.1190	10.2324
219	0.2887	18.2787	22.1629	28.3064	28.3893	32.0883	32.8340	26.5139	28.9872	24.1843	24.3296	28.6845	33.2093	14.2268
259	0.3157	19.7271	24.3945	28.7758	27.8868	31.5536	33.1825	27.1460	31.4154	24.7241	24.8277	31.4040	32.0505	22.3744
293	0.3225	22.1165	27.1001	29.2344	27.5274	30.6436	34.4626	27.6984	33.6576	24.6905	25.9899	35.3681	32.3629	27.7560
332	0.2688	22.2801	28.1548	29.0736	28.3456	30.1966	35.9285	28.2258	36.1566	26.6941	26.6262	37.6118	30.8100	30.6723
391	0.3803	19.5268	22.2243	25.8367	25.0187	27.6802	30.4357	20.4743	30.8168	26.3681	18.4246	29.9303	30.4528	34.9524
462	0.5884	14.5589	11.4885	16.1936	13.6488	17.4454	18.5280	11.7901	23.4601	21.9731	11.6543	19.0562	29.8510	25.1533
TVC	7	191	255	307	316	359	389	327	376	326	326	383	411	267

Table B-3: Tank C LISST data: volume concentration of particles (uL/L) by size class (um)

Resuspension event 1

particle diameter (um)	elapsed time (hours)													
	0.00	0.25	0.75	1.25	1.75	2.75	3.75	4.75	5.75	23.05	28.73	47.97	52.05	Off
2.73	0.0170	0.0002	0.0003	0.0013	0.0024	0.0087	0.0155	0.0393	0.0616	0.2734	0.6626	0.9994	1.1964	1.0287
3.22	0.0259	0.0010	0.0019	0.0044	0.0070	0.0207	0.0348	0.0757	0.1068	0.3657	0.8018	1.1514	1.3343	0.9775
3.8	0.0484	0.0071	0.0110	0.0203	0.0301	0.0718	0.1094	0.1951	0.2489	0.5696	1.0861	1.4633	1.6279	0.9632
4.48	0.0985	0.0461	0.0700	0.1114	0.1515	0.2822	0.3853	0.5537	0.6541	0.9286	1.5278	1.9277	2.0593	0.9832
5.29	0.1794	0.2291	0.3309	0.4539	0.5732	0.8431	1.0451	1.2580	1.4136	1.3736	2.0431	2.4767	2.5872	1.0669
6.24	0.2343	0.4955	0.6785	0.8429	1.0183	1.2920	1.5254	1.6973	1.8703	1.6424	2.4238	2.9145	3.0632	1.2231
7.36	0.2599	0.6124	0.8058	0.9650	1.1351	1.3589	1.5862	1.7415	1.9328	1.7928	2.7301	3.2605	3.4474	1.3240
8.69	0.3406	0.9415	1.2070	1.4065	1.6027	1.8419	2.1082	2.2378	2.5105	2.2141	3.3024	3.8059	3.9476	1.3454
10.2	0.4165	1.2292	1.5570	1.7816	2.0076	2.2958	2.5824	2.7054	3.0523	2.6276	3.8307	4.2944	4.4036	1.4951
12.1	0.4592	1.2389	1.5592	1.8212	2.0445	2.4066	2.7098	2.8554	3.2390	2.8719	4.2018	4.5785	4.6959	1.6305
14.3	0.5825	1.5438	1.9884	2.3615	2.6341	3.1149	3.4974	3.6242	4.1139	3.4703	4.9711	5.2317	5.3235	1.6863
16.8	0.6376	1.4672	2.0058	2.4605	2.7835	3.3610	3.8163	3.9849	4.5586	3.9191	5.5709	5.8340	5.9282	1.8048
19.9	0.6928	1.3777	1.9660	2.5170	2.8867	3.5514	4.1188	4.2881	4.9676	4.2686	5.9960	6.2862	6.3890	1.8661
23.5	0.8395	1.6002	2.2873	2.9476	3.3901	4.1602	4.8368	5.0274	5.8708	4.8147	6.6928	6.9932	7.1155	1.8811
27.7	1.0509	2.0066	2.7329	3.4588	3.8929	4.7887	5.4800	5.7902	6.7244	5.2379	7.3349	7.7157	7.9118	2.0245
32.7	1.3542	3.0018	4.0440	4.9651	5.4407	6.5156	7.3063	7.5324	8.6586	6.2802	8.6597	8.9777	9.2950	2.2855
38.5	1.4366	3.2735	4.7799	5.7577	6.3835	7.7238	8.6485	9.0243	10.1033	7.4208	10.0042	10.8094	11.2262	2.6485
45.5	1.6651	4.2459	6.4529	7.3555	8.2604	10.0397	11.0398	11.7300	12.6105	9.2269	12.0000	13.6493	14.1143	3.4776
53.7	1.9536	5.9342	8.8660	9.4423	10.6586	12.7669	13.7215	14.9334	15.4010	11.2168	14.4144	17.0190	17.7866	4.5491
63.3	2.0701	7.4819	11.4308	11.6889	13.3643	15.7329	16.8457	18.7919	18.9962	13.8833	17.5962	21.2294	22.9287	5.8175
74.7	2.1561	10.0895	14.9748	14.8752	17.0712	19.4191	20.6566	22.8887	23.3302	16.9231	21.3479	25.8320	28.4245	6.8998
88.2	2.0243	12.7987	18.4142	18.3786	21.2833	23.6223	24.8989	26.9087	27.8639	19.9900	25.4365	30.9532	33.6676	8.7172
104	1.7446	15.6474	22.2207	23.0734	26.3025	28.5645	29.6377	30.8784	32.7835	23.2396	29.8185	35.0406	37.2062	9.8550
128	1.5117	18.7099	26.1762	27.5804	31.2457	32.7576	33.2244	34.0654	35.7974	24.1443	31.3155	37.9472	38.6706	9.6387
157	1.2588	21.9837	30.8065	32.5989	36.9032	36.2442	36.4455	36.2559	37.6338	24.4799	32.2072	39.5216	37.9254	9.2276
186	1.1177	25.7001	34.1956	36.2422	39.9156	36.0630	37.0970	35.8880	37.5033	23.7575	30.7705	40.9038	37.5863	12.1684
219	0.9747	27.2923	33.6494	39.0734	40.3035	35.1248	38.0509	33.9862	38.2518	23.8222	31.3569	42.3814	37.7592	20.8673
259	1.0536	28.2634	29.6483	33.7074	33.7315	29.4567	35.8076	30.5664	34.5827	21.0539	29.1043	45.4229	41.1594	40.3355
293	1.0703	28.5985	26.9635	30.2223	29.9274	26.6485	36.6020	27.6069	32.9021	18.7356	27.0471	46.4558	45.0048	51.3790
332	1.2001	29.1600	24.6967	25.4071	26.4486	24.2640	34.6910	23.1439	31.2851	15.5583	25.4315	46.1724	52.3158	35.9989
391	1.2126	26.2779	28.0784	22.3928	28.7094	25.8463	35.1382	26.3223	34.6321	15.9343	27.6511	39.8067	52.3458	26.9636
462	1.6732	18.6074	23.3953	18.7733	26.7836	21.8892	30.7326	28.1282	33.4668	19.3363	32.0654	38.3387	52.9038	22.1890
TVC	31	300	366	383	427	422	484	455	507	331	459	599	631	294

Resuspension event 2

particle diameter (um)	elapsed time (hours)												
	0.00	0.25	0.75	1.25	1.75	2.75	3.75	4.75	21.02	28.87	43.90	53.27	Off
2.73	0.0640	0.0014	0.0020	0.0031	0.0045	0.0066	0.0109	0.0122	0.1216	0.2952	0.3997	0.7208	1.1529
3.22	0.0752	0.0041	0.0057	0.0082	0.0112	0.0157	0.0242	0.0270	0.2044	0.4409	0.5458	0.8883	0.7215
3.8	0.0972	0.0161	0.0228	0.0316	0.0407	0.0540	0.0753	0.0837	0.4337	0.7920	0.8752	1.2392	0.4169
4.48	0.1319	0.0762	0.1066	0.1415	0.1714	0.2114	0.2633	0.2899	0.9850	1.4931	1.4709	1.7875	0.2635
5.29	0.1768	0.2790	0.3777	0.4797	0.5492	0.6360	0.7173	0.7785	1.8483	2.4377	2.2083	2.3921	0.2473
6.24	0.2153	0.4754	0.6276	0.7782	0.8619	0.9660	1.0389	1.1130	2.2802	2.9017	2.5747	2.7395	0.3953
7.36	0.2462	0.5027	0.6561	0.8072	0.8855	0.9833	1.0562	1.1208	2.3011	2.9993	2.6614	2.9291	0.6416
8.69	0.2907	0.6738	0.8698	1.0564	1.1529	1.2697	1.3566	1.4317	2.8269	3.6278	3.1053	3.4054	0.6844
10.2	0.3264	0.7982	1.0266	1.2377	1.3523	1.4802	1.5847	1.6848	3.2874	4.1509	3.4855	3.8361	0.7500
12.1	0.3614	0.7863	1.0072	1.2267	1.3422	1.4670	1.6002	1.7112	3.4131	4.3585	3.6019	4.0821	0.8087
14.3	0.4299	1.0192	1.2977	1.5743	1.7324	1.8807	2.0651	2.1998	4.2541	5.3468	4.2794	4.8344	0.6726
16.8	0.5086	1.1505	1.4601	1.7688	1.9686	2.1368	2.3560	2.5108	4.8703	6.2449	4.9044	5.5869	0.6127
19.9	0.6047	1.2936	1.6357	1.9978	2.2243	2.4220	2.6514	2.8207	5.4919	7.1713	5.4776	6.3054	0.5058
23.5	0.7197	1.5087	1.9141	2.3340	2.6173	2.8296	3.0920	3.2590	6.3723	8.4571	6.2038	7.2083	0.4461
27.7	0.8212	1.5706	2.0022	2.4640	2.7784	3.0090	3.2687	3.4457	6.8316	9.1879	6.6001	7.8100	0.4279
32.7	0.8754	1.9665	2.5387	3.1128	3.5080	3.7966	4.0662	4.2705	8.3342	10.7745	7.7758	9.2369	0.3615
38.5	0.9128	2.3438	3.1449	3.8964	4.3777	4.7739	5.1598	5.3302	10.2622	12.8255	9.7618	11.5497	0.2554
45.5	0.8894	2.9627	4.1128	5.1620	5.7820	6.4085	6.9674	7.1396	13.1651	15.7342	12.7044	14.8002	0.2038
53.7	0.9255	3.8397	5.4749	6.8600	7.6679	8.4722	9.2315	9.3930	16.3180	19.4314	16.1092	18.2916	0.2131
63.3	1.0738	5.2089	7.6092	9.3791	10.3801	11.2023	11.9540	12.2748	21.2308	25.1889	21.5249	23.8441	0.2341
74.7	1.0935	6.4094	9.5468	11.6379	12.7366	13.4596	14.0710	14.6350	26.4494	31.3667	27.0528	29.8453	0.2716
88.2	0.9780	7.9897	11.5818	14.0088	15.3079	16.0993	16.6474	17.4981	32.0679	37.5587	32.8307	36.5795	0.3246
104	0.8295	10.3339	14.5778	17.2665	18.9113	19.5337	20.2704	21.7201	37.6021	42.7119	37.8091	42.7462	0.3524
128	0.6812	12.2890	16.9410	19.7469	21.3890	21.4809	22.0909	23.9308	41.6407	44.4358	41.9174	46.1954	0.3079
157	0.4564	13.3199	17.5842	20.6411	21.9311	21.3506	22.1804	24.0684	44.2133	44.2337	45.2089	48.0866	0.2688
186	0.3866	15.1165	19.2583	22.8383	23.7549	22.7685	23.0419	24.8812	44.4632	43.4417	47.3234	48.9770	0.2469
219	0.3375	16.1278	19.8308	23.5897	24.0649	23.9059	22.9102	24.6991	42.6188	42.7575	45.4889	49.2952	0.2448
259	0.3612	17.1468	21.0261	25.2604	25.2078	26.9197	23.5302	26.0904	37.7017	41.6396	44.1517	45.5708	0.2232
293	0.3376	17.4343	21.5416	25.6141	25.3819	29.1418	23.3483	27.1768	33.8360	41.8534	44.4696	41.9669	0.2100
332	0.3184	17.1078	21.4668	25.2835	24.7814	32.1814	22.6483	29.0900	33.2556	40.6050	46.7875	42.4928	0.2023
391	0.2408	12.8859	15.4158	17.4979	17.5480	29.3978	16.2997	23.2137	40.2903	30.4721	52.4833	50.4634	0.2447
462	0.3115	10.5808	8.4145	12.4557	13.0787	22.9763	12.2964	20.8684	39.1810	17.6672	58.2085	52.7613	0.3342
TVC	16	183	233	280	294	333	298	339	568	603	640	668	13

Table B-3: Tank C LISST data: volume concentration of particles (uL/L) by size class (um)

Resuspension event 3

particle diameter (um)	elapsed time (hours)													
	0.00	0.25	0.75	1.25	1.75	3.22	4.22	5.25	6.25	24.20	27.35	48.50	51.58	Off
2.73	0.0090	0.0047	0.0000	0.0000	0.0003	0.0000	0.0000	0.0002	0.0069	0.0162	0.0213	0.1017	0.0991	0.4782
3.22	0.0102	0.0037	0.0000	0.0000	0.0005	0.0003	0.0007	0.0013	0.0086	0.0335	0.0431	0.1600	0.1575	0.4140
3.8	0.0164	0.0030	0.0005	0.0006	0.0024	0.0040	0.0056	0.0081	0.0172	0.0952	0.1172	0.3128	0.3125	0.3633
4.48	0.0293	0.0064	0.0078	0.0094	0.0166	0.0299	0.0393	0.0514	0.0671	0.3001	0.3493	0.6500	0.6605	0.3324
5.29	0.0347	0.0320	0.0547	0.0698	0.0986	0.1627	0.1997	0.2441	0.2741	0.7401	0.8183	1.1384	1.1695	0.3477
6.24	0.0470	0.0865	0.1470	0.1935	0.2448	0.3523	0.4173	0.4895	0.5220	1.0230	1.1015	1.3715	1.4170	0.4393
7.36	0.0367	0.1211	0.1972	0.2622	0.3118	0.4105	0.4800	0.5505	0.5773	1.0327	1.1101	1.3825	1.4339	0.5646
8.69	0.0286	0.2003	0.3151	0.4204	0.4779	0.5966	0.6855	0.7717	0.7943	1.3116	1.3983	1.6648	1.7359	0.6370
10.2	0.0092	0.2581	0.3958	0.5305	0.5956	0.7330	0.8376	0.9390	0.9538	1.5459	1.6170	1.9124	2.0046	0.7278
12.1	0.0018	0.2284	0.3633	0.4913	0.5614	0.6959	0.8049	0.9071	0.9389	1.5562	1.6103	1.9684	2.0754	0.8393
14.3	0.0003	0.2518	0.4523	0.6225	0.7220	0.9014	1.0445	1.1788	1.2635	1.9248	1.9723	2.3764	2.5138	0.9379
16.8	0.0000	0.2001	0.4442	0.6386	0.7571	0.9785	1.1368	1.2895	1.4484	2.1378	2.2057	2.6345	2.7718	1.0340
19.9	0.0000	0.1319	0.3968	0.6164	0.7523	1.0038	1.1739	1.3532	1.5912	2.3940	2.4903	2.8472	2.9866	1.0831
23.5	0.0000	0.0821	0.3476	0.5924	0.7492	1.0242	1.2136	1.4382	1.7185	2.9196	3.0570	3.2486	3.4159	1.1993
27.7	0.0178	0.0491	0.2701	0.4963	0.6566	0.9298	1.1217	1.3518	1.5801	3.3124	3.4857	3.6348	3.8110	1.3434
32.7	0.0502	0.0517	0.3195	0.6131	0.8119	1.1437	1.3876	1.6655	1.7955	4.2681	4.4619	4.5885	4.8273	1.5687
38.5	0.0000	0.0949	0.4851	0.8780	1.1292	1.5854	1.9150	2.2279	2.1697	5.0050	5.2377	5.8329	6.0919	1.7943
45.5	0.0000	0.3700	1.1457	1.7903	2.1717	2.9495	3.4822	3.8814	3.6937	6.4027	6.4643	7.9159	8.2290	2.1672
53.7	0.0117	1.9465	3.1202	4.0001	4.5529	5.6483	6.4545	7.0437	7.2270	8.6016	8.6141	10.4424	10.8667	2.6016
63.3	1.8512	4.6573	5.7171	6.8080	7.6225	8.7377	9.8638	10.7921	11.6704	11.2290	11.3890	13.9389	14.5114	2.9000
74.7	0.0001	1.8697	3.9616	5.6933	6.8455	8.0907	9.4543	10.4969	10.4438	13.9547	14.2863	17.7918	18.7511	2.9921
88.2	0.0000	0.9574	3.1184	5.1860	6.5469	8.3430	9.8421	11.0928	10.9351	18.0463	17.9932	21.5919	23.1447	3.1919
104	0.0018	4.2269	7.5843	10.3266	12.0117	14.0378	15.6000	17.2014	17.2548	22.1147	21.6498	24.9327	27.1922	3.6550
128	0.0562	6.3867	9.9474	13.1671	14.8044	16.3796	17.8854	19.7713	18.6081	24.1982	23.5243	27.5288	30.1481	4.2158
157	0.0002	3.8328	8.1812	12.0920	13.8239	15.3278	17.2208	19.7817	18.6659	25.7767	23.9111	30.4231	33.5096	4.8088
186	0.3191	8.5531	13.0286	16.7676	18.1471	18.5218	20.7614	24.2904	22.4008	25.8219	23.4774	32.4682	35.7129	4.4278
219	0.0036	7.1248	11.7177	15.5618	15.9948	16.5745	18.8416	22.1673	20.7043	26.1010	24.3273	30.8136	34.0983	3.7560
259	0.0679	8.9014	12.5459	16.3631	16.0670	16.6882	18.5798	21.0530	20.6025	23.8586	24.6238	29.2146	30.5404	3.3605
293	0.1096	10.3203	12.6334	16.2860	15.8420	15.7663	17.2377	18.8514	19.6281	22.5381	25.5806	28.2933	27.4066	2.5779
332	0.1932	11.3054	12.6371	15.5554	15.4254	14.8112	16.2946	17.0924	19.7612	20.4256	23.9356	26.7585	24.5033	1.5681
391	0.4508	11.9684	10.7292	13.2349	14.2740	13.6315	15.0533	15.6812	21.3331	19.9569	19.0081	28.9230	29.2082	1.6900
462	0.6326	6.5776	6.0362	7.8561	11.7520	9.9749	12.2497	11.3538	19.1499	17.2668	17.6528	30.8199	34.9386	5.2851
TVC	4	91	126	167	184	196	221	245	258	316	318	398	420	63

Appendix C: Dissolved PCB data

C-1: Tank A

C-2: Tank B

C-3: Tank C

Table C-1: Tank A dissolved PCBs (ng/L)

Resuspension event 1

elapsed time (hours)	4, 10	8, 5	19	18	17	33, 21, 53	52	49	66, 95	110, 77
0	ND	ND	ND	ND	ND	ND	ND	NQ	NQ	ND
0	ND	ND	ND	ND	ND	ND	ND	NQ	NQ	ND
0.25	ND	ND	ND	ND	ND	ND	ND	NQ	NQ	NQ
0.25	ND	ND	ND	ND	ND	ND	ND	NQ	NQ	NQ
0.75	ND	ND	4.8	ND	ND	4.7	5.7	3.8	NQ	NQ
0.75	ND	ND	4.7	ND	ND	4.9	5.9	4.4	NQ	NQ
1.25	NQ	ND	6.2	3.8	1.1	6.1	6.7	5.4	3.7	NQ
1.25	NQ	ND	6.3	3.9	1.2	6.0	6.3	5.2	3.8	NQ
1.75	2.5	NQ	7.2	6.1	2.1	7.9	7.7	5.9	4.4	4.1
1.75	2.5	NQ	7.5	6.4	2.2	7.7	8.0	6.5	4.2	4.3
2.43	3.8	5.4	8.1	7.3	2.4	8.8	10.0	6.9	5.8	5.4
2.43	3.6	5.6	8.5	7.7	2.4	8.7	10.2	7.2	6.1	5.8
3.43	5.5	9.2	9.3	9.6	3.0	10.6	12.3	8.6	7.6	6.5
3.43	5.2	9.5	9.1	9.8	3.1	10.3	12.4	8.9	7.3	6.7
4.43	6.8	13.2	9.7	10.7	3.5	11.7	14.1	10.6	8.5	7.3
4.43	6.9	13.0	9.9	11.0	3.7	11.4	14.4	10.4	8.9	7.1
5.43	8.5	14.5	10.0	12.1	4.0	12.2	15.5	11.2	9.7	7.5
5.43	8.2	14.4	10.3	11.9	3.9	12.5	15.8	11.4	9.9	7.3
24.73	7.6	14.9	11.3	11.9	4.1	12.4	15.3	10.8	10.6	7.9
24.73	7.9	14.7	10.9	11.6	3.7	12.3	15.0	10.2	10.8	7.7
28.80	8.2	15.1	11.2	12.1	3.5	12.5	14.9	10.5	10.8	8.0
28.80	7.8	14.9	11.4	11.6	3.7	12.2	15.1	10.9	10.3	7.8
46.77	7.7	14.3	11.0	11.9	4.0	12.4	15.2	10.1	10.6	8.0
46.77	8.1	14.5	11.3	12.2	4.1	12.2	15.0	10.5	10.4	8.0
53.72	7.9	14.7	11.1	12.0	3.8	12.5	15.1	10.1	10.4	7.9
53.72	8.3	14.6	11.4	11.8	4.1	12.1	14.9	10.8	10.5	8.2

Resuspension event 2

elapsed time (hours)	4, 10	8, 5	19	18	17	33, 21, 53	52	49	66, 95	110, 77
0	ND	ND	ND	ND	ND	ND	ND	ND	ND	NQ
0	ND	ND	ND	ND	ND	ND	ND	ND	ND	NQ
0.25	ND	ND	2.2	NQ	ND	NQ	ND	NQ	ND	NQ
0.25	ND	ND	2.2	NQ	ND	NQ	ND	NQ	ND	NQ
0.75	NQ	NQ	2.8	NQ	NQ	3.6	NQ	3.5	ND	NQ
0.75	NQ	NQ	2.9	NQ	NQ	3.7	NQ	3.8	ND	NQ
1.25	2.1	5.6	3.4	NQ	NQ	4.3	6.2	4.0	NQ	NQ
1.25	1.9	5.8	3.5	NQ	NQ	4.2	6.3	3.9	NQ	NQ
1.75	2.4	7.2	3.9	4.2	NQ	5.0	8.3	4.2	NQ	NQ
1.75	2.4	6.9	4.1	4.1	1.0	5.2	8.2	4.4	NQ	NQ
3.25	2.9	8.0	4.7	4.7	1.2	6.2	9.5	4.7	2.8	3.4
3.25	2.7	8.2	4.4	4.8	1.3	6.4	9.6	4.5	2.6	3.3
4.25	3.5	8.7	5.1	5.0	1.5	6.9	11.6	5.0	2.9	5.1
4.25	3.2	8.9	4.9	5.4	1.4	7.1	11.3	5.1	3.1	4.9
5.25	3.6	9.3	5.4	5.2	1.5	7.3	12.5	5.3	3.3	6.1
5.25	3.8	9.1	5.5	5.6	1.6	7.2	12.3	5.5	3.2	5.8
6.25	3.9	9.7	5.6	5.9	1.6	7.3	13.0	5.6	3.4	6.4
6.25	3.7	9.5	5.7	5.7	1.7	7.5	12.9	5.5	3.5	6.1
25.58	4.2	10.0	6.1	6.3	2.0	7.8	13.6	6.0	3.7	7.0
25.58	4.1	10.2	5.9	6.1	1.9	8.1	13.8	6.2	3.9	6.8
29.25	4.3	9.8	6.2	6.3	2.0	7.9	13.8	6.1	4.0	7.1
29.25	4.0	10.0	6.0	6.2	2.1	8.1	14.1	5.9	3.8	6.6
46.68	4.0	10.2	6.4	6.4	1.9	8.1	14.1	6.2	4.2	6.9
46.68	4.1	10.0	6.3	6.2	2.1	8.2	14.4	6.4	4.1	6.7
53.22	4.2	10.3	6.1	6.5	2.0	8.2	14.3	6.1	4.0	6.5
53.22	4.4	10.1	6.2	6.3	2.0	8.0	14.1	5.9	4.1	7.0

ND = not detected
NQ = not quantifiable

Table C-1: Tank A dissolved PCBs (ng/L)

Resuspension event 3

elapsed time (hours)	4, 10	8, 5	19	18	17	33, 21, 53	52	49	66, 95	110, 77
0	ND	ND	ND	ND	ND	ND	ND	ND	ND	ND
0	ND	ND	ND	ND	ND	ND	ND	ND	ND	ND
0.25	NQ	NQ	2.9	ND	ND	NQ	NQ	ND	ND	ND
0.25	NQ	NQ	2.5	ND	ND	NQ	NQ	ND	ND	ND
0.75	NQ	NQ	3.3	NQ	NQ	4.4	6.2	3.3	NQ	NQ
0.75	NQ	NQ	3.5	NQ	NQ	4.3	6.4	3.3	NQ	NQ
1.25	2.2	5.5	3.9	NQ	NQ	4.7	8.8	4.4	3.2	3.8
1.25	2.4	5.7	4.1	NQ	NQ	4.6	8.7	4.3	3.0	3.5
1.75	2.6	7.5	4.3	NQ	1.1	5.4	10.8	4.9	3.5	4.4
1.75	2.3	7.3	4.5	NQ	1.1	5.1	11.1	5.0	3.6	4.2
3.23	3.2	8.3	5.0	4.1	1.2	6.3	12.0	5.2	3.9	5.0
3.23	3.1	8.5	5.1	4.2	1.3	6.4	12.1	5.3	4.1	4.8
4.23	3.5	8.9	5.3	4.4	1.4	7.3	12.4	5.5	4.1	5.0
5.23	3.6	9.0	5.6	4.5	1.3	7.5	12.5	5.5	4.2	5.1
5.23	3.8	9.2	5.7	4.7	1.4	7.4	12.3	5.6	4.2	5.2
6.23	3.9	9.4	5.8	4.6	1.3	7.6	12.5	5.6	4.2	5.3
6.23	3.7	9.5	5.9	4.8	1.4	7.5	12.6	5.7	4.3	5.1
24.22	4.2	9.9	6.3	4.9	1.5	7.8	12.9	6.0	4.4	5.5
24.22	4.3	10.1	6.1	5.1	1.5	7.9	13.0	6.1	4.6	5.4
28.22	4.2	10.1	6.4	5.0	1.4	7.9	13.0	5.9	4.3	5.6
28.22	4.4	10.2	6.2	5.2	1.5	8.0	13.1	6.0	4.5	5.3
48.98	4.4	10.1	6.3	4.9	1.5	8.1	13.1	6.0	4.5	5.5
48.98	4.5	10.3	6.0	5.1	1.6	8.0	13.2	6.0	4.6	5.4
53.23	4.5	10.2	6.4	5.2	1.5	7.9	13.2	6.0	4.5	5.6
53.23	4.4	10.3	6.3	5.0	1.5	8.1	13.0	6.1	4.4	5.4
71.17	4.8	10.8	6.7	5.1	1.6	8.1	13.2	5.9	4.5	5.6
71.17	4.7	11.0	6.5	5.2	1.6	8.2	13.4	6.1	4.4	5.5
95.12	4.9	12.2	7.0	5.2	1.7	8.5	14.6	6.6	4.6	5.5
95.12	5.0	12.6	7.2	5.4	1.8	8.4	14.4	6.4	4.5	5.7
118.90	5.5	12.7	7.6	5.6	1.6	8.9	15.0	7.0	4.7	5.8
118.90	5.3	13.6	7.8	5.4	1.7	8.6	14.8	7.2	4.6	5.7
143.55	5.6	13.4	8.0	5.8	1.8	9.1	15.5	7.6	4.8	5.6
143.55	5.8	14.7	8.1	5.7	1.9	9.2	15.7	7.4	4.7	5.8
168.80	5.8	15.0	8.6	6.1	2.0	9.4	16.0	7.7	4.8	5.9
168.80	6.0	15.2	9.4	5.9	1.9	9.4	16.1	7.8	4.8	6.0

ND = not detected
NQ = not quantifiable

Table C-2: Tank B dissolved PCBs (ng/L)

Resuspension event 1

elapsed time (hours)	4, 10	8, 5	19	18	17	33, 21, 53	52	49	66, 95	110, 77
0	NQ	ND	4.0	ND	ND	3.6	5.5	2.2	ND	ND
0	NQ	ND	4.1	ND	ND	3.7	5.7	2.3	ND	ND
0.25	2.1	NQ	5.4	4.1	1.2	4.4	9.9	3.5	NQ	NQ
0.25	2.2	NQ	5.6	4.4	1.2	4.4	9.0	3.1	NQ	NQ
0.75	2.6	3.5	6.0	5.8	1.5	5.7	12.5	4.4	4.1	NQ
0.75	2.8	3.0	5.9	5.5	1.6	5.6	12.3	4.6	4.2	NQ
1.90	3.3	5.5	7.6	6.3	2.4	7.0	16.5	6.9	5.3	3.9
1.90	3.5	5.6	7.4	6.2	2.4	7.0	16.2	6.8	5.2	3.6
2.92	4.5	8.0	8.0	7.4	2.7	8.9	19.4	8.5	6.3	5.6
2.92	4.6	8.2	7.9	7.6	2.9	8.2	19.2	8.6	6.1	5.7
3.90	5.7	10.2	8.7	8.7	3.2	11.2	21.2	9.9	7.9	6.6
3.90	5.5	10.5	8.5	8.8	3.3	11.6	21.0	9.6	7.5	6.4
4.90	6.5	12.4	9.1	9.4	3.6	13.0	23.3	11.2	8.9	7.2
4.90	6.3	12.3	9.5	9.6	3.9	12.9	23.8	11.4	9.2	7.4
5.92	6.6	13.8	10.0	11.0	4.3	16.6	24.6	13.8	10.5	8.0
5.92	6.9	13.6	10.5	11.2	4.2	16.6	24.2	13.6	10.2	8.2
24.83	6.8	15.9	13.7	10.9	3.6	16.4	23.5	12.3	9.8	7.8
24.83	7.0	17.0	13.4	11.0	3.5	16.2	23.2	12.4	10.1	8.0
28.82	7.4	16.7	13.5	11.2	4.0	15.4	23.0	12.5	10.1	7.7
28.82	7.5	17.0	14.0	10.8	4.2	15.8	23.2	12.1	9.9	7.9
47.67	7.6	17.2	14.3	10.9	4.5	16.4	23.4	11.9	10.2	8.3
47.67	7.8	17.4	14.5	11.0	4.2	16.0	23.6	11.7	10.0	8.1
52.82	7.5	17.4	14.7	11.1	3.9	15.9	23.2	12.2	10.2	7.8
52.82	7.7	17.1	14.5	10.9	4.1	16.1	23.0	12.1	10.6	7.9

Resuspension event 2

elapsed time (hours)	4, 10	8, 5	19	18	17	33, 21, 53	52	49	66, 95	110, 77
0	ND	ND	ND	ND	ND	5.5	NQ	NQ	ND	ND
0	ND	ND	ND	ND	ND	5.5	NQ	NQ	ND	ND
0.25	NQ	NQ	3.0	ND	NQ	6.2	5.5	NQ	ND	ND
0.25	NQ	NQ	3.0	ND	NQ	6.7	5.2	NQ	ND	ND
0.75	NQ	NQ	3.4	NQ	NQ	7.4	7.4	3.9	ND	ND
0.75	NQ	NQ	3.8	NQ	NQ	7.4	7.7	3.5	ND	ND
1.25	NQ	NQ	4.0	NQ	1.1	8.2	9.4	4.7	ND	NQ
1.25	NQ	NQ	4.2	NQ	1.1	8.3	9.3	4.9	ND	NQ
1.75	NQ	3.2	4.5	4.6	1.2	9.7	10.7	5.6	3.0	NQ
1.75	NQ	3.3	4.9	4.3	1.2	9.5	10.8	5.8	3.2	NQ
2.97	2.0	4.1	5.4	5.8	1.4	10.7	11.9	6.9	3.3	NQ
2.97	2.1	4.2	5.3	5.5	1.4	10.6	12.0	6.8	3.3	NQ
3.97	2.9	4.4	6.0	6.7	1.5	11.3	13.0	7.5	3.5	NQ
3.97	2.7	4.5	6.3	6.5	1.5	11.5	13.2	7.7	3.8	NQ
4.97	3.5	4.8	6.5	7.2	1.6	12.1	14.1	7.9	4.2	3.3
4.97	3.4	4.9	6.9	7.5	1.7	11.9	14.0	8.3	4.5	3.4
5.97	3.8	5.4	7.0	7.9	1.8	12.3	14.2	8.5	5.0	3.6
5.97	3.6	5.2	7.1	7.6	1.9	12.2	14.4	8.6	5.2	3.8
21.75	4.4	6.4	8.0	8.5	2.3	12.7	15.1	9.7	6.2	4.2
21.75	4.2	6.3	7.7	8.8	2.2	13.0	15.1	9.5	6.2	4.1
30.62	4.4	6.8	8.2	8.9	2.5	13.4	14.8	9.5	6.6	4.2
30.62	4.5	6.9	8.3	9.1	2.6	13.3	16.0	9.8	6.6	4.0
48.22	4.5	7.1	9.6	9.0	2.7	13.9	15.9	10.0	6.9	4.2
48.22	4.4	7.2	9.5	8.9	2.8	14.0	16.0	9.7	6.9	4.1
53.22	4.5	7.5	9.4	8.7	3.0	13.7	16.4	9.9	7.0	4.2
53.22	4.8	7.7	9.5	8.5	2.7	13.9	16.2	9.5	7.3	4.1

ND = not detected
NQ = not quantifiable

Tank C-2: Tank B dissolved PCBs (ng/L)

Resuspension event 3

elapsed time (hours)	4, 10	8, 5	19	18	17	33, 21, 53	52	49	66, 95	110, 77
0	ND	ND	ND	ND	ND	ND	ND	ND	ND	ND
0	ND	ND	ND	ND	ND	ND	ND	ND	ND	ND
0.25	ND	NQ	ND	ND	ND	4.1	NQ	NQ	ND	ND
0.25	ND	NQ	ND	ND	ND	4.3	NQ	NQ	ND	ND
0.75	NQ	NQ	2.9	ND	ND	4.9	NQ	1.6	NQ	ND
0.75	NQ	NQ	2.8	ND	ND	4.9	NQ	1.6	NQ	ND
1.25	NQ	NQ	3.8	NQ	ND	5.3	NQ	2.3	NQ	ND
1.25	NQ	NQ	3.6	NQ	ND	5.4	NQ	2.1	NQ	ND
1.75	NQ	NQ	4.8	NQ	ND	5.7	6.0	3.2	NQ	NQ
1.75	NQ	NQ	4.6	NQ	ND	5.5	5.8	3.3	NQ	NQ
2.75	NQ	NQ	5.2	NQ	NQ	6.0	6.6	4.4	NQ	NQ
2.75	NQ	NQ	5.3	NQ	NQ	6.1	6.7	4.4	2.9	NQ
3.75	NQ	NQ	5.5	NQ	NQ	6.3	7.9	5.3	3.4	NQ
3.75	NQ	NQ	5.5	NQ	NQ	6.6	7.7	5.3	3.3	NQ
4.75	2.2	NQ	5.8	NQ	NQ	7.2	8.4	6.1	4.2	NQ
4.75	2.2	NQ	5.9	NQ	NQ	7.2	8.2	5.9	4.1	NQ
5.75	2.3	NQ	5.8	NQ	1.0	7.9	8.9	6.4	4.5	NQ
22.75	2.6	NQ	5.9	3.8	1.1	9.4	11.5	7.7	4.7	3.3
22.75	2.6	NQ	5.9	3.9	1.2	9.2	11.4	7.9	4.9	3.4
29.75	2.9	NQ	6.1	4.0	1.2	9.6	12.0	8.1	5.1	3.5
29.75	2.8	NQ	6.1	4.1	1.1	9.4	12.2	7.9	4.9	3.6
47.25	2.9	NQ	6.3	4.2	1.1	10.2	12.3	8.1	5.1	3.5
47.25	2.9	NQ	6.2	4.1	1.1	10.2	12.3	8.2	5.2	3.6
52.75	2.8	NQ	6.1	4.1	1.2	10.1	12.4	8.2	5.2	3.7
52.75	3.0	NQ	6.2	4.2	1.1	10.2	12.3	8.1	5.1	3.5

ND = not detected
NQ = not quantifiable

Table C-3: Tank C dissolved PCBs (ng/L)

Resuspension event 1

elapsed time (hours)	4, 10	8, 5	19	18	17	33, 21, 53	52	49	66, 95	110, 77
0	NQ	ND	ND	ND	ND	NQ	NQ	ND	ND	ND
0	NQ	ND	ND	ND	ND	NQ	NQ	ND	ND	ND
0.25	NQ	ND	7.1	ND	ND	3.7	5.8	2.0	NQ	ND
0.25	NQ	ND	6.3	ND	ND	4.0	5.7	1.7	NQ	ND
0.75	1.9	NQ	8.8	4.0	NQ	5.0	6.1	2.7	NQ	ND
0.75	2.2	NQ	8.1	4.3	NQ	5.2	6.5	2.8	NQ	ND
1.25	2.5	NQ	9.1	4.8	1.1	6.1	7.2	3.0	3.3	NQ
1.25	2.4	NQ	9.2	5.0	1.1	6.3	7.3	3.3	3.8	NQ
1.75	2.9	3.6	9.8	6.1	1.6	6.0	8.4	3.8	4.6	NQ
1.75	3.0	3.3	10.0	5.8	1.5	6.2	8.3	4.1	4.3	NQ
2.75	3.9	4.4	10.5	7.2	2.1	7.0	9.4	4.9	6.3	NQ
2.75	4.1	4.2	10.4	7.6	2.0	7.4	9.2	4.7	6.5	NQ
3.75	4.8	5.0	10.6	8.4	2.4	7.5	10.7	5.7	7.0	4.4
3.75	4.4	4.8	11.1	8.1	2.3	7.5	10.9	5.5	7.3	4.2
4.75	5.8	5.4	11.5	9.2	2.5	7.6	12.6	6.3	8.7	4.9
4.75	6.0	5.2	11.9	9.0	2.7	8.0	12.2	6.4	8.1	5.0
5.75	7.2	5.4	12.0	10.4	2.7	7.9	13.8	6.8	9.6	5.5
5.75	7.3	5.5	12.4	10.1	2.9	8.1	13.6	7.0	9.5	5.3
23.05	6.4	6.3	13.4	9.9	2.9	8.8	14.0	6.4	9.5	5.7
23.05	6.5	6.2	13.6	9.7	2.9	8.5	14.4	6.1	9.6	5.6
28.73	6.8	6.1	13.9	10.0	3.0	8.9	14.3	6.3	9.7	5.6
28.73	6.5	6.4	13.1	9.8	3.0	8.7	14.3	6.5	9.9	5.5
47.97	6.7	6.1	13.4	10.2	3.0	9.5	14.3	6.4	9.7	5.8
47.97	6.8	6.3	13.7	10.0	3.1	9.4	14.5	6.2	10.0	5.7
52.05	7.0	6.0	13.5	10.0	2.9	9.7	14.2	6.3	9.8	5.8
52.05	6.7	6.2	13.8	9.9	3.0	9.5	14.0	6.6	10.1	5.5

Resuspension event 2

elapsed time (hours)	4, 10	8, 5	19	18	17	33, 21, 53	52	49	66, 95	110, 77
0	NQ	ND	ND	NQ	ND	NQ	NQ	NQ	ND	NQ
0	NQ	ND	ND	NQ	ND	NQ	NQ	NQ	ND	NQ
0.25	NQ	ND	5.6	NQ	NQ	NQ	NQ	NQ	NQ	NQ
0.25	NQ	ND	5.4	NQ	NQ	NQ	NQ	NQ	NQ	NQ
0.75	2.2	NQ	5.8	4.4	1.3	4.3	5.5	NQ	NQ	NQ
0.75	2.0	NQ	5.7	4.5	1.1	4.1	5.8	NQ	NQ	NQ
1.25	2.5	NQ	6.0	4.7	1.0	4.5	6.7	1.4	NQ	NQ
1.25	2.7	NQ	6.2	4.8	1.2	4.8	6.8	1.9	NQ	NQ
1.75	3.2	NQ	6.3	5.0	1.3	5.5	7.5	2.4	NQ	NQ
1.75	3.4	NQ	6.3	5.3	1.6	5.1	7.7	2.1	NQ	NQ
2.75	3.7	3.3	6.7	5.2	1.9	6.1	8.8	3.2	2.9	NQ
2.75	3.9	3.3	6.4	5.9	1.7	5.9	8.8	2.7	2.8	NQ
3.75	4.3	4.0	6.5	6.3	1.8	6.7	9.1	3.6	2.8	3.1
4.75	4.4	4.4	7.0	6.7	2.0	7.1	9.3	4.4	3.3	3.6
4.75	4.5	4.2	7.0	6.6	2.1	7.3	9.2	4.1	3.4	3.4
21.02	5.0	4.8	7.3	7.0	2.5	8.3	9.8	5.4	4.8	5.0
21.02	4.7	5.0	7.6	7.5	2.1	8.0	9.9	5.5	4.4	4.4
28.87	5.0	5.1	7.5	8.1	2.3	8.6	9.9	5.3	5.0	5.3
28.87	4.8	4.9	7.8	7.9	2.2	9.0	10	5.8	5.5	5.5
43.90	5.0	4.8	8.1	8.0	2.5	8.1	9.9	5.8	5.6	5.8
43.90	4.8	4.8	8.0	8.1	2.5	8.6	10.1	5.6	5.1	5.6
53.27	5.0	5.1	8.5	8.3	2.4	8.1	10.1	6.0	5.6	5.5
53.27	5.2	5.0	8.1	8.0	2.5	8.4	9.8	6.1	5.2	5.9

ND = not detected
NQ = not quantifiable

Table C-3: Tank C dissolved PCBs (ng/L)

Resuspension event 3

elapsed time (hours)	4, 10	8, 5	19	18	17	33, 21, 53	52	49	66, 95	110, 77
0	NQ	ND	ND	ND	ND	4.1	NQ	NQ	ND	ND
0	NQ	ND	ND	ND	ND	4.4	NQ	NQ	ND	ND
0.25	NQ	ND	3.3	NQ	ND	4.7	NQ	NQ	ND	ND
0.25	NQ	ND	3.1	NQ	ND	4.5	NQ	NQ	ND	ND
0.75	NQ	NQ	3.6	NQ	ND	5.1	NQ	NQ	ND	ND
0.75	NQ	NQ	3.5	NQ	ND	4.9	NQ	NQ	ND	ND
1.25	NQ	NQ	4.2	NQ	NQ	5.5	NQ	1.9	NQ	NQ
1.25	NQ	NQ	4.3	NQ	NQ	5.3	NQ	1.7	NQ	NQ
1.75	2.1	NQ	4.8	NQ	NQ	5.4	5.3	2.1	NQ	NQ
1.75	2.2	NQ	4.9	NQ	NQ	5.9	5.5	2.2	NQ	NQ
3.22	2.6	NQ	5.2	4.2	1.0	6.2	6.1	2.8	NQ	NQ
3.22	2.7	NQ	5.6	4.0	1.3	6.0	6.0	2.6	NQ	NQ
4.22	3.1	NQ	5.4	4.5	1.4	6.3	6.9	3.1	NQ	NQ
4.22	3.0	NQ	6.2	4.9	1.6	6.6	6.5	3.3	NQ	NQ
5.25	3.4	NQ	6.4	5.1	1.4	6.5	7.3	3.6	NQ	NQ
5.25	3.2	NQ	6.4	5.3	1.5	6.8	7.7	3.9	NQ	NQ
6.25	3.4	NQ	7.0	5.6	1.8	7.2	7.9	4.3	NQ	NQ
6.25	3.6	3.3	6.8	5.8	1.7	7.4	8.1	4.0	NQ	NQ
24.20	4.0	3.9	7.8	6.6	2.1	8.3	9.2	5.7	2.8	NQ
24.20	4.3	3.8	7.9	6.5	2.1	8.5	9.5	5.1	2.6	NQ
27.35	4.1	3.8	7.8	6.7	2.1	8.5	9.7	5.5	2.7	NQ
27.35	4.6	4.0	8.1	6.9	2.1	8.4	10.2	5.7	2.9	3.2
48.50	4.5	4.1	8.2	6.8	2.0	8.8	10.1	5.8	3.1	3.1
48.50	4.2	3.9	8.0	7.0	2.1	8.6	9.8	5.5	2.9	3.1
51.58	4.2	4.1	8.1	7.0	2.1	8.8	10.0	6.0	3.1	3.6
51.58	4.2	4.0	8.3	7.1	2.1	8.4	10.4	5.7	3.3	3.2

ND = not detected
 NQ = not quantifiable

Appendix D: Particulate PCB data

D-1: Tank A

D-2: Tank B

D-3: Tank C

Table D-1: Tank A particulate PCBs (ng/g)

Resuspension event 1

	0	0	0.25	0.25	0.75	0.75	1.25	1.25	1.75	1.75	2.43
elapsed time (hours)	150	150	150	150	150	150	150	150	150	150	150
sample vol (ml)	2.4	2.4	31	31	35.3	30.1	34.2	34.2	32.3	32.3	41.8
TSS (mg/L)	86	79	83	80	83	68	85	79	94	70	90
% 14 recovered	73	68	75	71	76	64	73	71	65	67	85
% 65 recovered	84	82	85	83	83	73	84	84	81	82	92
% 106 recovered											
congener	conc (ng/g)	conc (ng/g)	conc (ng/g)	conc (ng/g)	conc (ng/g)	conc (ng/g)	conc (ng/g)	conc (ng/g)	conc (ng/g)	conc (ng/g)	conc (ng/g)
4,10	NQ	NQ	304	292	216	216	225	276	275	289	363
7,9	NQ	NQ	99	75	67	67	82	85	83	87	52
6	ND	ND	191	161	133	153	171	197	192	199	153
8,5	NQ	NQ	2049	2007	1502	1908	1785	2025	2043	2093	2013
19	NQ	NQ	208	204	149	176	184	226	211	212	246
12,13	ND	ND	25	17	18	ND	ND	21	ND	ND	22
18	ND	ND	535	447	372	430	489	524	494	511	432
17	ND	ND	541	444	363	436	511	526	526	492	559
24	NQ	NQ	72	NQ	NQ	NQ	NQ	71	73	70	274
16,32	NQ	NQ	455	428	332	407	461	478	477	479	738
29	NQ	NQ	NQ	NQ	NQ	NQ	NQ	NQ	NQ	NQ	NQ
26	NQ	ND	634	491	442	436	649	585	605	774	606
25	ND	ND	158	117	101	113	142	146	165	ND	174
31,28	ND	ND	2185	1675	1585	457	2318	2191	2188	2019	2070
33,21,53	NQ	NQ	655	568	488	565	642	729	694	694	811
51	ND	ND	71	70	61	61	83	123	83	82	130
22	ND	ND	NQ	NQ	294	NQ	374	ND	362	355	200
45	ND	ND	75	68	58	64	72	86	78	85	110
46	ND	NQ	NQ	54	NQ	NQ	NQ	49	53	57	61
52	ND	ND	934	803	715	774	1009	984	959	917	1072
49	NQ	ND	580	509	455	478	610	578	568	567	680
47,48	494	424	326	316	249	264	335	312	355	312	716
44	ND	ND	186	210	140	97	154	254	146	135	115
37,42	ND	ND	281	166	182	148	223	196	207	190	248
41,64,71	ND	NQ	393	323	324	329	402	407	371	381	447
40	ND	ND	56	43	52	39	59	61	62	53	NQ
100	ND	ND	42	26	33	34	51	43	34	54	170
63	202	ND	66	70	78	39	90	ND	102	73	50
74	NQ	ND	177	148	118	106	156	123	196	168	166
70,76	NQ	NQ	200	175	NQ	NQ	192	NQ	171	168	150
66,95	ND	NQ	649	452	494	478	680	660	666	669	742
91	NQ	NQ	82	77	63	61	94	87	96	90	126
56,60(92,84)	NQ	NQ	429	333	306	323	475	464	453	412	363
89	ND	ND	154	120	ND	116	181	171	176	152	207
101	ND	NQ	NQ	NQ	114	NQ	82	87	82	84	93
99	ND	ND	44	38	33	35	58	46	39	50	47
119	NQ	NQ	NQ	NQ	NQ	NQ	NQ	NQ	NQ	NQ	NQ
83	ND	ND	5	ND	7	12	11	10	10	10	10
97	66	316	6	7	6	NQ	8	6	5	6	NQ
81,87	NQ	NQ	NQ	NQ	NQ	NQ	NQ	NQ	NQ	NQ	NQ
85	ND	ND	17	9	12	15	ND	25	17	30	23
136	ND	ND	22	ND	17	ND	ND	28	24	34	34
77,110	ND	ND	443	278	351	253	448	464	316	324	236
82,151	ND	ND	17	18	16	15	20	21	19	19	19
135,144	ND	ND	39	52	41	31	51	49	44	41	NQ
107	ND	47	20	30	23	15	22	22	25	21	36
123,149	ND	ND	108	107	107	80	129	125	105	115	121
118	NQ	NQ	64	49	47	48	66	55	61	67	73
134	NQ	NQ	NQ	NQ	14	NQ	NQ	NQ	NQ	NQ	NQ
146	NQ	NQ	NQ	NQ	NQ	NQ	NQ	NQ	NQ	NQ	71
132,153,105	NQ	NQ	NQ	NQ	NQ	NQ	NQ	NQ	NQ	NQ	NQ
141	ND	ND	14	12	11	49	17	70	50	76	NQ
137,130,176	NQ	NQ	NQ	NQ	NQ	NQ	NQ	NQ	NQ	NQ	NQ
163,138	85	ND	181	146	152	139	194	190	179	187	219
158	NQ	NQ	NQ	NQ	NQ	NQ	NQ	NQ	NQ	NQ	NQ
129,178	ND	ND	25	30	31	25	36	40	47	38	49
187,182	ND	ND	111	97	103	101	124	130	109	110	112
183	ND	ND	ND	20	30	ND	22	36	ND	20	NQ
128	ND	ND	5	8	8	ND	12	ND	ND	8	NQ
185	ND	ND	ND	ND	ND	ND	ND	ND	ND	ND	4
174	NQ	NQ	NQ	NQ	NQ	NQ	NQ	NQ	NQ	NQ	21
177	ND	ND	38	28	36	28	38	54	56	39	37
202,171,156	ND	NQ	ND	22	27	ND	35	24	ND	37	30
157,200	ND	ND	ND	ND	ND	ND	ND	ND	ND	ND	8
172	ND	ND	ND	ND	ND	ND	ND	ND	ND	ND	ND
197	ND	ND	ND	ND	ND	ND	ND	ND	ND	ND	ND
180	ND	ND	63	37	47	48	60	57	64	59	59
193	ND	ND	ND	ND	NQ	ND	ND	ND	NQ	29	ND
191	ND	ND	8	ND	ND	ND	ND	ND	ND	ND	ND
199	ND	NQ	NQ	NQ	NQ	NQ	NQ	NQ	NQ	NQ	NQ
170,190	ND	ND	67	36	46	40	74	78	50	45	65
198	ND	ND	ND	ND	ND	ND	ND	ND	ND	ND	ND
201	ND	ND	63	42	48	50	76	60	56	83	75
203,196	ND	ND	68	53	62	48	109	112	79	83	70
189	ND	ND	ND	ND	ND	ND	ND	ND	ND	ND	ND
208,195	ND	ND	52	28	ND	ND	75	61	ND	ND	61
207	ND	ND	ND	ND	ND	ND	ND	ND	ND	ND	ND
194	ND	ND	NQ	NQ	NQ	NQ	21	NQ	32	ND	NQ
205	ND	ND	ND	ND	ND	ND	ND	ND	ND	ND	ND
206	ND	ND	NQ	22	23	31	42	57	54	52	40
209	ND	ND	NQ	NQ	NQ	ND	ND	NQ	NQ	NQ	NQ
total (ng/g)	847	787	14232	12091	10780	9749	14729	14558	14691	14496	15878
total (ug/g)	0.8	0.8	14.2	12.1	10.8	9.7	14.7	14.6	14.7	14.5	15.9

ND = not detected
NQ = not quantifiable

Table D-1: Tank A particulate PCBs (ng/g)

Resuspension event 1

	3.43	4.43	5.43	24.73	28.8	46.77	46.77	53.72	Off
elapsed time (hours)	150	150	150	150	150	150	150	150	150
sample vol (ml)	42.9	34.8	36	71.8	53.7	62.9	62.9	62.2	5.4
TSS (mg/L)	87	70	89	77	72	80	98	76	76
% 14 recovered	74	71	72	68	77	72	89	78	76
% 65 recovered	88	86	84	51	76	60	91	82	63
% 166 recovered									
congener	conc (ng/g)	conc (ng/g)	conc (ng/g)	conc (ng/g)	conc (ng/g)	conc (ng/g)	conc (ng/g)	conc (ng/g)	conc (ng/g)
4,10	250	298	222	206	209	159	174	240	1052
7,9	84	80	83	70	47	59	37	36	301
6	176	186	180	144	133	127	126	108	574
8,5	1811	1905	1742	1165	1535	1201	1279	1235	8032
19	211	232	187	210	232	194	200	184	866
12,13	24	ND	23	19	26	18	12	18	ND
18	508	526	479	422	396	349	321	299	1944
17	509	474	474	422	492	328	329	350	1826
24	66	71	64	57	177	46	231	133	NQ
16,32	426	491	427	401	679	519	530	501	2148
29	NQ	NQ	NQ	NQ	NQ	NQ	NQ	NQ	NQ
26	628	538	729	562	687	454	518	498	2391
25	139	125	195	116	202	103	140	133	593
31,28	2274	2028	2207	1818	2253	1606	1759	1637	7829
33,21,53	673	677	649	595	800	592	566	599	3108
51	125	82	78	79	109	60	117	82	374
22	ND	349	375	233	ND	252	264	187	165
45	82	86	69	75	94	58	94	71	317
46	43	60	NQ	34	45	29	46	31	NQ
52	959	927	964	828	1086	775	809	779	4662
49	571	582	565	470	673	500	525	491	2853
47,48	313	310	333	253	594	411	422	427	1346
44	138	201	121	121	129	97	84	84	705
37,42	200	259	179	172	237	139	175	173	888
41,64,71	388	375	371	298	452	275	360	321	1981
40	69	65	68	62	70	47	NQ	53	275
100	48	43	55	35	130	32	NQ	36	36
63	72	ND	69	45	40	48	62	25	548
74	164	140	150	114	148	108	178	116	811
70,76	194	NQ	159	122	139	98	98	113	NQ
66,95	535	623	640	544	707	568	571	548	2253
91	91	81	89	72	113	78	96	80	413
56,60(92,84)	448	375	453	329	393	313	289	267	2240
89	167	157	166	139	158	117	171	148	704
101	74	74	75	81	88	55	72	67	NQ
99	46	42	48	37	57	33	44	34	236
119	NQ	NQ	NQ	NQ	ND	NQ	NQ	NQ	NQ
83	10	8	8	7	24	7	7	5	59
97	7	6	6	6	ND	5	21	NQ	33
81,87	NQ	NQ	NQ	NQ	ND	NQ	NQ	NQ	NQ
85	38	21	ND	13	27	14	20	17	62
136	25	24	24	18	36	17	26	24	97
77,110	317	317	324	177	290	164	178	184	885
82,151	18	17	21	11	21	10	15	14	68
135,144	42	40	53	24	ND	25	NQ	NQ	162
107	30	17	28	11	29	11	18	10	61
123,149	123	96	128	67	137	62	83	77	384
118	81	43	81	27	33	38	37	37	139
134	NQ	NQ	NQ	NQ	ND	NQ	NQ	NQ	NQ
146	NQ	NQ	NQ	NQ	ND	NQ	NQ	NQ	NQ
132,153,105	NQ	NQ	NQ	NQ	NQ	NQ	NQ	NQ	NQ
141	21	18	12	6	17	9	NQ	12	55
137,130,176	NQ	NQ	NQ	NQ	NQ	NQ	NQ	NQ	NQ
163,138	200	174	174	102	207	93	151	197	569
158	NQ	NQ	NQ	NQ	ND	NQ	NQ	ND	NQ
129,178	45	28	37	17	50	12	32	31	81
187,182	111	106	110	56	110	ND	79	73	383
183	31	20	23	9	23	12	NQ	14	ND
128	14	7	6	3	15	6	NQ	11	ND
185	ND	ND	ND	ND	ND	ND	ND	ND	ND
174	NQ	NQ	NQ	NQ	29	NQ	15	19	NQ
177	43	34	39	20	46	22	29	26	123
202,171,156	34	23	26	15	39	20	21	26	NQ
157,200	ND	ND	ND	ND	ND	ND	7	ND	ND
172	ND	ND	ND	ND	ND	ND	9	ND	ND
197	ND	ND	ND	ND	ND	ND	ND	ND	ND
180	63	70	46	27	64	28	40	34	157
193	ND	ND	ND	ND	ND	ND	ND	ND	ND
191	ND	ND	ND	ND	ND	ND	ND	ND	ND
199	NQ	NQ	NQ	NQ	ND	NQ	NQ	NQ	NQ
170,190	76	86	49	26	76	33	43	40	150
198	ND	ND	ND	ND	ND	ND	ND	ND	ND
201	61	71	68	26	72	31	53	43	230
203,196	105	120	64	27	75	35	56	49	217
189	ND	ND	ND	ND	ND	ND	ND	ND	ND
208,195	73	69	54	18	67	31	42	43	218
207	ND	ND	ND	ND	ND	4	ND	ND	33
194	26	25	20	NQ	32	10	NQ	16	NQ
205	NQ	ND	NQ	NQ	ND	ND	ND	ND	ND
206	49	59	40	15	56	23	30	30	133
209	18	33	NQ	NQ	11	NQ	NQ	4	NQ
total (ng/g)	14149	13992	14127	10936	15214	10581	11889	11120	55811
total (ug/g)	14.1	14.0	14.1	10.9	15.2	10.6	11.7	11.1	55.8

ND = not detected
NQ = not quantifiable

Table D-1: Tank A particulate PCBs (ng/g)

Settling after resuspension event 3

elapsed time (min.)	before	3	3	8	8	20	20	60	60	120	1365	
sample vol (ml)	150	150	150	150	150	150	150	150	300	300	300	
TSS (mg/L)	58	58	42.5	42.5	34.5	21.5	21.5	18.3	18.3	13.8	8.2	
% 14 recovered	69	63	77	66	74	55	86	61	77	52	82	
% 65 recovered	68	80	83	86	77	74	87	83	78	70	88	
% 166 recovered	82	76	85	79	83	83	82	76	79	79	86	
congener	conc (ng/g)	conc (ng/g)	conc (ng/g)	conc (ng/g)	conc (ng/g)	conc (ng/g)	conc (ng/g)	conc (ng/g)	conc (ng/g)	conc (ng/g)	conc (ng/g)	conc (ng/g)
4,10	246	190	298	197	270	202	307	249	256	191	328	386
7,9	39	81	37	85	38	78	54	93	28	77	50	54
6	105	135	119	135	114	118	120	143	78	114	100	110
8,5	1251	1537	1590	1668	1482	1575	1963	1966	1188	1450	1700	1727
19	180	144	205	148	188	135	220	167	173	128	210	216
12,13	ND	34	ND	29	17	30	ND	31	ND	22	ND	ND
18	256	378	326	374	279	352	387	463	229	359	316	296
17	376	479	483	486	433	450	509	534	374	439	490	440
24	125	151	143	160	138	152	183	201	117	144	154	156
16,32	490	559	568	571	578	551	689	686	491	531	617	615
29	NQ	NQ	NQ	NQ	NQ	NQ	NQ	NQ	NQ	NQ	NQ	NQ
26	485	486	553	489	538	408	641	512	494	381	599	492
25	133	158	146	146	153	123	246	197	142	108	167	168
31, 28	1647	1623	1903	1657	1825	1334	2064	1660	1570	1198	1988	1342
33,21,53	585	780	714	798	656	741	785	914	528	738	714	684
51	81	96	87	95	146	94	102	116	75	93	99	109
22	175	269	180	265	ND	304	254	366	133	296	215	242
45	72	96	78	95	89	90	83	108	57	94	81	73
46	32	37	40	36	48	41	71	NQ	NQ	42	57	NQ
52	769	822	910	861	911	770	1069	1012	866	733	1083	1025
49	471	513	552	542	579	486	734	674	547	459	669	659
47,48	425	453	496	474	517	420	586	578	456	399	583	644
44	91	141	112	156	107	163	169	172	115	133	160	95
37,42	188	228	226	248	208	246	291	270	310	197	287	132
41,64,71	321	481	377	529	378	531	488	667	344	522	441	424
40	50	73	61	81	60	80	82	81	58	78	64	55
100	40	36	42	40	36	32	44	34	34	44	44	43
63	34	22	44	34	36	30	82	ND	56	18	43	45
74	108	120	196	222	159	155	226	166	176	124	150	125
70,76	131	140	155	167	149	136	215	141	187	97	156	136
66,95	557	734	656	802	577	733	847	643	338	739	745	616
91	76	101	80	133	94	100	111	122	84	97	101	109
56,60,92,84	278	379	348	408	346	384	465	465	102	375	348	398
89	139	226	174	455	182	214	205	269	153	210	195	192
101	63	91	79	ND	79	90	110	117	69	92	94	95
99	39	58	48	48	51	46	57	57	52	41	51	50
119	NQ	24	NQ	31	NQ	36	NQ	53	NQ	39	NQ	NQ
83	7	11	11	12	10	11	13	13	9	11	8	8
87	NQ	45	NQ	43	NQ	39	NQ	57	NQ	49	NQ	NQ
81, 87	NQ	NQ	NQ	NQ	NQ	NQ	NQ	NQ	NQ	NQ	NQ	NQ
85	17	25	25	24	21	25	39	33	15	25	21	29
136	25	39	30	39	29	43	37	46	26	40	30	34
77,110	159	223	204	224	200	233	219	231	187	205	208	185
82, 151	14	21	16	22	13	22	18	25	17	21	15	22
135,144	ND	NQ	NQ	NQ	NQ	NQ	NQ	NQ	NQ	NQ	NQ	NQ
167	107	12	13	19	12	13	18	13	34	16	25	39
123,149	79	128	90	134	99	145	125	164	116	140	116	128
118	50	50	49	50	55	68	114	49	70	43	54	61
134	NQ	NQ	NQ	NQ	NQ	NQ	NQ	333	NQ	NQ	NQ	NQ
146	47	105	NQ	126	NQ	171	NQ	251	NQ	180	NQ	NQ
132,153,105	NQ	NQ	NQ	NQ	NQ	NQ	NQ	NQ	NQ	NQ	NQ	NQ
141	9	17	ND	22	15	22	13	26	17	24	8	54
137,130,176	NQ	NQ	ND	NQ	NQ	NQ	NQ	NQ	NQ	NQ	NQ	NQ
163,138	182	187	186	179	186	195	207	220	143	185	187	208
158	NQ	NQ	NQ	NQ	NQ	NQ	NQ	NQ	NQ	NQ	NQ	NQ
129,178	56	39	60	59	63	66	61	119	45	74	45	53
187,182	87	111	93	114	97	116	118	153	89	118	97	139
183	ND	21	18	20	114	25	100	89	14	27	16	23
128	12	15	17	19	12	9	18	17	10	16	21	ND
185	5	5	4	6	ND	ND	ND	14	4	5	ND	ND
174	21	49	21	41	NQ	38	NQ	48	25	51	NQ	NQ
177	36	35	33	38	38	37	39	43	28	43	35	54
202,171,156	21	30	24	32	32	36	56	21	29	28	23	44
157,200	ND	22	ND	10	ND	ND	45	ND	ND	12	ND	ND
172	ND	13	ND	9	ND	ND	ND	39	ND	12	ND	ND
197	ND	ND	ND	3	ND	ND	ND	ND	4	ND	ND	ND
180	51	51	48	53	52	47	81	54	49	49	56	56
193	NQ	NQ	ND	NQ	NQ	NQ	ND	NQ	NQ	NQ	NQ	NQ
191	ND	3	ND	ND	13	ND	16	ND	ND	5	ND	18
199	ND	71	NQ	32	NQ	33	ND	145	NQ	NQ	154	NQ
170,190	56	52	62	51	57	48	44	42	50	51	44	67
198	ND	ND	ND	ND	ND	ND	ND	ND	ND	ND	ND	ND
201	46	60	58	53	71	54	64	57	62	50	65	75
203,196	48	64	57	62	77	71	86	95	60	68	75	79
189	ND	ND	ND	ND	ND	ND	19	ND	ND	ND	ND	ND
208,195	61	45	47	49	37	57	110	51	57	46	44	59
207	ND	NQ	NQ	NQ	NQ	NQ	ND	NQ	ND	NQ	ND	ND
194	NQ	NQ	NQ	NQ	NQ	NQ	NQ	NQ	NQ	NQ	NQ	NQ
205	ND	ND	ND	ND	NQ	NQ	NQ	NQ	NQ	NQ	NQ	NQ
206	NQ	NQ	NQ	NQ	NQ	NQ	NQ	NQ	NQ	NQ	NQ	NQ
209	NQ	ND	NQ	NQ	NQ	NQ	NQ	NQ	NQ	NQ	NQ	NQ
total (ng/g)	11164	13422	13200	14200	12773	13063	16124	16383	11037	12389	14446	13366
total (ug/g)	11.2	13.4	13.2	14.2	12.8	13.1	16.1	16.4	11.0	12.4	14.4	13.4

ND = not detected
NQ = not quantifiable

Table D-2: Tank B particulate PCBs (ng/g)

Resuspension event 1

elapsed time (hours)	0.00	0.25	0.25	0.75	1.25	1.25	1.90	2.92	3.90	4.90
sample volume (m)	150	150	150	150	150	150	150	150	150	150
TSS (mg/L)	3	54	54	65	64	64	64	64	65	73
% recovery 14	77	80	91	89	81	90	82	74	82	91
% recovery 65	69	84	95	90	85	88	87	79	88	103
% recovery 166	77	85	103	100	93	91	94	88	89	95

congener	conc (ng/g)	conc (ng/g)	conc (ng/g)	conc (ng/g)	conc (ng/g)	conc (ng/g)	conc (ng/g)	conc (ng/g)	conc (ng/g)	conc (ng/g)
4,10	NQ	406	559	479	535	621	542	502	329	409
7,9	NQ	67	78	59	83	37	87	61	46	73
6	ND	134	213	154	206	112	211	167	141	163
8,5	NQ	1801	2576	1866	2444	1815	2282	1995	1847	1976
19	NQ	369	473	398	466	520	468	452	314	401
12,13	ND	34	35	30	48	ND	69	53	34	41
18	ND	445	543	427	555	370	578	459	357	507
17	ND	517	650	519	657	538	671	583	501	610
24	436	232	295	232	289	841	300	262	216	270
16,32	NQ	657	864	677	847	745	842	739	646	760
29	NQ	NQ	NQ	NQ	NQ	NQ	NQ	NQ	NQ	NQ
26	NQ	551	662	515	667	814	660	677	616	688
25	ND	143	191	147	194	167	182	192	183	186
31, 28	ND	2209	2666	2059	2736	3221	2594	2773	2579	2729
33,21,53	NQ	864	1115	868	1104	948	1167	1010	862	1154
51	ND	145	183	140	181	330	193	177	143	201
22	ND	194	232	169	247	322	280	268	272	268
45	ND	120	157	128	163	133	177	134	96	141
46	NQ	49	78	69	75	38	81	65	39	55
52	432	1090	1221	961	1184	1350	1194	1228	1127	1307
49	NQ	607	764	548	665	777	672	692	643	721
47,48	ND	492	585	459	563	647	ND	578	537	605
44	ND	97	100	91	122	101	121	103	112	117
37,42	ND	211	269	211	295	231	283	276	255	257
41,64,71	NQ	424	507	388	501	494	497	476	446	510
40	ND	102	79	106	86	97	99	94	84	107
100	ND	ND	ND	50	ND	ND	ND	ND	ND	ND
63	ND	46	61	53	53	67	48	53	31	36
74	NQ	120	162	121	152	141	140	148	117	119
70,76	ND	112	148	125	149	134	150	153	130	122
66,95	NQ	830	942	720	932	943	922	919	840	984
91	74	112	128	96	128	210	126	131	127	141
56,69,92,84	NQ	308	401	297	403	428	401	418	423	420
89	194	204	242	187	238	292	251	242	233	265
101	251	73	91	73	88	91	91	96	85	85
99	ND	37	44	34	41	50	47	46	47	44
119	NQ	18	20	15	18	21	20	14	14	15
83	ND	10	11	8	11	11	11	10	11	11
97	NQ	10	NQ	NQ	NQ	NQ	NQ	NQ	11	8
81, 87	ND	ND	ND	ND	ND	ND	ND	ND	ND	ND
85	ND	19	19	15	23	31	22	24	22	21
136	ND	ND	ND	32	44	51	ND	44	41	46
77,110	102	226	298	213	287	339	271	294	330	285
82, 151	22	20	23	17	22	27	23	24	25	24
136,144	50	48	55	39	53	73	56	58	63	59
107	ND	16	22	15	19	25	21	22	23	20
123,149	75	102	115	87	115	131	113	123	127	123
118	NQ	51	75	45	67	58	73	82	76	72
134	NQ	10	10	8	9	18	10	5	NQ	7
146	NQ	77	78	63	79	62	81	64	71	81
132, 153, 105	NQ	NQ	NQ	NQ	NQ	NQ	NQ	NQ	NQ	NQ
141	NQ	14	11	12	11	13	17	12	14	13
137, 130, 176	NQ	NQ	NQ	NQ	NQ	NQ	NQ	NQ	NQ	NQ
163, 138	265	215	256	204	267	258	255	263	222	247
158	NQ	ND	ND	ND	ND	ND	ND	ND	ND	ND
129, 178	ND	49	59	40	55	60	66	53	56	62
187, 182	ND	109	119	92	114	122	129	126	108	129
183	ND	27	28	23	29	28	33	28	22	27
128	ND	11	15	8	19	24	15	7	17	17
185	ND	ND	5	ND	5	ND	ND	4	5	6
174	NQ	28	27	21	27	23	34	29	34	32
177	83	42	50	39	53	44	48	52	46	47
202, 171, 156	ND	29	38	27	32	29	39	38	34	32
157, 200	ND	14	15	9	11	16	10	12	12	15
172	ND	14	15	9	13	26	12	21	ND	ND
197	ND	ND	ND	ND	ND	ND	ND	7	ND	ND
180	45	65	70	63	75	63	71	79	63	68
193	NQ	NQ	NQ	NQ	NQ	NQ	NQ	NQ	NQ	NQ
191	ND	ND	ND	NQ	NQ	ND	ND	NQ	ND	ND
199	NQ	NQ	NQ	NQ	NQ	NQ	NQ	NQ	NQ	NQ
170,190	NQ	NQ	NQ	NQ	NQ	NQ	NQ	NQ	NQ	NQ
198	ND	ND	ND	ND	ND	ND	ND	4	ND	ND
203,196	ND	72	90	78	90	82	100	98	84	76
189	136	78	88	77	92	84	57	95	81	85
208,195	ND	62	64	56	76	63	63	76	73	66
207	ND	ND	7	6	ND	ND	ND	7	ND	ND
194	ND	NQ	NQ	NQ	NQ	NQ	NQ	NQ	NQ	NQ
205	ND	ND	ND	ND	ND	ND	ND	ND	ND	ND
206	ND	52	72	63	78	50	66	77	57	58
209	NQ	11	9	8	9	8	10	8	8	11
total (ng/g)	2154	15285	19099	14822	18915	19453	18156	18103	16226	18236
total (ug/g)	2.2	15.3	19.1	14.8	18.9	19.5	18.2	18.1	16.2	18.2

ND= not detected
NQ = not quantifiable

Table D-2: Tank B particulate PCBs (ng/g)

Resuspension event 1

elapsed time (hours)	5.92	24.83	28.82	47.67	52.82	52.82	OFF	OFF
sample volume (ml)	150	150	150	150	150	150	150	150
TSS (mg/L)	73	63	76	81	75	75	6	6
% recovery 14	61	50	71	79	73	74	78	95
% recovery 65	64	72	79	85	84	79	84	91
% recovery 166	70	76	88	90	91	88	96	94
congener	conc (ng/g)	conc (ng/g)	conc (ng/g)	conc (ng/g)	conc (ng/g)	conc (ng/g)	conc (ng/g)	conc (ng/g)
4,10	339	156	454	407	609	486	1510	1680
7,9	47	13	68	65	73	62	325	292
6	109	29	165	133	201	174	558	523
8,5	1413	445	1997	1610	1192	1188	7888	7360
19	356	217	491	432	442	472	759	735
12,13	29	4	44	33	52	41	20	35
18	365	186	523	467	595	488	1564	1596
17	458	188	668	540	666	659	1631	1445
24	232	140	325	269	345	353	492	730
16,32	665	377	908	762	997	1005	2086	1739
29	NQ	NQ	NQ	NQ	NQ	NQ	NQ	NQ
26	576	309	837	606	757	917	2570	2522
25	156	74	231	166	213	243	490	420
31, 23	2223	1059	3264	2411	3099	3237	7865	7426
33,21,53	862	582	1331	1026	1445	1360	3312	3022
51	160	109	238	183	246	242	379	474
22	226	110	332	259	330	345	210	350
45	110	59	163	144	197	171	190	200
46	42	25	59	56	90	56	48	88
52	1072	732	1532	1204	1444	1685	2763	2199
49	602	401	838	667	797	826	1170	2043
47,48	500	306	724	550	668	774	976	945
44	100	53	142	115	135	146	602	674
37,42	218	98	313	242	328	330	885	840
41,64,71	406	255	604	454	586	628	842	685
40	85	53	125	101	138	75	117	117
100	ND	ND	ND	ND	ND	ND	ND	ND
63	48	27	47	48	52	63	430	470
74	105	56	144	127	155	165	285	297
70,75	95	46	151	124	152	157	87	109
66,95	753	490	1153	914	1075	1194	2377	2870
91	115	75	172	125	148	183	156	327
56,60,92,84	367	215	531	389	464	580	1553	1561
89	218	135	324	244	287	344	403	445
101	71	46	110	78	105	118	209	157
99	40	25	59	40	52	64	52	151
119	14	NQ	18	15	15	19	135	NQ
83	12	6	17	12	11	17	ND	10
97	12	NQ	18	14	8	17	NQ	9
81, 87	ND	ND	ND	ND	ND	ND	ND	ND
85	19	12	33	18	26	34	39	30
136	37	24	59	43	62	58	62	103
77,110	246	131	363	243	319	367	208	400
82, 151	21	13	31	21	28	35	31	38
135,144	52	33	78	51	67	86	70	107
107	18	11	27	17	25	28	23	42
123,149	109	70	163	112	139	168	157	184
118	49	30	89	54	82	91	NQ	NQ
134	5	NQ	6	9	8	5	97	ND
146	68	57	92	79	73	92	300	397
132, 153, 105	NQ	NQ	NQ	NQ	NQ	NQ	NQ	NQ
141	11	NQ	21	16	12	23	NQ	NQ
137, 130, 176	NQ	NQ	NQ	NQ	NQ	NQ	NQ	NQ
163, 138	196	114	311	229	295	341	490	390
158	ND	ND	ND	ND	ND	ND	ND	ND
129, 178	49	30	76	54	64	83	111	99
187, 182	98	69	156	104	141	163	232	327
183	21	11	33	25	25	37	ND	ND
128	10	8	25	17	14	25	30	40
185	5	2	5	4	4	10	ND	ND
174	30	16	47	33	30	50	NQ	ND
177	44	23	120	45	60	69	74	120
202, 171, 156	30	15	ND	34	39	49	NQ	ND
157, 200	11	6	14	12	13	19	ND	ND
172	13	ND	17	13	14	23	ND	ND
197	ND	ND	ND	ND	ND	ND	ND	ND
180	58	33	86	63	84	95	98	83
193	NQ	NQ	NQ	NQ	NQ	NQ	NQ	ND
191	ND	ND	ND	ND	NQ	ND	ND	ND
199	NQ	NQ	NQ	NQ	NQ	NQ	NQ	NQ
170,190	NQ	NQ	NQ	NQ	NQ	NQ	NQ	NQ
198	ND	1	ND	ND	ND	ND	ND	ND
201	64	45	106	78	106	112	136	162
203,196	72	40	109	73	103	122	163	285
189	ND	ND	ND	ND	ND	ND	ND	ND
208,195	52	30	91	57	93	93	70	60
207	ND	ND	ND	ND	ND	11	ND	ND
194	NQ	NQ	NQ	NQ	NQ	NQ	ND	ND
205	ND	ND	ND	ND	ND	ND	ND	ND
206	54	27	74	103	87	81	34	10
209	6	NQ	9	27	11	11	5	12
total (ng/g)	14640	7974	21360	16668	20168	21334	46780	47541
total (ug/g)	14.6	8.0	21.4	16.7	20.2	21.3	46.8	47.5

ND= not detected
NQ = not quantifiable

Table D-2: Tank B particulate PCBs (ng/g)

Settling after resuspension event 3

elapsed time (min.)	before	3	8	20	20	60	120	1160
sample volume (ml)	100	100	150	150	150	150	300	300
TSS (mg/L)	63	47.5	32	17	17	9.5	6.8	2.5
% recovery 14	78	83	76	81	73	81	83	81
% recovery 65	86	88	80	84	79	84	86	89
% recovery 166	84	82	76	90	85	88	91	86
congener	conc (ng/g)	conc (ng/g)	conc (ng/g)	conc (ng/g)	conc (ng/g)	conc (ng/g)	conc (ng/g)	conc (ng/g)
4,10	556	477	497	692	667	500	589	690
7,9	75	43	44	124	111	77	84	161
6	231	208	155	257	233	195	220	276
8,5	2208	2627	2189	3646	3385	3392	3152	5053
19	533	514	463	562	569	508	469	720
12,13	ND	45	22	40	53	ND	27	44
18	523	455	403	689	687	590	625	886
17	802	757	628	900	942	875	824	1169
24	364	330	295	369	357	335	325	515
16,32	1090	1032	884	1052	1121	1048	944	1666
29	NQ	NQ	NQ	NQ	NQ	NQ	NQ	NQ
26	960	961	858	875	854	839	875	960
25	276	300	255	291	265	281	312	324
31, 28	3963	4134	3288	3567	3527	3249	3056	3297
33,21,53	1609	1612	1188	1440	1483	1350	1306	1923
51	265	259	220	225	229	239	221	280
22	ND	514	329	363	336	NQ	471	NQ
45	ND	159	125	213	212	174	171	262
46	67	70	51	117	118	107	124	240
52	1861	2088	1628	1835	1912	2141	1842	2816
49	1030	1155	928	1062	1085	1251	1062	1709
47,48	877	954	818	927	883	992	943	1372
44	ND	200	152	109	156	164	168	229
37,42	594	447	315	353	388	361	350	475
41,64,71	747	774	613	766	766	870	792	1257
40	145	176	111	171	145	162	149	142
100	ND	ND	ND	ND	ND	ND	ND	ND
63	81	80	87	94	96	115	150	69
74	200	289	166	237	261	260	263	521
70,76	193	231	168	190	227	213	222	ND
66,95	1369	1605	1151	1402	1547	1673	1525	2412
91	203	225	180	189	189	236	199	315
56,60,92,84	664	755	565	614	610	754	669	1003
89	377	408	309	376	382	405	377	572
101	132	162	107	149	148	157	150	270
99	70	80	57	56	70	64	70	97
119	20	27	27	NQ	NQ	105	66	NQ
83	20	18	33	14	11	16	34	30
97	NQ	NQ	NQ	NQ	NQ	NQ	NQ	NQ
81, 87	ND	ND	ND	ND	ND	ND	ND	ND
85	33	41	26	ND	26	53	32	83
136	ND	79	ND	ND	ND	78	69	120
77,110	417	492	373	413	412	454	407	669
82, 151	36	47	32	42	38	40	43	55
135,144	85	116	79	94	96	96	80	132
107	ND	42	30	35	ND	32	43	53
123,149	197	230	166	190	205	216	216	314
118	84	120	98	111	123	86	91	127
134	8	NQ	NQ	30	31	39	37	103
146	135	134	96	173	164	318	195	471
132, 153, 105	NQ	NQ	NQ	NQ	NQ	NQ	NQ	NQ
141	25	22	20	NQ	NQ	NQ	NQ	NQ
137, 130, 176	NQ	NQ	NQ	NQ	NQ	NQ	NQ	NQ
163, 138	363	397	283	415	424	456	430	ND
158	NQ	NQ	NQ	NQ	NQ	NQ	NQ	NQ
129, 178	ND	100	ND	104	88	116	88	ND
187,182	174	198	148	222	220	ND	260	390
183	41	32	28	29	39	64	ND	71
128	22	30	18	10	9	37	ND	24
185	ND	ND	ND	ND	4	ND	ND	ND
174	54	60	38	46	48	NQ	105	NQ
177	72	84	72	85	79	87	109	130
202, 171, 156	84	58	41	68	57	63	79	103
157, 200	26	14	ND	ND	19	ND	ND	ND
172	ND	ND	ND	ND	ND	ND	ND	ND
197	ND	ND	ND	ND	4	ND	ND	ND
180	95	113	78	119	121	113	115	158
193	NQ	NQ	ND	NQ	NQ	ND	ND	ND
191	ND	ND	ND	ND	NQ	ND	ND	ND
199	NQ	NQ	NQ	NQ	NQ	NQ	NQ	NQ
170,190	NQ	NQ	NQ	NQ	NQ	NQ	NQ	NQ
198	ND	ND	ND	ND	ND	ND	ND	ND
201	120	145	100	132	155	161	141	264
203,196	130	140	87	128	153	169	198	288
189	ND	ND	ND	ND	ND	ND	ND	ND
208,195	128	111	62	112	121	134	164	211
207	ND	ND	ND	ND	ND	ND	ND	ND
194	NQ	NQ	NQ	NQ	NQ	NQ	NQ	ND
205	ND	ND	ND	ND	ND	ND	ND	ND
206	69	94	61	83	108	81	96	86
209	10	14	ND	NQ	NQ	NQ	NQ	NQ
total (ng/g)	25511	27086	21244	26586	26764	26094	25825	34917
total (ug/g)	25.5	27.1	21.2	26.6	26.8	26.1	25.8	34.9

ND= not detected
NQ = not quantifiable

Table D-3: Tank C particulate PCBs (ng/g)

Resuspension event 1

elapsed time (hours)	0	0.75	1.25	1.75	2.75	2.75	3.75
sample volume (ml)	150	150	150	150	150	150	150
TSS (mg/L)	6.5	46	46	43.5	54.5	54.5	56.5
% recovery 14	75	80	81	101	84	73	84
% recovery 65	81	86	84	86	85	81	88
% recovery 166	85	93	88	85	91	83	91
congener	conc (ng/g)	conc (ng/g)	conc (ng/g)	conc (ng/g)	conc (ng/g)	conc (ng/g)	conc (ng/g)
4,10	NQ	414	365	291	313	298	378
7,9	70	91	85	43	79	60	86
6	142	225	198	104	202	158	232
8,5	NQ	2817	2474	1235	2383	2144	2617
19	200	238	212	147	183	175	216
12,13	ND	41	28	ND	30	27	25
18	375	647	636	364	606	557	647
17	496	775	709	308	675	656	699
24	NQ	194	185	127	172	219	191
16,32	676	867	750	448	726	817	789
29	NQ	NQ	NQ	NQ	NQ	NQ	NQ
26	444	843	709	394	680	728	745
25	176	221	184	88	194	189	192
31, 28	450	2983	2466	1159	2479	2631	2539
33,21,53	115	930	893	502	857	877	915
51	65	118	126	61	116	144	118
22	ND	350	283	101	329	271	315
45	ND	112	100	45	102	98	105
46	NQ	56	58	44	53	45	48
52	620	1181	1104	677	1017	1214	1083
49	442	762	672	431	637	749	672
47,48	NQ	687	597	648	675	680	642
44	ND	170	133	72	160	135	152
37,42	95	339	245	53	312	287	282
41,64,71	NQ	541	462	269	453	486	486
40	ND	96	72	43	72	NQ	76
100	ND	NQ	NQ	NQ	NQ	NQ	NQ
63	ND	42	39	28	36	58	39
74	ND	192	144	77	172	167	175
70,76	ND	232	159	51	182	176	180
66,95	ND	877	745	345	749	797	765
91	72	119	110	66	112	138	117
56, 60/92, 84	NQ	469	398	183	407	414	405
89	145	236	215	110	208	484	218
101	NQ	108	98	50	101	ND	98
99	46	61	58	25	61	58	56
119	NQ	NQ	NQ	NQ	NQ	NQ	NQ
83	ND	21	9	6	ND	21	10
97	NQ	NQ	NQ	NQ	20	22	20
81, 87	NQ	NQ	NQ	NQ	NQ	NQ	NQ
85	40	26	27	15	30	23	21
136	ND	37	35	19	37	35	30
110, 77	249	267	236	132	245	255	216
82, 151	25	22	21	11	21	23	20
135, 144	NQ	NQ	NQ	NQ	NQ	NQ	NQ
107	ND	22	32	11	27	32	40
123, 149	96	126	128	60	119	135	133
118	ND	89	80	29	80	82	83
134	NQ	NQ	NQ	NQ	NQ	NQ	NQ
146	NQ	54	53	NQ	60	69	54
132, 153, 105	NQ	NQ	NQ	NQ	NQ	NQ	NQ
141	ND	16	15	9	20	NQ	12
137, 130, 176	NQ	NQ	NQ	NQ	NQ	NQ	NQ
163, 138	243	229	222	113	211	212	204
158	NQ	NQ	NQ	NQ	NQ	NQ	NQ
129, 178	ND	54	52	31	50	40	43
187, 182	174	107	111	54	106	105	101
183	ND	27	24	14	21	NQ	20
128	ND	25	17	11	24	14	17
185	61	ND	ND	ND	9	ND	2
174	ND	NQ	NQ	NQ	NQ	NQ	NQ
177	94	NQ	NQ	NQ	NQ	NQ	NQ
202, 171, 156	ND	ND	ND	NQ	26	NQ	ND
157, 200	ND	ND	ND	NQ	ND	ND	ND
172	ND	ND	ND	NQ	ND	ND	ND
197	ND	ND	ND	ND	ND	ND	ND
180	ND	ND	59	31	61	65	55
193	188	ND	ND	NQ	NQ	ND	ND
191	90	ND	ND	6	12	ND	ND
199	ND	ND	NQ	NQ	NQ	NQ	NQ
170, 190	NQ	NQ	NQ	NQ	NQ	NQ	NQ
198	ND	ND	ND	ND	ND	ND	ND
201	121	73	64	39	70	72	55
203, 196	ND	69	64	41	81	74	62
189	ND	ND	ND	ND	ND	ND	ND
208, 195	ND	56	ND	NQ	59	NQ	57
207	ND	ND	ND	ND	ND	ND	ND
194	ND	24	NQ	NQ	21	NQ	17
205	ND	ND	ND	ND	ND	ND	ND
206	ND	NQ	NQ	NQ	NQ	NQ	NQ
209	ND	NQ	NQ	NQ	NQ	NQ	NQ
total (ng/g)	6009	19378	16960	9217	16946	17215	17576
total (ug/g)	6.0	19.4	17.0	9.2	16.9	17.2	17.6

ND = not detected
NQ = not quantifiable

Table D-3: Tank C particulate PCBs (ng/g)

Resuspension event 1

elapsed time (hours)	4.75	5.75	23.05	28.73	47.97	52.05	Off
sample volume (ml)	150	150	150	150	150	150	150
TSS (mg/L)	56.5	50	67	71	82	83	11.07
% recovery 14	77	93	79	62	83	81	79
% recovery 65	80	90	88	68	79	87	74
% recovery 166	87	96	92	81	79	91	78
congener	conc (ng/g)	conc (ng/g)	conc (ng/g)	conc (ng/g)	conc (ng/g)	conc (ng/g)	conc (ng/g)
4,10	319	466	369	256	210	243	1334
7,9	86	111	90	60	38	48	251
6	193	258	180	141	101	125	528
8,5	2293	2941	2169	1556	1185	1391	7981
19	206	310	246	186	148	183	803
12,13	25	29	32	21	10	19	35
18	640	882	683	480	299	355	1361
17	741	975	678	540	351	418	1464
24	190	275	203	157	119	133	194
16,32	805	1065	818	625	488	554	2800
29	NQ	NQ	NQ	NQ	NQ	NQ	NQ
26	767	1132	743	610	425	483	2469
25	201	295	180	160	109	132	461
31, 28	2704	3743	2517	2176	1400	1735	7259
33,21,53	925	1306	962	770	564	666	3644
51	125	182	130	103	73	86	397
22	385	418	297	286	127	186	272
45	117	160	119	96	66	79	341
46	52	ND	60	43	34	ND	NQ
52	1105	1696	1106	912	673	856	4186
49	699	984	691	575	412	479	2661
47,48	708	1034	632	534	418	429	1691
44	166	213	151	139	92	107	690
37,42	323	427	264	256	160	192	708
41,64,71	505	675	500	407	299	334	1424
40	96	119	91	75	47	60	140
100	NQ	NQ	NQ	NQ	NQ	NQ	NQ
63	33	38	23	31	23	23	421
74	169	283	157	177	123	152	874
70,76	189	246	164	148	91	122	145
66,95	838	1117	800	658	444	548	2737
91	125	165	115	100	64	78	312
56, 60/92, 84	440	535	404	356	221	283	2213
89	254	314	228	193	122	156	771
101	104	133	96	83	57	68	94
99	57	81	59	47	32	42	149
119	NQ	NQ	NQ	NQ	NQ	NQ	NQ
83	11	17	9	8	5	6	8
97	21	40	23	17	NQ	14	NQ
81, 87	NQ	148	NQ	NQ	NQ	NQ	NQ
85	25	41	30	22	14	16	17
136	41	54	41	33	19	22	31
110, 77	273	342	230	226	126	155	587
82, 151	23	28	22	18	10	14	17
135, 144	NQ	NQ	NQ	NQ	NQ	NQ	NQ
107	15	21	17	12	19	10	19
123, 149	133	150	113	98	71	79	203
118	72	87	61	63	42	50	57
134	NQ	NQ	NQ	NQ	NQ	NQ	NQ
146	51	80	62	50	NQ	49	NQ
132, 153, 105	NQ	NQ	NQ	NQ	NQ	NQ	NQ
141	18	31	29	15	10	10	20
137, 130, 176	NQ	NQ	NQ	NQ	NQ	NQ	NQ
163, 138	245	298	222	200	108	157	407
158	NQ	NQ	NQ	NQ	NQ	NQ	NQ
129, 178	61	81	51	53	30	41	24
187, 182	118	166	113	ND	54	87	NQ
183	29	49	26	25	13	18	ND
128	31	33	24	24	9	14	12
185	ND	ND	ND	ND	ND	ND	ND
174	NQ	NQ	NQ	NQ	NQ	NQ	NQ
177	NQ	NQ	NQ	NQ	NQ	NQ	NQ
202, 171, 156	NQ	44	NQ	NQ	NQ	ND	NQ
157, 200	ND	ND	ND	ND	NQ	ND	ND
172	ND	ND	ND	ND	NQ	ND	ND
197	ND	ND	ND	ND	ND	ND	ND
180	65	76	62	57	31	47	148
193	ND	ND	ND	ND	NQ	ND	ND
191	ND	ND	ND	ND	3	ND	ND
199	NQ	NQ	ND	NQ	NQ	ND	NQ
170, 190	NQ	NQ	NQ	NQ	NQ	NQ	NQ
198	ND	ND	ND	ND	ND	ND	ND
201	84	84	60	65	34	60	168
203, 196	81	106	86	67	31	58	178
189	ND	ND	ND	ND	ND	ND	ND
208, 195	NQ	80	ND	NQ	25	ND	NQ
207	ND	ND	ND	ND	ND	ND	ND
194	26	36	16	22	NQ	18	ND
205	ND	ND	ND	ND	ND	ND	ND
206	NQ	NQ	NQ	NQ	NQ	NQ	ND
209	NQ	ND	ND	NQ	NQ	NQ	NQ
total (ng/g)	18008	24697	17252	14030	9674	11691	52704
total (ug/g)	18.0	24.7	17.3	14.0	9.7	11.7	52.7

ND = not detected
NQ = not quantifiable

Table D-3: Tank C particulate PCBs (ng/g)

Settling after resuspension event 3

elapsed time (min.)	before	3	8	8	20	60	120	1136
sample volume (ml)	150	150	150	150	200	300	400	300
TSS (mg/L)	59.5	48	34	34	26.5	15	10.5	5
% recovery 14	62	87	85	90	101	87	84	85
% recovery 65	74	84	85	84	91	86	88	86
% recovery 166	83	85	87	86	91	81	89	87
congener	conc (ng/g)	conc (ng/g)	conc (ng/g)	conc (ng/g)	conc (ng/g)	conc (ng/g)	conc (ng/g)	conc (ng/g)
4,10	173	302	300	273	231	314	NQ	NQ
7,9	32	57	53	46	38	55	42	NQ
6	95	163	148	155	101	151	139	124
8,5	1288	2022	2029	1982	1583	2048	1940	NQ
19	120	182	176	164	132	177	130	179
12,13	16	24	18	11	11	13	19	ND
18	284	394	389	424	323	367	369	396
17	424	556	572	614	462	554	559	537
24	136	142	131	207	179	134	143	192
16,32	570	655	622	689	627	639	583	833
29	NQ	NQ	NQ	NQ	NQ	NQ	NQ	NQ
26	497	585	605	608	535	570	593	488
25	143	167	194	234	158	184	190	186
31, 28	1745	2138	2301	2593	1856	2134	2017	359
33,21,53	650	741	701	879	655	675	655	NQ
51	110	98	97	138	98	83	106	102
22	212	241	289	293	178	193	261	300
45	74	79	80	80	50	70	59	49
46	40	50	47	61	NQ	48	47	NQ
52	890	949	1003	1224	979	1016	1071	1037
49	563	598	659	796	617	640	688	734
47,48	534	572	588	622	923	652	691	898
44	110	149	145	159	114	131	138	120
37,42	217	271	281	304	214	246	305	225
41,64,71	389	426	418	519	385	417	443	551
40	NQ	78	69	NQ	NQ	64	NQ	NQ
100	NQ	NQ	NQ	NQ	NQ	NQ	NQ	NQ
63	46	38	41	61	80	44	130	NQ
74	137	210	177	243	150	163	226	197
70,76	152	183	187	220	137	180	248	179
66,95	632	705	727	847	639	718	789	842
91	105	99	102	143	97	99	122	129
56,60/92,84	332	361	376	435	336	365	409	NQ
89	180	186	188	236	177	186	200	214
101	77	87	96	105	75	88	95	121
99	46	50	49	62	56	50	64	53
119	NQ	NQ	NQ	NQ	NQ	NQ	NQ	NQ
83	8	9	9	12	6	6	12	12
97	NQ	NQ	NQ	NQ	NQ	NQ	NQ	NQ
81, 87	NQ	NQ	NQ	NQ	NQ	NQ	NQ	NQ
85	22	19	24	27	19	19	24	23
136	27	29	30	39	24	30	33	39
77,110	192	205	220	256	186	220	244	228
82, 151	16	ND	ND	21	16	ND	21	23
135,144	NQ	NQ	NQ	NQ	NQ	NQ	NQ	NQ
107	20	32	14	30	18	41	24	26
123,149	96	121	97	125	96	133	117	133
118	63	66	64	76	55	77	74	77
134	NQ	NQ	NQ	NQ	NQ	NQ	NQ	NQ
146	44	51	NQ	NQ	NQ	NQ	90	NQ
132,153,105	NQ	NQ	NQ	NQ	NQ	NQ	NQ	NQ
141	NQ	17	81	NQ	NQ	13	NQ	NQ
137,130,176	NQ	NQ	NQ	NQ	NQ	NQ	NQ	NQ
163,138	312	187	220	221	158	186	217	213
158	NQ	NQ	NQ	NQ	NQ	NQ	NQ	NQ
129,178	33	41	42	44	26	43	41	48
187,182	83	91	98	113	78	92	123	170
183	NQ	20	29	NQ	NQ	18	NQ	ND
128	11	18	21	16	NQ	14	NQ	ND
185	ND	ND	ND	ND	ND	ND	ND	ND
174	20	26	27	30	NQ	27	32	NQ
177	30	39	40	39	24	56	47	NQ
202,171,156	24	24	ND	40	NQ	39	31	NQ
157,200	ND	ND	ND	ND	ND	ND	ND	ND
172	ND	9	ND	ND	ND	12	ND	ND
197	ND	ND	ND	ND	ND	ND	ND	ND
180	45	49	56	62	39	54	66	61
193	ND	ND	NQ	ND	NQ	NQ	NQ	ND
191	ND	ND	ND	ND	ND	ND	ND	ND
199	NQ	NQ	NQ	NQ	NQ	NQ	NQ	NQ
170,190	NQ	NQ	NQ	NQ	NQ	NQ	NQ	NQ
198	ND	ND	ND	ND	ND	ND	ND	ND
201	48	60	73	79	46	63	68	83
203,196	54	76	66	70	43	52	75	97
189	ND	ND	ND	ND	ND	ND	ND	ND
208,195	37	33	ND	70	39	51	65	ND
207	ND	ND	ND	ND	ND	ND	ND	ND
194	NQ	NQ	ND	NQ	NQ	NQ	NQ	ND
205	ND	NQ	ND	ND	ND	ND	ND	ND
206	NQ	NQ	ND	NQ	NQ	ND	NQ	NQ
209	NQ	NQ	ND	NQ	NQ	ND	NQ	NQ
total (ng/g)	12203	14783	15069	16795	13066	14712	14873	10279
total (ug/g)	12.20	14.78	15.07	16.79	13.07	14.71	14.87	10.28

ND = not detected
NQ = not quantifiable

Appendix E: Sediment PCB data

Table E-1: Sediment PCB concentrations (ng/g)

	Tank A R1	Tank A R2	Tank A R3	Tank B R1	Tank B R2	Tank B R3	Tank C R1	Tank C R2	Tank 4 R1	Tank 4 R2
% water	74	76	75	68	68	68	62	60	76	77
% 14 recovered	88	77	81	97	68	70	90	90	69	73
% 65 recovered	84	93	85	89	95	80	89	89	79	87
% 166 recovered	85	85	88	91	74	82	93	93	79	79
congener	ng/g dry	ng/g dry	ng/g dry	ng/g dry	ng/g dry	ng/g dry	ng/g dry	ng/g dry	ng/g dry	ng/g dry
4,10	275	320	211	210	219	276	136	110	358	270
7,9	45	85	66	38	45	41	26	21	40	41
6	122	151	153	180	92	126	66	53	87	73
8,5	1723	1726	1700	1266	1379	1325	1004	958	949	1003
19	129	146	137	109	107	108	164	154	176	129
12,13	18	31	32	ND	22	26	12	10	ND	13
18	299	445	387	311	259	245	164	132	264	254
17	450	752	404	454	747	451	243	205	366	477
24	40	144	97	35	112	80	22	18	48	124
16,32	363	544	506	387	438	448	190	153	294	387
29	1	2	4	1	NQ	3	NQ	NQ	2	NQ
26	710	649	483	705	529	539	408	328	624	478
25	195	165	100	260	157	113	105	84	145	104
31,28	2484	2033	2318	2625	2643	2411	1440	1559	2010	1998
33,21,53	570	614	449	583	475	567	338	272	505	449
51	87	90	88	78	70	70	42	34	83	75
22	266	361	219	426	339	284	175	141	232	239
45	44	92	61	41	50	44	25	20	51	54
46	13	21	27	13	18	22	7	6	12	12
52	763	733	675	710	606	702	415	334	695	580
49	447	444	415	409	349	337	221	178	384	357
47,48	281	393	306	229	304	255	136	109	244	330
44	83	81	75	157	74	74	55	44	87	77
37,42	248	210	193	254	163	164	147	119	231	158
41,64,71	243	329	277	234	270	243	128	103	230	298
40	54	96	50	64	108	48	27	22	53	85
100	NQ	NQ	NQ	NQ	NQ	23	NQ	13	NQ	NQ
63	28	17	16	24	14	18	16	13	29	15
74	132	104	100	110	73	82	75	60	122	97
70,76	135	86	99	171	88	117	101	82	147	76
66,95	391	476	429	421	424	410	224	181	393	410
91	94	79	60	88	72	57	50	40	85	67
56,60,92,84	310	266	296	360	262	273	210	169	351	249
89	115	162	126	117	138	111	62	50	116	132
101	47	60	49	49	53	44	24	19	46	55
99	41	42	37	34	33	28	16	13	36	37
119	1	6	2	1	3	2	0	0	1	3
83	6	8	8	8	5	7	4	3	8	7
97	3	NQ	5	5	NQ	4	3	2	5	NQ
81,87	10	52	14	11	29	16	8	6	10	39
85	18	17	14	19	16	14	12	10	ND	17
136	13	26	18	15	25	18	8	7	20	21
77,110	212	186	168	261	167	182	125	100	223	170
82,151	13	16	12	15	17	11	8	7	15	14
135,144	28	NQ	29	30	NQ	26	16	13	32	NQ
107	12	12	12	12	10	6	5	5	12	9
123,149	66	91	70	62	75	57	31	25	62	72
118	68	57	58	66	52	48	36	29	69	49
134	0	7	2	3	16	1	0	0	0	NQ
146	11	34	22	11	26	20	6	5	14	25
132,153,105	78	141	127	78	88	110	48	39	83	105
141	6	11	9	6	5	8	4	3	9	8
137,130,176	7	14	8	6	11	9	4	3	7	11
163,138	115	134	110	119	118	120	65	53	115	116
158	NQ	NQ	5	NQ	NQ	2	NQ	NQ	NQ	NQ
129,178	21	36	21	24	33	25	12	10	22	29
187,182	53	66	67	50	52	71	32	26	49	52
183	11	16	16	10	10	13	6	5	11	11
128	12	13	7	9	10	7	5	4	7	11
185	2	3	2	3	4	3	ND	ND	2	2
174	12	23	21	12	14	18	7	6	12	14
177	26	26	27	25	25	30	12	10	26	24
202,171,156	15	20	18	16	21	19	9	7	15	18
157,200	7	9	8	8	9	8	6	5	7	7
172	8	9	11	10	8	9	7	6	8	7
197	ND	ND	ND	ND	ND	ND	ND	ND	ND	NQ
180	35	41	44	32	30	40	18	15	34	33
193	3	4	5	3	ND	5	ND	ND	3	4
191	ND	4	3	ND	ND	ND	ND	ND	ND	NQ
199	NQ	2	4	NQ	2	4	NQ	NQ	NQ	2
170,190	38	40	43	35	33	44	20	16	35	33
198	ND	ND	ND	ND	ND	3	ND	ND	ND	ND
201	40	43	51	40	45	56	20	16	37	43
203,196	40	45	50	41	46	53	24	19	44	43
189	ND	ND	ND	ND	ND	ND	ND	ND	ND	ND
208,195	35	36	37	37	40	46	20	16	38	40
207	ND	ND	5	ND	4	6	ND	ND	ND	3
194	17	16	16	22	17	20	10	8	20	16
205	ND	7	ND	ND	ND	ND	ND	ND	ND	ND
206	30	29	34	39	37	40	18	14	33	33
209	NQ	NQ	NQ	NQ	NQ	NQ	NQ	NQ	NQ	NQ
total (ng/g)	12320	13250	11828	12298	11837	11350	7086	6297	10584	10293
total (ug/g)	12.3	13.3	11.8	12.3	11.8	11.4	7.1	6.1	10.6	10.3

ND = not detected
NQ = not quantifiable

Appendix F: Matlab Code for the Radial Diffusion Model

```
clear
%program to calculate Deff and plot the radial diffusion model as c(t)/c steady state

%molecular diffusion coefficient of compound in water [cm2/s] PCB 18
Dm=5.7e-6;
%partitioning coefficient [cm3/g]
Kd=5e4;
%porosity of the floc
n=0.92;
%dry solids density ps [g/cm3]
ps=2.27;
%Deff is the effective intraparticle diffusivity
Deff=(Dm*n^2)/((1-n)*ps*Kd+n)*60*60;
%change in diameter as a function of resuspension time (till steady state is
%reached)
syms x y k diam diamln rad
diamln=(-0.022*x)+ 4.9281;
diam=exp(diamln);
rad=(diam/2)*10^-4;
%Crank's solution for the radial diffusion model
y=(1-0.60792*symsum(1/k^2*exp(-((Deff*k^2*pi^2*x)/(rad)^2)),k,1,1000));
ezplot(y,[0,9.5]);
hold on;
%radius is constant at steady state
rad=0.0056;
%Crank's solution for the radial diffusion model
y=(1-0.60792*symsum(1/k^2*exp(-((Deff*k^2*pi^2*x)/(rad)^2)),k,1,1000));
ezplot(y,[9,30]);
hold on;
title ('Tank A Event 1: PCB 18')
xlabel ('resuspension time in hours')
hold on;
```

References

- Accardi-Dey, A. and Gschwend, P.M., 2003. Reinterpreting literature sorption data considering both absorption into organic carbon and adsorption onto black carbon. *Environ. Sci. Technol.*, 37(1): 99-106.
- Achman, D.R., Brownawell, B.J. and Zhang, L.C., 1996. Exchange of polychlorinated biphenyls between sediment and water in the Hudson River Estuary. *Estuaries*, 19(4): 950-965.
- Alkhatib, E. and Weigand, C., 2002. Parameters affecting partitioning of 6 PCB congeners in natural sediments. *Environ. Monit. Assess.*, 78(1): 1-17.
- Allen-King R.M., Grathwohl, P. and Ball, W.P. 2002. New modeling paradigms for the sorption of hydrophobic organic chemicals to heterogeneous carbonaceous matter in soils, sediments, rocks. *Adv. Water Res.*, 25: 985-1016.
- Aochi, Y.O. and Farmer, W.J., 1997. Role of microstructural properties in the time dependent sorption/desorption behavior of 1,2-dichloroethane on humic substances. *Environ. Sci. Technol.*, 31(9): 2520-2526.
- Arthur, C.L. and Pawliszyn, J., 1990. Solid-phase microextraction with thermal-desorption using fused-silica optical fibers. *Anal. Chem.*, 62(19): 2145-2148.
- Baker, J.E., Eisenreich, S.J. and Eadie, B.J., 1991. Sediment Trap Fluxes and Benthic Recycling of Organic-Carbon, Polycyclic Aromatic-Hydrocarbons, and Polychlorobiphenyl Congeners in Lake-Superior. *Environ. Sci. Technol.*, 25(3): 500-509.
- Baker, J.E. et al., 2001. *PCBs in the Upper Hudson River: The Science Behind the Dredging Controversy*. Hudson River Foundation. October.
- Ball W.P. and Roberts P.V. 1991. Long term sorption of halogenated organic chemicals by aquifer material 2. Intraparticle diffusion. *Environ. Sci. Technol.* 25(7): 1237-1249.
- Baltussen, E., Sandra, P., David, F., Janssen, H.G. and Cramers, C., 1999. Study into the equilibrium mechanism between water and poly(dimethylsiloxane) for very apolar solutes: Adsorption or sorption? *Anal. Chem.*, 71(22): 5213-5216.
- Bamford, H.A., Ko, F.C. and Baker, J.E., 2002. Seasonal and annual air-water exchange of polychlorinated biphenyls across Baltimore Harbor and the northern Chesapeake Bay. *Environ. Sci. Technol.* 36(20): 4245-4252.
- Bamford, H.A., Ko, F.C. and Baker, J.E., 2002. Seasonal and annual air-water exchange of polychlorinated biphenyls across Baltimore Harbor and the northern Chesapeake Bay. *Environ. Sci. Technol.*, 36(20): 4245-4252.

- Bamford, H.A., Offenberg, J.H., Larsen, R.K., Ko, F.C. and Baker, J.E., 1999. Diffusive exchange of polycyclic aromatic hydrocarbons across the air-water interface of the Patapsco River, an urbanized subestuary of the Chesapeake Bay. *Environ. Sci. Technol.*, 33(13): 2138-2144.
- Borglin, S., Wilke, A., Jepsen, R. and Lick, W., 1996. Parameters affecting the desorption of hydrophobic organic chemicals from suspended sediments. *Environ. Toxicol. Chem.*, 15(12): 2254-2262.
- Brusseau, M.L., 1991. Cooperative Sorption of Organic-Chemicals in Systems Composed of Low Organic-Carbon Aquifer Materials. *Environ. Sci. Technol.*, 25(10): 1747-1752.
- Brusseau, M.L., Jessup, R.E. and Rao, P.S.C., 1991. Nonequilibrium Sorption of Organic-Chemicals - Elucidation of Rate-Limiting Processes. *Environ. Sci. Technol.*, 25(1): 134-142.
- Burban, P.Y., Xu, Y.J., McNeil, J. and Lick, W., 1990. Settling Speeds of Floccs in Fresh-Water and Seawater. *J. Geophys. Res.-Oceans*, 95(C10): 18213-18220.
- Butcher, J.B., Garvey, E.A. and Bierman, V.J., 1998. Equilibrium partitioning of PCB congeners in the water column: Field measurements from the Hudson River. *Chemosphere*, 36(15): 3149-3166.
- Cardoso, V.V., Rodrigues, A., Correia, J. and Benoliel, M.J., 2000. Application of SPME in the analysis of polynuclear aromatic hydrocarbons in water by HPLC with DAD detection. *Polycycl. Aromat. Comp.*, 19(1-4): 227-239.
- Carroll, K.M., Harkness, M.R., Bracco, A.A. and Balcarcel, R.R., 1994. Application of a permeant polymer diffusional model to the desorption of Polychlorinated-Biphenyls from Hudson River Sediments. *Environ. Sci. Technol.*, 28(2): 253-258.
- Chai, M. and Pawliszyn, J., 1995. Analysis of environmental air samples by solid-phase microextraction and gas-chromatography ion-trap mass-spectrometry. *Environ. Sci. Technol.*, 29(3): 693-701.
- Chang, M.-L. and Sanford, L.P., 2005. Modeling the effects of tidal resuspension and deposition on early diagenesis of contaminants. *Aquatic Ecosystem Health and Management*, 8(1): 41-51.
- Chapra S.C. 1996. *Surface Water Quality Modeling*. McGraw-Hill Science.
- Cheng, C.Y., Atkinson, J.F. and Depinto, J.V., 1995. Desorption during resuspension events - kinetic v equilibrium model. *Mar. Freshwater Res.*, 46(1): 251-256.
- Connolly, J.P. et al., 2000. A model of PCB fate in the Upper Hudson River. *Environ. Sci. Technol.*, 34(19): 4076-4087.

Cornelissen, G., Elmquist, M., Groth, I. and Gustafsson, O., 2004. Effect of sorbate planarity on environmental black carbon sorption. *Environ. Sci. Technol.*, 38(13): 3574-3580.

Cornelissen, G., Rigterink, H., van Noort, P.C.M. and Govers, H.A.J., 2000. Slowly and very slowly desorbing organic compounds in sediments exhibit Langmuir-type sorption. *Environ. Toxicol. Chem.*, 19(6): 1532-1539.

Cornelissen, G., vanNoort, P.C.M. and Govers, H.A.J., 1997. Desorption kinetics of chlorobenzenes, polycyclic aromatic hydrocarbons, and polychlorinated biphenyls: Sediment extraction with Tenax(R) and effects of contact time and solute hydrophobicity. *Environ. Toxicol. Chem.*, 16(7): 1351-1357.

Crank, J., 1975. *The Mathematics of Diffusion*. Oxford University Press, Oxford, England, pg 91.

DiToro, D.M. et al., 1991. Technical basis for establishing sediment quality criteria for nonionic organic-chemicals using equilibrium partitioning. *Environ. Toxicol. Chem.*, 10(12): 1541-1583.

Droppo, I.G., Leppard, G.G., Flannigan, D.T. and Liss, S.N., 1997. The freshwater floc: A functional relationship of water and organic and inorganic floc constituents affecting suspended sediment properties. *Water Air and Soil Poll.*, 99(1-4): 43-53.

Frame, G.M., Cochran, J.W. and Bowadt, S.S., 1996. Complete PCB congener distributions for 17 aroclor mixtures determined by 3 HRGC systems optimized for comprehensive, quantitative, congener-specific analysis. *HRC-J. High Res. Chrom.*, 19(12): 657-668.

Fugate, D.C. and Friedrichs, C.T., 2002. Determining concentration and fall velocity of estuarine particle populations using ADV, OBS and LISST. *Cont. Shelf Res.*, 22(11-13): 1867-1886.

General Electric. 2001. Press release statement from August 17, 2001.

Ghosh, U., Weber, A.S., Jensen, J.N. and Smith, J.R., 1999. Congener level PCB desorption kinetics of field-contaminated sediments. *J. Soil Contam.*, 8(5): 593-613.

Ghosh, U., Zimmerman, J.R. and Luthy, R.G., 2003. PCB and PAH speciation among particle types in contaminated harbor sediments and effects on PAH bioavailability. *Environ. Sci. Technol.*, 37(10): 2209-2217.

Girvin, D.C., Sklarew, D.S., Scott, A.J. and Zipperer, J.P., 1997. Polychlorinated biphenyl desorption from low organic carbon soils: Measurement of rates in soil-water suspensions. *Chemosphere*, 35(9): 1987-2005.

- Gobas, F. and MacLean, L.G., 2003. Sediment-water distribution of organic contaminants in aquatic ecosystems: The role of organic carbon mineralization. *Environ. Sci. Technol.*, 37(4): 735-741.
- Gramatica, P., Navas, N. and Todeschini, R., 1998. 3D-modelling and prediction by WHIM descriptors. Part 9. Chromatographic relative retention time and physico-chemical properties of polychlorinated biphenyls (PCBs). *Chemometr. Intell. Lab. Sys.*, 40(1): 53-63.
- Hawley, N., 1991. Preliminary-observations of sediment erosion from a bottom resting flume. *J. Great Lakes Res.*, 17(3): 361-367.
- Huckins, J.N., Manuweera, G.K., Petty, J.D., Mackay, D. and Lebo, J.A., 1993. Lipid-containing semipermeable membrane devices for monitoring organic contaminants in Water. *Environ. Sci. Technol.*, 27: 2489-2496.
- Huckins, J.N., Tubergen, M.W. and Manuweera, G.K., 1990. Semipermeable membrane devices containing model lipid: A new approach to monitoring the bioavailability of lipophilic contaminants and estimating their bioconcentration potential. *Chemosphere*, 20(5): 533-552.
- Jepsen, R. and Lick, W., 1996. Parameters affecting the adsorption of PCBs to suspended sediments from the Detroit River. *J. Great Lakes Res.*, 22(2): 341-353.
- Jepsen, R., Borglin, S., Lick, W. and Swackhamer, D.L., 1995. Parameters affecting the adsorption of hexachlorobenzene to natural sediments. *Environ. Toxicol. Chem.*, 14(9): 1487-1497.
- Jonker, M.T.O. and Koelmans, A.A., 2002. Sorption of polycyclic aromatic hydrocarbons and polychlorinated biphenyls to soot and soot-like materials in the aqueous environment mechanistic considerations. *Environ. Sci. Technol.*, 36(17): 3725-3734.
- Karickhoff, S.W. and Morris, K.R., 1985. Sorption dynamics of hydrophobic pollutants in Sediment Suspensions. *Environ. Toxicol. Chem.*, 4(4): 469-479.
- Karickhoff, S.W., Brown, D.S. and Scott, T.A., 1979. Sorption of hydrophobic pollutants on natural sediments. *Water Res.*, 13: 241-248.
- Kim, E.H., Mason, R.P., Porter, E.T. and Soulen, H.L., 2004. The effect of resuspension on the fate of total mercury and methyl mercury in a shallow estuarine ecosystem: a mesocosm study. *Mar. Chem.*, 86(3-4): 121-137.
- Kleineidam S., Rugner, H. and Grathwohl, P. 2004. Desorption kinetics of Phenanthrene in aquifer material lacks hysteresis. *Environ. Sci. Technol.* 38: 4169-4175.

- Kopinke, F.D., Poerschmann, J. and Georgi, A., 1999. Application of SPME to study sorption phenomena on dissolved humic organic matter. In: J. Pawliszyn (Editor), Applications of Solid Phase Microextraction. Chromatography Monographs. Royal Society of Chemistry, Cambridge, pp. 111-128.
- Kranck, K. and Milligan, T.G., 1992. Characteristics of suspended particles at an 11-hour anchor station in San-Francisco Bay, California. *J. Geophys. Res. Oceans*, 97(C7): 11373-11382.
- Krone, R.B. (Editor), 1976. Engineering interest in the benthic boundary layer. *The Benthic Boundary Layer*. Plenum Press, New York, 143-156 pp.
- Kucklick, J.R., Harvey, H.R., Ostrom, P.H., Ostrom, N.E. and Baker, J.E., 1996. Organochlorine dynamics in the pelagic food web of Lake Baikal. *Environ. Toxicol. Chem.*, 15(8): 1388-1400.
- Kucklick, J.R., Hinckley, D.A. and Bidleman, T.F., 1991. Determination of Henry Law constants for hexachlorocyclohexanes in distilled water and artificial seawater as a function of temperature. *Mar. Chem.*, 34(3-4): 197-209.
- Kukkonen, J.V.K. et al., 2003. Sediment characteristics affecting desorption kinetics of select PAH and PCB congeners for seven laboratory spiked sediments. *Environ. Sci. Technol.*, 37(20): 4656-4663.
- Lamoureux, E.M. and Brownawell, B.J., 1999. Chemical and biological availability of sediment-sorbed hydrophobic organic contaminants. *Environ. Toxicol. Chem.*, 18(8): 1733-1741.
- Landin, P., Llompart, M., Lourido, M. and Cela, R., 2001. Determination of tri- through heptachlorobiphenyls in water samples by SPME-GC-MS-MS: Comparison of PDMS and PDMS-DVB coatings. *J. Microcolumn Sep.*, 13(7): 275-284.
- Langenfeld, J.J., Hawthorne, S.B. and Miller, D.J., 1996. Quantitative analysis of fuel-related hydrocarbons in surface water and wastewater samples by solid-phase microextraction. *Anal. Chem.*, 68(1): 144-155.
- Latimer, J.S., Davis, W.R. and Keith, D.J., 1999. Mobilization of PAHS and PCBs from in-place contaminated marine resuspension events. *Estuar. Coast. and Shelf Sci.*, 49(4): 577-595.
- Lee, C., Wu, C.H. and Hoopes, J.A., 2004. Automated sediment erosion testing system using digital Imaging. *J. Hydrol. Eng.*, 130(8): 771-782.
- Lee, S., Gan, J., Liu, W.P. and Anderson, M.A., 2003. Evaluation of K-d underestimation using solid phase microextraction. *Environ. Sci. Technol.*, 37(24): 5597-5602.

- Lick, W. and Rapaka, V., 1996. A quantitative analysis of the dynamics of the sorption of hydrophobic organic chemicals to suspended sediments. *Environ. Toxicol. Chem.*, 15(7): 1038-1048.
- Lick, W., Lick, J. and Ziegler, C.K., 1994. The Resuspension and transport of fine-grained sediments in Lake Erie. *J. Great Lakes Res.*, 20(4): 599-612.
- Lick, W., Xu, Y.J. and McNeill, J., 1995. Resuspension properties of sediments from the Fox, Saginaw, and Buffalo Rivers. *J. Great Lakes Res.*, 21(2): 257-274.
- Llompart, M., Li, K. and Fingas, M., 1998. Solid phase microextraction and headspace solid phase microextraction for the determination of polychlorinated biphenyls in water samples. *Anal. Chem.*, 70(13): 2510-2515.
- Lohmann, R., MacFarlane, J.K. and Gschwend, P.M., 2005. Importance of black carbon to sorption of native PAHs, PCBs, and PCDDs in Boston and New York, Harbor sediments. *Environ. Sci. Technol.*, 39(1): 141-148.
- Maa, J.P.Y., Sanford, L. and Halka, J.P., 1998. Sediment resuspension characteristics in Baltimore Harbor, Maryland. *Mar. Geol.*, 146(1-4): 137-145.
- Manning, A.J. and Dyer, K.R., 1999. A laboratory examination of floc characteristics with regard to turbulent shearing. *Mar. Geol.*, 160(1-2): 147-170.
- Martinez, E., Landin, P., Carro, A.M., Llompart, M.P. and Cela, R., 2002. Strategically designed sample composition for fastest screening of polychlorinated biphenyl congeners in water samples. *J. Environ. Monitor.*, 4(4): 490-497.
- Mayer, P., Vaes, W.H.J. and Hermens, J.L.M., 2000a. Absorption of hydrophobic compounds into the poly(dimethylsiloxane) coating of solid-phase microextraction fibers: High partition coefficients and fluorescence microscopy images. *Anal. Chem.*, 72(3): 459-464.
- Mayer, P. et al., 2000. Sensing dissolved sediment porewater concentrations of persistent and bioaccumulative pollutants using disposable solid-phase microextraction fibers. *Environ. Sci. Technol.*, 34(24): 5177-5183.
- Mikkelsen, O.A. and Pejrup, M., 2001. The use of a LISST-100 laser particle sizer for in-situ estimates of floc size, density and settling velocity. *Geo-Mar. Lett.*, 20(4): 187-195.
- Mikkelsen, O.A., 2002. Examples of spatial and temporal variations of some fine-grained suspended particle characteristics in two Danish coastal water bodies. *Oceanol. Acta*, 25(1): 39-49.

Muller, L., 1999. Field Analysis by SPME. In: J. Pawliszyn (Editor), Applications of Solid Phase Microextraction. RSC Chromatography Monographs. Royal Society of Chemistry, Cambridge, pp. 269-283.

New York State Department of Health, 1998. Health Consultation. *Survey of Hudson River Angelers and an Estimate of their Exposure to PCBs*.

Oomen, A.G., Mayer, P. and Tolls, J., 2000. Nonequilibrium solid phase microextraction for determination of the freely dissolved concentration of hydrophobic organic compounds: Matrix effects and limitations. *Anal. Chem.*, 72(13): 2802-2808.

Opperhuizen, A., Gobas, F., Vandersteen, J.M.D. and Hutzinger, O., 1988. Aqueous Solubility of Polychlorinated-Biphenyls Related to Molecular-Structure. *Environ. Sci. Technol.*, 22(6): 638-646.

Pawliszyn, J., 1999. Quantitative aspects of SPME. In: J. Pawliszyn (Editor), Applications of Solid Phase Microextraction. Chromatography Monographs. Royal Society of Chemistry, Cambridge, pp. 3-21.

Pignatello, J.J. and Xing, B.S., 1996. Mechanisms of slow sorption of organic chemicals to natural particles. *Environ. Sci. Technol.*, 30(1): 1-11.

Poerschmann, J., Gorecki, T. and Kopinke, F.D., 2000. Sorption of very hydrophobic organic compounds onto poly(dimethylsiloxane) and dissolved humic organic matter. 1. Adsorption or partitioning of VHOC on PDMS-coated solid-phase microextraction fibers - A never-ending story? *Environ. Sci. Technol.*, 34(17): 3824-3830.

Porschmann, J., Kopinke, F.D. and Pawliszyn, J., 1998. Solid-phase microextraction for determining the binding state of organic pollutants in contaminated water rich in humic organic matter. *J. Chromatogr.*, 816(2): 159-167.

Porter, E.T., Sanford, L.P., Gust, G. and Porter, F.S., 2004. Combined water-column mixing and benthic boundary-layer flow in mesocosms: key for realistic benthic-pelagic coupling studies. *Mar. Ecol. Prog. Ser.*, 271: 43-60.

Porter, E.T., Sanford, L.P., Porter, F.S. and Mason, R.P., 2005. STORM: Resuspension mesocosms with realistic bottom shear and water column turbulence for benthic-pelagic coupling studies. *Limnol. Oceanogr.*

Potter, D.W. and Pawliszyn, J., 1994. Rapid-Determination of Polyaromatic Hydrocarbons and Polychlorinated-Biphenyls in Water Using Solid-Phase Microextraction and Gcms. *Environ. Sci. Technol.*, 28(2): 298-305.

Ramos, E.U., Meijer, S.N., Vaes, W.H.J., Verhaar, H.J.M. and Hermens, J.L.M., 1998. Using solid-phase microextraction to determine partition coefficients to humic acids and

bioavailable concentrations of hydrophobic chemicals. *Environ. Sci. Technol.*, 32(21): 3430-3435.

Rantalainen, A.L., Cretney, W.J. and Ikonou, M.G., 2000. Uptake rates of semipermeable membrane devices (SPMDs) for PCDDs, PCDFs and PCBs in water and sediment. *Chemosphere*, 40(2): 147-158.

Sanford, L.P. et al., 2005. Variability of suspended particle concentrations, sizes, and settling velocities in the Cheapeake Bay turbidity maximum. In: I.G. Droppo (Editor), *Flocculation in natural and engineered environmental systems*. CRC Press, Boca Raton, FL, pp. 211-235.

Sanford, L.P., 1997. Turbulent mixing in experimental ecosystem studies. *Mar. Ecol. Prog. Ser.*, 161: 265-293.

Shiu, W.Y. and Ma, K. C. 2000. Temperature dependence of physical chemical properties of selected chemicals of environmental interest II. Chlorobenzenes, Polychlorinated Biphenyls, Polychlorinated Dibenzo-p-dioxins and Dibenzofurans. *J. Phys. Chem. Ref. Data* 29(30): 387-462.

Sobek, A., Gustafsson, O., Hajdu, S. and Larsson, U., 2004. Particle-water partitioning of PCBs in the photic zone: A 25-month study in the open Baltic Sea. *Environ. Sci. Technol.*, 38(5): 1375-1382.

Sukola, K., Koziel, J., Augusto, F. and Pawliszyn, J., 2001. Diffusion-based calibration for SPME analysis of aqueous samples. *Anal. Chem.*, 73(1): 13-18.

Ten Hulscher, T.E.M. et al., 1999. Triphasic desorption of highly resistant chlorobenzenes, polychlorinated biphenyls, and polycyclic aromatic hydrocarbons in field contaminated sediment. *Environ. Sci. Technol.*, 33(1): 126-132.

Ten Hulscher, T.E.M., Vrind, B.A., van Noort, P.C.M. and Govers, H.A.J. 2002. Resistant sorption of in situ chlorobenzenes and a polychlorinated biphenyl in river Rhine suspended matter. *Chemosphere*, 49(10): 1231-1238.

Thomann, R.V., Mueller, J.A., Winfield, R.P. and Huang, C.R. 1991. Model of Fate and Accumulation of Pcb Homologs in Hudson Estuary. *J. Environ. Eng. Sci.*, 117(2): 161-178.

Tolhurst, T.J. et al., 2000. A comparison and measurement standardisation of four in situ devices for determining the erosion shear stress of intertidal sediments. *Cont. Shelf Res.*, 20(10-11): 1397-1418.

Totten, L.A. et al., 2001. Dynamic air-water exchange of polychlorinated biphenyls in the New York - New Jersey Harbor Estuary. *Environ. Sci. Technol.*, 35(19): 3834-3840.

- Traykovski, P., Latter, R.J. and Irish, J.D. 1999. A laboratory evaluation of the laser in situ scattering and transmissometry instrument using natural sediments. *Mar. Geol.*, 159(1-4): 355-367.
- Tsai, C.H. and Lick, W., 1988. Resuspension of Sediments from Long-Island Sound (USA). *Water Sci. Technol.*, 20(6-7): 155-164.
- Tsai, C.H., Iacobellis, S. and Lick, W. 1987. Flocculation of fine-grained lake sediments due to a uniform shear-stress. *J. Great Lakes Res.*, 13(2): 135-146.
- Tye, R., Jepsen, R. and Lick, W. 1996. Effects of colloids, flocculation, particle size, and organic matter on the adsorption of hexachlorobenzene to sediments. *Environ. Toxicol. Chem.*, 15(5): 643-651.
- United States Environmental Protection Agency 2000. Hudson River PCB Superfund Site (New York) Superfund Site Proposed Plan, December.
- United States Environmental Protection Agency *Phase 2 Report-Review Copy: Data Evaluation and Interpretation Report*; Hudson River PCBs Reassessment RI/FS. U.S. Environmental Protection Agency, U.S. Government Printing Office, Washington, DC, 1997.
- Vaes, W.H.J., Ramos, E.U., Verhaar, H.J.M., Seinen, W. and Hermens, J.L.M., 1996. Measurement of the free concentration using solid-phase microextraction: Binding to protein. *Anal. Chem.*, 68(24): 4463-4467.
- Valsaraj, K.T. and Thibodeaux, L.J., 1999. On the linear driving force model for sorption kinetics of organic compounds on suspended sediment particles. *Environ. Toxicol. Chem.*, 18(8): 1679-1685.
- Van der Lee, W.T.B., 2000. Temporal variation of floc size and settling velocity in the Dollard estuary. *Cont. Shelf Res.*, 20(12-13): 1495-1511.
- Van Leussen, W., 1999. The variability of settling velocities of suspended fine-grained sediment in the Ems estuary. *J. Sea Res.*, 41(1-2): 109-118.
- Van Noort, P.C.M. et al., 2003. Slow and very slow desorption of organic compounds from sediment: influence of sorbate planarity. *Water Res.*, 37(10): 2317-2322.
- Voulgaris, G. and Meyers, S.T., 2004. Temporal variability of hydrodynamics, sediment concentration and sediment settling velocity in a tidal creek. *Cont. Shelf Res.*, 24(15): 1659-1683.
- Wang, X. Tang, S. Liu S., Cui, S., and Wang, W. 2003. Molecular hologram derived quantitative structure-property relationships to predict physico-chemical properties of polychlorinated biphenyls. *Chemosphere*, 51: 617-632.

Wells, M., Wick, L.Y. and Harms, H., 2004. Perspectives on modeling the release of hydrophobic organic contaminants drawn from model polymer release systems. *J. Mater. Chem.*, 14(15): 2461-2472.

Wu, S.C. and Gschwend, P.M., 1986. Sorption kinetics of hydrophobic organic-compounds to natural sediments and soils. *Environ. Sci. Technol.*, 20(7): 717-725.

Wu, S.C. and Gschwend, P.M., 1988. Numerical modeling of sorption kinetics of organic compounds to soil and sediment particles. *Water Resources Research*, 24(8): 1373-1383.

Xia, G., 1998. Sorption behavior of nonpolar organic chemicals on natural sorbents, Johns Hopkins University, Baltimore Maryland.

Xia, X.M. et al., 2004. Observations on the size and settling velocity distributions of suspended sediment in the Pearl River Estuary, China. *Cont. Shelf Res.*, 24(16): 1809-1826.

Yang, Y., Miller, D.J. and Hawthorne, S.B., 1998. Solid-phase microextraction of polychlorinated biphenyls. *J. Chromatogr.*, 800(2): 257-266.

Zeng, E.Y. and Noblet, J.A., 2002. Theoretical considerations on the use of solid-phase microextraction with complex environmental samples. *Environ. Sci. Technol.*, 36(15): 3385-3392.

Zeng, E.Y., Tsukada, D. and Diehl, D.W., 2004. Development of solid-phase microextraction-based method for sampling of persistent chlorinated hydrocarbons in an urbanized coastal environment. *Environ. Sci. Technol.*, 38(21): 5737-5743.

Zygmunt, B., Jastrzebska, A. and Namiesnik, J., 2001. Solid phase microextraction - A convenient tool for the determination of organic pollutants in environmental matrices. *Crit. Rev. Anal. Chem.*, 31(1): 1-18.